

Untersuchung der stromalen Alterung

-

**Proteom- und Sekretomstudie *in situ* gealterter
humaner dermaler Fibroblasten**

Inaugural-Dissertation

zur Erlangung des Doktorgrades
der Mathematisch-Naturwissenschaftlichen Fakultät
der Heinrich-Heine-Universität Düsseldorf

vorgelegt von

Daniel Michael Waldera-Lupa
aus Bochum

Düsseldorf, Juni 2014

aus dem Molecular Proteomics Laboratory
des Instituts für Molekulare Medizin
an der Heinrich-Heine Universität Düsseldorf

Gedruckt mit der Genehmigung der
Mathematisch-Naturwissenschaftlichen Fakultät der
Heinrich-Heine-Universität Düsseldorf

Referent: Prof. Dr. Kai Stühler
Korreferent: Prof. Dr. Lutz Schmitt

Tag der mündlichen Prüfung:

*„Der Zweifel ist der Beginn der Wissenschaft.
Wer nichts anzweifelt, prüft nichts. Wer nichts
prüft, entdeckt nichts. Wer nichts entdeckt, ist
blind und bleibt blind.“*

Teilhard de Chardin

Inhaltsverzeichnis

Abkürzungen	VI
Zusammenfassung	X
Summary	XII
1 Einleitung	1
1.1 Das Altern	1
1.1.1 Definition des Alterns	1
1.1.2 Zelluläre und molekulare Charakteristika des Alterns	2
1.2 Die Haut als Modellsystem des Alterns	9
1.2.1 Aufbau und Funktion der Haut	9
1.2.2 Die Alterung der Haut	10
1.2.3 Mechanismen der stromalen Alterung	13
1.3 Die Proteomanalyse	19
1.3.1 Methoden der qualitativen und quantitativen Proteomanalyse	20
1.3.2 Identifizierung von Proteinen mittels Massenspektrometrie	21
1.3.3 Quantifizierung von Proteinen mittels LC-MS	24
2 Ziele der Arbeit	27
3 Manuskripte	28
3.1 Übersicht und Zusammenfassungen	28
3.2 Publikation I: <i>The fate of b-ions in the two worlds of collision-induced dissociation</i>	36
3.3 Publikation II: <i>Application of label-free proteomics for differential analysis of lung carcinoma cell line A549</i>	54
3.4 Publikation III: <i>Proteome-wide analysis of primary cultures of in situ aged human fibroblasts reveals a moderate age-associated cellular phenotype</i>	65
3.5 Publikation IV: <i>Characterization of skin aging associated secreted proteins (SAASP) produced by dermal fibroblast isolated from intrinsically aged human skin</i>	110

4	Abschlussdiskussion	158
4.1	Die massenspektrometrie-basierte Proteomanalyse	158
4.1.1	Evaluierung eines Massenspektrometers für die Identifizierung von Proteinen	158
4.1.2	Etablierung eines Arbeitsablaufs zur Charakterisierung humaner Proben	160
4.1.3	Proteomanalyse humaner dermaler Fibroblasten	161
4.2	Charakterisierung <i>in situ</i> gealterter humaner dermaler Fibroblasten	163
4.2.1	Intrazelluläre altersassoziierte Veränderungen	163
4.2.2	Altersassoziierte Veränderungen des Sekretoms	165
4.3	Schlussfolgerung	168
4.4	Ausblick	170
5	Literaturverzeichnis	171
Publikationen und Manuskripte im Journalformat		XIV
Veröffentlichungen und Präsentationen		XXIX
Danksagung		XXXII
Lebenslauf		XXXIII
Erklärung		XXXV

Abkürzungen

1D	eindimensional
2D	zweidimensional
3D	dreidimensional
AASP	altersassoziiertes sekretorischer Phänotyp (<i>age-associated secretory phenotype</i>)
ABC	Ammoniumhydrogencarbonat (<i>ammoniumbicarbonat</i>)
Ac	acetyliert (<i>acetylated</i>)
ACN	Acetonitril
AMPK	<i>AMP-activated protein kinase</i>
ANOVA	Varianzanalyse (<i>analysis of variance</i>)
APEX	<i>absolute proteomics expression</i>
AQUA	absolute Quantifizierung (<i>absolute quantification</i>)
ATP	Adenosintriphosphat
bCID	<i>beam-type collision-induced dissociation</i>
CDH	<i>cadherin</i>
CID	<i>collision-induced dissociation</i>
COL	<i>collagen</i>
CV	Variationskoeffizient (<i>coefficient of variation</i>)
CXCL	<i>C-X-C motif chemokine</i>
Da	Dalton
DAVID	<i>database for annotation, visualization and integrated discovery</i>
DB	Datenbank (<i>data base</i>)
DIGE	Differentielle Gelelektrophorese (<i>difference gel electrophoresis</i>)
DMEM	<i>Dulbecco's Modified Eagle's Medium</i>
DNA	Desoxyribonukleinsäure (<i>deoxyribonucleic acid</i>)
DNA-SCARS	<i>DNA Segments with Chromatin Alterations Reinforcing Senescence</i>
DSB	Doppelstrangbruch
DTT	Dithiothreitol
ECM	Extrazelluläre Matrix (<i>extracellular matrix</i>)
EGF	<i>epidermal Growth Gactor</i>
EGFR	<i>epidermal Growth Factor Receptor</i>
ELISA	<i>enzyme linked immunosorbent assay</i>

Abkürzungen

emPAI	<i>exponentially modified protein abundance index</i>
ER	Endoplasmatisches Retikulum (<i>endoplasmic reticulum</i>)
ESI	Elektrospray-Ionisation (<i>electrospray ionization</i>)
ETD	Elektronentransferdissoziation (<i>electron transfer dissociation</i>)
<i>ex vivo</i>	Außerhalb des Lebendigen
FA	Ameisensäure (<i>formic acid</i>)
F-Aktin	filamentöses Aktin
FBS	Fetales Kälberserum (<i>fetal bovine serum</i>)
G-Aktin	globuläres Aktin
gero-miR	Gerontologische microRNA
GO	<i>gene ontology</i>
HCD	Hochenergie-Kollisionsdissoziation (<i>higher-energy collisional dissociation</i>)
HF	Hydrophobizitätsfaktor (<i>hydrophobicity factor</i>)
HPLC	Hochleistungsflüssigkeitschromatographie (<i>high performance liquid chromatography</i>)
HSD	<i>honestly significant difference</i>
i.d.	Innendurchmesser (<i>inner diameter</i>)
IAA	Iodacetamid
iBAQ	<i>intensity based absolute quantification</i>
ICAT	<i>isotope-coded affinity tag</i>
ICPL	<i>isotope-coded protein label</i>
IEF	Isoelektrische Fokussierung
IIS	<i>insulin/IGF-like signalling</i>
IL	Interleukin
<i>in silico</i>	Computerbasiert
<i>in situ</i>	In der natürlichen Lage im Körper
<i>in vivo</i>	Im lebendigen Organismus
IPTL	<i>isobaric peptide termini labeling</i>
iTRAQ	<i>isobaric tags for relative and absolute quantitation</i>
LC-MS	Kopplung von HPLC und MS
LIT	lineare Ionenfalle (<i>linear ion trap</i>)
<i>m/z</i>	Masse-zu-Ladung-Verhältnis (<i>mass-to-charge ratio</i>)
MALDI	Matrix-unterstützte Laser-Desorption/Ionisation (<i>matrix-assisted laserdesorption/ionisation</i>)

Abkürzungen

MEF	embryonale Mausfibroblasten (<i>mouse embryonic fibroblast</i>)
MFAP	<i>microfibrillar-Associated Protein</i>
MIF	<i>migration Inhibitory Factor</i>
miR/miRNA	<i>micro ribonucleic acid</i>
MMP	Matrix-Metalloproteinase
mRNA	<i>messenger ribonucleic acid</i>
MS	Massenspektrometrie
MS/MS	Tandemmassenspektrometrie
mtDNA	Mitochondriale DNA
mTOR	<i>mammalian target of rapamycin</i>
MudPIT	<i>multidimensional protein identification technology</i>
nAc	nicht acetyliert (<i>non-acetylated</i>)
NER	Nukleotidexzisions-Reparatur
NF- κ B	<i>nuclear factor 'kappa-light-chain-enhancer' of activated B-cells</i>
NHDF	<i>normal human dermal fibroblasts</i>
NHEJ	<i>non-homologous endjoining</i>
NLRP3	<i>NOD-like receptor family, pyrin domain containing 3</i>
p53	<i>cellular tumor antigen p53</i>
PAGE	Polyacrylamid-Gelelektrophorese
PBS	phosphatgepufferte Salzlösung (<i>phosphate buffered saline</i>)
PCA	<i>principle component analysis</i>
PI	Propidiumiodid (<i>propidium iodide</i>)
PID	<i>protein interaction database</i>
PML	<i>promyelocytic Leukaemia</i>
PN	Passagen-Nummer (<i>passage number</i>)
pRB	<i>retinoblastoma-associated protein</i>
PTM	Posttranslationale Modifikation
Q	Quadrupol
QIT	dreidimensionale Ionenfalle (<i>three-dimensional ion trap</i>)
QQQ	Triplequadrupol
QToF	Quadrupole time-of-flight
R	Auflösung (<i>resolution</i>)
rCID	<i>resonant excitationcollision-induced dissociation</i>

Abkürzungen

RNA	Ribonukleinsäure (<i>ribonucleic acid</i>)
ROS	Reaktive Sauerstoffspezies (<i>reactive oxygen species</i>)
SAASP	<i>skin aging-associated secreted proteins</i>
SASP	seneszenz-assoziiierter sekretorischer Phänotyp (<i>senescence-associated secretory phenotype</i>)
SC	<i>spectral counting</i>
SDS	<i>sodium dodecyl sulfate</i>
SI	<i>signal intensity</i>
SILAC	<i>stable isotope labelling by amino acids in cell culture</i>
SMS	<i>senescence-messaging secretome</i>
T3PQ	<i>top 3 protein quantification</i>
TFA	Trifluoressigsäure (<i>trifluoroacetic acid</i>)
TGFB	<i>transforming growth factor beta</i>
TMT	<i>tandem mass tag</i>
TNF	Tumornekrosefaktor
TOF	Flugzeitmassenspektrometer (<i>time-of-flight</i>)
TOST	<i>two one-sided test</i>
UPLC	<i>ultra performance liquid chromatography</i>
UV	Ultraviolettstrahlung
VEGF	<i>vascular endothelial growth factor</i>
γ H2AX	phosphoryliertes Histon H2AX

Zusammenfassung

In den letzten Jahren wurden große Fortschritte erzielt die molekularen Mechanismen des Alterns von Zellen und Organismen zu verstehen. Dabei wurde evident, dass in diesen Mechanismen unterschiedliche Klassen von Biomolekülen involviert sind. Ziel dieser Arbeit ist es die Rolle der Proteine in der stromalen Alterung zu untersuchen und einen Beitrag zur Aufklärung des stromalen Alterungsprozesses zu leisten sowie die Mechanismen des Alterns zu ergänzen. Um eine komplexe Mischung von Proteinen quantitativ mittels Massenspektrometrie untersuchen zu können, wurden zunächst methodische Arbeiten durchgeführt. Infolge der Verfügbarkeit unterschiedlicher Massenspektrometer stellte sich die Frage, welches für das geplante Experiment in Hinsicht auf Sensitivität und Genauigkeit am geeignetsten ist. Aufgrund der signifikant höheren Detektionsrate von b-Ionen und auch y-Ionen und der daraus resultierenden gesteigerten Identifizierungsrate von Proteinen wurde ein Orbitrap-Massenspektrometer für die Analyse humaner Zellen ausgewählt. Nachfolgend wurde ein Arbeitsablauf für die labelfreie Quantifizierung von Proteinen mittels Massenspektrometrie etabliert. Im Anschluss wurde ein zelluläres *ex vivo* Hautalterungsmodell unter Verwendung *in situ* gealterter primärer adulter humaner dermaler Fibroblasten, als Hauptzelltyp des Stromas, von 15 verschiedenen Individuen mittels labelfreier Proteomanalyse auf Ebene der intrazellulären und sezernierten Proteine untersucht. Ergänzt wurden die Daten durch Arbeiten weiterer molekularer Aspekte, wie Telomerlängen, genomische Stabilität und Analysen der mRNA und miRNA, welche im Rahmen des Verbundprojekts „*GerontoSys - stromal ageing*“ in Kooperation erstellt wurden. Durch die quantitative Analyse des Proteoms konnten 43 altersabhängig veränderte Proteine identifiziert werden, die einen moderaten altersassoziierten zellulären Phänotyp ausbilden und in acht übergeordnete biologische Prozesse, wie die Differenzierung, die Proliferation, die Proteostase, den RNA-Metabolismus, die Zellkommunikation, die Zellorganisation, den Zellstress und den Zelltod, involviert sind. Der Abgleich mit mRNA -Daten gab Hinweise darauf, dass 77 % dieser Proteine nicht durch die Genexpression reguliert werden. Zudem konnte durch die Berücksichtigung von miRNA-Daten gezeigt werden, dass drei Proteine einer potentiell posttranskriptionalen Regulation durch miRNAs unterliegen. Die meisten der Proteine wurden noch nicht im Rahmen der Alterung von Fibroblasten beschrieben, gleichwohl bestätigen die identifizierten Prozesse die bekannten molekularen Charakteristika des Alterns. Durch die quantitative Analyse des Sekretoms konnten 70 altersabhängig

veränderte Proteine identifiziert werden, die in die Organisation der extrazellulären Matrix, die Formation von elastischen Fasern, die Inflammation und die interzelluläre Kommunikation involviert sind. In dieser Arbeit wurde erstmals der altersassoziierte sekretorische Phänotyp dermalen Fibroblasten auf Ebene der Proteine charakterisiert. Durch den Vergleich mit dem in der Literatur beschriebenen Seneszenz-assoziierten sekretorischen Phänotyp wurde gezeigt, dass die Sekretion pro-inflammatorischer Zytokine und Matrix-Metalloproteinasen ein gemeinsamer Aspekt der induzierten Seneszenz und des *in situ* Alters ist, obgleich die Phänotypen deutliche Unterschiede aufweisen. Die Ergebnisse dieser Arbeit erlauben Rückschlüsse auf die intra- und extrazellulären Veränderungen der Fibroblasten während des Alterns zu ziehen und tragen zu einem besseren Verständnis des Alterungsprozesses, der Mechanismen der Hautalterung und der Beteiligung der Fibroblasten an der Stromalalterung bei.

Summary

In recent years, great progress has been achieved to understand the molecular mechanisms of cellular and organismal ageing. It became evident that different classes of biomolecules are involved in these mechanisms. The aim of this study is to investigate the role of proteins in stromal ageing and to complement the mechanisms of the ageing process. For quantitative analysis of a complex protein mixture methodological development has been performed first. Due to the availability of different mass spectrometers the question arose, which of them is suitable for the planned experiments in terms of sensitivity and accuracy. Because of the significantly higher detection rate of b-ions and y-ions, and the resulting increased rate of protein identification an Orbitrap mass spectrometer has been selected for the analysis of human cells. Subsequently, a label-free mass spectrometric workflow for quantification of proteins was established. Next, the intracellular and secreted proteins of an *ex vivo* skin ageing model of *in situ* aged primary adult human dermal fibroblasts, as the major cell type within the stroma, of 15 different individuals were analysed using the established approach. The data were supplemented by analyses of other molecular aspects, such as telomere length, genomic stability, and alterations on mRNA and miRNA level, which were analysed within the research project “GerontoSys – stromal ageing”. Quantitative analysis of the proteome revealed 43 proteins exhibiting an age-associated abundance change, thereby developing a moderate age-associated cellular phenotype. The age-associated proteins are involved in eight biological categories, such as differentiation, proliferation, proteostasis, RNA metabolism, cell communication, cell organisation, response to stress and cell death. Comparing the results obtained from proteomics with mRNA and miRNA data revealed that at least 77 % of altered proteins were not regulated via gene expression, and at least three candidate proteins were potentially post-transcriptionally regulated by miRNAs. Most of the identified proteins have not been described in the context of the fibroblasts’ ageing yet, but the deduced processes confirmed known molecular hallmarks of ageing. Quantitative analysis of secreted proteins revealed 70 proteins exhibiting an age-dependent secretion pattern. The proteins are involved in extracellular matrix organisation, elastic fiber formation, inflammation and intercellular communication. Within this work, the age-associated secretory phenotype of dermal fibroblasts was characterised for the first time at the level of proteins. The comparison of the identified phenotype with the described senescence-associated secretory phenotype revealed that the secretion of pro-inflammatory cytokines and matrix metalloproteinases are common

Summary

aspects of induced senescence as well as *in situ* ageing. Furthermore, the comparison revealed that the secretory phenotype of *in situ* aged human dermal fibroblasts significantly differs from the senescence-associated secretory phenotype. The results of this work allow a comprehensive insight into the intra- and extracellular alterations of fibroblasts during *in vivo* ageing. In addition, they contribute to a better understanding of the mechanisms of the ageing process and the involvement of fibroblasts in stromal ageing.

1 Einleitung

1.1 Das Altern

1.1.1 Definition des Alterns

Das Altern ist ein hochkomplexer Prozess, welcher stetig voranschreitet und mit dem Tod des Organismus endet. Der Alterungsprozess kann durch fünf charakteristische Veränderungen beschrieben werden: Zunahme der Mortalität, Reduktion physiologischer Funktionen und Kapazitäten, Abnahme adaptiver Fähigkeiten, erhöhte Anfälligkeit und Vulnerabilität für Krankheiten und biochemische Veränderungen im Gewebe (zusammengefasst in Treon, 2003).

Eine frühe Definition beschreibt das Altern als Wahrscheinlichkeit der Sterblichkeit. Dies bedeutet, dass je älter ein Organismus ist, desto höher ist die Wahrscheinlichkeit seines Todes (Gompertz, 1825). Ein Charakteristikum dieser Definition ist die Stetigkeit, welche im Laufe eines menschlichen Lebens jedoch nicht gegeben ist. So ist die Wahrscheinlichkeit beim Menschen in den ersten drei Lebensmonaten zu versterben deutlich höher als zwischen dem achten und zehnten Lebensjahr, das ein Minimum aufweist (Treon, 2003). Eine weiterentwickelte Definition beschreibt das Altern als eine fortschreitende, zeitabhängige Reduktion der Funktionsfähigkeit (Shock, 1985). Es gibt diverse physiologische Funktionen, die bereits in früheren Jahren abnehmen, wie z.B. die Immunfunktionen, das Hören und die Flexibilität des vaskulären Systems (Bowen und Atwood, 2004). Allerdings gibt es auch physiologische Funktionen, die noch im Alter von 20 Jahren nicht vollständig entwickelt sind. Demnach kann kein eindeutiger Zeitpunkt definiert werden, ab wann das Altern beginnt. Wenn das Altern mit der Beendigung der Entwicklung und der Abnahme aller Funktionen beginnt, dann Altern wir vermutlich erst nach dem 60. Lebensjahr. Eine aktuelle Definition beschreibt den Organismus als eine komplexe Kombination chemischer Reaktionen, und somit das Altern als Resultat von jeglichen Veränderungen im Laufe der Zeit (Bowen und Atwood, 2004). In dieser Definition werden nicht nur die Veränderungen im Bezug auf den Verlust von Funktionen, sondern auch den Gewinn von Funktionen, d.h. die Entwicklung berücksichtigt. Im Umkehrschluss kann somit gefolgert werden, dass wenn alle chemischen Reaktionen gestoppt werden, keine Veränderung mehr stattfinden kann und der Organismus nicht altert (Bowen und Atwood, 2004).

1.1.2 Zelluläre und molekulare und Charakteristika des Alterns

Es existieren eine Vielzahl von verschiedenen hypothetischen und auch wissenschaftlich fundierten Alterstheorien, die sich großteils ergänzen (zusammengefasst in Weinert und Timiras, 2003). Diese unterscheiden sich in ihren Ansätzen, obgleich es viele Übereinstimmungen gibt. Die Gemeinsamkeiten lassen sich auf zelluläre und molekulare Charakteristika, die das Altern determinieren, reduzieren (Lopez-Otin *et al.*, 2013). Zu diesen Charakteristika gehören die genomische Instabilität, Telomerverkürzungen, epigenetische Veränderungen, der Verlust der Proteostase, die Dysregulation von Nährstoffsignalwegen, die mitochondriale Dysfunktion, die zelluläre Seneszenz, der Verbrauch von Stammzellen und eine veränderte interzelluläre Kommunikation (Abb. 1).



Abbildung 1: Übersicht der zellulären und molekularen Charakteristika des Alterns (modifiziert nach Lopez-Otin *et al.*, 2013). Dazu gehören die genomische Instabilität, Telomerverkürzungen, epigenetische Veränderungen, der Verlust der Proteostase, die Dysregulation von Nährstoffsignalwegen, die mitochondriale Dysfunktion, die zelluläre Seneszenz, der Verbrauch von Stammzellen und eine veränderte interzelluläre Kommunikation.

Genomische Instabilität

Das Genom beschreibt die Gesamtheit der genetischen Information eines Organismus, welche auf der Desoxyribonukleinsäure (*deoxyribonucleic acid*, DNA) kodiert ist. Es gibt Hinweise darauf, dass genomische Schäden mit steigendem Alter akkumulieren und eine künstliche Schädigung des Genoms Aspekte einer beschleunigten Alterung hervorrufen (Moskalev *et al.*, 2013). Des Weiteren sind viele Krankheiten des vorzeitigen Alterns mit der Akkumulation von DNA-Schäden assoziiert (Amor-Guéret, 2006; Burtner und Kennedy, 2010). Die Stabilität und Integrität der DNA wird kontinuierlich durch eine Vielzahl unterschiedlicher Faktoren gestört. Hierzu gehören sowohl exogene Faktoren, wie z.B. chemische und biologische Agenzien, als auch endogene Faktoren, wie Replikationsfehler oder reaktive Sauerstoffspezies (*reactive oxygen species*, ROS) (Hoeijmakers, 2009). Die daraus resultierenden Veränderungen der DNA beinhalten Punktmutationen, Translokationen, Chromosomenaberrationen, Telomerverkürzungen und den Verlust von Genen, die größtenteils durch ein komplexes Netzwerk diverser Reparaturmechanismen behoben werden können (Lopez-Otin *et al.*, 2013). Die Schädigung der DNA und Defekte in den Reparaturmechanismen können in dysfunktionalen Zellen resultieren, die einen schädlichen Einfluss auf Ihre Umgebung und die Homöostase des Gewebes haben und zur beschleunigten Alterung führen (Rossi *et al.*, 2008; Gregg *et al.*, 2012).

Telomerverkürzung

Telomere sind kurze, wiederkehrende DNA-Sequenzen an den Chromosomenenden mit der Funktion diese zu schützen (Greider, 1996). Die Verkürzung der Telomere wurde in der Telomer-Hypothese im Zusammenhang mit dem Alterungsprozess beschrieben (Harley *et al.*, 1992). Die Hypothese besagt, dass je mehr Zellteilungen eine Zelle durchlaufen hat, umso kürzer sind ihre Telomere. Die stetige Verkürzung der Telomere resultiert in der Reduktion der Proliferationsrate und ist der Grund für die replikative Seneszenz *in vitro* (Blackburn, 2000). Auch während der *in vivo* Alterung wurde eine Verkürzung der Telomere beobachtet (Blasco, 2007). Des Weiteren konnte gezeigt werden, dass die Länge der Telomere unmittelbar mit der maximalen Lebenserwartung korreliert (Armanios *et al.*, 2009; Tomas-Loba *et al.*, 2008). Ein wichtiges altersassoziiertes Protein im Zusammenhang mit Telomeren ist die Telomerase, einer reversen Transkriptase, die in der Lage ist die Telomere wiederherzustellen, indem sie hexamerische DNA-Sequenzen repetitiv an die Enden der

Chromosomen hängt (Greider und Blackburn, 1985). In den meisten somatischen Zellen wird die Telomerase allerdings nicht exprimiert, was zur Verkürzung der Telomere mit jeder Zellteilung führt (Olovnikov, 1996). Es gibt Hinweise darauf, dass die Reaktivierung der Telomerase das vorzeitige Altern inhibiert (Jaskelioff *et al.*, 2011) und das physiologische Altern verzögert (Bernardes de Jesus *et al.*, 2012).

Epigenetische Veränderungen

Der Begriff Epigenetik umschreibt molekulare Mechanismen vererbbarer Chromosomenmodifikationen, die nicht auf Veränderungen der DNA-Sequenz beruhen und für die Regulation der Aktivität von Genen verantwortlich sind. Epigenetische Veränderungen werden durch eine Vielzahl unterschiedlicher Proteine reguliert. Dazu gehören unter anderem Methyltransferasen, Methylasen, Demethylasen, Histonacetylasen und Deacetylasen (Lopez-Otin *et al.*, 2013). Das Gewebe und die Zellen eines Organismus werden im Verlauf des Lebens von einer Vielzahl epigenetischer Veränderungen beeinflusst (Talens *et al.*, 2012). Diese treten auf Ebene der posttranslationalen Modifikation von Histonen und der DNA-Methylierung auf. Die Methylierung der DNA ist ein elementarer Regulator der Genexpression (Beck und Rakyán, 2008). Es gibt Hinweise darauf, dass die DNA mit zunehmendem Alter an verschiedenen Loci, wie Tumorsuppressorgenen, hypermethyliert wird (Maegawa *et al.*, 2010). Die Veränderung im Methylierungsmuster der DNA können zu einer Dysregulation der Transkription und einer aberranten Produktion von mRNAs führen, die eine wichtige Rolle in inflammatorischen, mitochondrialen und lysosomalen Signalwegen spielen (de Magalhaes *et al.*, 2009; Harries *et al.*, 2011). Zudem gibt es Hinweise darauf, dass spezielle microRNAs (gero-miRs), welche die Genexpression auf posttranskriptionaler Ebene regulieren, einer altersabhängigen Regulation unterliegen (Boulias und Horvitz, 2012; Ugalde *et al.*, 2011). Diese gero-miRs sind direkt in den Alterungsprozess involviert und haben einen Einfluss auf die Lebenserwartung (Toledano *et al.*, 2012; Liu *et al.*, 2012; Shen *et al.*, 2012).

Verlust der Proteostase

Die Protein-Homöostase, auch als Proteostase bezeichnet, ist ein elementarer Bestandteil der zellulären Homöostase und von großer Bedeutung für die Stressresistenz (Balch *et al.*, 2008). Die Proteostase beinhaltet die Proteinbiogenese, -faltung, -transport und -degradation. Die Aufgabe dieser Prozesse ist die Instandhaltung der Stabilität und der Funktionalität der

Proteine einer Zelle (Powers *et al.*, 2009). Die Proteostase spielt eine essentielle Rolle beim Alterungsprozess und verändert sich mit zunehmendem Alter (Zhang und Cuervo, 2008). Hierbei sind zwei Mechanismen von elementarer Bedeutung: die Chaperon-vermittelte Proteinfaltung und das proteolytische System (Koga *et al.*, 2011). Chaperone sind in der Faltung von Proteinen und in der Antwort auf zellulären Stress involviert (Ellis und van der Vies, 1991). Die Stress-induzierte Synthese von Chaperonen ist mit zunehmendem Alter signifikant beeinträchtigt (Calderwood *et al.*, 2009). Des Weiteren konnte gezeigt werden, dass die Abnahme von Chaperonen zu einer beschleunigten Alterung (Min *et al.*, 2008) und die Zunahme zu einer erhöhten Lebenserwartung führen (Swindell *et al.*, 2009). Es wird postuliert, dass der altersabhängige Verlust von Chaperonen zur vermehrten Aggregation fehlgefalteter Proteine führt, welches in proteotoxischen Schädigungen resultiert (Lopez-Otin *et al.*, 2013). Der andere altersassoziierte Mechanismus betrifft das proteolytische System, welches an der Beseitigung fehlgefalteter und funktionsloser Proteine beteiligt ist (Koga *et al.*, 2011). Es gibt Hinweise darauf, dass die Funktionalität des proteolytischen Systems negativ mit dem Alter korreliert, was in der Akkumulation geschädigter Proteine resultiert (Rubinsztein *et al.*, 2011; Tomaru *et al.*, 2012). Die induzierte Zunahme der proteasomalen Aktivität führt zum Abbau von toxischen Proteinen (Lee *et al.*, 2010) und zu einer Erhöhung der replikativen Lebensspanne (Kruegel *et al.*, 2011).

Dysregulation von Nährstoffsignalwegen

Seit langem ist bekannt, dass die Restriktion von Nährstoffen, auch Kalorienrestriktion genannt, mit der durchschnittlichen und auch maximalen Lebenserwartung assoziiert ist (Weindruch *et al.*, 1986). In vielen eukaryotischen Spezies, auch in Primaten, führt die Kalorienrestriktion zu einer Verlängerung der Lebenserwartung (Fontana *et al.*, 2010; Mattison *et al.*, 2012). Dies lässt vermuten, dass die Signalwege, die in der Nährstoffaufnahme involviert sind, eine entscheidende Rolle im Alterungsprozess spielen. Es gibt Hinweise darauf, dass der *insulin/insulin-like growth factor 1* (IGF-1)-Signalweg (IIS), der *mammalian target of rapamycin* (mTOR)-Signalweg und der *5'-AMP-activated protein kinase* (AMPK)-Signalweg Einfluss auf die Alterung haben (Houtkooper *et al.*, 2010). So resultieren die Abnahme der Aktivität des IIS, die Inhibition von mTOR sowie die Aktivierung von AMPK in einer erhöhten Lebenserwartung (Fontana *et al.*, 2010; Harrison *et al.*, 2009; Alers, *et al.*, 2012). Es wird postuliert, dass die Regulation dieser Signalwege lebensverlängernde Mechanismen der Zelle sind bei denen das Zellwachstum und der

Metabolismus verringert werden und somit weniger zelluläre Schäden entstehen (Garinis *et al.*, 2008).

Mitochondriale Dysfunktion

Mitochondrien haben verschiedene Funktionen, wie z.B. den Energiestoffwechsel, die Calcium-Homöostase und die Apoptose (Green, 1998; Hajnóczky *et al.*, 2006). Die Dysfunktion der Mitochondrien kann den Alterungsprozess beschleunigen (Vermulst *et al.*, 2008). Es wurde postuliert, dass durch die Schädigung der Mitochondrien bzw. der mitochondrialen DNA (mtDNA) vermehrt ROS gebildet werden, welche wiederum die mtDNA schädigen (Harman, 1972). Die zunehmende Dysfunktion der Mitochondrien durch freie Radikale begünstigt somit die Bildung neuer Radikale und der exponentielle Anstieg der ROS führt zur Seneszenz bzw. Apoptose der Zelle (Mandavilli, 2002). Diese Theorie konnte *in vivo* jedoch nicht verifiziert werden (Zhang *et al.*, 2009; Kalfalah *et al.*, 2014). Gleichwohl führt eine Beeinträchtigung mitochondrialer Funktionen zu einem beschleunigten Altern (Edgar *et al.*, 2009; Hiona *et al.*, 2010). Die Dysfunktion der Mitochondrien mit zunehmendem Alter kann durch diverse Mechanismen induziert werden. Hierzu gehören unter anderem Mutationen in der mtDNA, oxidative Schädigungen mitochondrialer Proteine, Veränderung in der Lipidzusammensetzung der mitochondrialen Membran, defekte in der Mitophagie und Beeinträchtigungen in dem proteolytischen Abbau beschädigter Mitochondrien (Wang und Klionsky, 2011). Die zugrundeliegenden Mechanismen beeinflussen die Stressantwort, den Energiemetabolismus, die Biogenese, die Apoptose und die Kommunikation zwischen den Organellen, und fördern inflammatorische Reaktionen (Green *et al.*, 2011; Raffaello und Rizzuto, 2011).

Zelluläre Seneszenz

Die zelluläre Seneszenz wurde von Hayflick und Moorhead (1961) beschrieben und beruht auf der *in vitro* Replikation von Fibroblasten, die nur eine endliche Zahl von Replikationszyklen durchlaufen können (Hayflick-Limit). Der Zustand der zellulären Seneszenz ist definiert als dauerhafter Zellzyklusarrest in der G₀/G₁-Phase, wobei die Zellen nicht mehr in der Lage sind in die S-Phase einzutreten (Sherwood *et al.*, 1988). Seneszente Zellen sind weiterhin lebensfähig, haben einen aktiven Metabolismus und sind resistent gegenüber Apoptose (zusammengefasst in Campisi und d'Adda di Fagagna, 2007). Die

zelluläre Seneszenz geht zudem mit phänotypischen Veränderungen einher, wobei sich die Morphologie der Zelle verändert (Collado *et al.*, 2007; Kuilman *et al.*, 2010). Des Weiteren bilden seneszente Fibroblasten einen seneszenz-assoziierten sekretorischen Phänotyp (SASP) aus, welcher vermehrt pro-inflammatorische Zytokine und Matrix-Metalloproteinasen (MMPs) sezerniert (Coppe *et al.*, 2010). Es wird zwischen zwei Arten der Seneszenz unterschieden: der replikativen und der stressinduzierten Seneszenz (Toussaint *et al.*, 2000). Die replikative Seneszenz wird durch die Verkürzung der Telomere determiniert (siehe „Telomerverkürzung“) (Harley *et al.*, 1990; Harley *et al.*, 1992), wobei nach Erreichen einer kritischen Länge das Seneszenz-Programm der Zelle aktiviert wird (Martens *et al.*, 2000). Die stressinduzierte Seneszenz wird durch unterschiedliche Stressfaktoren, wie Onkogene, ROS und DNA-Schädigungen, hervorgerufen (Collado *et al.*, 2007). Auch während der *in vivo* Alterung können seneszente Zellen beobachtet werden. So verdoppelt sich die Anzahl seneszenten Zellen in bestimmten Geweben, wie der Leber oder der Haut mit zunehmendem Alter (Wang *et al.*, 2009). Als Hauptursache für die Induktion der altersassoziierten Seneszenz werden Schädigungen der DNA und übermäßig aktive mitogene/onkogene Signalwege postuliert (Collado *et al.*, 2007). Seneszente Zellen können einen negativen Effekt auf benachbarte Zellen und die Gewebemöostase haben (Coppe *et al.*, 2010).

Verbrauch von Stammzellen

Das deutlichste Charakteristikum des Alters ist die Reduktion des regenerativen Potentials von Geweben, welches durch somatische Stammzellen determiniert wird (Barrilleaux *et al.*, 2006; Gimble *et al.*, 2007). Es wird postuliert, dass der Verbrauch von Stammzellen einen wichtigen Aspekt des Alterns darstellt (Edelberg und Ballard, 2008). So nimmt beispielweise die Hämatopoese, die Blutbildung aus Stammzellen, mit zunehmendem Alter ab, was zu einer reduzierten Produktion von adaptiven Immunzellen und somit zur Immunoseneszenz führt (Shaw *et al.*, 2010). Des Weiteren wird davon ausgegangen, dass auch die Schädigung von Stammzellen von großer Bedeutung für den Alterungsprozess ist und deren Verjüngung das Altern verlangsamen kann (Rando und Chang, 2012). Ein weiterer Aspekt von Stammzellen im Alterungsprozess ist die Fähigkeit der Stimulation benachbarter Zellen (Conboy und Rando, 2012). Es wurde gezeigt, dass durch die Transplantation von jungen Stammzellen die Lebenserwartung gesteigert und die Degeneration von Gewebe verlangsamt wird (Lavasani *et al.*, 2012). Die positiven Effekte konnten auch in Geweben beobachtet werden, in denen keine

Stammzellen gefunden wurden. Daher wird angenommen, dass Stammzellen durch sezernierte Faktoren Einfluss auf das umliegende Gewebe nehmen (Lavasani *et al.*, 2012).

Veränderte interzelluläre Kommunikation

Die Kommunikation zwischen Zellen ist für viele physiologische Prozesse von elementarer Bedeutung. Sie wird durch verschiedene Moleküle, wie Zytokine und Wachstumsfaktoren, vermittelt. Es gibt Hinweise darauf, dass sich die endokrine und die neuroendokrine interzelluläre Kommunikation mit dem Alter verändert (Rando und Chang, 2012; Zhang *et al.*, 2013). Neurohormonale Signalwege, wie z.B. der IIS, nehmen mit zunehmendem Alter ab und Zytokin-vermittelte inflammatorische Reaktionen nehmen zu (Coppe *et al.*, 2010). Die prominenteste altersassoziierte Veränderung der interzellulären Kommunikation ist als Entzündungsaltern bekannt (Salminen *et al.*, 2012). Hierbei handelt es sich um einen pro-inflammatorischen Phänotyp, welcher während der Alterung auftritt. Es gibt diverse Gründe für das Entzündungsaltern, wie beispielweise die Akkumulation von inflammatorischen Gewebeschäden, ein dysfunktionales Immunsystem, pro-inflammatorische seneszente Zellen, die erhöhte Aktivierung des NF- κ B-Signalwegs oder die abnehmende Fähigkeit der Autophagie (Salminen *et al.*, 2012). Diese Veränderungen führen zu einer Aktivierung des *NOD-like receptor family, pyrin domain containing 3* (NLRP3)-Inflammasoms und anderen pro-inflammatorischen Signalwegen. Dies resultiert in der erhöhten Produktion von Interferonen, Interleukinen und Tumornekrosefaktoren (Green *et al.*, 2011; Salminen *et al.*, 2012). Das Entzündungsaltern ist zudem in die Immunoseneszenz involviert, fungiert als Inhibitor epidermaler Stammzellen (Doles *et al.*, 2012) und gilt als Induktor altersassoziiierter Krankheiten (Barzilai *et al.*, 2012; Deeks, 2011). Die Reduktion der Regenerationsfähigkeit des Gewebes und der immunologischen Funktionen durch eine erhöhte Inflammation könnte dazu führen, dass seneszente, pro-inflammatorische Zellen nicht mehr abgebaut werden und akkumulieren, und so das Gewebe kontinuierlich geschädigt wird (Senovilla *et al.*, 2012).

1.2 Die Haut als Modellsystem des Alterns

1.2.1 Aufbau und Funktion der Haut

Die Haut ist das größte und funktionell vielseitigste Organ. Sie ist die Abgrenzung des Organismus gegenüber der Außenwelt und schützt als Barriere vor physikalischen, chemischen und biologischen Einflüssen. Des Weiteren dient die Haut als Regulator des Wasser-, Temperatur- und Elektrolythaushalts sowie der Immunabwehr (Fritsch, 2009). Die humane Haut setzt sich aus drei Schichten zusammen: der Epidermis, der Dermis und der Subkutis (Abb. 2).

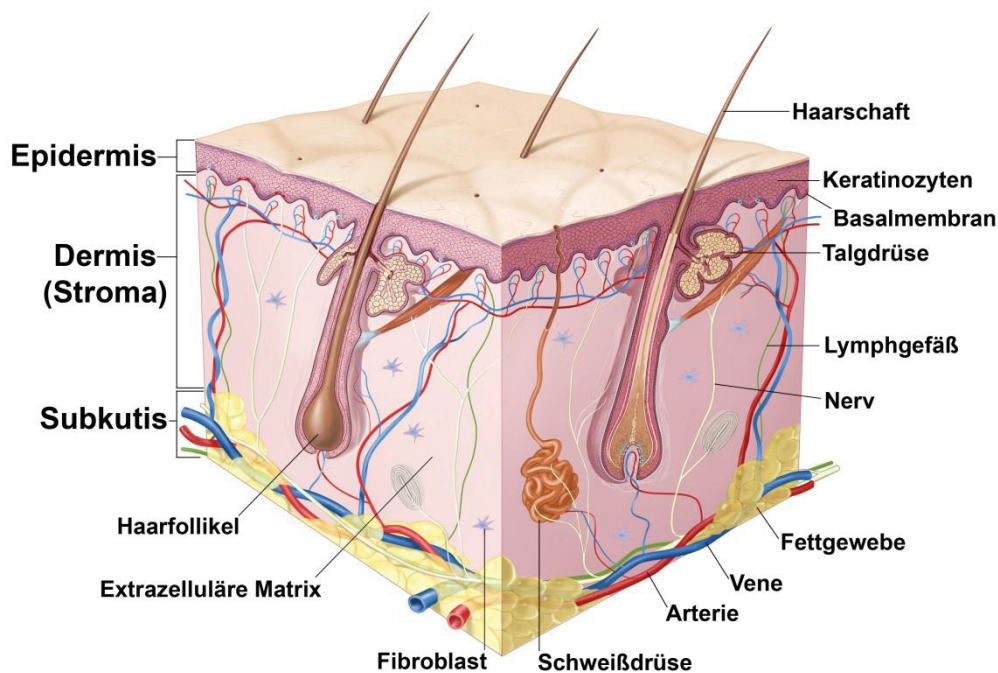


Abbildung 2: Schematischer Aufbau humaner Haut (modifiziert nach Terese Winslow, 2008).

Die Haut setzt sich aus drei Schichten zusammen: der Epidermis, der Dermis und der Subkutis. Die Epidermis besteht hauptsächlich aus Keratinozyten und ist durch die Basalmembran von der Dermis abgetrennt. Die Dermis besteht größtenteils aus Fibroblasten und der extrazellulären Matrix. Zudem befinden sich in dieser Talg- und Schweißdrüsen, Lymphgefäße, Nerven und Haarfollikel. Die Subkutis besteht aus lockerem Binde- und Fettgewebe. In dieser befinden sich vor allem größere Blutgefäße und Nerven.

Die äußerste Hautschicht ist die Epidermis. Sie gehört zu den Epithelgeweben und besteht aus einem mehrschichtigen, verhornenden Plattenepithel, das hauptsächlich aus Keratinozyten besteht (McGrath *et al.*, 2004). Die zweite Hautschicht ist die Dermis, das Stroma der Haut.

Sie stellt das kollagenfaserreiche, fibroelastische Bindegewebe unterhalb der Epidermis und oberhalb der Subkutis dar. In der Dermis befinden sich im Gegensatz zur Epidermis Blutgefäße, Nerven und Drüsen. Der Hauptzelltyp der Dermis ist der Fibroblast, welcher für die Stabilität und Integrität der Dermis zuständig ist (McGrath *et al.*, 2004). Weitere in der Dermis vorkommende Zelltypen sind Mastzellen, die für die hypersensitiven Reaktionen der Haut verantwortlich sind und Makrophagen, die als immunologisch aktive Zellen anfallende Abbauprodukte und abgestorbene Zellen phagozytieren und durch die Speicherung von Antigenen und Produktion von Interferon an der Immunantwort der Haut beteiligt sind (Jung, 1998; Chu *et al.*, 2003). Ein weiterer wichtiger Bestandteil der Dermis ist die extrazelluläre Matrix (*extracellular matrix*, ECM). Die ECM besteht aus einem Gemisch diverser Komponenten, die von Fibroblasten synthetisiert und abgebaut werden. Zu den synthetisierten Faktoren gehören Strukturproteine wie Laminin, Fibronectin, Elastin und Kollagen sowie Proteoglykane und Glukosaminglykane, als auch spezifische MMPs, die in der Degradation und Modifikation von Kollagenen und somit im Um- und Abbau der ECM involviert sind (Fritsch, 2009). Der andauernde Abbau und die Erneuerung der ECM stellen einen wichtigen Aspekt der Gewebemöostase dar und sind von großer Bedeutung für die Integrität und Stabilität von Organen (Cox und Erler, 2011). Die unterste Hautschicht ist die Subkutis. Diese besteht hauptsächlich aus lockerem Binde- und Fettgewebe. In der Subkutis befinden sich vor allem größere Blutgefäße und Nerven, die für die Versorgung der darüber liegenden Hautschichten verantwortlich sind. Zudem dient das in der Subkutis enthaltene Fettgewebe als Isolator und Energiespeicher.

1.2.2 Die Alterung der Haut

Die Alterung der Haut wird durch intrinsische und extrinsische Faktoren beeinflusst. Die intrinsische Hautalterung wird hauptsächlich durch eine genetische Prädisposition (Yaar und Gilchrist, 2001) und den Hormonstatus determiniert (Phillips *et al.*, 2001). Die extrinsische Hautalterung hingegen wird durch äußere Faktoren, wie z.B. der UV-Strahlung (Schroeder *et al.*, 2006; Krutmann, 2012), bestimmt. Beide Formen der Hautalterung führen zu einem Verlust der Elastizität des Gewebes und zur Bildung von Falten, wobei diese bei der extrinsischen Alterung früher einsetzen und deutlich stärker ausgeprägt sind (Escoffier *et al.*, 1989; Warren *et al.*, 1991). Des Weiteren treten bei beiden Formen der Hautalterung phänotypische Veränderungen der Hautzellen und der ECM auf (Abb. 3) (Naylor *et al.*, 2011).

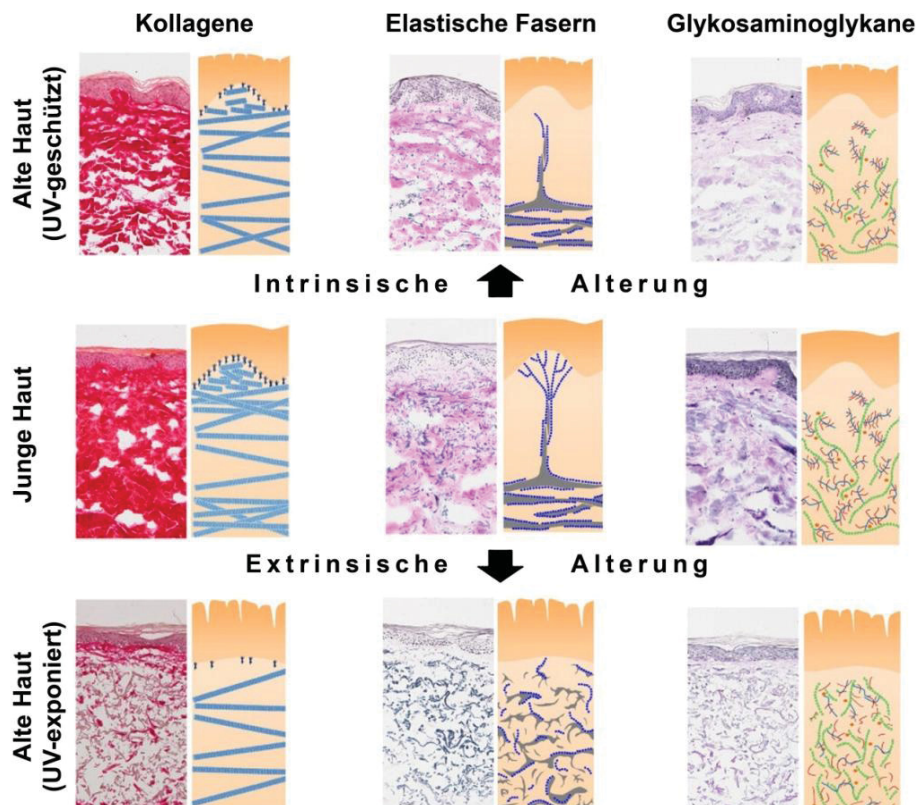


Abbildung 3: Veränderungen der extrazellulären Matrix intrinsisch (UV-geschützt) und extrinsisch (UV-exponiert) gealterter Haut (modifiziert nach Naylor *et al.*, 2011). Junge Haut: 23 Jahre, oberer Innenarm; alte Haut (UV-geschützt): 75 Jahre, unterer Rücken; alte Haut (UV-exponiert): 75 Jahre, Unterarm. Dermale Kollagene, elastische Fasern und Glykosaminoglykane weisen eine signifikante Veränderung sowohl während der intrinsischen als auch der extrinsischen Alterung auf. Des Weiteren unterscheiden sich die Veränderungen zwischen den beiden Alterungsformen in Art und Ausprägung.

In intrinsisch gealterter Haut gibt es Hinweise auf die Degradation der Kollagene I, III, IV und Elastin sowie den Abbau von Glykoproteinen und Proteoglykanen, die essentiell für die Gewebekompetenz sind (El-Domyati *et al.*, 2002; Naylor *et al.*, 2011). Ein Charakteristikum extrinsisch gealterter Haut, mit UV-Strahlung als häufigste exogene Noxe (Gilchrest, 1989), ist die Elastose (Krutmann, 2003). Dabei ist ein Verlust der fibrillären Kollagene I und III in der Dermis und von Kollagen VII-Ankerfibrillen zu beobachten (El-Domyati *et al.*, 2002; Craven *et al.*, 1997; Talwar *et al.*, 1995). Zudem kommt es zum Verlust von Fibrillin-1 (Watson *et al.*, 1999) und -5 (Kadoya *et al.*, 2005), was zu einer Destabilisierung des elastischen Fasernetzwerks führt. Diese Hinweise lassen darauf schließen, dass die zugrundeliegenden Mechanismen der intrinsischen und extrinsischen Hautalterung sich in Teilbereichen unterscheiden.

Die Haut stellt ein ideales Modellsystem für die Untersuchung intrinsischer Alterungsprozesse dar, da das komplette Organ der intrinsischen Alterung unterliegt, wohingegen nur umwelt-exponierte Areale extrinsisch altern. Ein Merkmal der intrinsischen Hautalterung ist die Verdünnung der Epidermis, die mit einer Abnahme der Barrierefunktion und der Wundheilung einhergeht (zusammengefasst in Tigges *et al.*, 2014). Die Verdünnung von Geweben beruht zumeist auf der Dysfunktion von Stamm- und Vorläuferzellen. Hingegen konnte bei der Haut gezeigt werden, dass epidermale Stammzellen mit zunehmendem Alter ihre Funktion behalten (Stern und Bickenbach, 2007). Es gibt zudem Hinweise darauf, dass die Instandhaltung eines Gewebes nicht durch die Funktionalität der Stammzellpopulation limitiert wird (Rando, 2006; Blagosklonny, 2008). Hingegen konnte beobachtet werden, dass gealterte Stammzellen durch ein junges Milieu verjüngt werden (Conboy *et al.*, 2005). Infolgedessen wurde postuliert, dass das intrinsische Altern der Haut durch die Dermis und nicht durch Stammzellen determiniert wird (Boukamp, 2005; Parrinello *et al.*, 2005).

Die Dermis ist ein statisches Gewebekompartiment und dysfunktionale Zelle können nicht unmittelbar beseitigt werden, weshalb die Gewebemöostase hauptsächlich auf der zellulären Anpassung und der Beseitigung von Schäden basiert. Der Hauptzelltyp der Dermis ist der Fibroblast (McGrath *et al.*, 2004), eine langlebige Zelle mit einer geringen Proliferationsrate meist in einem Zustand des reversiblen Zellzyklusarrests, welcher auch als Quieszenz bezeichnet wird (Burton, 2009). Aus diesem Grund müssen zelluläre Funktionen angepasst werden und altersassoziierte Veränderungen können akkumulieren. Daher wird angenommen, dass die treibende Kraft für das intrinsische Altern der Haut bzw. eines Organs das statische Stroma und die Wechselwirkung von Fibroblasten mit der ECM ist (Boukamp, 2005). Hinweise für die Relevanz von Fibroblasten in Alterungsprozessen bzw. in altersabhängigen Veränderungen des Gewebes können auch in anderen Organen gefunden werden. So sind seneszente Fibroblasten im Eierstock eng mit der Initiation und Progression von Ovarialkarzinomen assoziiert (Yang *et al.*, 2006). Im Epithelium der Brust sezernieren Fibroblasten Faktoren, die die Homöostase des Gewebes mit zunehmendem Alter verändern (Parrinello *et al.*, 2005). Aufgrund der Langlebigkeit, der altersabhängigen Akkumulation von zellulären Schäden und der Bedeutung für die Alterung von Organen sind Fibroblasten ein häufig verwendetes Modellsystem zur Untersuchung der Mechanismen des Alterungsprozesses.

1.2.3 Mechanismen der stromalen Alterung

Fibroblasten sind ein akzeptiertes zelluläres Alterungsmodell (de Magalhaes, 2004). Bereits Hayflick und Moorhead (1961) haben für die Untersuchung altersassoziierter Mechanismen Fibroblasten verwendet. Hierbei muss zwischen zwei Modellen unterschieden werden: der *in vitro* und der *ex vivo* Alterung (Boraldi *et al.*, 2010). Bei *in vitro* Alterungsmodellen werden primäre Fibroblasten durch Replikation oder Stressinduktion, z.B. durch UV-Bestrahlung, in die Seneszenz geführt (Collado *et al.*, 2007). Die dadurch hervorgerufenen Veränderungen werden als Repräsentativ für den Alterungsprozess angesehen. Allerdings ist die Seneszenz lediglich ein Teilaspekt des Alterns und daher besteht die Möglichkeit, dass die Ergebnisse aus induzierten Modellen nicht mit den tatsächlichen *in vivo* Alterungsprozessen übereinstimmen (Mondello *et al.*, 1999). Bei *ex vivo* Alterungsmodellen hingegen werden primäre Fibroblasten direkt aus dem Hautgewebe gealterter Individuen isoliert, eine definierte Zeit kultiviert und noch im teilungsfähigen Zustand analysiert. Diese Vorgehensweise hat den Vorteil, dass nicht die Effekte der Seneszenz, sondern altersassozierte Prozesse untersucht werden (Boraldi *et al.*, 2010). Eine Vielzahl von *in vitro* und *ex vivo* Alterungsmodellen unter der Verwendung dermalen Fibroblasten wurden bereits untersucht. Die darin identifizierten biologischen Prozesse stimmen partiell mit den allgemeinen zellulären und molekularen Charakteristika des Alterns überein. Die altersassozierten Veränderungen in Fibroblasten finden auf Ebene des Genoms, der Transkription, der Mitochondrien, der Proteostase, des Zytoskeletts und der interzelluläre Kommunikation statt. Gleichwohl gibt es immer noch große Lücken im Verständnis der Alterungsprozesse von Fibroblasten innerhalb ihrer physiologischen Gewebeumgebung.

DNA-Schäden und -Reparatur

Die Instandhaltung des Genoms ist elementar für die Stabilität und Integrität des Genoms, und wird durch DNA-Reparaturmechanismen gewährleistet. Dazu gehören unter anderem die Nukleotidexzisions-Reparatur (NER) und die Doppelstrangbruch-(DSB)-Reparatur. Die NER ist für die Beseitigung von Addukten und *intra-crosslinks*, welche durch UV-Strahlung erzeugt werden können, zuständig. In gealterten Fibroblasten kann eine Reduktion der NER-Aktivität mit zunehmendem Alter beobachtet werden, wobei die Fähigkeit fehlerhafte Nukleotide zu entfernen unverändert bleibt (Takahashi *et al.*, 2005). Daher wird angenommen, dass nur Komponenten betroffen sind, die nach dem Herausschneiden der

Nukleotide agieren. Die DSB-Reparatur hingegen besteht aus zwei komplementären Mechanismen, der homologen Rekombination und dem *non-homologous endjoining* (NHEJ) und ist für die Reparatur von Doppelstrangbrüchen zuständig (Martínez und Blasco, 2010). In replikativ seneszenten Fibroblasten konnte eine geringere Effizienz und Präzision des NHEJ beobachtet werden, aber keine Veränderung auf Ebene der Expression (Seluanov *et al.*, 2004). Eine mögliche Erklärung dafür ist die Zunahme von irreparablen Doppelstrangbrüchen (Fumagalli *et al.*, 2012). Hinweise darauf liefert die Akkumulation von phosphorylierten Histon H2AX (γ H2AX)-Foci in stress-induzierten Fibroblasten, welche DSB-Reparaturkomplexe beinhalten und nicht an den Telomeren lokalisiert sind. γ H2AX ist ein Marker für DNA-Doppelstrangbrüche sowie der genomischen Instabilität (Valdiglesias *et al.*, 2013). Somit kann der Anstieg von γ H2AX-Foci als repräsentativ für die Zunahme von DSB und Chromosomenaberrationen mit zunehmendem Alter gesehen werden (Sedelnikova *et al.*, 2004). Allerdings kann die Zunahme von γ H2AX-Foci auch ein Hinweis auf den Anstieg von DNA-Segmenten mit Chromatinveränderungen (*DNA segments with chromatin alterations reinforcing senescence*), den sogenannten DNA-SCARS sein, welche mit der Seneszenz assoziiert sind (Rodier *et al.*, 2011). Die DNA-SCARS sind permanente DNA-Schadens-Foci die sich unabhängig von p53, pRB oder anderen Zellzykluskontrollproteinen bilden, in Verbindung mit *PML nuclear bodies* auftreten und keine DNA-Reparaturproteine und einzelsträngige DNA aufweisen. Dies bedeutet, dass die DNA-SCARS eine aktive DNA-Schadens-Antwort signalisieren, jedoch keine DNA-Reparatur vermitteln. Es wird angenommen, dass die DNA-SCARS Einfluss auf mehrere Aspekte des seneszenten Phänotyps nehmen. Dazu gehören der permanente Zellzyklusarrest und die Ausbildung des SASP (Rodier *et al.*, 2011). In Fibroblasten wurden DNA-SCARS bisher nur in induzierten Alterungsmodellen nachgewiesen.

Telomerverkürzung

Die Verkürzung der Telomere wurde bisher ausschließlich in induzierten Alterungsmodellen nachgewiesen. Da der Fibroblast eine quieszente Zelle ist wird postuliert, dass die Telomerverkürzung keine Relevanz für die *in vivo* Alterung in der Haut hat (Tigges *et al.*, 2014). Es gibt jedoch Hinweise darauf, dass DNA-Schadens-Foci in dermalen Zellen mit zunehmendem Alter ansteigen und mit Telomeren kolokalisieren (Herbig *et al.*, 2006). Somit besteht die Möglichkeit, dass die Schädigungen der DNA an den Telomeren in der Induktion

der Seneszenz und Apoptose resultieren und deshalb die Regenerationsfähigkeit des Gewebes mit zunehmendem Alter abnimmt (Fumagalli *et al.*, 2012; Martinez und Blasco, 2010).

Epigenetik

Während der Hautalterung kommt es zu Veränderungen im Methylierungsmuster der DNA epidermaler und stromaler Zellen. In *in situ* gealterten dermalen Fibroblasten wurden 75 Loci identifiziert, die mit zunehmendem Alter hyper- oder hypomethyliert werden (Koch *et al.*, 2011). So liegt der *cyclin-dependent kinase 4 inhibitor B* (CDKN2B), ein Regulator des Zellzyklus, im Alter hypermethyliert vor, was Auswirkungen auf die Regeneration der Haut und die Karzinogenese haben kann (Zhang *et al.*, 2012). Das altersassoziierte Methylierungsmuster einer Zelle oder eines Gewebes ist sehr spezifisch und kann als Marker für das Alter verwendet werden (Horvath, 2013). Allerdings ist bisher unbewiesen, ob die epigenetischen Veränderungen lediglich eine Begleiterscheinung des Alterns sind oder einen Mechanismus der stromalen Alterung repräsentieren.

Mitochondrien

Ein Aspekt der mitochondrialen Veränderung im Alterungsprozess ist die mitochondriale Masse (Mitomasse). In induzierten Alterungsmodellen dermalen Fibroblasten konnte gezeigt werden, dass die Mitomasse während der replikativen Seneszenz zunimmt (Lee *et al.*, 2002). Es wird postuliert, dass der Anstieg der Mitomasse eine retrograde mito-biogene Stressantwort auf eine erhöhte ROS-Produktion oder permanenter DNA-Schäden dysfunktionaler Mitochondrien, welche aufgrund einer geminderten Autophagie nicht abgebaut werden können, ist (Yen und Klionsky, 2008; Finley und Haigis, 2009). Kalfalah *et al.* (2014) konnten jedoch zeigen, dass die Mitomasse in *in vivo* gealterten dermalen Fibroblasten signifikant abnimmt. Es wird angenommen, dass die retrograden mito-biogenen Signalwege mit zunehmendem Alter gestört sind, was in einer Reduktion der Mitomasse resultiert und dramatische Folgen für den Energiemetabolismus der Zelle und deren Funktion hat. Eine weitere Veränderung der Mitochondrien während der Alterung betrifft die Atmungskette. Dabei wird mittels oxidativer Phosphorylierung Adenosintriphosphat (ATP) gebildet, welches der Hauptenergiespeicher der Zelle ist. Greco *et al.* (2003) konnten in *in vivo* gealterten Fibroblasten zeigen, dass die oxidative Phosphorylierung mit dem Alter abnimmt und somit die ATP-Produktion ineffizient wird. Zudem wurde in gealterten

Individuen eine signifikante Reduktion des mitochondrialen Membranpotentials beobachtet (Greco *et al.*, 2003). Diese Befunde deuten auf eine Reduktion der Energiegewinnung und einen gestörten Energiemetabolismus mit zunehmendem Alter hin.

Proteolytisches System

Während der Hautalterung kommt es zur Akkumulation von oxidierten, funktionslosen Proteinen, welche durch das Proteasom abgebaut (Bulteau *et al.*, 2007) oder durch Autophagie entfernt (Cuervo *et al.*, 2005) werden müssen. Es gibt keine Hinweise darauf, dass die Autophagie während der Hautalterung beeinträchtigt ist. Jedoch konnte gezeigt werden, dass die Funktion des Proteasoms mit zunehmendem Alter und durch UV-Strahlung abnimmt (Bulteau *et al.*, 2007). Es wird vermutet, dass die Reduktion der proteasomalen Funktion durch eine geminderte Expression proteasomaler Untereinheiten oder der Akkumulation von endogenen Inhibitoren verursacht wird. Dies hat zur Folge, dass die Zellatmung abnimmt (Kozziel *et al.*, 2011) und Matrix-Metalloproteinasen induziert werden, was zur Degradation der ECM und einer gestörten Gewebemöostase führt (Catalgol *et al.*, 2009).

Transkription

Transkriptionelle Veränderungen in Fibroblasten während der Alterung betreffen sowohl die kodierende mRNA als auch die nicht-kodierende, regulatorische miRNA (miR). Auf Ebene der mRNA konnten in Fibroblasten gealterter Individuen 105 Gene mit einer altersassoziierten Expression gefunden werden (Lener *et al.*, 2006). Die involvierten biologischen Prozesse beinhalten die Zellzykluskontrolle, inflammatorische Reaktionen und den Metabolismus. In einer weiteren Studie *in situ* gealterter Fibroblasten konnten 138 altersassoziierte Gene identifiziert werden (Kalfalah *et al.*, 2014). Hierbei wurden die folgenden Prozesse als negativ mit dem Alter korrelierend gefunden: der mitochondriale Metabolismus, die Elektronentransportkette, die Instandhaltung der ECM, der Zellzyklus und der Proteintransport. Hingegen wurden der Cholesterinmetabolismus, Immunreaktionen und die mRNA-Prozessierung als im Alter ansteigend beobachtet (Kalfalah *et al.*, 2014). Auf Ebene der regulatorischen Transkripte sind mehrere miRNAs bekannt, die eine Rolle in der Entwicklung der Haut und der Gewebemöostase spielen. So ist beispielweise die miR-203 essentiell für epidermale Morphogenese (Sand *et al.*, 2009). In Experimenten mit stress-

induzierten, seneszenten Fibroblasten konnte die Überexpression der miR-101 beobachtet werden (Greussing *et al.*, 2013). Ein spezifisches Ziel der miR-101 ist die *histone-lysine N-methyltransferase EZH2* (EZH2) (Suvà *et al.*, 2009), welche in Verbindung mit der Tumorpromotion steht (Crea *et al.*, 2011). Die Überexpression der miR-101 führt zur Inhibition der mRNA-Expression von EZH2 und somit zur Seneszenz der Zelle (Greussing *et al.*, 2013). In replikativ seneszenten Fibroblasten hingegen konnten die miR-152 und die miR-181a als überexprimiert identifiziert werden (Mancini *et al.*, 2012). Als spezifische Ziele dieser miRNAs wurden *integrin alpha-5* (ITGA5) und *collagen alpha-1(XVI) chain* (COL16A1) identifiziert. Mancini *et al.* (2012) postulieren, dass diese miRNAs wichtige Akteure der Zelladhäsion und des Umbaus der ECM während des Alterns sind. Es gibt jedoch keine Hinweise darauf, dass diese miRNAs in die *in vivo* Alterung involviert sind.

Proteom und Zytoskelett

Die altersabhängige Veränderung des Proteoms ist sowohl für die induzierte Seneszenz als auch für die *in vivo* Alterung beschrieben. In einer Studie *in situ* gealterter Fibroblasten konnten 38 altersabhängig veränderte Proteine identifiziert werden, die in den Metabolismus, den Zellzyklus, die Proteindegradation und zelluläre Abwehrmechanismen involviert sind (Boraldi *et al.*, 2003). Ein weiteres Charakteristikum ist die Veränderung des Zytoskeletts. Diese resultieren in einem Anstieg des Zellvolumens und der Zelloberfläche sowie in Veränderungen der Morphologie (Hwang *et al.*, 2009). Replikativ seneszente Fibroblasten sind große und flache Zellen, die einen erhöhten Anteil an Mikrotubuli und Intermediärfilamenten aufweisen (Wang und Gundersen, 1984). Besonders auffällig ist der Anstieg von Vimentin bei der *in vitro* Alterung (Nishio und Inoue, 2005). Allerdings gibt es bisher keine Hinweise darauf, dass sich Vimentin auch während der *in vivo* Alterung verändert. Neben den Veränderungen der Morphologie steigt auch die Steifheit der Fibroblasten mit zunehmendem Alter an. Es wird postuliert, dass der Anstieg der Steifheit durch Aktin determiniert wird (Schulze *et al.*, 2010). So kommt es zu einer Veränderung des Verhältnisses von filamentösen F-Aktin zu globulären G-Aktin. Dabei steigt die Konzentration von F-Aktin an und die von G-Aktin nimmt ab, wobei die Gesamtmenge an Aktin unverändert bleibt (Sprenger *et al.*, 2010). Dies resultiert in der Zunahme der Steifheit und der Abnahme der Mobilität.

Interzelluläre Kommunikation

Die interzelluläre Kommunikation und die Instandhaltung der ECM sind elementare Aufgaben des Fibroblasten. Während der replikativen und stress-induzierten Seneszenz kommt es zur Ausbildung eines, sekretorischen Phänotyps, dem sogenannten SASP (zusammengefasst in Coppe *et al.*, 2010). Dieser zeichnet sich durch die erhöhte Sekretion pro-inflammatorischer Proteine, wie Interleukine (IL1, IL6 und IL8), ECM-Degradationsproteinen, wie Matrix-Metalloproteinasen (MMP1 und MMP3), und Wachstumsfaktoren, wie *vascular endothelial growth factor* (VEGF) und *transforming growth factor beta* (TGF- β) aus (Abb. 4). Coppe *et al.* (2010) postulieren, dass der SASP eine negative Wirkung auf benachbarte Zellen und das Gewebe hat. So kann die erhöhte Sekretion pro-inflammatorische Zytokine und MMPs mit zunehmendem Alter zu einem Anstieg von Entzündungsreaktionen und zum Verlust der Gewebeelastizität führen. Des Weiteren könnte der SASP die Karzinogenese stimulieren und die Gewebekomöostase stören. Da seneszente Fibroblasten mit dem Alter in der Haut akkumulieren (Wang *et al.*, 2009), könnte der SASP eine Rolle in der *in vivo* Alterung spielen. Allerdings gibt es bisher keine detaillierte Untersuchung des Sekretoms *in situ* gealterter Fibroblasten.

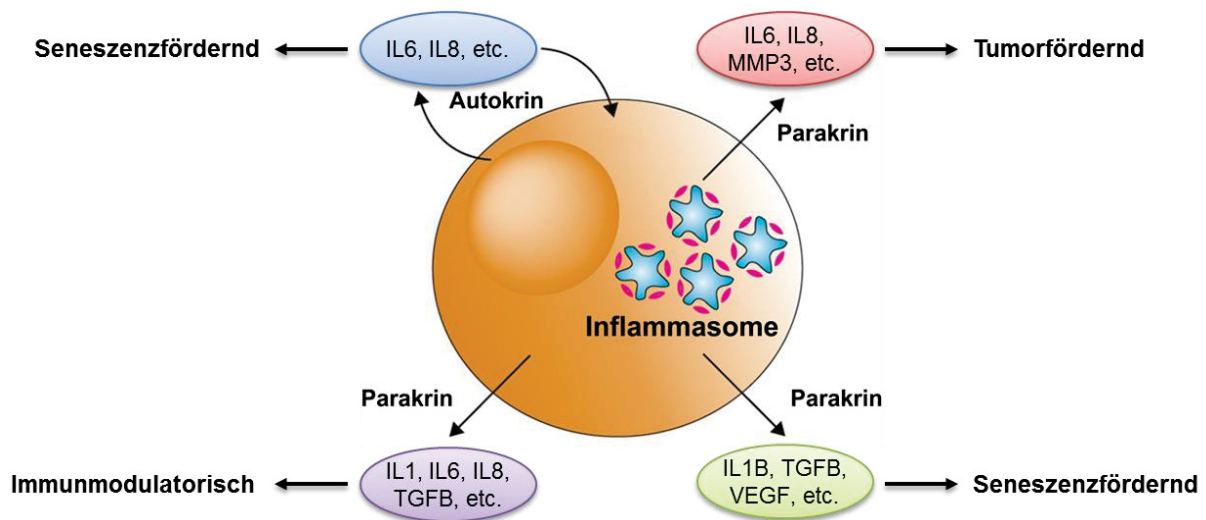


Abbildung 4: Auswahl sezernierter Proteine des SASP und dessen autokrine und parakrine Wirkung (modifiziert nach Hoare und Narita, 2013). Das Inflammasom ist der zentrale Regulator des SASP. Dieser kann die Seneszenz in einem autokrinen Mechanismus verstärken und wirkt zudem seneszenzfördernd auf das umliegende Gewebe. Des Weiteren wirkt der SASP bei prämaligen Epithelzellen tumorfördernd und reguliert den immunologischen Abbau seneszenter Zellen.

1.3 Die Proteomanalyse

Nahezu alle Prozesse, die in den Zellen lebender Organismen ablaufen, beruhen auf der Wirkung von Proteinen. Es wird davon ausgegangen, dass etwa 10.000 - 20.000 verschiedene Proteinspezies gleichzeitig zu einem definierten Zeitpunkt in einer Eukaryotenzelle präsent sind, wobei ein Abundanzbereich von mindestens sieben Größenordnungen abgedeckt wird (Zuo *et al.*, 2001; Beck *et al.*, 2011). Die Gesamtheit aller Proteine, die zu einem bestimmten Zeitpunkt eines definierten Zustands in einem Organismus, einem Gewebe oder einer Zelle von dessen Genom exprimiert werden, werden analog zum Genom als Proteom bezeichnet (Wilkins *et al.*, 1996). Im Gegensatz zum Genom, der Gesamtheit aller Gene, mit seiner zeitlich konstanten und exakt definierbaren DNA-Sequenz, ist das Proteom dynamisch und wird von einer Vielzahl endo- und exogener Faktoren, wie Zellstress oder Temperatur, beeinflusst. Hierdurch kann sich sowohl die Zusammensetzung des Proteoms, als auch die Abundanz der Proteine verändern (Anderson und Anderson, 1996). Zudem können Proteine, je nach Stimulus, posttranslational modifiziert werden und somit in verschiedenen Isoformen vorliegen (Graves und Haystead, 2002; Rotilio *et al.*, 2012). Posttranslationale Modifikationen (PTM) sind Proteinveränderungen, die nach der Proteinsynthese stattfinden und die Funktion eines Proteins verändern können (zusammengefasst in Karve und Cheema, 2011). Brett *et al.* (2002) haben postuliert, dass für jedes humane Gen durchschnittlich drei unterschiedlich modifizierte Proteinspezies mit einer verschiedenartigen Funktion existieren. Die Proteomik beinhaltet die Erforschung des Proteoms von Zellen, Geweben oder Organismen und ist ein Teilaspekt der Systembiologie, die die Bereiche der Genomik, der Transkriptomik, der Proteomik, der Interaktomik und der Metabolomik abdeckt. Die Proteomik befasst sich zum einen mit der Identifizierung und Quantifizierung von Proteinen komplexer biologischer Systeme (Jungblut *et al.*, 1999), wobei auch PTMs analysiert werden (Lottspeich, 2009). Zum anderen widmet sich die Proteomik der Aufklärung von Proteinstrukturen (Konermann *et al.*, 2011) und Protein-Protein-Interaktionen (Stumpf *et al.*, 2008) zur Kartierung komplexer zellulärer Netzwerke. Die Analyse des Proteoms stellt eine wichtige Ergänzung zur Genomanalyse dar, da bei dieser auch Informationen über Proteinisoformen erhalten werden können, die durch alternatives Spleißen der prä-mRNA erzeugt werden (Stastna und Van Eyk, 2012). Zudem kann die Quantifizierung von Proteinen eukaryotischer Zellen aufgrund einer geringen Korrelation zwischen Genexpression und Proteinabundanz erst auf Basis der Proteine stattfinden (Gygi *et al.*, 1999; Gry *et al.*, 2009; Schwanhäusser *et al.*, 2011).

1.3.1 Methoden der qualitativen und quantitativen Proteomanalyse

Für die qualitative und quantitative Analyse des Proteoms einer Zelle, eines Gewebes oder eines Organismus stehen drei häufig verwendete methodische Ansätze zur Verfügung: die gelbasierte ein- oder zweidimensionale Polyacrylamidgelelektrophorese (1D/2D-PAGE) in Kombination mit der Massenspektrometrie, die Protein-Microarray-Analyse und der Flüssigchromatographie- und Massenspektrometrie-basierte Ansatz (*liquid chromatography and mass spectrometry*, LC-MS).

Beim gelbasierten Ansatz werden Proteingemische mittels *sodium dodecyl sulfate* (SDS)-PAGE aufgetrennt und zur Identifizierung der Proteine massenspektrometrisch analysiert (Roepstorff, 2012). Aufgrund der hohen Komplexität des eukaryotischen Proteoms wird der SDS-PAGE zur besseren Trennung der Proteine eine isoelektrische Fokussierung (IEF) vorgeschaltet (Marcus *et al.*, 2009). Diese Art der 2D-PAGE besitzt ein Auflösungsvermögen von bis zu 10.000 Proteinspezies, wobei auch die Auftrennung von Proteinisoformen möglich ist (Klose *et al.*, 1995; O’Farrell *et al.*, 1975). Eine differentielle Analyse von Proteinen unterschiedlicher Proben mittels 2D-PAGE kann beispielweise unter Verwendung proteinbindender Fluoreszenzfarbstoffe realisiert werden (*difference gel electrophoresis*, DIGE; Tonge *et al.*, 2001; Minden *et al.*, 2009).

Bei der Protein-Microarray-Analyse handelt es sich um einen gelfreien Ansatz der mit dem DNA-Microarray verwandt ist. Der Ansatz ist vergleichbar mit dem *enzyme linked immunosorbent assay* (ELISA) und beruht auf der Immobilisierung von Proteinen auf einem Trägerchip (MacBeath und Schreiber, 2000). Durch Miniaturisierung ist es möglich über 9.000 humane Proteine auf einem einzigen Protein-Microarray zu immobilisieren (Luo, 2012). Nach Inkubation der immobilisierten Proteine mit der biologischen Probe erfolgt die Detektion der erfolgreich gebundenen Proteine mittels Fluoreszenz. Unter Verwendung von Referenzproteinen oder -peptiden, die ebenfalls auf dem Trägerchip immobilisiert sind, ist es möglich Proteine zu quantifizieren (Pratsch *et al.*, 2014).

Bei der LC-MS-Analyse handelt es sich ebenfalls um einen gelfreien Ansatz. Hierbei werden komplexe Peptid- oder Proteingemische mittels Hochleistungsflüssigkeitschromatographie (*high performance liquid chromatography*, HPLC), meist Umkehrphasen-HPLC, aufgetrennt und sequentiell in das Massenspektrometer überführt (Roepstorff, 2012). Durch den Prozess der Elektrosprayionisation (ESI) gehen die eluierenden Proteine oder Peptide aus der Flüssigphase in die Gasphase über und werden anschließend massenspektrometrisch analysiert (Fenn *et al.*, 1989).

1.3.2 Identifizierung von Proteinen mittels Massenspektrometrie

Eine der ersten Methoden zur qualitativen Charakterisierung von Proteinen war der Edman-Abbau (Edman und Begg, 1967). Diese Methode erlaubt die Sequenzierung von Proteinen und somit die Entschlüsselung der Aminosäuresequenz. Durch die DNA-Sequenzierung und die damit verbundene Entschlüsselung ganzer Genome kann die Proteinidentifizierung heutzutage auch mithilfe der Massenspektrometrie durchgeführt werden (Mann *et al.*, 1993).

Die Massenspektrometrie ist eine Methodik, mit der gasförmige Ionen mittels unterschiedlichen physikalischen Techniken nach ihrem Masse-zu-Ladung-Verhältnis (m/z) getrennt und anschließend detektiert werden. Ein Massenspektrometer besteht aus einer Ionenquelle, die geladene Moleküle generiert, einem Massenanalysator, der Ionen anhand ihres m/z -Verhältnis auftrennt und einem Detektor, der die Anzahl der Ionen zu jedem m/z -Verhältnis bestimmt (Aebersold *et al.*, 2003). Der Vorteil der massenspektrometrischen Analyse gegenüber anderen Methoden zur Proteinidentifizierung liegt in der hohen analytischen Genauigkeit der Massenbestimmung sowie der Sensitivität (Mann und Kelleher, 2008). Es gibt zwei verschiedene massenspektrometrische Ansätze für die Identifizierung von Proteinen: die *top-down*- und die *bottom-up*-Methode (Catherman *et al.*, 2014). Bei der *top-down*-Methode werden die intakten Proteine mittels ESI (Fenn *et al.*, 1989) oder Matrix-unterstützte Laser-Desorption/Ionisation (*matrix-assisted laser desorption/ionization*, MALDI) (Karas und Hillenkamp, 1988; Tanaka *et al.*, 1988) in die Gasphase überführt. Aufgrund der milden Ionisation, bei der die Proteine positive Ladungen erhalten kommt es nicht zur Fragmentierung und die Proteine können im Ganzen analysiert werden. Die *top-down*-Methode benötigt aufgrund der hohen Ladungszustände der Proteine ein besonders hochauflösendes Massenspektrometer ($R > 240.000$ bei $400 m/z$) (Michalski *et al.*, 2012) und eignet sich nur bedingt für die Identifizierung von Proteinen aus komplexen Gemischen (Catherman *et al.*, 2014). Bei der *bottom-up*-Methode hingegen werden die Proteine zunächst proteolytisch verdaut, die generierten Peptide mittels ESI oder MALDI ionisiert, wobei niedrig geladene Peptidionen gebildet werden (+1, +2, +3 und +4), und anschließend massenspektrometrisch analysiert. Aufgrund der Analyse von niedrig geladenen Peptidionen ist bei dieser Methode eine moderate Auflösung ($R = 50.000$ bei $400 m/z$) ausreichend, um eine Identifizierung zu erreichen (Nagaraj *et al.*, 2012). Aufgrund der hohen Komplexität humaner Proben und der Möglichkeit der vorgeschalteten Trennung mittels HPLC wird bevorzugt die ESI eingesetzt.

Für die Analyse von ESI-Peptiden stehen verschiedene Massenanalysatoren zur Verfügung: das Quadrupol- und Triplequadrupol-MS (Q und QQQ), das Flugzeit-MS (*quadrupole time-of-flight*, QToF), die lineare Ionenfalle (*linear ion trap*, LIT), die dreidimensionale Ionenfalle (*three-dimensional ion trap*, QIT) und die Orbitrap (Paul, 1989; Wollnik, 1993; Paul und Raether, 1995; Makarov, 2000). Jeder dieser Massenanalysatoren hat seine spezifischen Vor- und Nachteile und die Verwendung hängt von dem durchzuführenden Experiment ab. Der Ablauf der Analyse ist jedoch nahezu identisch. Zunächst wird ein Übersichtsspektrum (MS-Spektrum) akquiriert und das m/z -Verhältnis des in der Proteinanalytik meist positiv geladenen Peptidions bestimmt. Anschließend wird das Peptidion (*precursor*) isoliert und definiert fragmentiert. Das resultierende Massenspektrum (MS/MS-Spektrum) enthält die m/z -Verhältnisse der spezifisch gebildeten Fragmentionen (*fragment ions*). Für die Fragmentierung von Peptiden können verschiedene Methoden verwendet werden, wobei sich je nach Fragmentierungsmethode unterschiedliche Fragmentionen bilden (Abbildung 5).

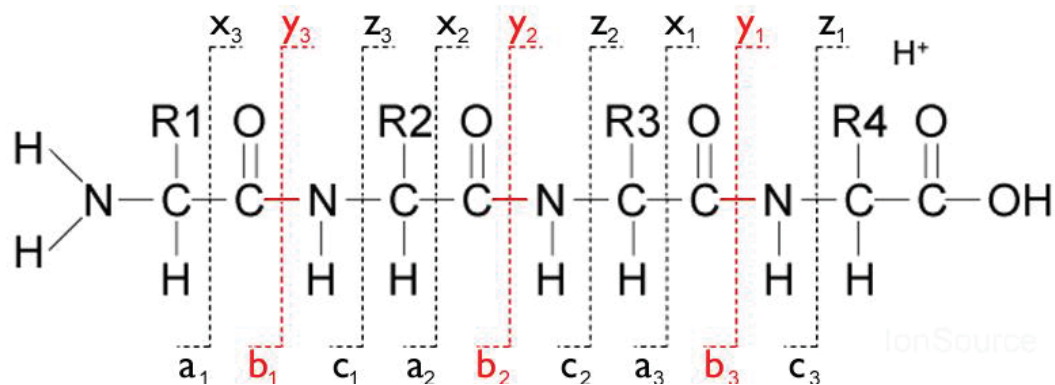


Abbildung 5: Schematische Darstellung und Nomenklatur der Fragmentionen, die bei der Fragmentierung von Peptidionen entstehen können (modifiziert nach Roepstorff und Fohlman, 1984). Bei der in dieser Arbeit eingesetzten Fragmentierungsart, der kollisionsinduzierten Dissoziation, werden bevorzugt N-terminale b-Ionen und C-terminale y-Ionen gebildet.

Bei der Fragmentierung durch die Kollision des Peptidions mit einem Inertgas (meist He oder N_2), auch kollisionsinduzierten Dissoziation (*collision-induced dissociation*, CID) oder Hochenergie-Kollisionsdissoziation (*higher-energy collisional dissociation*, HCD) genannt, erfolgt der Bruch bevorzugt entlang des Peptidrückgrates zwischen dem Carbonylkohlenstoff und dem Amidstickstoff, wobei verschiedene N-terminale b-Ionen und C-terminale y-Ionen gebildet werden (Roepstorff und Fohlman, 1984). Diese weisen eine unterschiedliche Stabilität auf, wobei b-Ionen instabiler sind und zudem zyklisieren können, wodurch

wiederum a-Ionen gebildet werden (Tabb *et al.*, 2003; Paizs und Suhai, 2005; Harrison, 2009). Zudem gibt es Hinweise darauf, dass die Detektion von b-Ionen durch den verwendeten CID-Typ determiniert wird (Lau *et al.*, 2009; Barsnes *et al.*, 2011). Bei der CID kann zwischen zwei Typen unterschieden werden, der resonanz-angeregten CID (*resonant excitation*, rCID) und der Beam-CID (*beam-type*, bCID). Bei der rCID, welche in Ionenfallen-MS (LIT, QIT) verwendet wird, werden die Peptidionen im Beisein eines Inertgas mit einer spezifischen Energie angeregt bis diese mit dem Inertgas kollidieren und fragmentieren. Bei der bCID hingegen, welche in QToF-MS und QQQ-MS verwendet wird, werden die Peptidionen mit Überschall in die mit einem Inertgas gefüllte Kollisionszelle transferiert, was in der Kollision und der Fragmentierung resultiert. Aufgrund der hohen Energie bei CID-Experimenten werden PTMs häufig nicht detektiert, da diese abgespalten werden (Tang *et al.*, 2006). Daher können meist nur stabile Modifikationen, wie beispielweise Acetylierungen oder Oxidationen, identifiziert werden.

Eine weitere Fragmentierungsmethode stellt die Elektronentransferdissoziation (*electron transfer dissociation*, ETD) dar. Hierbei wird innerhalb der Kollisionszelle ein Elektron von einem Anion, z.B. Fluoranthen, auf das Peptidion übertragen, wodurch die Fragmentierung induziert wird und bevorzugt c- und z-Ionen gebildet werden (Syka *et al.*, 2004). Durch die Verwendung von ETD können ergänzend zum CID Fragmentionen erhalten werden, die wegen der geringeren Energie bei der Fragmentierung Aufschluss über PTMs, wie beispielweise Phosphorylierungen und Glykosylierungen, geben können (Zubarev *et al.*, 2000).

Die mittels CID, HCD oder ETD generierten MS/MS-Spektren können für die Identifizierung von Proteinen durch den Abgleich mit einer Sequenzdatenbank unter Verwendung eines Suchalgorithmus, wie MASCOT (Perkins *et al.*, 1999) oder Sequest (Eng *et al.*, 1994), verwendet werden. Dabei werden *in silico* Proteine zu Peptiden verdaut, die dazugehörigen Fragmentionenmassen bestimmt und mit den experimentellen *m/z*-Verhältnissen verglichen. Die Suchalgorithmen geben anschließend Wahrscheinlichkeitswerte für die Übereinstimmung zwischen theoretischen und experimentellen MS/MS-Spektren an. Nach statistischer Evaluation werden mithilfe der identifizierten Peptide die dazugehörigen Proteine identifiziert (Perkins *et al.*, 1999; Steen und Mann, 2004). Die Wahrscheinlichkeit für die richtige Identifizierung eines Proteins nimmt mit steigender Sequenzabdeckung zu, wobei ein Protein basierend auf wenigen Peptiden bereits signifikant identifiziert werden kann (Mann *et al.*, 1993).

1.3.3 Quantifizierung von Proteinen mittels LC-MS

Die LC-MS-Analyse ermöglicht neben der Identifizierung auch die Quantifizierung von Proteinen aus komplexen Gemischen. Mithilfe der Quantifizierung ist es möglich Unterschiede in der Abundanz von Proteinen verschiedener Zustände, z.B. jung und alt, zu vergleichen. Hierbei kann zwischen der relativen und der absoluten Quantifizierung von Proteinen unterschieden werden (Bantscheff *et al.*, 2007).

Bei der relativen Quantifizierung von Proteinen mittels LC-MS werden zwei oder mehr Zustände miteinander verglichen und ins Verhältnis gesetzt. Hierbei wird die Information über die Abnahme bzw. Zunahme einzelner Proteine relativ zur Kontrollgruppe erhalten. Für die relative Quantifizierung von Proteinen und Peptiden sind folgende Ansätze etabliert: die metabolische Markierung, die chemische Markierung und die labelfreie Analyse (Abb. 6; zusammengefasst in Bantscheff *et al.*, 2007).

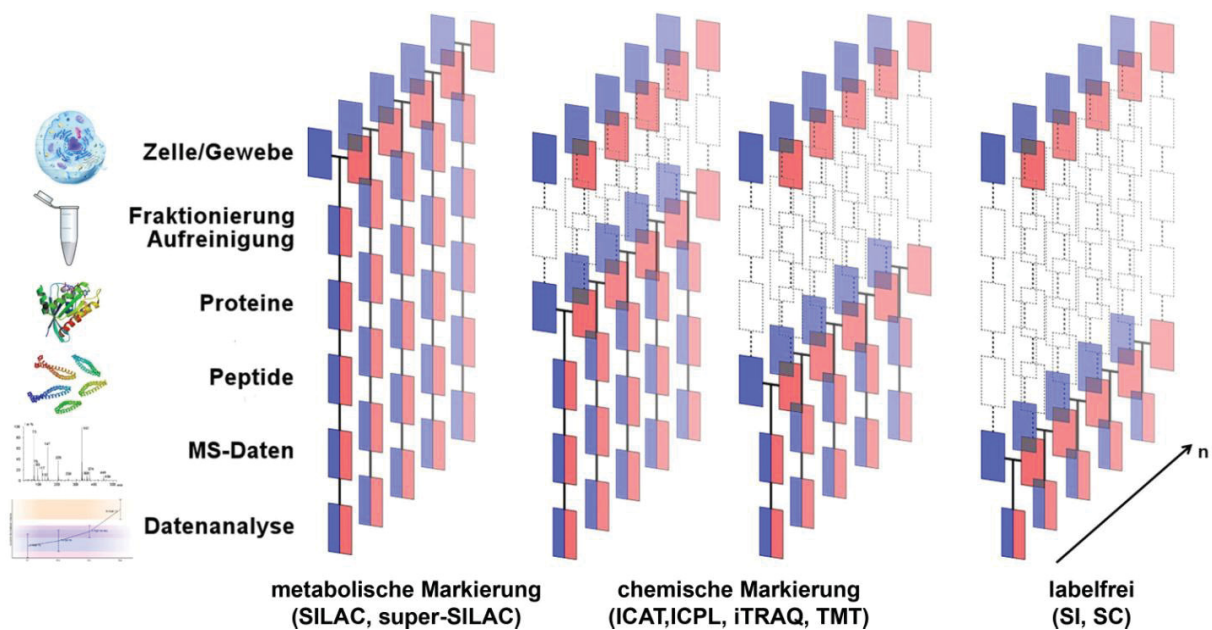


Abbildung 6: Methoden zur Quantifizierung von Proteinen mittels massenspektrometrie-basierter Proteomanalyse (modifiziert nach Bantscheff *et al.*, 2007). Die blauen und roten Markierungen repräsentieren jeweils unterschiedliche experimentelle Zustände sowie die dazugehörigen biologischen Replikate (n). Die horizontalen Linien zeigen an, auf welcher Ebene die Proben für die Quantifizierung kombiniert werden. SILAC, *stable isotope labelling by amino acids in cell culture*; ICAT, *isotope coded affinity tag*, ICPL, *isotope coded protein label*; iTRAQ, *isobaric tag for relative and absolute quantitation*; TMT, *tandem mass tag*; SI, *signal intensity*; SC, *spectral counting*.

Bei der metabolischen Markierung werden während der Kultivierung von Zellen spezifische natürliche Aminosäuren durch isotope markierte (^{13}C und ^{15}N) Aminosäuren ausgetauscht, weshalb der Ansatz als *stable isotope labelling by amino acids in cell culture* (SILAC) bezeichnet wird (Ong *et al.*, 2002). Der Austausch der Aminosäuren führt aufgrund identischer biochemischer Eigenschaften meist nicht zur Ausbildung eines Phänotyps. Vor Beginn des Experiments muss dieses jedoch verifiziert werden. Zur Quantifizierung werden die Proben im äquimolaren Verhältnis kombiniert. Durch die eingeführten Massenverschiebung (4-10 Da) kann auf Ebene der Signalintensitäten (endogen/markiert) die Quantifizierung durchgeführt werden. Aufgrund der vorgeschalteten Kultivierung ist der Ansatz für klinische Proben ungeeignet. Eine Weiterentwicklung dieses Ansatzes, das sogenannte super-SILAC, beruht auf der Erstellung eines isotope markierten Standards, der aus verschiedenen Zelllinien besteht und zu jeder Probe im äquimolaren Verhältnis hinzugefügt wird (Geiger *et al.*, 2010). Durch die Verwendung des super-SILAC-Ansatzes besteht die Möglichkeit klinische Proben zu quantifizieren. Bei der chemischen Markierung werden auf Ebene der Proteine oder Peptide Markierungen eingeführt, die zur Quantifizierung mittels Signalintensitäten genutzt werden können. Die Markierung erfolgt mithilfe von isotope markierten Reagenzien über reaktive Seitengruppen der Aminosäuren. Zu den chemischen Markierungen gehören das *isotope coded affinity tag* (ICAT), bei dem auf Peptidebene Reportergruppen an Cysteine gebunden werden (Gygi *et al.*, 1999), das *isotope coded protein label* (ICPL), bei dem Reportergruppen auf Proteinebene an freie Aminofunktionen gebunden werden (Schmidt *et al.*, 2005) und die Ansätze mit isobaren Markierungen, wie das *isobaric tag for relative and absolute quantitation* (iTRAQ) und das *tandem mass tag* (TMT), bei denen auf Protein- oder Peptidebene Reportergruppen an den N-Terminus addiert werden (Thompson *et al.*, 2003; Ross *et al.*, 2004). Für die Quantifizierung werden die jeweiligen Zustände im äquimolaren Verhältnis kombiniert und auf MS- oder MS/MS-Ebene quantifiziert. Die chemische Markierung ist für eine Quantifizierung von Proteinen aus komplexen Proben nur bedingt geeignet. So ist Cystein eine eher selten vorkommende Aminosäure und die gebildete Thioetherbindung ist oxidationsempfindlich (Lottspeich *et al.*, 2006). Des Weiteren können Proteine N-terminal modifiziert vorliegen, weshalb die Addition einer Reportergruppe nicht möglich ist (Bantscheff *et al.*, 2007). Bei der labelfreien Analyse hingegen wird keine Markierung eingeführt und die jeweiligen Proben werden erst *in silico* kombiniert (Chelius und Bondarenko, 2002). Die labelfreie Quantifizierung basiert auf der Signalintensität (*signal intensity*, SI) oder auf der Anzahl

akquirierter MS/MS-Spektren einer spezifischen Peptidmasse (*spectral counting*, SC) (Bantscheff *et al.*, 2007). Bei dem SI-Ansatz werden die spezifischen Peptidmuster (m/z -Verhältnis und Retentionszeit) detektiert, die Signalfläche aller detektierten Peptide definiert und die dazugehörigen Intensitäten berechnet. Durch den Vergleich der einzelnen LC-MS-Experimente ist es möglich die Peptide bzw. Proteine zwischen den jeweiligen Zuständen relativ zu quantifizieren, da die Signalintensität mit der Peptid- und Proteinabundanz korreliert. Dieser Ansatz setzt eine hohe Reproduzierbarkeit der Chromatographie und eine hohe Massengenauigkeit des Massenspektrometers voraus, wobei Abweichungen der Retentionszeit *in silico* korrigiert werden können (Cox und Mann, 2011). Bei dem SC-Ansatz wiederum werden die akquirierten MS/MS-Spektren einer spezifischen Peptidmasse für die Quantifizierung herangezogen, da die Anzahl der MS/MS-Spektren mit der Peptid- und Proteinabundanz korreliert (Old *et al.*, 2005). Der labelfreie Ansatz eignet sich sowohl für die Analyse von Zellkulturproben, als auch klinischer Proben (Neilson *et al.*, 2011).

Bei der absoluten Quantifizierung von Proteinen mittels LC-MS wird die Konzentration bzw. die Kopienzahl der Proteine pro Zelle bestimmt. Dazu wird der zur quantifizierenden Probe ein Analyt mit bekannter Konzentration beigefügt und aus dem Verhältnis der Signalintensitäten bzw. Signalflächen (bekannt/unbekannt) die absolute Menge bestimmt (Desiderio und Kai, 1983; Bantscheff *et al.*, 2007). Für eine akkurate absolute Quantifizierung ist essentiell, dass die beigefügten Analyten die gleiche Ionisierungseffizienz aufweisen. Daher werden der Probe proteotypische synthetische isopenmarkierte Peptide bekannter Konzentration, welche identische physikochemische Eigenschaften aufweisen, beigefügt. Dieser Ansatz der absoluten Quantifizierung wird auch als *absolute quantification of proteins* (AQUA) bezeichnet (Gerber *et al.*, 2003). Aufgrund der Komplexität humaner Proben eignet sich dieser Ansatz nur für eine gezielte Analyse weniger Kandidatenproteine. Die profunde absolute Quantifizierung komplexer Proben ist ebenfalls möglich. Hierzu stehen verschiedene Ansätze wie LCMS^E (Silva *et al.*, 2006), *top 3 protein quantification* (T3PQ; Grossmann *et al.*, 2010), *intensity based absolute quantification* (iBAQ; Schwanhäusser *et al.*, 2011), *exponentially modified protein abundance index* (emPAI; Ishihama *et al.*, 2005) und *absolute proteomics expression* (APEX; Lu *et al.*, 2007) zur Verfügung (zusammengefasst in Arike *et al.*, 2012). Die absolute Konzentration von Proteinen hat eine hohe klinische Relevanz, spielt jedoch in der Grundlagenforschung eine eher untergeordnete Rolle.

2 Ziele der Arbeit

Das Altern ist ein komplexer Prozess, der mit verschiedenen Veränderungen auf molekularer, zellulärer und systemischer Ebene einhergeht. Die zugrundeliegenden Mechanismen des Alterungsprozesses sind noch nicht gänzlich erforscht und verstanden. Für die Untersuchung altersassoziierter Prozesse wurden bisher überwiegend induzierte Alterungsmodelle verwendet, die nur bedingt repräsentativ für das *in vivo* Altern sind. Daher besteht die Notwendigkeit für die Charakterisierung *in situ* gealterter zellulärer Modellsysteme. Ziel dieser Arbeit ist es mithilfe der quantitativen massenspektrometrie-basierten Proteomanalyse einen Beitrag zur Aufklärung des stromalen Alterungsprozesses zu leisten und die zugrundeliegenden Mechanismen des Alterns zu ergänzen. Dazu soll ein zelluläres *ex vivo* Hautalterungsmodells unter Verwendung *in situ* gealterter primärer adulter humaner dermaler Fibroblasten mittels labelfreier differentieller Proteomanalyse sowohl auf Ebene der intrazellulären Proteine, als auch der sezernierten Proteine untersucht werden. Dafür wurde im Rahmen dieser Dissertation Folgendes durchgeführt:

- I. Evaluierung eines geeigneten Massenspektrometers für die Identifizierung von Proteinen und Peptiden aus komplexen Gemischen (*The fate of b-ions in the two worlds of collision-induced dissociation*, Waldera-Lupa *et al.*, 2013).
- II. Etablierung eines massenspektrometrischen Arbeitsablaufs zur Quantifizierung der Proteine humaner Zellen unter der Verwendung eines online nano-HPLC-ESI-MS-Systems (*Application of label-free proteomics for differential analysis of lung carcinoma cell line A549*, Sitek *et al.*, 2012).
- III. Untersuchung des Proteoms *in situ* gealterter Fibroblasten, und Validierung mittels Transkriptomanalyse und miRNA-profiling (*Proteome-wide analysis of primary cultures of in situ aged human fibroblasts reveals a moderate age-associated cellular phenotype*, Waldera-Lupa *et al.*, 2014a).
- IV. Charakterisierung des Sekretoms *in situ* gealterter Fibroblasten und Vergleich mit dem in der Literatur beschriebenen SASP (*Characterization of skin aging associated secreted proteins (SAASP) produced by dermal fibroblast isolated from intrinsically aged human skin*, Waldera-Lupa *et al.*, 2014b).

Diese Arbeit wird einen Beitrag zum Verständnis der Mechanismen des Alterungsprozesses, der Hautalterung und der Rolle der Fibroblasten bei der stromalen Alterung leisten.

3 Manuskripte

3.1 Übersicht und Zusammenfassungen

Publikation I

The fate of b-ions in the two worlds of collision-induced dissociation

Daniel M. Waldera-Lupa¹, Anja Stefanski¹, Helmut E. Meyer², Kai Stühler¹

¹Molecular Proteomics Laboratory, Biologisch-Medizinisches Forschungszentrum, Heinrich-Heine-Universität, Düsseldorf, Germany

²Medizinisches Proteom-Center, Ruhr-Universität Bochum, Bochum, Germany

Art der Autorenschaft:	Erstautor
Anteil an der Publikation:	85 %
Beitrag zur Publikation:	Studiendesign, Planung und Durchführung aller Experimente, Erhebung der Daten, Datenanalyse und Auswertung, Interpretation der Ergebnisse, Verfassen der Publikation
Journal:	<i>Biochimica et Biophysica Acta - Proteins and Proteomics</i>
Impact Factor:	3,733
Stand der Veröffentlichung:	Publiziert im Dezember 2013
Ergänzende Angaben:	<i>Biochim Biophys Acta</i> . 2013 Dec;1834(12):2843-8
DOI:	10.1016/j.bbapap.2013.08.007
PubMed-ID:	23994226

Zusammenfassung Publikation I

The fate of b-ions in the two worlds of collision-induced dissociation

Die Identifizierung von Proteinen komplexer Gemische mittels Massenspektrometrie basiert auf der Fragmentierung von Peptidionen zu definierten Fragmentionen. Untersuchungen von Fragmentionen synthetischer Peptide haben ergeben, dass sich die bei der CID gebildeten b-Ionen und y-Ionen in ihrer Stabilität unterscheiden. Dies resultiert in einer Unterrepräsentation von b-Ionen. Des Weiteren wurde gezeigt, dass b-Ionen zyklische Strukturen bilden, die für eine Identifizierung nicht verwendet werden können. Die Evaluation von Spektrendatenbanken gab zusätzlich einen Hinweis darauf, dass das Fragmentierungsmuster durch den verwendeten CID-Typ (rCID und bCID) determiniert wird. Allerdings gibt es bisher keine experimentelle Evaluation und Quantifizierung der Unterrepräsentation von b-Ionen der beiden CID-Typen.

In dieser Publikation wurde die Unterrepräsentation von b-Ionen detailliert evaluiert und quantifiziert. Dazu wurde ein systematischer Vergleich von rCID und bCID mit unterschiedlichen Massenspektrometern, einem QToF-MS, einem LIT-MS und einem QIT-MS, durchgeführt. Die detaillierte Analyse der generierten MS/MS-Spektren tryptischer Peptide ergab, dass b-Ionen bei allen verwendeten Massenspektrometern signifikant unterrepräsentiert sind. Zudem kommen y-Ionen bei bCID-MS etwa fünfmal so häufig vor wie b-Ionen. Durch die Einführung einer N-terminalen Acetylierung wurde der Einfluss der Zyklisierung auf die Unterrepräsentation von b-Ionen analysiert. Durch die N-terminale Acetylierung wurde zum ersten Mal gezeigt, dass die Zyklisierung signifikant zu einem Verlust von etwa 16 % der b-Ionen beiträgt, und dass dieser Verlust sowohl bei bCID-MS, als auch bei rCID-MS auftritt. Des Weiteren konnte gezeigt werden, dass die Ringschlussreaktion der hauptsächliche Grund für die Unterrepräsentation von b-Ionen bei rCID-MS ist. Bei bCID-MS hingegen sind die b-Ionen auch nach der Acetylierung signifikant unterrepräsentiert. Ferner wurde gezeigt, dass bei bCID-MS, anders als bei rCID-MS, nur wenig langkettige b-Ionen ($> b_6$) detektiert werden.

Publikation II

Application of label-free proteomics for differential analysis of lung carcinoma cell line A549

Barbara Sitek¹, Daniel M. Waldera-Lupa^{1,2}, Gereon Poschmann^{1,2}, Helmut E. Meyer¹, Kai Stühler²

¹Department of Medical Proteomics/Bioanalytics, Medizinisches Proteom-Center, Ruhr-Universität Bochum, Bochum, Germany

²Molecular Proteomics Laboratory, Biologisch-Medizinisches Forschungszentrum, Heinrich-Heine-Universität, Düsseldorf, Germany

Art der Autorenschaft:	Koautor
Anteil an der Publikation:	30 %
Beitrag zur Publikation:	Optimierung des LC-MS-Arbeitsablaufs sowie der LC-MS-Parameter, Verfassen der Publikation
Journal:	<i>Methods in Molecular Biology</i>
Impact Factor:	1,238
Stand der Veröffentlichung:	Publiziert im Juni 2012
Ergänzende Angaben:	<i>Methods Mol Biol.</i> 2012 ;893:241-8
DOI:	10.1007/978-1-61779-885-6_16
PubMed-ID:	22665305

Zusammenfassung Publikation II

Application of label-free proteomics for differential analysis of lung carcinoma cell line A549

Mithilfe der labelfreien massenspektrometrie-basierten Proteomanalyse ist es möglich Unterschiede in der Abundanz von Proteinen verschiedener Proben zu vergleichen. Die labelfreie Quantifizierung von Proteinen basiert auf einem stabilen und hoch-reproduzierbaren LC-MS-System. Aufgrund der hohen Komplexität humaner Proben und der großen Anzahl biologischer Replikate in einer Studie ist es unabdingbar sowohl die Probenvorbereitung, als auch das LC-MS-System zuvor zu optimieren. Dazu gehören die Proteinextraktion, der Proteinverdau, die Chromatographie, die massenspektrometrischen Parameter und die Datenauswertung, welche die Identifizierung, die Quantifizierung und die statistische Auswertung inkludiert.

In dieser Publikation wurde ein labelfreier massenspektrometrischer Ansatz für die relative Quantifizierung von Proteinen aus komplexen humanen Zellen entwickelt und optimiert. Dieser beinhaltet die Lyse der Zellen, die Extraktion der Proteine, einen tryptischen Flüssigverdau der extrahierten Proteine, die LC-MS/MS-Analyse mithilfe eines nano-HPLC-ESI-MS-Systems und die Datenauswertung mittels Quantifizierungs- und Identifizierungssoftware. Der entwickelte labelfreie LC-MS-Arbeitsablauf wurde erfolgreich in einer Proteomstudie angewendet, bei der ein Lungenfibrosemodell untersucht wurde. In dieser Studie wurde die humane Lungenkarzinomzelllinie A549 mit dem *transforming growth factor beta 1* (TGF- β 1) behandelt und anschließend mittels LC-MS analysiert. In der Analyse von 2 x 7 Einzelproben mit je 1 μ g Gesamtprotein wurden insgesamt 732 Proteine identifiziert. Durch die statistische Auswertung konnten 202 Proteine identifiziert werden, die sich in ihrer Abundanz zwischen behandelten und unbehandelten Lungenkarzinomzellen signifikant unterscheiden. Die mittlere technische Varianz der LC-MS-Analyse betrug ca. 25 % und der dynamische Abundanzbereich etwa vier Größenordnungen. Der entwickelte Arbeitsablauf ermöglicht die Durchführung quantitativer Proteomanalysen und eignet sich für die Analyse humaner Proben, wobei mehrere hundert Proteine gleichzeitig identifiziert und quantifiziert werden können.

Publikation III

Proteome-wide analysis of primary cultures of in situ aged human fibroblasts reveals a moderate age-associated cellular phenotype

Daniel M. Waldera-Lupa^{1,2}, Faiza Kalfalah³, Ana-Maria Florea⁴, Steffen Sass⁵, Fabian Kruse^{1,2}, Vera Rieder^{1,2}, Julia Tigges⁶, Ellen Fritsche⁶, Jean Krutmann⁶, Hauke Busch^{7,8,9}, Melanie Boerries^{7,8,9}, Helmut E. Meyer¹⁰, Fritz Boege³, Fabian Theis¹¹, Guido Reifenberger^{4*}, Kai Stühler^{1,2*}

* These authors contributed equally

¹Institute for Molecular Medicine, Heinrich-Heine-University, Düsseldorf, Germany

²Molecular Proteomics Laboratory, Biomedical Research Centre, Heinrich-Heine-University, Düsseldorf, Germany

³Institute of Clinical Chemistry and Laboratory Diagnostics, Heinrich-Heine-University, Med. Faculty, Düsseldorf, Germany

⁴Department of Neuropathology, Heinrich-Heine-University, Düsseldorf, and German Cancer Consortium, German Cancer Research Center, Heidelberg, Germany

⁵Institute of Computational Biology, Helmholtz Center Munich, German Research Center for Environmental Health, Neuherberg, Germany

⁶Leibniz Research Institute for Environmental Medicine, Düsseldorf, Germany

⁷Institute of Molecular Medicine and Cell Research, Albert-Ludwigs-University Freiburg, Freiburg, Germany.

⁸German Cancer Consortium, Freiburg, Germany

⁹German Cancer Research Center, Heidelberg, Germany

¹⁰Department of Biomedical Research, Leibniz-Institute for Analytical Science, Dortmund, Germany

¹¹Department of Mathematics, Technical University Munich, Garching, Germany

Art der Autorenschaft:	Erstautor
Anteil an der Publikation:	80 %
Beitrag zur Publikation:	Studiendesign, Planung und Durchführung der Experimente, Erhebung der Proteom-Daten, Datenanalyse und Auswertung, Interpretation der Ergebnisse, Verfassen der Publikation
Journal:	<i>Aging Cell</i>
Impact Factor:	5,705
Stand der Veröffentlichung:	Eingereicht im Juni 2014

Zusammenfassung Publikation III

Proteome-wide analysis of primary cultures of in situ aged human fibroblasts reveals a moderate age-associated cellular phenotype

Die Alterung eines Organs wird durch das statische Stroma determiniert. Der Hauptzelltyp im Stroma ist der Fibroblast, eine langlebige und quieszente Zelle, die sich im Ruhezustand befindet und daher eine nur geringe Proliferationsrate aufweist. Aus diesem Grund müssen zelluläre Funktionen angepasst werden und altersassoziierte Veränderungen können akkumulieren. Für den Alterungsprozess von Fibroblasten wurden verschiedene Charakteristika definiert. Allerdings wurden bisher die meisten Studien an Zellen durchgeführt, die durch die Replikation *in vitro*, die Induktion von zellulärem Stress oder die Überexpression von Onkogenen in die zelluläre Seneszenz geführt wurden.

In dieser Publikation wurde mithilfe eines *ex vivo* Hautalterungsmodells unter der Verwendung *in situ* gealterter humaner dermaler Fibroblasten von 15 verschiedenen Individuen aus drei Altersgruppen die zellulären Alterungsprozesse untersucht. Mittels labelfreier massenspektrometrie-basierter Proteomanalyse wurden 43 altersabhängig veränderte Proteine identifiziert. Der Vergleich mit kürzlich publizierten Transkriptomdaten identischer Individuen gab Hinweise darauf, dass 77 % der altersassoziierten Proteine nicht durch die Genexpression reguliert werden. Durch ein *miRNA-profiling* konnten zwölf altersabhängig veränderte miRNAs identifiziert werden, die potentiell drei der 43 altersassoziierten Proteine posttranskriptional regulieren. Auf Ebene des Transkriptoms, des Proteoms und des miRNAoms konnte gezeigt werden, dass Fibroblasten während der *in vivo* Alterung einen moderaten altersassoziierten zellulären Phänotyp ausbilden. Die systematische Analyse ergab, dass auf allen beschriebenen Ebenen größtenteils identische biologische Prozesse involviert sind. Zu diesen gehören die Differenzierung, die Proliferation, die Proteostase, der RNA-Metabolismus, die Zellkommunikation, die Zellorganisation, der Zellstress und der Zelltod. Die meisten Kandidatenproteine wurden noch nicht im Rahmen der Alterung von Fibroblasten beschrieben, gleichwohl können den identifizierten Proteinen biologische Prozesse zugeordnet werden, die eine starke Relevanz für die bekannten Charakteristika des Alterns aufweisen. Die Ergebnisse dieser Publikation gestatten einen detaillierten Einblick in die intrazellulären Veränderungen der Fibroblasten während des *in vivo* Alterns.

Publikation IV

Characterization of skin aging associated secreted proteins (SAASP) produced by dermal fibroblast isolated from intrinsically aged human skin

Daniel M. Waldera-Lupa^{1,2}, Faiza Kalfalah³, Petra Boukamp⁴, Kai Safferling⁵, Gereon Poschmann^{1,2}, Christine Götz-Rösch⁶, Françoise Bernerd⁷, Laura Haag³, Hanzen Birgit³, Ulrike Huebenthal⁵, Ellen Fritsche⁶, Niels Grabe⁵, Fritz Boege³, Julia Tigges^{6*}, Jean Krutmann^{1,6*}, Kai Stühler^{1,2*}

* Authors contributed equally

¹Institute of Molecular Medicine, University of Duesseldorf, Duesseldorf, Germany

²Molecular Proteomics Laboratory, Heinrich-Heine-University, Düsseldorf, Germany

³Institute of Clinical Chemistry and Laboratory Diagnostics, Heinrich-Heine-University, Med. Faculty, Düsseldorf, Germany

⁴German Cancer Research Centre, Heidelberg, Germany

⁵Hamamatsu Tissue Imaging and Analysis Center, BIOQUANT, Ruprecht-Karls-University, Heidelberg, Germany

⁶IUF – Leibniz Research Institute for Environmental Medicine, Düsseldorf, Germany

⁷L'Oréal Recherche, Clichy, Paris, France

Art der Autorenschaft:	Erstautor
Anteil an der Publikation:	70 %
Beitrag zur Publikation:	Studiendesign, Zellkultur, Planung und Durchführung der Experimente, Erhebung der Sekretom-Daten, Datenanalyse und Auswertung, Interpretation der Ergebnisse, Verfassen der Publikation
Journal:	<i>Journal of Investigative Dermatology</i>
Impact Factor:	6,193
Stand der Veröffentlichung:	Eingereicht im Juni 2014

Zusammenfassung Publikation IV

Characterization of skin aging associated secreted proteins (SAASP) produced by dermal fibroblast isolated from intrinsically aged human skin

Viele Altersstudien wurden unter der Verwendung *in vitro* gealterter Fibroblasten durchgeführt. Dabei wurden die Zellen durch unterschiedliche Noxen in die zelluläre Seneszenz geführt. Der durch die *in vitro* Alterung generierte seneszente Phänotyp beinhaltet einen irreversiblen Zellzyklusarrest, eine erhöhte Heterochromatisierung, die Formierung von DNA-SCARS, die Verkürzung der Telomere und die Ausbildung eines sekretorischen Phänotyps, dem sogenannten SASP. Dieser zeichnet sich durch eine aberrante Sekretion von über 80 Faktoren aus. Zu diesen gehören Zytokine, Wachstumsfaktoren, MMPs sowie lösliche Rezeptoren und deren Liganden. Es wird angenommen, dass der SASP einen negativen Einfluss auf das umliegende Gewebe hat, und die Karzinogenese stimulieren sowie die Gewebemöostase stören kann. Allerdings gibt es keine experimentellen Evidenzen, ob sich der SASP während des *in vivo* Alterns ausbildet.

In dieser Publikation wurde der altersabhängige sekretorische Phänotyp *in situ* gealterter humaner dermaler Fibroblasten von 15 verschiedenen Individuen aus drei Altersgruppen charakterisiert. Dazu wurden zunächst die in der Literatur beschriebenen Merkmale für die zelluläre Seneszenz, wie die Bildung von DNA-SCARS, das Apoptoseverhalten und die Telomerlängen, untersucht. In dieser Studie wurde erstmals gezeigt, dass sich mit zunehmendem Alter DNA-SCARS bilden, und dass diese weder mit der Zunahme von DNA-Doppelstrangbrüchen, noch mit der Abnahme der Zellviabilität korrelieren. Des Weiteren ergab die Untersuchung der Telomere keine Verkürzung mit zunehmendem Alter. Mittels labelfreier massenspektrometrie-basierter Proteomanalyse und einer gezielten Zytokinanalyse konnten 998 sekretierte Proteine identifiziert werden, wovon 70 eine altersabhängige Veränderung der Abundanz aufwiesen. Diese Proteine sind in die Organisation der extrazellulären Matrix, die Formation von elastischen Fasern, die Inflammation und die interzellulären Kommunikation involviert. Der Vergleich mit dem SASP ergab, dass die Sekretion von Zytokinen und MMPs ein gemeinsamer Aspekt der induzierten Seneszenz und der *in situ* Alterung sind. Insgesamt wurden 27 Proteine identifiziert, die bisher nicht durch den SASP beschrieben wurden. In dieser Publikation wurde erstmals der altersassoziierte sekretorische Phänotyp auf Ebene der Proteine charakterisiert und gezeigt, dass dieser sich vom SASP unterscheidet.

3.2 Publikation I

The fate of b-ions in the two worlds of collision-induced dissociation

Daniel M. Waldera-Lupa¹, Anja Stefanski¹, Helmut E. Meyer², Kai Stühler¹

¹Molecular Proteomics Laboratory, Biologisch-Medizinisches Forschungszentrum (BMFZ), Heinrich-Heine-Universität, Düsseldorf, Germany

²Medizinisches Proteom-Center, Ruhr-Universität Bochum, Bochum, Germany

ABSTRACT

Fragment analysis of proteins and peptides by mass spectrometry using collision-induced dissociation (CID) revealed that the pairwise generated N-terminal b- and C-terminal y-ions have different stabilities resulting in underrepresentation of b-ions. Detailed analyses of large-scale spectra databases and synthetic peptides underlined these observations and additionally showed that the fragmentation pattern depends on utilized CID regime. To investigate this underrepresentation further we systematically compared resonant excitation energy and beam-type CID facilitated on different mass spectrometer platforms: (i) quadrupole time-of-flight, (ii) linear ion trap and (iii) three-dimensional ion trap. Detailed analysis of MS/MS data from a standard tryptic protein digest revealed that b-ions are significantly underrepresented on all investigated mass spectrometers. By N-terminal acetylation of tryptic peptides we show for the first time that b-ion cyclization reaction significantly contributes to b-ion underrepresentation even on ion trap instruments and accounts for at most 16 % of b-ion loss.

INTRODUCTION

The application of mass spectrometry (MS) has become an indispensable tool in proteomics [1-4]. In combination with soft ionization techniques such as matrix-assisted laser-desorption/ionization (MALDI) [5] and electrospray ionization (ESI) [6] as well as different mass analyzers like e.g. time-of-flight, ion trap, orbitrap, MS provides a broad range of applications for detailed characterization of proteins and peptides. The commonly used bottom up approach of analyzing peptides after tryptic digestion has been successfully applied to quantify proteomes [1-3] as well as in-depth analysis of the phosphoproteome [7-8]. To obtain sequence information and characterize proteins' primary structure as well as posttranslational modifications fragment analysis using collision-induced dissociation (CID), electron transfer dissociation (ETD) or higher-energy collisional dissociation (HCD) is routinely applied [9-12]. In low-energy CID experiments the selected precursor ions undergo energetic collisions with an inert gas such as nitrogen or helium predominantly leading to so-called N-terminal b-ions and C-terminal y-ions [11-16]. At this point it must be distinguished between two different instrument specific CID fragmentation techniques: beam-type and resonance excitation CID. Beam-type CID is a quadrupole based technique (QToF, QQQ) where fragmentation is achieved by transferring precursor ions with ultrasonic speed from the analytical quadrupole into the gas-filled collision cell [9-10]. Formed fragment ions can undergo unintended secondary fragmentation leading to non-sequence specific ions. In contrast, fragmentation in ion trap instruments (LIT, QIT) is achieved by resonance excitation of precursor ions. Here, the ions are excited with a precursor specific energy and collisions with the inert gas cause fragmentation [9-10]. The excitation energy is not sufficient for exciting previously formed fragment ions.

Due to the specific fragmentation pattern, sequence information can be deduced from the b- and y-ion series. In case of *de novo* sequencing nearly complete b- or y-ion series are mandatory, whereas searching of fragment spectra against a protein database via peptide fragment mass fingerprint analysis even partial b- and y-ion series can successfully identify a peptide sequence [17]. The broad application of CID experiments for peptide characterization revealed early that b- and y-ions have different stabilities leading to product ion spectra with high numbers of y-ions but often a minor number of b-ions (19-20). Especially, analyzing tryptic digest the different intensity of b- and y-ions is more pronounced because y-ion *per se* contain a C-terminal basic amino acids (arginine and lysine) which produce more intense signals in the positive analysis mode [18-20].

It has been accepted that y-ions are protonated amino acids or protonated truncated peptides, whereas the structures of b-ions are much more complex and variable [21]. In general, b-ions have an oxazolone structure [14, 21] and can form linear as well as cyclic conformers [21-29]. There is evidence that b₂ and larger b-ions form fully cyclic structures [21-22, 30-35]. These cyclic structures are formed via a C-terminal oxazolone intermediate (ring formation) by nucleophilic attack of the N-terminal amine function on the carbonyl function of the oxazolone structure of the b-ion (head-to-tail cyclization) [31]. The possible reopening of the cyclic peptide at several positions can lead to scrambling of the initial amino acid sequence and thus lead to a complex variety of oxazolones [21, 25, 31, 34]. Further fragmentation of these scrambled b-ions leads to fragment ions (a-ions or lower b-ions) that are hard to assign to the initial peptide [30-31]. Quantifying the proportion of b-ion cyclization is still object of recent research [36].

Detailed analyses of large-scale spectra databases underlined these observations and additionally revealed that the fragmentation pattern depends on CID technique [37]. First reports on underrepresentation of b-ions were shown for QToF instruments (beam-type CID) [37-38], but also slight differences were reported for ion trap instruments (resonance excitation CID) [19-20]. But until now, data experimentally evaluating and quantifying the underrepresentation of b-ions on different MS platforms is missing. Here, we systematically analyzed a standard tryptic protein digest on two ion trap instruments, linear ion trap (LIT) and three-dimensional ion trap (QIT), and one quadrupole time-of-flight instrument (QToF) statistically evaluating b- and y-ion series in a prospective approach. By N-terminal acetylation of tryptic peptides we show for the first time that b-ion cyclization reaction significantly contributes to b-ion underrepresentation on all examined instrument platforms even on ion traps.

MATERIAL AND METHODS

Sample preparation

The proteins Glucose oxidase (*Aspergillus Niger*) (Serva, Heidelberg, Germany), Lipase (*Burkholderia Glumae*) (Serva, Heidelberg, Germany) and Alpha-crystallin (*Bos Taurus*) (Sigma-Aldrich, München, Germany) were separately digested and afterwards mixed together. For digestion 1 mg of each protein was solved in 100 μ L 40 mM ammonium bicarbonate with 10 μ L acetonitrile (Biosolve, Valkenswaard, Netherlands) and digested with trypsin 1:50 (Promega, Mannheim, Germany) at 37 °C for 16 h. Finally the digests were filtered using 3 kDa cut-off CentriconsTM (Millipore, Schwalbach, Germany) at 16,000 x g for 15 min and mixed together. For peptide acetylation 3 pmol of the digested 3-protein-mix was dried in a SpeedVacTM, dissolved in 20 μ L 50 mM ammonium bicarbonate and incubated with acetic anhydride (Acros Organics, Nidderau, Germany) dissolved in ethanol (1:3) (Sigma-Aldrich, München, Germany) for 1 h [39-40]. The pH was adjusted to be acidic (pH 6) during the acetylation reaction to ensure that monoacetylation occurred at the amino terminus. For LC-MS/MS analysis 3 ng (25 fmol of each protein) of acetylated (Ac) and non-acetylated (nAc) protein-mix were applied.

LC-MS/MS data collection

LC-ESI-MS/MS measurements were carried out using different HPLC-MS systems. Bruker MaxisTM (QToF) and HCTultra IITM (QIT) mass spectrometers (Bruker Daltonics, Bremen, Germany) were coupled with nanoHPLC UltiMate 3000TM (Thermo Fisher Scientific, Bremen, Germany) and Thermo LTQ VelosTM (LIT) mass spectrometer (Thermo Fisher Scientific, Bremen, Germany) were coupled with RSLCnanoTM UPLC (Thermo Fisher Scientific, Bremen, Germany). Both LC systems were operated with a pre-column (C₁₈) and analytical column (C₁₈) setup. After injection of 15 μ L of each sample peptides were trapped, desalted (0.1 % aqueous trifluoroacetic acid) and then separated using a linear gradient from 4 % to 40 % (45 min) gradient solvent (84 % acetonitrile and 0.1 % formic acid in water). The flow rate was 400 nL/min. For all mass spectrometers the mass range for survey full scan MS spectra was m/z 300-1500. For fragmentation collision-induced dissociation (CID) was applied. All other mass spectrometer parameters were set to system specific standard values and were not changed during the acetylation experiment.

Database search and statistical analysis

Result files were converted into MASCOT Generic Format (.mgf) files using Data AnalysisTM (Bruker Daltonics, Bremen, Germany) for HCTultra IITM und MaxisTM and Proteome DiscovererTM (Thermo Fisher Scientific, Bremen, Germany) for LTQ VelosTM data. The MS data were searched against a UniProtKB/Swiss-Prot shuffled decoy database (519,348 sequences) using MASCOTTM (v2.2.0) algorithm (Matrix Science, London, United Kingdom). The following parameters were applied: enzyme: trypsin, missed cleavages: allow up to one, variable modifications: oxidation (methionine) and acetylation (N-term/lysine for acetylated samples), peptide tolerance: 15 ppm (Maxis), 0.3 Da (HCTultra IITM) and 0.4 Da (LTQ VelosTM), MS/MS tolerance: 0.1 Da (MaxisTM), 0.3 Da (HCTultra IITM) and 0.4 Da (LTQ VelosTM), peptide charge: 2+ and 3+ and monoisotopic mass. For the analysis of identified ion series the Fragmentation Analyzer tool [41] was used. Briefly, Fragmentation Analyzer can analyze the influence of the following parameters: (i) the instrument used for the identifications; (ii) the modification status of the N- and C-terminus of the identified peptides; (iii) the charge of the identified peptides; and (iv) post-translational modifications detected for the identified peptides. First, it is required to load an input file of a MS search engine (MASCOT, OMSSA, etc.) into the Fragmentation Analyzer tool. After selection of parameters, the tool finds a set of matching identifications, groups these by peptide sequence, and presents them for further analysis [41]. MASCOT input files (.dat) were loaded into the Fragmentation Analyzer and the peptides were filtered according to the following properties: all peptides had a precursor charge of 2+, unmodified C-terminals (acetylation of lysine and arginine were not considered) and acetylated or unmodified N-terminals. Only peptides confidently identified by a MASCOT score (≥ 30) search were considered. Twenty common peptides (supplement) were selected for analysis eluting over the whole LC gradient and reproducibly detected in three LC-MS/MS runs per instrument at least. For statistical analysis the occurrence of ions in MS spectra was used. The calculation of b- and y-ions occurrence was performed using a fragment ion probability plot generated by the Fragmentation Analyzer tool [41]. For the comparison between different MS platforms b-ion occurrence was normalized by y-ion occurrence. For testing of statistical significance of ion occurrence between different MS platforms Tukey's honestly significant difference (HSD) Post-Hoc-Test ($p < 0.05$) was applied. For calculation of significance difference of $p < 0.05$ between b- and y-ions occurrences on the same instrument Student's *t*-test was used.

RESULTS AND DISCUSSION

Fragment analysis of proteins and peptides by mass spectrometry using collision-induced dissociation revealed that the pairwise generated N-terminal b- and C-terminal y-ions have different stabilities [21]. Detailed analyses of large-scale spectra databases and synthetic peptides underlined these observations and additionally revealed that the fragmentation pattern is instrument-specific [37-38]. It has been shown that instruments facilitating beam-type CID (triple quadrupole instruments, QToF) with excitation energies of around 100 eV exhibit an underrepresentation of b-ions [37-38, 42]. For ion traps (QIT, LIT) utilizing resonant-excitation energy CID (< 2eV) it was reported that y-ions were more than twice as intense as b-ions; however systematic evaluation has not been performed [19]. A detailed analysis of the influence of amino acids' basicity on fragmentation ion peak intensities on ion trap instruments revealed that fragment ions containing the basic amino acids arginine, lysine and histidine generate more intense peaks [20]. But until now, no experimental approach has been undertaken to analyze underrepresentation of b-ions facilitating different CID types. For the experimental evaluation of the observation of underrepresentation of b-ions on different MS platforms we decided to analyze tryptic proteins digest instead of synthetic peptides to approach the realistic situation of MS-based protein analysis. To avoid the above mentioned influence of basic amino acids on ion intensity we only consider tryptic peptides represented on all MS platforms containing arginine and lysine and normalized the b-ions occurrence by the y-ions. Because it has been shown that averaged spectra are more reliable to analyze ion series we decided to consider Fragment Analyzer tool instead of representative spectra [38, 41]. Furthermore, we decided to consider the ion occurrence instead of the ion intensity because protein identification in common proteomics strategies relies not on ion intensities. Altogether 95 LC-MS/MS runs, including non-acetylated and acetylated samples, were performed using a QIT, a LIT and a QToF instrument. In total more than 15,000 spectra (≥ 2 per peptide) were evaluated. All peptides considered for statistic evaluation were consistently identified by MASCOTTM. Over 75,000 b- and y-ions could be assigned to the twenty common peptides (Tab 1S) in all LC-MS/MS runs. The selected peptides elute over the whole LC gradient to prevent any potential bias in the data due to differing distributions of amino acid frequencies or compositions in the sequences of the peptides. Analysis of ion statistics based on average values of b-ion and of y-ion occurrence of twenty selected peptides identified in at least three LC-MS/MS runs per MS. To avoid any potential bias by different ionization efficiency and fragmentation techniques of used MS platforms b-ion occurrence

was normalized by the y-ion occurrence. Statistical significance of ion occurrence between MS platforms was determined by Tukey's HSD Post-Hoc-Test. Tukey's HSD test is a single-step multiple comparison procedure in conjunction with an ANOVA to find if normalized means of b-ions are significantly different between the instruments.

Determination of b-ion statistic on different mass spectrometer platforms

Fragmentation and fragment ion analysis is a favorite technique to characterize peptides primary structure by mass spectrometry. Although major processes of peptide fragmentation have already been described [15, 21, 25] the detailed elucidation of peptides' fragmentation reaction in the gas-phase or even prediction of fragment spectra is still far from realization. In the past experiments ranging from single synthetic peptide analysis [22-32] to the in-depth data analysis of spectra databases have been performed to elucidate the fragmentation process of peptides [37-38]. In recent years the gas-phase chemistry of b-ions became of increasing interest. The analysis of spectra databases has shown that b-ions in comparison to y-ions are underrepresented in MS/MS spectra acquired on MS instruments with beam-type CID [37-38, 42]. The instability of b-ions in applied CID conditions makes them more susceptible to post-CID reactions leading to much more complex and variable structures of b-ions' gas-phase chemistry [21, 25].

Our aim was to answer the question if the underrepresentation of b-ions varies significantly on different MS platforms (QIT, LIT, QToF) depending on their CID type and quantify b-ion degradation via head-to-tail-cyclization reaction as one major pathway.

In agreement with the discussed observation of Lau *et al.* [37] we could confirm that b-ions in comparison with y-ions are underrepresented on the QToF instrument (see Figure 1 non-acetylated example peptide EM(Ox)GGVVDNAAR). We could also show that beside underrepresentation of b-ions on the QToF instrument b-ions are also significantly underrepresented on ion trap instruments and therewith statistically confirm the observation of Tabb *et al.* [19-20] (Figure 2 QIT and LIT). Although the underrepresentation of b-ions is significant on all considered platforms, the QToF instrument with a normalized b-ion occurrence of around 25 % exhibit the greatest difference between b- and y-ions. The normalized b-ion occurrence for QIT and LIT is about 71 % and 82 %, respectively. Furthermore, detailed inspection showed that the resonant-excitation energy CID utilizing ion trap instruments exhibit an even distribution of b-ions and y-ions over the entire m/z range without any maximum (Figure 2 QIT and LIT), whereas the beam-type CID applying QToF

instrument showed a maximum for y-ions at y_6 and for b-ions at b_3 (Figure 2 QToF). The absence of long-chained b-ions on the QToF instrument could be a hint of secondary fragmentation of b-ions ($b_n \rightarrow a_n \rightarrow b_{n-1} \rightarrow \dots$) or other degradation pathways [25, 43]. However, no significant increase of a-ions in the QToF instrument could be detected (data not shown).

Determining the influence of head-to-tail cyclization on b-ion occurrence

As a next step we were aiming at experimentally elucidating the role of b-ions' head-to-tail cyclization as one pathway of significant underrepresentation of b-ions. In contrast to stable y-ions ("protonated amino acids") b-ions tend to stabilize their structure in the gas-phase by cyclization or rearrangement reactions [21]. Beside CO loss and building of a-ions, sequence scrambling after head-to-tail cyclization and re-opening have been described as post-CID fragmentation and rearrangement processes of b-ions. Especially this unpredictable sequence scrambling infers with data analysis and hampers protein identification by common search algorithm.

The influence of initial head-to-tail cyclization on b-ion occurrence was determined by acetylation of the N-terminus of tryptic peptides. It has been shown that acetylation of the amino-N-atom at the N-terminus blocks the head-to-tail-cyclization reaction of b-ions [32, 34-35]. Effects on b-ion stability by acetylation can be neglected because it has been shown that monoacetylation has not significant influence in the overall basicity of peptides [18]. Therefore, only monoacetylated peptides were considered for further data interpretation. As already described for single peptides N-terminal acetylation leads to an increase in b-ion occurrence [32, 42] (see Figure 1 acetylated example peptide EM(Ox)GGVVDNAAR). As depicted for the selected peptide EM(Ox)GGVVDNAAR acetylation leads to an increase in b-ion occurrence (Figure 1). We assume that un-matched m/z values are peptide species coming from internal fragments or scrambled sequences.

Statistical analysis revealed a significant increase of b-ions on all instruments, whereas acetylation does not influence y-ion occurrence (Figure 3 Box-Plot). On the QToF instrument b-ion occurrence improved by 17 % after blocking head-to-tail cyclization by acetylation and has its maximum at b-ion b_3 (Figure 3 QToF). For the ion trap instruments we could observe the same effect. The b-ion occurrence on QIT and LIT increased by 16 % and 15 %, respectively. On ion trap instruments (performing resonant-excitation energy CID) acetylation of peptides abolishes the difference between b-ion and y-ion occurrence and therefore b-ions

head-to-tail cyclization appears to be the dominant process leading to b-ion underrepresentation on ion trap instruments. For the QToF (performing beam-type CID) instrument the difference between y-ion and b-ion abundance is still statically significant (Figure 3 QToF). A possible explanation of this observation could be the impact of collisional energies on beam-type CID fragmentation which is more likely optimal for y-ion intensities. It would be interesting to analyze the impact of different collision energies on the intensity of b- and y-ions on beam-type CID-based instruments. Our experimental approach clearly demonstrates that b-ion cyclization contributes to a maximum of 16 % of the underrepresentation of b-ions independent of the utilized CID type. The comparison with recent reports relying on the prediction and assignment of scrambled ions is hindered by the unclear data situation. Goloborodko *et al.* reported that < 1 % of ions in the SwedCAD library (15,897 low energy CAD MS/MS spectra) could be matched to scrambled ion [36], whereas Dong *et al.* showed that in 390,000 CID spectra more than 10 % of ions could be matched to scrambled ions [44]. In the work of Saminathan *et al.* in 35 % of 43 peptides scrambling could be observed [45]. Therefore it would be interesting to combine both approaches of prediction of scrambled ions as well as experimental evaluation (N-terminal acetylation of peptides) and to adapt search engines for full interpretation of MS/MS spectra.

CONCLUSIONS

The underrepresentation of b-ions is a common feature of both beam-type (QToF) and resonant-excitation energy (LIT and QIT) CID type performing instruments.

The significant increase of b-ion occurrence by acetylation of peptides' N-terminus on all investigated instrument types let us conclude that the head-to-tail cyclization as an initial step for downstream degradation pathways of b-ions i.e. scrambling followed by fragmentation to a-ions and smaller species accounts for a maximum of 16 % of b-ion loss. The abolition of differences between b- and y-ion occurrence revealed that the underrepresentation of b-ions not only exist on resonant-excitation energy CID performing ion trap MS but also that head-to-tail cyclization is the dominant process and responsible for this loss.

As long as specific search algorithms don't reward for complete b- and y-ion series the loss of b-ions can be neglected in shotgun proteome analyses as shown by recent reports [36, 45]. But, in case of detailed sequence analysis like e.g. *de novo* sequencing or phosphorylation site determination when complete sequence coverage is required, underrepresentation of b-ion becomes an issue. Therefore, the adaption of sample preparation protocols or selection of instrument facilitating resonant-excitation energy CID will help to obtain more sequence information.

REFERENCES

- [1] Aebersold, R., Mann, M. Mass spectrometry-based proteomics. *Nature* **2003**, *422*, 198-207
- [2] Domon, B., Aebersold, R. Mass spectrometry and protein analysis. *Science* **2006**, *312*, 212-217
- [3] Yates III, J.R., Ruse, C.I., Nakorchevsky, A. Proteomics by Mass Spectrometry: Approaches, Advances and Applications. *Annu. Rev. Biomed. Eng.* **2009**, *11*, 49-79
- [4] Han, X., Aslanian, A., Yates III, J.R. Mass Spectrometry for Proteomics. *Curr. Opin. Chem. Biol.* **2008**, *12*, 483-490
- [5] Karas, M., Hillenkamp, F. Laser desorption ionization of proteins with molecular masses exceeding 10,000 Da. *Anal. Chem.* **1988**, *60*, 2299-2301
- [6] Fenn, J.B., Mann, M., Meng, C.K., Wong, S.F., Whitehouse, C.M. Electrospray ionization mass spectrometry of large molecules. *Science* **1989**, *246*, 64-71
- [7] Muñoz J., Heck A.J. Quantitative proteome and phosphoproteome analysis of human pluripotent stem cells. *Methods Mol Biol.* **2011**, *767*, 297-312
- [8] Zhou H., Di Palma S., Preisinger C., Peng M., Polat A.N., Heck A.J., Mohammed S. Toward a comprehensive characterization of a human cancer cell phosphoproteome. *J Proteome Res.* **2013**, *12*, 260-271
- [9] Busch, K.L., Glish, G.L., McLuckey, S.A. Mass Spectrometry/Mass Spectrometry: Techniques and Applications of Tandem Mass Spectrometry, VCH: New York, **1988**
- [10] McLafferty, F.W. Tandem Mass Spectrometry; Wiley: New York, **1983**
- [11] Johnson, R., Martin, S., Biemann, K., Stults, J., Watson, J. Novel fragmentation process of peptides by collision-induced decomposition in a tandem mass spectrometer: differentiation of leucine and isoleucine. *Anal. Chem.* **1987**, *59*, 2621-2625
- [12] Zubarev, R.A., Kelleher, N.L., McLafferty, F.W. Electron capture dissociation of multiply charged protein cations. A nonergodic process. *J. Am. Chem. Soc.* **1998**, *120*, 3265-3266
- [13] Zubarev, R.A., Haselmann, K.F., Budnik, B., Kjeldsen, F., Jensen, F. Towards an understanding of the mechanism of electron-capture dissociation: a historical perspective and modern ideas. *Eur. J. Mass Spectrom.* **2002**, *8*, 337-349
- [14] Wysocki, V.H. *et al.* Principles of mass spectrometry applied to biomolecules, Ed. by J. Laskin and C. Lifshitz; Wiley: New York, **2006**

- [15] Roepstorff, P., Fohlman, J. Proposal for a common nomenclature for sequence ions in mass spectra of peptides. *Biomed. Mass Spectrom.* **1984**, *11*, 601
- [16] Biemann, K. Contributions of Mass Spectrometry to Peptide and Protein Structure. *Biomed. Environ. Mass Spectrom.* **1988**, *16*, 99-111
- [17] McCormack, A.L., Eng, J., Yates III, J.R. Peptide Sequence Analysis on Quadrupole Mass Spectrometers. A Companion to Methods in Enzymology. *Academic Press* **1994**, *6*, 274-283
- [18] Dongré, A.R., Jones, J.L., Somogyi, A., Wysocki, V.H. Influence of Peptide Composition, Gas-Phase Basicity and Chemical Modification on Fragmentation Efficiency: Evidence for the Mobile Proton Model. *J. Am. Chem. Soc.* **1996**, *118*, 8365-8374
- [19] Tabb, D.L., Smith, L.L., Breci, L.A., Wysocki, V.H., Lin, D., Yates III, J.R. Statistical Characterization of Ion Trap Tandem Mass Spectra from Doubly Charged Tryptic Peptides. *Anal. Chem.* **2003**, *75*, 1155
- [20] Tabb, D.L., Huang, Y., Wysocki, V.H., Yates III, J.R. Influence of Basic Residue Content on Fragment Ion Peak Intensities in Low-Energy Collision-Induced Dissociation Spectra of Peptides. *Anal. Chem.* **2004**, *76*, 1243
- [21] Harrison, A.G. To b or not to b: The ongoing Saga of Peptide b Ions. *Mass. Spec. Rev.* **2009**, *28*, 640-654
- [22] Harrison, A.G., Csizmadia, I.G., Tang, T.H. Structure and fragmentation of b₂ ions in peptide mass spectra. *J. Am. Soc. Mass Spectrom.* **2000**, *11*, 427-436
- [23] Yalcin, T., Khouw, C., Csizmadia, I.G., Peterson, M.R., Harrison, A.G. Why are B Ions Stable Species in Peptide Mass Spectra? *J. Am. Soc. Mass Spectrom.* **1995**, *6*, 1165-1174
- [24] Yalcin, T., Csizmadia, I.G., Peterson, M.R., Harrison, A.G. The Structures and Fragmentation of B_n ($n \geq 3$) Ions in Peptide Mass Spectra. *J. Am. Soc. Mass Spectrom.* **1996**, *7*, 233-242
- [25] Paizs, B., Suhai, S. Fragmentation Pathways of Protonated Peptides. *Mass. Spectrom. Reviews* **2005**, *24*, 508-548
- [26] Paizs, B., Lendvay, G., Vékey, K., Suhai, S. Formation of b₂⁺ Ions from Protonated Peptides. An Ab Initio Study. *Rapid Commun. Mass Spectrom.* **1999**, *13*, 525-533

- [27] Nold, M.J., Wesdemiotis, C., Yalcin, T., Harrison, A.G. Amide Bond Dissociation in Protonated Peptides. Structures of the N-terminal Ionic and Neutral Fragments. *Int. J. Mass Spectrom. Ion Process.* **1997**, *164*, 137–153
- [28] Rodriguez, C.F., Shoeib, T., Chu, I.K., Siu, K.W.M., Hopkinson, A.C. Comparison between Protonation, Lithiation and Argentionation of 5-Oxazolones. A Study of a Key Intermediate in Gas-Phase Peptide Sequencing. *J. Phys. Chem. A* **2000**, *104*, 5335-5342
- [29] Harrison, A.G., Csizmadia, I.G., Tang, T.H. Structures and Fragmentation of b_2 Ions in Peptide Mass Spectra. *J. Am. Soc. Mass Spectrom.* **2000**, *11*, 427-436
- [30] Yague, J., Paradela, A., Ramos, M., Ogueta, S., Marina, A., Barabona, F., de Castro, J.A., Vazquez, J. Peptide Rearrangement During Ion Trap Fragmentation: Added Complexity to MS/MS Spectra. *Anal. Chem.* **2003**, *75*, 1524-1535
- [31] Harrison, A.G., Young, A.B., Bleiholder, C., Suhai, S., Paizs, B. Scrambling of Sequence Information in Collision-Induced Dissociation of Peptides. *J. Am. Chem. Soc.* **2006**, *32*, 10364-10365
- [32] Jia, C., Qi, W., He, Z. Cyclization Reactions of Peptide Fragment Ions during Multistage Collisionally Activated Decomposition: An Inducement to Lose Internal Amino Acid Residues. *J. Am. Soc. Mass Spectrom.* **2007**, *18*, 663-678
- [33] Mous, L., Aubagnac, J.L., Martinez, J., Enjalbal, C. Low Energy Peptide Fragmentations in an ESI-Q-ToF Type Mass Spectrometer. *J. Proteome Res.* **2007**, *6*, 1378-1391
- [34] Harrison, A.G. Peptide Sequence Scrambling through Cyclization of b_5 Ions. *J. Am. Soc. Mass Spectrom.* **2008**, *19*, 1776-1780
- [35] Harrison, A.G. Cyclization of Peptide b_9 Ions. *J. Am. Soc. Mass Spectrom.* **2009**, *20*, 2248-2253
- [36] Goloborodko, A.A., Gorshkov, M.V., Good, D.M., Zubarev, R.A. Sequence Scrambling in Shotgun Proteomics is Negligible. *J. Am. Soc. Mass Spectrom.* **2011**, *22*, 1121-1124
- [37] Lau, K.W., Hart, S.R., Lynch, J.A., Wong, S.C.C., Hubbard, S.J., Gaskell, S.J. Observations on the detection of b- and y-type ions in the collisionally activated decomposition spectra of protonated peptides. *Rapid Commun. Mass Spectrom.* **2009**, *23*, 1508-1514
- [38] Barsnes, H., Eidhammer, I., Martens, L. A Global Analysis of Peptide Fragmentation Variability. *Proteomics* **2011**, *11*, 1181-1188

- [39] Samgina, T.Y., Kovalev, S.V., Gorshkov, V.A., Artemenko, K.A., Poljakov, N.B., Lebedev, A.T. N-Terminal Tagging Strategy for De Novo Sequencing of Short Peptides by ESI-MS/MS and MALDI-MS/MS. *J. Am. Soc. Mass. Spectrom.* **2010**, *21*, 104-111
- [40] Riordan, J.F., Vallee, B.L., Hirs, C.H., Serge, N.T. Acetylation. *In Methods in Enzymology, Academic Press: Oxford* **1972**, *15*, 494–499
- [41] Barsnes, H., Eidhammer, I., Martens, L. Fragmentation Analyzer: an open-source tool to analyze MS/MS fragmentation data. *Proteomics* **2010**, *10*, 1087-1090
- [42] Vachet, R.W., Bishop, B.M., Erickson, W., Glish, G.L. Novel Peptide Dissociation: Gas-Phase Intramolecular Rearrangement of Internal Amino Acid Residues. *J. Am. Chem. Soc.* **1997**, *24*, 5481-5488
- [43] Paizs, B., Bythell, B.J., Maître, P. Rearrangement Pathways of the a4 Ion of Protonated YGGFL Characterized by IR Spectroscopy and Modeling. *J. Am. Soc. Mass. Spectrom.* **2012**, *23*, 664-675
- [44] Dong, N., Liang, Y., Yi, L. Investigation of Scrambled Ions in Tandem Mass Spectra. Part 1. Statistical Characterization. *J. Am. Soc. Mass. Spectrom.* **2012**, *23*, 1209-1220
- [45] Saminathan, I.S., Wang, X.S., Guo, Y., Krakovska, O., Voisin, S., Hopkinson, A.C., Siu, K.W.M. The Extent and Effects of Peptide Sequence Scrambling Via Formation of Macrocyclic *b* Ions in Model Proteins. *J. Am. Soc. Mass. Spectrom.* **2010**, *21*, 2085-2094
- [46] Krokhin, O.V., Spicer, V. Peptide retention standards and hydrophobicity indexes in reversed-phase high-performance liquid chromatography of peptides. *Anal. Chem.* **2009**, *22*, 9522-9530

FIGURES

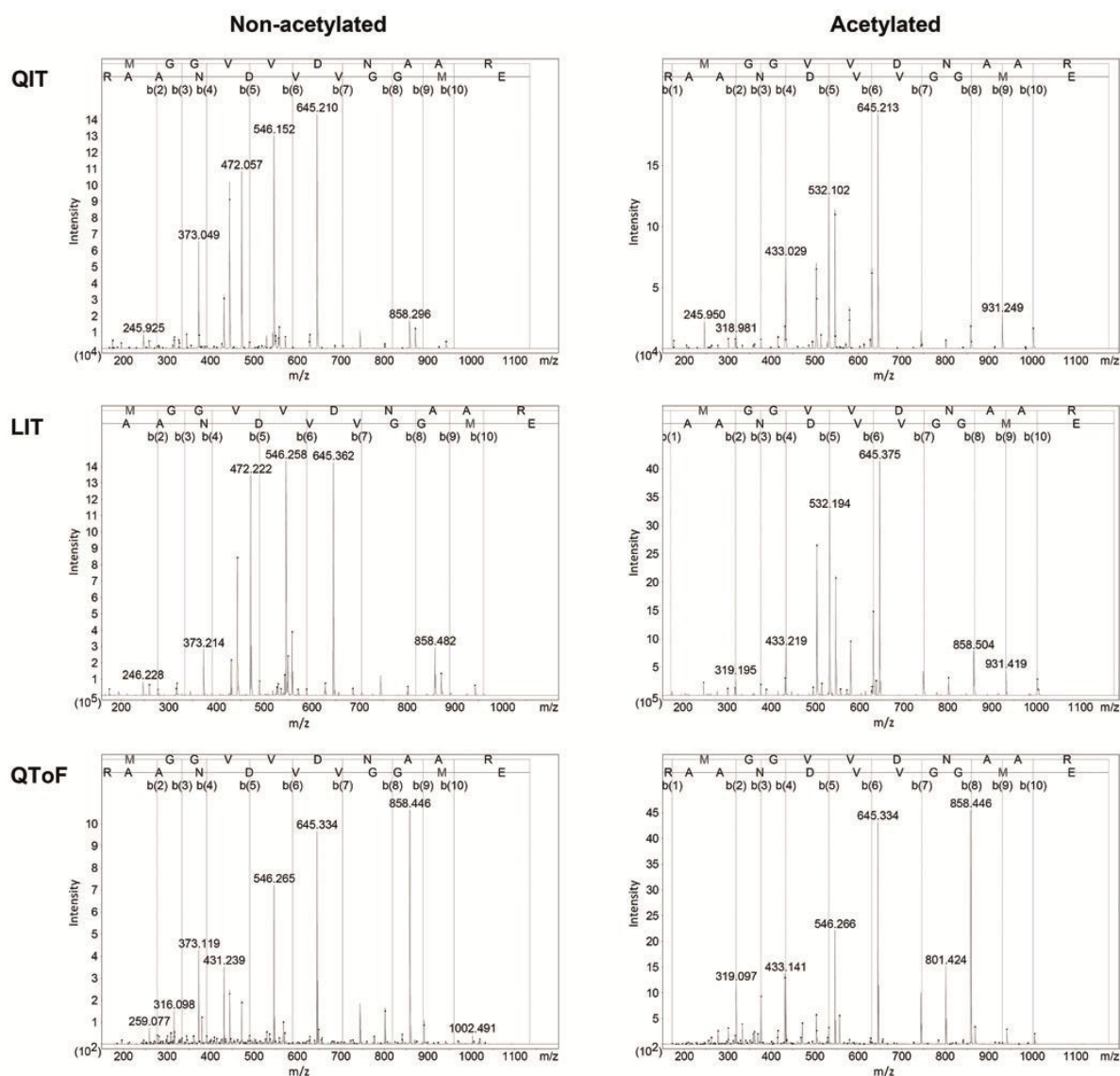


Figure 1 Representative fragment spectra (CID) of a single peptide (sequence: EM(Ox)GGVVDNAAR) from digested protein mix measured with different mass spectrometers (QIT, LIT and QToF) before and after acetylation. Continuous lines indicate identified b-ions, whereas the dashed lines indicate unmatched b-ions.

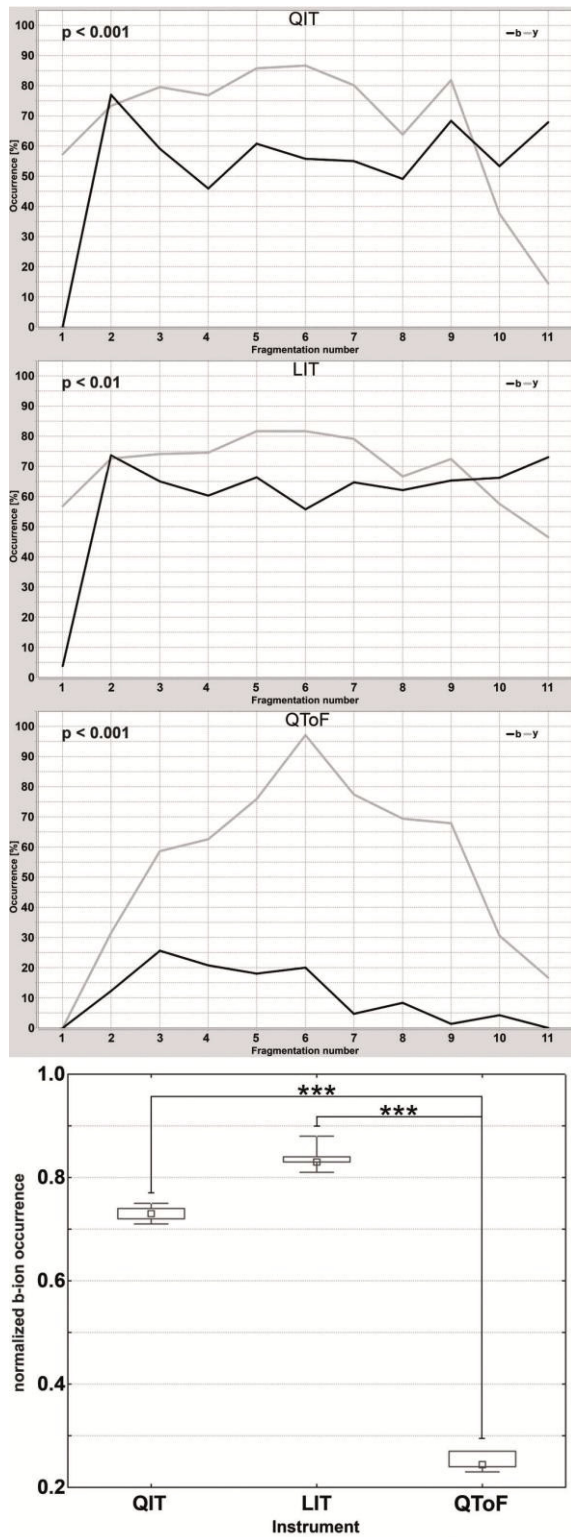


Figure 2 Occurrence of b- and y-ions on different mass spectrometer platforms of digested protein mix. On the x-axis fragment number and on the y-axis occurrence in percent (%) is plotted. The black line represents the b-ion occurrence and the gray line the y-ion occurrence. The plotted p-value describes the difference between b- and y-ion occurrence of the same mass spectrometer calculated by Student's *t*-test. The Box-Whisker-Plot shows the normalized b-ion occurrence of the mass spectrometers. Significance is calculated across ion trap and QToF instruments by Tukey's HSD Post-Hoc-Test.

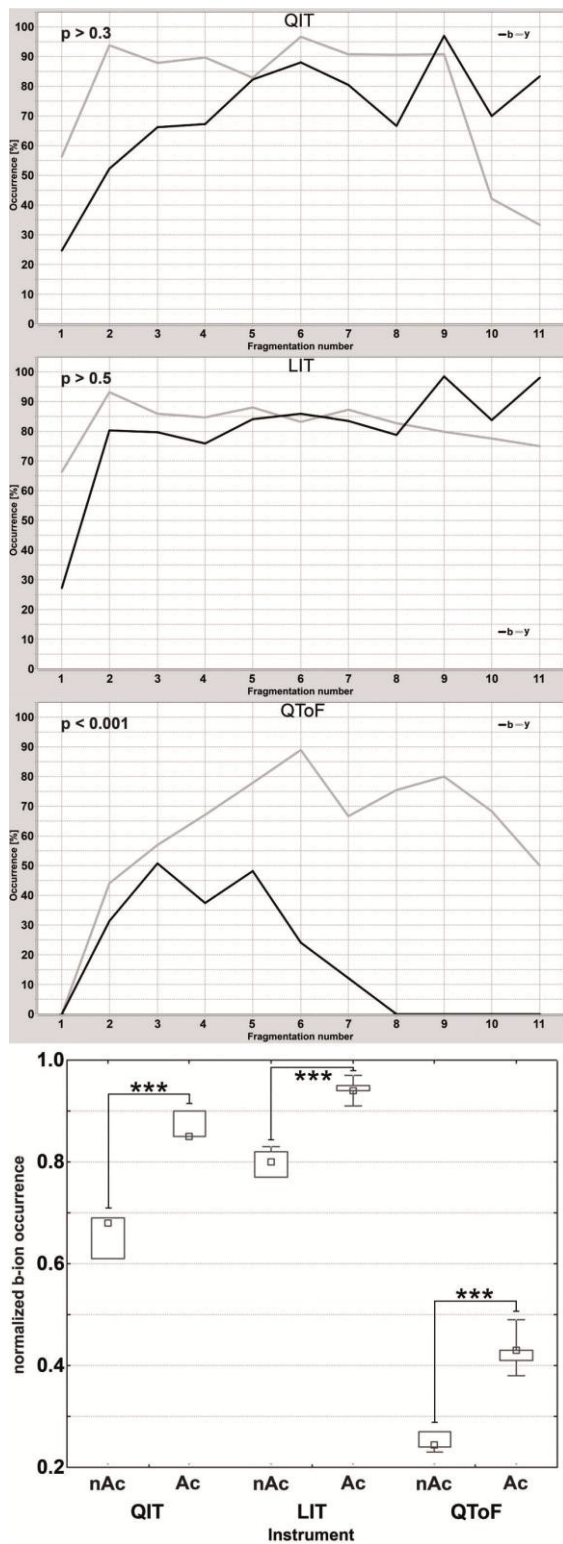


Figure 3 Occurrence of b- and y-ions on different mass spectrometer platforms analyzing acetylated peptide mixture. On the x-axis fragment number and on the y-axis occurrence in percent (%) is plotted. The black line represents the b-ion occurrence and the gray line the y-ion occurrence. The p-value of Student's *t*-test was considered as a measure to analyze significance between b- and y-ions occurrences. The Box-Whisker-Plot shows the normalized b-ion occurrence of the different MS instruments with p-value calculated by Tukey's HSD Post-Hoc-Test.

SUPPLEMENTARY MATERIAL

Table 1S Selected peptides used for statistical evaluation. Calculation of the hydrophobicity factor (HF) is based on Krokhin *et al.* [46].

Sequence	Accession	Gene ID	Protein	Organism	Length	HF
EEKPSSAPSS	P02470	CRYAA	Alpha-crystallin	<i>Bos Taurus</i>	10	2.17
GNTHNVYAK	P13006	GOX	Glucose oxidase	<i>Aspergillus Niger</i>	9	4.52
AAATQLAR	P13006	GOX	Glucose oxidase	<i>Aspergillus Niger</i>	8	10.16
EEKPAVTAAPK	P02510	CRYAB	Alpha-crystallin	<i>Bos Taurus</i>	11	11.01
QDDHGYSR	P02470	CRYAA	Alpha-crystallin	<i>Bos Taurus</i>	9	11.16
AHELLNTK	P13006	GOX	Glucose oxidase	<i>Aspergillus Niger</i>	8	11.98
ASGQNDGLVSR	Q05489	LIPA	Lipase	<i>Burkholderia Glumae</i>	11	12.46
IPSGVDAGHSER	P02470	CRYAA	Alpha-crystallin	<i>Bos Taurus</i>	12	13.71
QDEHGFISR	P02510	CRYAB	Alpha-crystallin	<i>Bos Taurus</i>	9	14.33
QVLAATGATK	Q05489	LIPA	Lipase	<i>Burkholderia Glumae</i>	10	15.48
AVGVEFGTHK	P13006	GOX	Glucose oxidase	<i>Aspergillus Niger</i>	10	16.51
TLTTAQTATYNR	Q05489	LIPA	Lipase	<i>Burkholderia Glumae</i>	12	19.45
VYGVQGLR	P13006	GOX	Glucose oxidase	<i>Aspergillus Niger</i>	8	19.96
GYVHLDK	P13006	GOX	Glucose oxidase	<i>Aspergillus Niger</i>	8	19.97
EMGGVVDNAAR	P13006	GOX	Glucose oxidase	<i>Aspergillus Niger</i>	11	21.22
GANAEDEVAVIR	Q05489	LIPA	Lipase	<i>Burkholderia Glumae</i>	12	21.87
ALMSAVEDR	P13006	GOX	Glucose oxidase	<i>Aspergillus Niger</i>	9	23.44
DTGDDYSPIVK	P13006	GOX	Glucose oxidase	<i>Aspergillus Niger</i>	11	24.64
TVLDSGISEVR	P02470	CRYAA	Alpha-crystallin	<i>Bos Taurus</i>	11	26.94
TLGPFYPSR	P02470	CRYAA	Alpha-crystallin	<i>Bos Taurus</i>	9	28.75

3.3 Publikation II

Application of label-free proteomics for differential analysis of lung carcinoma cell line A549

Barbara Sitek¹, Daniel M. Waldera-Lupa^{1,2}, Gereon Poschmann^{1,2}, Helmut E. Meyer¹, Kai Stühler²

¹Department of Medical Proteomics/Bioanalytics, Medizinisches Proteom-Center, Ruhr-Universität Bochum, Bochum, Germany

²Molecular Proteomics Laboratory, Biologisch-Medizinisches Forschungszentrum (BMFZ), Heinrich-Heine-Universität, Düsseldorf, Germany

ABSTRACT

A label-free solution basing on a highly reproducible and stable LC-MS/MS system allows quantitative proteome analyses. Due to nonlabeling approach, the label-free method has the potential to measure samples from clinical specimen monitoring and comparing thousands of proteins. The presented label-free workflow includes in-solution digest, LC-MS analyses, data evaluation by the means of Progenesis™ software, and validation of the differential proteins. We successfully applied this workflow in a proteomics study analyzing the human lung carcinoma cell line A549 treated with transforming growth factor beta 1, a cell culture model of lung fibrosis. The differential analysis of only 1 µg protein per sample led to 202 significantly regulated proteins.

INTRODUCTION

A label-free solution for relative quantitative proteomics is based on two different strategies for protein quantification. On the one hand, the relative peptide ion intensities measured by liquid

Chromatography in combination with mass spectrometry to calculate expression levels of proteins can be used. The high correlation of mass spectral peak intensities of peptide ions and protein abundances has been demonstrated in numerous studies (1, 2). On the other hand, the label-free quantification can be performed by counting the number of fragment spectra identifying peptides of a given protein (see Chapters 20 and 22). Spectral count or peptide ion intensity are measured for individual LC-MS/MS runs and differences in protein abundances are calculated by direct comparison between different runs.

In contrast to labeling-based quantification techniques such as ICAT (see Chapter 24), iTRAQ (see Chapter 8), TMT (see Chapter 9), IPTL (see Chapter 10), ICPL (see Chapter 11), or SILAC (see Chapters 13, 14, 25, and 26), the label-free approach is proceeding without any isotopic or chemical labeling. For this reason, the limitation caused by the labeling (e.g., high cost of the reagents, incomplete labeling, or higher sample concentration) can be omitted in the label-free technique. Otherwise there are some challenges which are important requirements for successful realization of label-free quantification in biological samples. Due to a high sample complexity, the reproducibility and stability of the LC-MS system as well as appropriate software solution for data analysis are essential. This is challenging, especially when a large number of biological samples is analyzed. Therefore, all steps of the label-free approach have to be optimized in order to get valid data. Usually, this approach includes the following steps: (a) sample preparation with protein extraction and digestion; (b) peptides separation by liquid chromatography; and (c) data analysis including quantification, identification, and statistical analysis. Recent improvements in the sensitivity of MS and the reproducibility of LC have shown that label-free proteomics for a proteome-wide quantification of proteins in complex biological samples is feasible. This technique has the potential to become a significant complement to current quantification methods. The high-throughput compatibility of a label-free approach allows processing of large numbers of biological samples, which is required for statistically significant quantification.

We describe the application of a label-free approach for the identification of new candidate proteins involved in the development of lung fibrosis. We used human lung carcinoma cell line A549 as a biological system. Transforming growth factor beta 1 (TGF- β 1) is a key

effector cytokine in the development of lung fibrosis. The treatment of A549 cells using TGF- β is a well-established model for lung fibrosis. For the differential proteome study, seven biological replicates of A549 cell line were treated with TGF- β 1 and as control seven cell replicates without TGF- β 1 were applied. We used nano-HPLC coupled to an LTQ-Orbitrap™ mass spectrometer for generating peptide profiles and the Progenesis™ software for statistical analysis of the data (Fig. 1). Altogether 202 proteins have been found to be differentially expressed (fold change > 1.5 or < -1.5 , $p < 0.01$).

MATERIALS

Sample Preparation and Digestion

1. Ultrasonic bath (VWR, Darmstadt, Germany).
2. Hand homogenizer.
3. Lysis buffer: 2 M thiourea, 7 M urea, 30 mM Tris–HCl, pH 8.0.
4. Digestion: 50 mM ammonium bicarbonate (ABC), 45 mM DTT, 100 mM iodoacetamide (IAA), 100 ng/mL trypsin, formic acid (FA).

Liquid Chromatography

1. Dionex UltiMate 3000 Nano LC System (Dionex, Idstein, Germany).
2. Trap column: Acclaim PepMap100 C18 Nano-Trap Column (C18, particle size 5 mm, pore size 300 Å, I.D. 200 mm, length 1 cm; Dionex).
3. Nano column: Acclaim PepMap100 C18 Column (C18, particle size 3 mm, pore sizes 100 Å, I.D. 75 mm, length 25 cm; Dionex).
4. Loading solvent: 0.1 % (v/v) Trifluoroacetic acid (TFA) (MS grade).
5. Gradient solvent A: 0.1 % (v/v) FA (MS grade).
6. Gradient solvent B: 0.1 % (v/v) FA (MS grade), 84 % (v/v) Acetonitrile (ACN) (HPLC-S gradient grade).

Mass Spectrometry

1. LTQ-Orbitrap XL with an online nano-ESI source (Thermo Fisher Scientific, Bremen, Germany).
2. Distal Coated SilicaTips™ (New Objective, Woburn, USA).
3. Collision gas: nitrogen.

Data Analysis

1. Mascot v. 2.2.0 (Matrix Science, London, UK) (see Chapter 28).
2. Progenesis™ v. 2.5 (Nonlinear Dynamics, Newcastle, UK).

METHODS

General Practice

The human lung adenocarcinoma cell line A549 (ATCCCL-185) was grown in DMEM (high glucose, GlutaMAX and Pyruvate; Invitrogen Nr. 31966047) supplemented with 10 % FBS in a humidified incubator at 37 °C and 5 % CO₂ until cells were confluent. Subsequently, cells have been detached by trypsin and transferred to 2 × 7 10 cm diameter dishes (2.5 × 10⁶ cells/dish). Twenty-four hours later, the medium was removed and exchanged by serum-free medium. After 24 h of serum starvation and exchange of medium, TGF-β1 (25 ng/10 mL serum-free medium, RD-Systems 240-B, lot AV406041) was added to seven dishes and TGF-β1 reconstitution buffer to the other seven dishes. Twenty four hours after cell stimulation cells were harvested, washed with PBS, scraped using a rubber policeman, washed with PBS again, pelleted, snap frozen, and stored at –80 °C.

Sample Preparation and Enzymatic Digestion

1. Lyse the cells in lysis buffer (1.4 mL/mg sample; 4 °C) and sonicate the samples six times for 10 s on ice and finally centrifuge (16,000 × *g* for 15 min) the lysate and store the supernatant at –80 °C (see Note 1).
2. For the further analysis, it is necessary to know the concentration of the samples. To determine the concentrations a Bradford assay is performed.
3. For the proteolysis of proteins a tryptic in-solution digest is performed. Therefore, solve 5 mg protein (5 mL) in 129 mL ABC and reduce with 0.8 mL DTT (45 mM) for 15 min at 50 °C. Afterwards alkylate with 0.8 mL IAA (100 mM) in the dark at room temperature for 15 min. Add trypsin (1:50, w/w) to digest the protein overnight (max. 14 h) at 37 °C. Stop the digestion by adding 5 mL 1 % FA to the solution.
4. Before performing the LC-MS experiments centrifuge (16,000 × *g* for 30 min) the digested samples and transfer them into a clear vial (see Note 2). Afterwards add 0.1 % TFA to a final concentration of 1 mg/15 mL.

Peptide Separation with Reversed Phase High-Performance Liquid Chromatography

1. For separation of digested proteins, a reversed phase high-performance liquid chromatography is performed using the UltiMate™ 3000 Nano LC System (Dionex).

Therefore, a system comprising a nano-trap column (C18) and a nano-column (C18) is used. Heating the columns to a temperature of 60 °C allows high flow rate (400 nL/min) at tolerable pressure (see Note 3).

2. For injection of the samples, a volume of 15 mL is used. After injection the peptides will be trapped while detergents and salts will be washed out for 5 min (see Note 4). For loading, a flow rate of 30 mL/min is used.
3. A shallow gradient is applied for separation: (a) linear gradient from 5 % B to 35 % B over 150 min, then (b) to 95 % B in 2 min, (c) constant 95 % B for 3 min and finally (d) 20 min at 5 % B for equilibration (see Note 5). As flow rate of the gradient pump 400 nL/min is used.

Detection of Separated Peptides with Mass Spectrometry

1. The LTQ-Orbitrap™ mass spectrometer (Thermo Fisher Scientific) is operated in the data-dependent mode to switch automatically between MS and MS/MS acquisition.
2. Set the mass range for survey full scan MS spectra and MS/MS spectra to m/z 300–1,500.
3. For fragmentation collision-induced dissociation (CID) with nitrogen as collision gas is applied. Therefore, a top six methods based on the intensity is used (see Note 6). The minimal required signals for precursor ions are 5,000 counts and the isolation width is 2 ppm.
4. Reject charge state 1+ and prefer charge states 2+, 3+, and 4+ for precursor ion isolation.
5. Utilize dynamic exclusion with an exclusion duration of 35 s and one repeat count within 30 s. Exclusion list size of 500 precursor ions with an exclusion mass width of 5 ppm is used.
6. Finally export LC-MS analysis data as Thermo .RAW file format.

Differential Proteome Analysis

1. The differential proteome analysis is performed with Progenesis™ (Nonlinear Dynamics). Import the LC-MS analysis data files which are described previously.
2. Select the reference run that all other runs are aligned to. Therefore, select a run that has minimal noise and represents stable LC/MS conditions by consideration of the two-dimensional map (Fig. 2).

3. Alignment is the most important step in the label-free workflow. So it is necessary that the alignment will be done with high accuracy. Apply automatic alignment and afterwards check the alignment carefully. If automatic alignment does not work, manually add vectors to align the run.
4. Feature detection, normalization and quantification will be done automatically. Exclude or include features from the analysis results. Therefore, the LC washing and equilibration step is excluded. Include only charge states between 2+ and 5+ to exclude contaminations from the analysis (see Note 7).
5. Create the design of the experiment, e.g., untreated vs. treated samples. Runs which have no stable LC-MS conditions can be sorted out.
6. For differential analysis, it is necessary to have significant results. Therefore, features are filtered based on p -value ($p < 0.05$) and tagged for further analysis.
7. Perform a principal component analysis (PCA) to check the runs cluster based on the expected groups. Features also can be filtered based on their q -value to report false discovery rates and their statistical power within the experimental analysis.
8. Identify features which are differentially regulated (Fig. 3). Therefore, export these features in an .mgf file format and perform a Mascot™ (Matrix Science) (see Chapter 28) MS/MS-Ions search.

Identification of Differentially Regulated Proteins

1. For protein identification the Mascot™ search engine is used. The following parameters are used: (a) database: ipi.human. decoy, (b) enzyme: trypsin, (c) missed cleavages: allow up to one, (d) fixed modifications: propionamide (cysteine), (e) variable modifications: oxidation (methionine), (f) peptide tolerance: 4 ppm, (g) MS/MS tolerance: 0.4 Da, (h) peptide charge: 2+ and 3+, (i) monoisotopic, and (j) data format: mascot generic.
2. Export identification data as .xml file format and import these in Progenesis™. The imported data are not filtered yet, e.g., peptides with a low mascot score are included. Filter the identified peptides based on mascot score and decoy entries.
3. Check the identified proteins manually and solve problems with protein isoforms if possible. Afterwards validate the differentially regulated proteins manually.
4. Finally create a report of the analysis results.

NOTES

1. For tissue and body fluids the procedure can also be applied. This workflow could already be carried out successfully.
2. A tryptic digestion is never complete. To avoid clogging of the trap column it is necessary to remove undigested proteins. If the trap column is closed the LC/MS runs will not be reproducible.
3. Heating the columns is necessary to reduce the pressure of the system and to get a better separation of the peptides. But if the columns are heated the flow rate must be higher, because the HPLC need a minimum of pressure to work. The higher the flow rate, the worse the sensitivity. A compromise between separation and sensitivity is necessary.
4. The time for trapping and washing the samples depends on the length of the capillaries to the trap column and on the purity of the samples. If high salt concentrations were used it is necessary to expand the time for washing.
5. To avoid a bad reproducibility time for equilibration should be 20 min in minimum. If early eluting peptides in the LC-MS runs are not reproducible increase the time for equilibration.
6. A top six method means that the six most intense peaks of a full scan MS are selected for fragmentation (MS/MS).
7. The charge states of tryptic peptides are between 2+ and 5+. Contaminations mostly have charge state +1. If another protease as trypsin is used the charge states could be different.

REFERENCES

1. Bondarenko PV, Chelius D, Shaler TA (2002) Identification and relative quantitation of protein mixtures by enzymatic digestion followed by capillary reversed-phase liquid chromatography-tandem mass spectrometry. *Anal Chem* 74:4741–4749
2. Chelius D, Bondarenko PV (2002) Quantitative profiling of proteins in complex mixtures using liquid chromatography and mass spectrometry. *J Proteome Res* 1:317–323

FIGURES

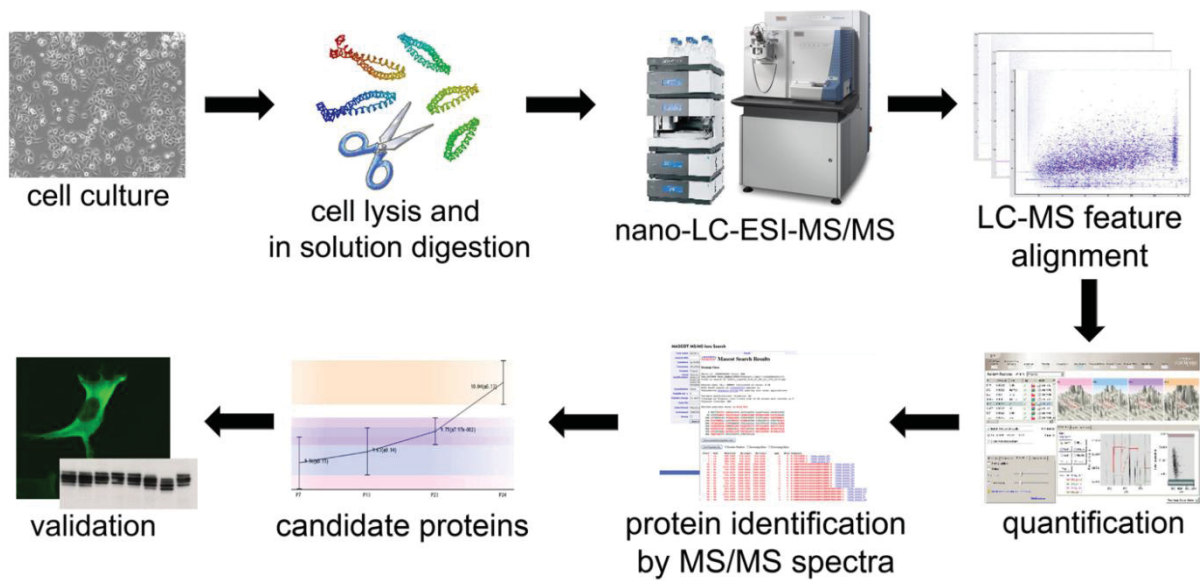


Figure 1 Workflow of the label-free proteomic approach applying LC-MS/MS. First the proteins will be extracted and digested with trypsin. After the digest LC-MS/MS data will be generated and evaluated with Progenesis™. The differential regulated proteins will be identified by using Mascot™. For validation of candidate proteins Western blots and immunohistochemistry will be performed.

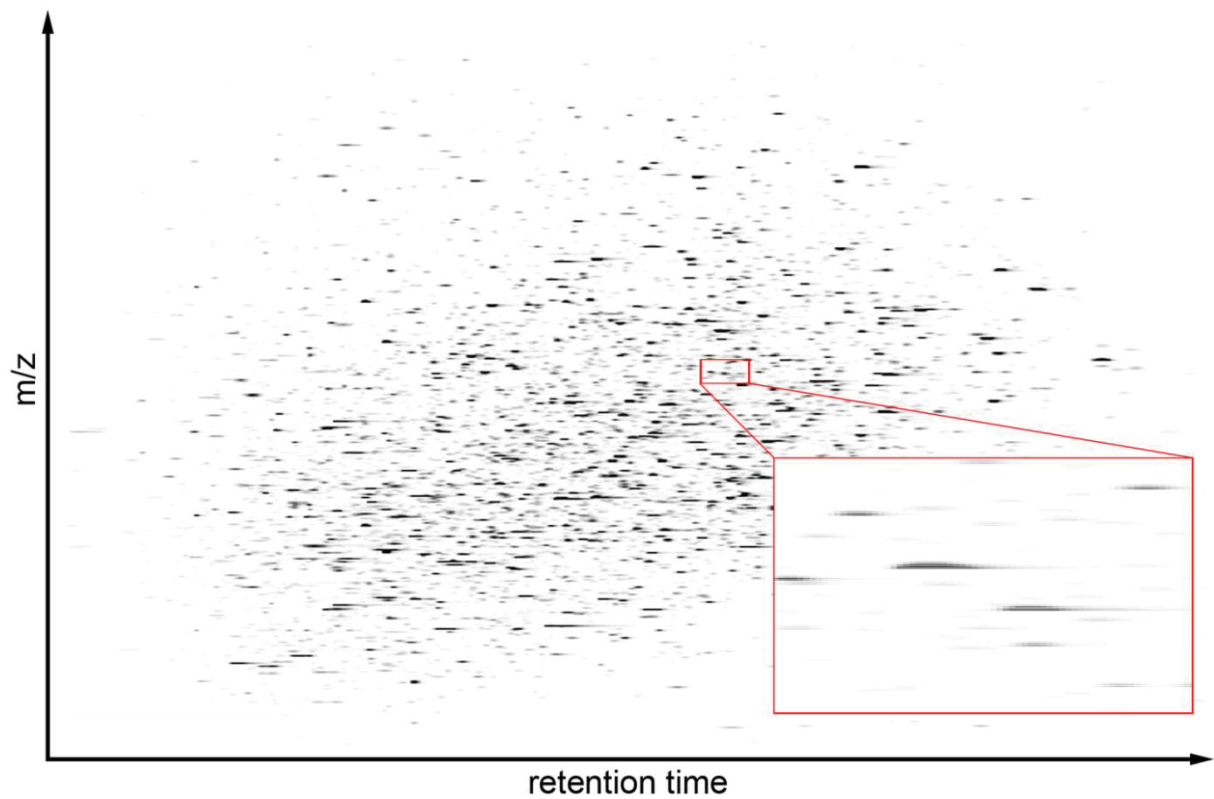


Figure 2 Two-dimensional display of the peptide LC-MS analysis from A549. The survey view displays m/z vs. retention time of the LC-MS run. The enlarged area shows the isotope pattern of the eluting peptides. The automated alignment of Progenesis™ is based on paired feature detection at the LC-MS level and does not reduce the data to the total ion chromatogram. This is followed by regression analysis in peptides retention time and m/z to produce an alignment grid used to accurately overlay the data.

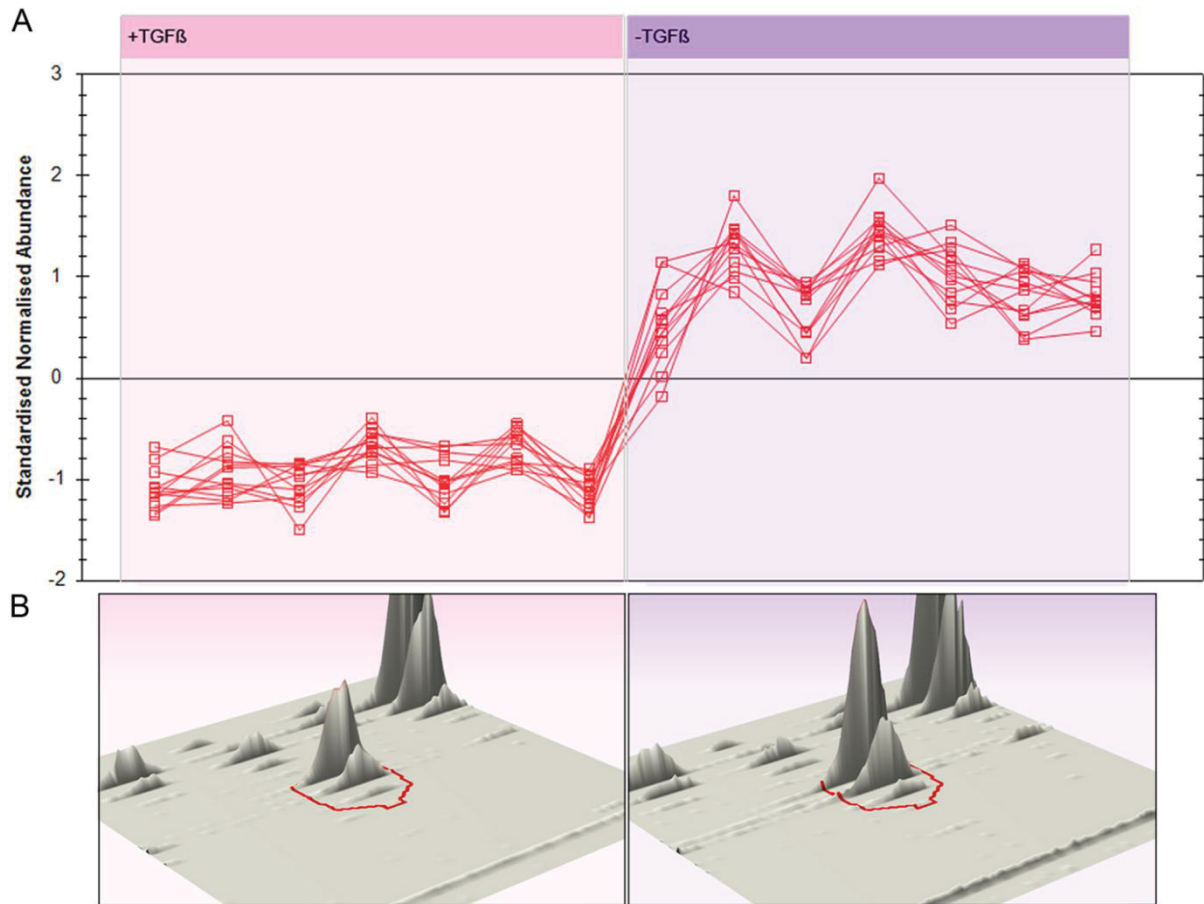


Figure 3 Regulation of the identified peptides from one single protein. (a) Twelve differentially regulated peptides from one protein which were identified in all samples. Each *square* stands for one peptide in each replicate for the respective condition. (b) Three-dimensional display of one specific peptide in both conditions. This view shows the regulation and also the isotopic pattern of the eluting peptide.

3.4 Publikation III

Proteome-wide analysis of primary cultures of *in situ* aged human fibroblasts reveals a moderate age-associated cellular phenotype

Daniel M. Waldera-Lupa^{1,2}, Faiza Kalfalah³, Ana-Maria Florea⁴, Steffen Sass⁵, Fabian Kruse^{1,2}, Vera Rieder^{1,2}, Julia Tigges⁶, Ellen Fritsche⁶, Jean Krutmann⁶, Hauke Busch^{7,8,9}, Melanie Boerries^{7,8,9}, Helmut E. Meyer¹⁰, Fritz Boege³, Fabian Theis¹¹, Guido Reifenberger^{4*} and Kai Stühler^{1,2*}

* These authors contributed equally

¹Institute for Molecular Medicine, Heinrich-Heine-University, Düsseldorf, Germany

²Molecular Proteomics Laboratory, Biomedical Research Centre (BMFZ), Heinrich-Heine-University, Düsseldorf, Germany

³Institute of Clinical Chemistry and Laboratory Diagnostics, Heinrich-Heine-University, Med. Faculty, Düsseldorf, Germany

⁴Department of Neuropathology, Heinrich-Heine-University, Düsseldorf, and German Cancer Consortium (DKTK), German Cancer Research Center (DKFZ), Heidelberg, Germany

⁵Institute of Computational Biology, Helmholtz Center Munich, German Research Center for Environmental Health, Neuherberg, Germany

⁶Leibniz Research Institute for Environmental Medicine (IUF), Düsseldorf, Germany

⁷Institute of Molecular Medicine and Cell Research, Albert-Ludwigs-University Freiburg, Freiburg, Germany.

⁸German Cancer Consortium (DKTK), Freiburg, Germany

⁹German Cancer Research Center (DKFZ), D-69120, Heidelberg, Germany

¹⁰Department of Biomedical Research, Leibniz-Institute for Analytical Science - ISAS, Dortmund, Germany

¹¹Department of Mathematics, Technical University Munich, Garching, Germany

SUMMARY

Several hallmarks for the aging process of fibroblasts have been defined. However, most studies on fibroblast aging focused on senescence and therefore considered cell models driven into replicative or stress-related senescence *in vitro*. Here, we analysed an *ex vivo* model of *in situ* aged human dermal fibroblasts, obtained from 15 adult healthy donors from three different age groups using an unbiased quantitative proteome-wide approach applying label free mass spectrometry. Thereby, we identified 2409 proteins, including 43 proteins with an age-associated abundance change. Most of the differentially abundant proteins have not been described in the context of fibroblasts' aging before, but the deduced biological processes confirmed known hallmarks of aging and led to a consistent picture of eight biological categories involved in fibroblast aging, namely proteostasis, cell cycle and proliferation, development and differentiation, cell death, cell organisation and cytoskeleton, response to stress, cell communication and signal transduction, as well as RNA metabolism and translation. The exhaustive analysis of protein and mRNA data revealed that 77 % of the age-associated proteins were not linked to expression changes of the corresponding transcripts. This is in line with an associated miRNA study and led us to conclusion that most of the age-associated alterations detected at the proteome level are likely caused post-transcriptionally rather than by differential gene expression regulation. In summary, our findings led to novel biomarkers of fibroblasts' aging and revealed that primary cultures of *in situ* aged fibroblasts are characterised by moderate age-related proteomic changes comprising the multifactorial process of aging.

INTRODUCTION

Aging is a multifactorial process that is characterised by distinct molecular and biological changes, such as increased genomic instability, telomere attrition, epigenetic alterations, loss of proteostasis, deregulated nutrient-sensing, mitochondrial dysfunction, cellular senescence and altered intercellular communication (Lopez-Otin *et al.*, 2013). It has been suggested that the aging process of the skin is mainly determined by alterations of its dermal stroma consisting predominantly of dermal fibroblasts and the extracellular matrix (Boukamp, 2005). The dermis is a highly stationary tissue compartment of mostly quiescent cells that cannot be removed quickly in case of dysfunction. Thus, the homeostasis of the dermis is primarily based on cellular adaptation and damage clearance and thereby prone to age-related changes. As the major cell source in the dermis and a long-lived cell system, dermal fibroblasts are able to accumulate aging-associated alterations and adapt their cellular functions. Therefore, dermal fibroblasts are a favored cell model to analyse the aging process of the skin. A broadly applied fibroblast aging model is based on the limited replicative lifespan of these cells (Tigges *et al.*, 2014). Although cellular senescence is one of the hallmarks of aging, it is unclear to which extent *in vitro* senescence models are representative for cell and organ aging *in vivo*. Moreover, most studies analysing *in vivo* and *in vitro* aging of fibroblasts focused on single genes or pathways (Tigges *et al.*, 2014), while comprehensive investigations of aging-associated alterations at the transcriptome-, miRNAome- and proteome-wide levels are sparse. In previous transcriptome-wide studies, replicative senescent (Kim *et al.*, 2013) and photo-aged fibroblasts (Greussing *et al.*, 2013) were analysed. These approaches revealed activation of the p53/p21 and p16(INK4a)/pRb pathways, differential expression of interleukins and differential expression of matrix metalloproteinases and their inhibitory proteins. There also is evidence that miRNA alterations are involved in the aging process. It was found that overexpression of the two miRNAs miR-152 and miR-181a is sufficient to induce senescence in fibroblasts (Mancini *et al.*, 2012). At the protein level, most studies analysed *in vitro* aging models of fibroblasts (Tigges *et al.*, 2014). Another model based on *in situ* aged fibroblasts which were cultured *ex vivo* was suggested for the investigation of the aging process. A proteome-wide study of *in situ* aged fibroblasts was reported by Boraldi *et al.* who used two-dimensional gel electrophoresis coupled with MALDI-MS (Boraldi *et al.*, 2003). Altogether, they identified several cellular processes as being altered during aging, including proliferation, metabolism, response to stress, cytoskeletal organisation, as well as protein synthesis and degradation. So far, a detailed systems biological study simultaneously

analysing aging-associated changes at the mRNA, miRNA and proteome levels has not been conducted. Here, we report a proteome-wide study integrating transcriptome and miRNAome data of primary, *ex vivo* cultured adult human dermal fibroblasts obtained from 15 donors of different ages. By performing combined bioinformatic analyses of the distinct large-scale data sets, we aimed to characterise aging-associated molecular changes and to identify relevant biological processes and regulatory mechanisms.

RESULTS

To reveal relevant biological processes and candidate proteins involved in the adaption of human dermal fibroblasts during the process of human skin aging, we analysed an *ex vivo* model of *in situ* aged human dermal fibroblasts by proteome-wide approach integrating large-scale data from associated transcriptome and miRNA studies. In a previous work (Waldera-Lupa *et al.*, unpublished data) we have shown that this model encompasses DNA-SCARS, which are neither accompanied by induced DNA double strand breaks nor decreased cell viability nor telomere shortening, and exhibit a secretory phenotype differing from the senescence-associated secretory phenotype (Coppe *et al.*, 2010) of common aging model systems.

Proteome-wide characterisation of *in situ* aged and *ex vivo* cultured dermal fibroblasts

At first, we analysed proteins expressed in *ex vivo* cultured human dermal fibroblasts by a proteomic approach using quantitative mass spectrometry (MS). Using a label-free MS approach, we identified a total of 2409 proteins analysing 15 primary fibroblast cultures obtained from each five young (20-30), middle aged (40-50) and old (60-70) female donors. Due to high reproducibility of our label-free MS analysis we were able to consider 1607 proteins for quantitative analysis. Statistical analysis revealed 43 proteins with a significant age-associated expression ($p \leq 0.05$), whereof 20 and 23 proteins exhibit positive and negative correlation with age, respectively (Tab. 1 and Tab. S1). However, principal component analysis revealed an almost homogeneous protein expression pattern of the three age groups with a low separation within the aged samples (Fig. S1). By detailed analysis of the proteome data we revealed that over 47 % (755 proteins) of quantified proteins exhibited a constant abundance across all age groups and thus likely account for this homogeneous protein expression pattern (Tab. S2; Fig. S2). By means of enrichment analysis we found that fibroblasts maintain protein abundance for biological processes such as ‘translation’, ‘metabolism of proteins’ and ‘metabolism of RNA’ during aging (Tab. S3). To reveal proteomic changes beyond the housekeeping processes, we analysed the proteome data considering proteins’ abundances. Therefore, we ranked the quantified proteins into four abundance classes over a dynamic abundance range of approximately five orders of magnitude (Fig. 1). This approach revealed that groups of proteins linked to specific biological processes demonstrated coordinated abundance changes during aging. For instance

a group of five proteins (MTCO2, NDUFA5, NDUFA9, NDUFA10, NDUFS6) linked to the biological process ‘mitochondrial ATP synthesis coupled electron transport’ appeared among the semi-abundant proteins (class III) for the young and middle age group, but among the low-abundant proteins in the old aged donors (class IV; Tab. S4-6). For the other abundance classes (class I-II) we found no age-associated changes. Due to observed age-associated changes of mitochondrial proteins we performed a detailed analysis of proteins related to mitochondria. Cluster analysis revealed 23 age-associated mitochondrial proteins ($p \leq 0.1$; 14 negative and 9 positive). Under the proteins with negative age-correlation the biological processes ‘ATP synthesis’ and ‘cellular respiration’ were significantly enriched. The biological processes ‘response to stress’ and ‘catabolism’ were enriched for proteins with a positive age-correlation (Fig. S3; Tab. S7). Proteome-wide characterisation revealed that *in situ* aged fibroblasts exhibit a moderate age-associated cellular phenotype with a large number of proteins exhibiting a constant abundance across the three age groups.

Transcriptome-wide characterisation of *in situ* aged and *ex vivo* cultured dermal fibroblasts

At next, we considered gene expression data from the same *in situ* aged fibroblasts already published by Kalfalah and colleagues (Kalfalah *et al.*, 2014). It was reported that about 17,000 transcripts were successfully quantified, whereof a total of 137 genes exhibited a significant age-associated differential expression (Tab. S8). Comparison between the proteome and transcriptome data revealed that for almost all proteins (98 %) gene expression data were available, but on the contrary the coverage for the 137 age-associated gene by proteome data was quite low (Fig. 2A). Only eight of the 137 differentially changed genes were successfully quantified at the proteomic level and exhibited no agreement with the respective mRNA data concerning age-associated differential expression. Due to intraspecies comparison with an 87 % and 98 % correlation within the proteome and transcriptome data, respectively, we exclude technical problems for the minor overlap of the expression data. The interspecies comparison with about 30 % correlation between proteins and mRNAs data was in the expected range (Fig. 2B; Fig. S4). Further detailed analysis revealed that over 63 % (10665 quantified mRNAs) of the analysed genes exhibited constant expression across the different age groups (Fig. S5; Tab. S9). In contrast, for all of the 43 age-associated proteins we obtained gene expression data and found out that 77 % (33 proteins) of the corresponding transcripts were not changed during aging. Comparison of these age-associated proteins with

transcriptome data revealed that age-associated proteins were not differentially regulated at the transcript level.

MicroRNA profiling of *in situ* aged and *ex vivo* cultured dermal fibroblasts

Here, we were interested, whether age-associated changes in miRNA expression might be related to the proteome data and transcriptome data listed above. Microarray-based miRNA profiling revealed 12 miRNAs showing evidence of age-related differential expression (Röck *et al.*, unpublished data) (Tab. 2). To determine if these miRNAs play a role in mRNA abundance, we compared their targets with the mRNAs from Kalfalah and colleagues (Kalfalah *et al.*, 2014). This comparison revealed 164 mRNAs as candidate targets of the 12 candidate miRNAs (Fig. 3; Tab. S10). However, none of the targeted mRNAs were found to be significantly altered with age. Moreover 59 % (96 mRNAs) exhibited a constant expression during aging. At the protein level we detected three proteins with age-associated alteration that possibly may be explained by miRNA mediated regulation (Tab. 2; Fig. 4). DNAJC3, DDX3X and CALM1 exhibited an anti-correlation with the miRNAs miR-107, miR-29c as well as with miR181a and miR-409-3p, respectively.

Age-associated biological processes

With the integration of data from proteome, transcriptome and miRNA analysis we assessed a broad spectrum of candidate genes/proteins involved in aging processes. Next, we were interested to reveal the biological processes which allow us to predict aging processes at the functional level. Kalfalah and colleagues reported on 117 age-related biological processes based on the transcriptome data (Tab. S11) (Kalfalah *et al.*, 2014). From the proteome data, we deduced for the 43 age-associated proteins 71 unique biological processes as significantly enriched ($p \leq 0.01$; Tab. S12). We found eight main categories of GO terms: ‘proteostasis’, ‘response to stimuli and stress’, ‘development and differentiation’, ‘cell organisation’, ‘cell communication and signal transduction’, ‘RNA metabolism’, ‘cell cycle and proliferation’ and ‘cell death’ (Fig. 5). Remarkably, comparison of biological processes related to the identified age-associated mRNA and protein candidates revealed ‘cell cycle’, ‘development’, ‘transcription’, ‘translation’, ‘regulation of actin cytoskeleton’, ‘proteasome’, ‘RNA and protein metabolism’, ‘signaling’, ‘RNA biosynthesis’, ‘oxidative phosphorylation’, ‘respiratory electron transport’ and ‘signal transduction’ as highly enriched in both

transcriptome and proteome data. Interestingly we revealed most of these processes by the enrichment analysis of 164 target mRNAs of the 12 identified age-associated candidate miRNAs (Tab. S13). Although not confirmed at the protein level or by mRNA alteration, enrichment analysis showed that identical age-associated biological processes such as ‘signal transduction’, ‘cell communication’, ‘cell death’, ‘RNA and protein metabolism’, ‘cell communication’, ‘response to stimuli’, ‘development’, ‘proliferation’, ‘cellular component organisation’ and ‘RNA and protein biosynthesis’ were highly enriched. The comparisons between different data sets by the deduced biological processes resulted in a significant overlap and led to a biological processes-oriented picture of aging in fibroblasts not expected from the single gene/protein level.

DISCUSSION

Deciphering the molecular and cellular mechanisms of aging *in vivo* is far from complete. Here, we analysed an *ex vivo* model of *in situ* aged human dermal fibroblasts by means of an unbiased proteome-wide approach and integrated the data with those obtained by mRNA and miRNA expression profiling. Previous study proposed that the aging process of an organ is mainly determined by stromal changes, as exemplified by the role of dermal fibroblasts and the dermal extracellular matrix in skin aging (Boukamp, 2005). As the stroma is a highly stationary compartment, homeostasis is primarily based on cellular adaptation and damage clearance and thereby prone to age-related changes. As the major cell source in the stroma and a long-lived cell system, fibroblasts are able to accumulate aging-associated alterations and consequently adapt their cellular functions. An *ex vivo* model of *in situ* aged fibroblasts has been suggested to closer represent the *in vivo* situation of aging than the commonly used senescence-related *in vitro* aging models, as it has been shown that the majority of fibroblasts *in situ* is in a reversible growth arrested state and only a minority is senescent (Mondello *et al.*, 1999; Burton, 2009). Based on the integration of comprehensive data sets from expression studies at the protein, mRNA and miRNA levels, we revealed a moderate age-associated cellular phenotype in *ex vivo* cultured dermal fibroblasts. We showed that 47 % and 63 % of the proteins and transcripts expressed in these cells exhibited a constant abundance across different donor age groups. A further observation supporting the moderate age-associated cellular phenotype was the low number of significantly changed mRNAs, proteins and miRNAs. In our previous study, a total of 117 mRNAs (Kalfalah *et al.*, 2014) and 12 miRNAs (Röck *et al.*, unpublished data) revealed age-dependent alteration in the same dermal fibroblast cultures investigated here. Our present analyses showed 43 proteins with altered expression in these cells according to the different donor age groups. Remarkably, we found no overlap between the mRNA and these 43 protein expression data. This could be due to the fact that individual proteins or transcripts may not meet the threshold for statistical significance as the used technologies have different noise levels. On the other hand, it has been shown and confirmed by our data that in mammalian cells approximately only one third of the mRNA abundance is reflected in the proteome (Gry *et al.*, 2009). However, the fact that 77 % of the age-associated proteins were not linked to expression changes of the corresponding transcripts suggested that most of the age-associated alterations detected at the proteome level are likely caused by other processes, such as post-transcriptional regulation, translation efficiency, protein stability or modifications, rather than by differential regulation

of gene expression. The analysis of the miRNA data suggest that the age-associated abundance changes observed for three candidate proteins (DNAJC3, DDX3X, CALM1) are caused by post-transcriptional regulation through corresponding miRNAs, i.e. miR-107, miR-29c, miR-181a and miR-409-3p, which may target these proteins and showed an inverse expression pattern compared to these proteins in our fibroblast cultures. Furthermore, considering the abundance of the proteins we showed that the age-associated alterations occur mostly in the groups of proteins with middle to low abundance. The observed age-associated decrease of low abundant proteins in fibroblast cultures was linked to electron transport chain, oxidative phosphorylation and cellular respiration. This is in agreement with our previous work showing that a decline in cell proliferation and protein synthesis of *in situ* aged fibroblasts is a consequence of inadequate mito-nuclear signaling (Kalfalah *et al.*, 2014). Although only moderate alterations of the proteome as well as transcriptome and miRNome of *in situ* aged fibroblasts were observed, we confirmed several hallmarks of the fibroblast aging process (Tigges *et al.*, 2014) and identified novel markers not yet described in this context. These age-associated processes point to the following eight categories dominant in aging of fibroblasts: proteostasis, cell cycle and proliferation, development and differentiation, cell death, cell organisation and cytoskeleton, response to stress and stimuli, cell communication and signal transduction, and RNA metabolism and translation.

Proteostasis in aging

Our analyses revealed a role of alterations in proteostasis in fibroblast aging. The central role of proteostasis has been intensively analysed in the context of aging, whereas defects of proteostasis may commonly lead to misfolding, aggregation, and accumulation of proteins resulting in cellular damage and tissue dysfunction (Lopez-Otin *et al.*, 2013). We identified five chaperones and co-chaperones with altered expression in *in situ* aged fibroblasts, which fits to the role of chaperones as part of the proteostasis network during aging. Expression of the co-chaperone DNAJC3 was found to be decreased with age. DNAJC3 plays an important role in the unfolded protein response during ER stress (van Huizen *et al.*, 2003). The chaperones TCP1 and CCT6A, which are involved in the folding of cytoskeleton proteins, also showed decreased expression levels in fibroblasts from older donors. In contrast, expression of certain chaperones of the Hsp70 family (HSPA1A/B and HSPA2) increased with age. Both proteins are involved in protein folding and unfolded protein response (Luders *et al.*, 2000). The abundance change of chaperones of the Hsp70 family could be seen as a

response of the aged fibroblasts to cope with increasing amount of unfolded proteins due to a decline of proteasome activity. We found that two proteasomal proteins, PSMD1 and PSMD14, which are involved in the ATP-dependent degradation of ubiquitinated proteins, demonstrated reduced expression in aged fibroblasts. The decrease of regulatory and catalytically components of the proteasome may result in an accumulation of age-associated toxic aggregates. The proteins related to protein folding and proteasome activity that demonstrated age-associated differential expression in our proteome analyses thus point to a dominant role of impaired proteostasis in *in situ* aged dermal fibroblasts.

Cell cycle and proliferation in aging

The limited proliferating potential of *in vitro* cultured cells has been widely investigated in context of cellular aging (Tigges *et al.*, 2014). We identified six proteins known to be involved in cell cycle regulation as showing age-associated expression changes in dermal fibroblasts. These included reduced expression of the two subunits TCP1 and CCT6A of the T-complex protein 1 that plays an important role in the transition from S to M phase (Yokota *et al.*, 2001). Another protein with age-associated decreased expression was CAPNS1 which is the regulatory subunit of the calcium-regulated non-lysosomal thiol-protease. Knock-down of CAPNS1 inhibited proliferation and cell growth (Zhang *et al.*, 1996). Similarly, DNAJC3, an inhibitor of the kinase PKR, showed reduced expression in aged fibroblasts. Lower expression of DNAJC3 results in increased activity of PKR and phosphorylation of EIF2A, whereby protein translation and cell growth is down-regulated (Gale *et al.*, 1998). The protein DDX3X, a multifunctional ATP-dependent RNA helicase involved in several steps of gene expression, also demonstrated lower expression fibroblasts from aged versus young donors. DDX3X is important for translation of Cyclin E1 mRNA and thereby may stimulate cell cycle progression (Lai *et al.*, 2010). In contrast THBS1 protein abundance increased with age in cultured fibroblasts. Previous data indicate that THBS1 may cause cell cycle arrest of endothelial cells by increasing the amounts of p21 and unphosphorylated RB1 (Yamauchi *et al.*, 2007). Collectively, our findings on aging-associated expression of cell cycle regulatory proteins are in line with a role of reduced proliferation capacity of aged fibroblast discussed in skin aging and provide candidate proteins for further functional validation of this concept.

Development and differentiation in aging

Fibroblasts are known to undergo phenotypic changes when they change from their normal, relatively quiescent state to a proliferative and contractile phenotype, in which they are referred to as myofibroblasts. Differentiation to myofibroblasts can be mediated by TGF- β 1 and also involves EGFR signaling (Simpson *et al.*, 2009). In our study, we found reduced expression of ARHGEF2, a downstream effector of EGFR signaling, in fibroblasts from aged donors. ARHGEF2 is an activator of Rho-GTPases and involved in barrier permeability, cell motility and innate immune response (Fukazawa *et al.*, 2008). The decrease of ARHGEF2 could lead to an impaired EGFR signaling and a loss of cell motility, which in turn leads to a reduction of wound healing capabilities of aged skin. This confirms previous findings showing that the reduction of EGFR resulting decreases differentiation capacity and cell motility of fibroblasts (Midgley *et al.*, 2014). We found three additional proteins (BASP1, CAP1, TWF2) with a potential role in development and differentiation of fibroblasts, which demonstrated age-associated expression changes. Among these, CAP1 is crucial for the epidermal permeability barrier and is, thereby, indispensable for skin development (Leyvraz *et al.*, 2005).

Cell organisation and cytoskeleton in aging

Impaired cell organisation and cytoskeletal alterations lead to morphological changes such as an increased cell volume and cell surface (Tigges *et al.*, 2014). We identified CAP1 as showing decreased expression in aged fibroblasts. CAP1 accelerates the depolymerisation of F-actin, regenerates polymerisable G-actin and recycles cofilin, which binds to F-actin and exhibits pH-sensitive F-actin depolymerising activity (Moriyama & Yahara, 2002). Down-regulation of CAP1 results in accumulation of F-actin, decrease of G-actin, changes in cofilin phosphorylation, larger cell size and altered cell motility (Zhang *et al.*, 2013). This is in line with the findings of an increase in filamentous F-actin and a decrease of G-actin in *in situ* aged fibroblasts (Schulze *et al.*, 2010). We also found increased expression of SYNPO2, a protein that stabilizes F-actin by bundling it to fibrils. SYNPO2 up-regulation may lead to an increase of actin filaments and thereby to increased stiffness (Schulze *et al.*, 2010). A third interesting protein involved in actin dynamics is TWF2, whose expression was decreased during *in situ* aging. TWF2 inhibits actin polymerisation by sequestering G-actin (Paavilainen *et al.*, 2007). Down-regulation of TWF2 may result in an increased polymerisation of G-actin

to F-actin filaments and a decline in cell motility. In the context of cellular transport and complex assembly, we identified nine proteins related to endocytosis as showing age-associated expression differences, including reduced expression of two essential subunits of the AP-2 adaptor complex (AP2A1 and AP2A2), which is necessary for the assembly of vesicles. Because fibroblasts have been estimated to internalize more than 200 % of their entire surface area each hour (Steinman *et al.*, 1983), a decrease in clathrin-mediated endocytosis may lead to impaired cellular and pericellular homeostasis in aged skin.

Cell death in aging

Impaired regulation of apoptosis may lead to an accumulation of damaged and nonfunctional cells in aging (Tigges *et al.*, 2014). An important aspect of the apoptotic machinery is the endocytic uptake of IGFBP3 which targets nuclear regulators of apoptosis (Lee *et al.*, 2005). We identified several proteins related to endocytosis as showing age-associated expression differences (see above). This may cause decreased uptake of IGFBP3, which in turn may contribute to apoptosis resistance of fibroblasts (Marcotte *et al.*, 2004). Other authors found that IGFBP3 accumulates at senescence in the conditioned medium of human fibroblasts and not in the nucleus where it promotes apoptosis (Goldstein *et al.*, 1991). We also identified proteins directly involved in apoptosis. Expression of HSPA1A/B, which protects proteins against aggregation, was found as being increased with age. HSPA1A/B may prevent active CASP3 from cleaving the transcription factor GATA-1 and inducing apoptosis (Ribeil *et al.*, 2007). Higher levels of HSPA1A/B thus may inhibit CASP3-mediated apoptosis and cause resistance of senescent fibroblasts to apoptotic cell death by down-regulating CASP3 (Marcotte *et al.*, 2004). One may speculate that age-associated impaired apoptosis may lead to an accumulation of nonfunctional fibroblasts which are no longer able to maintain a proper stroma. Instead, they release inflammatory cytokines and disturb the extracellular matrix. Thus, our data support the conclusion that cell death via apoptosis is diminished in dermal fibroblasts during *in situ* aging.

Stress response in aging

Activated stress response has been suggested to be a part of the aging process (Calabrese *et al.*, 2010). The ER is sensitive to the accumulation of misfolded proteins, and relays stress signals to the ER mitochondria calcium cycle (Lautenschlaeger *et al.*, 2012). In addition,

alterations in cellular calcium homeostasis correlate with the occurrence of ER stress and increased susceptibility to protein folding stress (Torres *et al.*, 2011). There is evidence that ER calcium homeostasis plays an important role in maintaining cells, since depletion of ER calcium causes growth arrest and cell death (Paschen & Doutheil, 1999). We found eight proteins with age-associated altered expression that are functionally related to calcium stimuli and unfolded protein response. DNAJC3 is an important player in unfolded protein response and its decreased expression leads to an increased accumulation of the transcription factors ATF4 and CHOP, followed by suppressed PPARG transcription (van Huizen *et al.*, 2003). Due to the suppression of PPARG, ER stress can enhance pro-inflammatory NF- κ B activation, which in turn leads to an increase of IL8 production (Park *et al.*, 2010). An increased level of IL8 is closely associated with cellular senescence (Coppe *et al.*, 2010) and aging in dermal fibroblasts (Waldera-Lupa *et al.*, unpublished data). We also identified several calcium sensitive proteins, which demonstrated age-associated expression changes. Thus, *in situ* aged fibroblasts undergo an alteration in calcium homeostasis and an increase of unfolded/misfolded proteins leading to an activation of ER stress response.

Cell communication and signal transduction in aging

An interactive communication exists between fibroblasts and their environment (Tigges *et al.*, 2014). We recently investigated the age-associated secretory phenotype (AASP) of *in situ* aged fibroblasts, which was characterised by altered secretion of a various matrix metalloproteases, cytokines and other proteins (Waldera-Lupa *et al.*, unpublished data). However, little is known about the intracellular pathways leading to the AASP of *in situ* aged fibroblasts. Recently, NF- κ B signaling was found to be activated in several tissues with aging (Tilstra *et al.*, 2011). One of the proteins involved in NF- κ B signaling is ANXA6, whose expression increased with age. Overexpression of ANXA6 results in NF- κ B activation (Campbell *et al.*, 2013). We also found two target proteins of NF- κ B, HSPA1A/B and THBS1, as being up-regulated in fibroblasts from aged donors. This might be a direct response to stress mediated by inflammation factors, such as cytokines and is in agreement with our secretome study, where we found increased secretion of several cytokines with age. In addition, our study suggests that mTOR signaling, a key modulator of aging and age-related disease (Johnson *et al.*, 2013), is involved in fibroblast aging. We identified increased age-associated expression of SRSF9, a promoter of mTOR activation. Thus, our data support

a role of mTOR and NF- κ B signaling in fibroblast aging and the development of a fibroblast-specific AASP.

RNA metabolism and translation in aging

Impaired function of the RNA machinery plays an important role in aging (Cookson, 2012). Our proteome study revealed decreased expression of a modulator of RNA-polymerase II activity, CGI-99, in aged fibroblasts. Further, we found evidence that RNA-processing may be altered during fibroblast aging. In fact other authors reported that expression patterns of alternatively spliced mRNA change during aging (Tigges *et al.*, 2014). We identified age-associated expression changes of four proteins (SRSF9, DDX1, DDX3X, DHX15) involved in RNA-splicing, with three of the proteins are functioning as RNA-helicases and therefore are important for translation. For example, an age-associated decrease of DDX3X expression may result in decreased protein synthesis and impaired protein homeostasis (see above). A further indication of impaired translation during aging is provided by altered expression levels of ribosomal proteins, of which we identified three (RPS5, RPS6, RPS29) in our study. The observed up-regulation of HASPA1A/B, a regulator of AUF1, is of interest since AUF1 is involved cytokine mRNA degradation, which is blocked by binding to HASPA1A (Laroia *et al.*, 1999). Thus, HASPA1A/B up-regulation may increase cytokine mRNA abundance and hence cytokine production. This is in agreement with our previous data on the aging-associated secretome of dermal fibroblasts (Waldera-Lupa *et al.*, unpublished data). A further aspect of RNA-degradation is the elimination of harmful RNAs generated at DNA double-strand breaks (DSB). The helicase DDX1 plays an RNA clearance role at DSB sites, thereby facilitating the template-guided repair of transcriptionally active regions of the genome (Li *et al.*, 2008). Moreover, we identified the oligoribonuclease REXO2 as being down-regulated during aging. REXO2 is involved in the degradation of small single-stranded RNA and DNA oligomers, and in the recycling of nucleotides (Nguyen *et al.*, 2000). Decrease of DDX1 and REXO2 thus might lead to the synthesis and accumulation of defect or misfolded proteins in aged fibroblasts.

EXPERIMENTAL PROCEDURES

Cell isolation and culture

Cell isolation and culture were performed as previously described (Kalfalah *et al.*, 2014)

Sample preparation, MS analysis, and protein identification and quantification

Detailed experimental procedures are reported as Data S1 (Supporting Information). Human dermal fibroblasts were cultivated under standardised conditions until passage three as described above. Cells were harvested, homogenised and lysed in urea-buffer. After determination of protein amount 10 µg of each sample were proteolytic digested with trypsin. Peptides of each sample were analysed with a nano-HPLC/ESI-MS system composed of an RSLCnano HPLC and a LTQ Orbitrap Velos (Thermo Fisher Scientific, Bremen, Germany). For protein identification, the Proteome Discoverer (version 1.3, Thermo Fisher Scientific) and MASCOT search engine (version 2.4.1, Matrix Science, London, UK) were used. MS/MS-spectra were searched against the UniProtKB database (date 04/03/2013). The false discovery rate was set to 1 %. For label-free quantification only proteins identified in 14 of 15 samples were regarded. Statistical analysis for the proteomes was performed using multiple t-tests (ANOVA) and Pearson correlation applying a significance threshold of 5 %. Stability of protein and mRNA abundance was determined as described elsewhere (Peterson *et al.*, 2012).

Functional annotation, network and enrichment analysis of proteins

Gene set analysis of unchanged proteins was carried out using Consensus Path DB (<http://cpdb.molgen.mpg.de/>). We discarded gene sets that were redundant, had ≤ 5 members or a p-value above 0.01. Enrichment analyses of abundance classes and mitochondria related proteins were carried out using DAVID (<http://david.abcc.ncifcrf.gov/>) and the Gene Ontology Biological Process categorisation. We discarded processes that had a p-value above 0.05. Network and enrichment analysis was carried out using Cytoscape environment (<http://www.cytoscape.org/>) and ClueGo plug-in (<http://www.ici.upmc.fr/cluego/>).

mRNA/protein correlation analysis

Correlation analysis between measured mRNA-expression levels and protein abundance was performed using R (<http://www.r-project.org>). The mRNA intensities were log₂-scaled, the

lowest 25 % based on the median intensities as well as probes with no corresponding EntrezID were discarded. In the case of Entrez GeneIDs corresponding to multiple AgilentIDs the mean intensities were used for further analysis, whereas the maximum value was set to 100 %. For each identified protein the sum intensities were divided by the underlying number of quantified peptides. The data was log₂-scaled and the maximum value was set to 100 %.

miRNA network and enrichment analysis

We built up an initial network for the reported age-associated miRNAs (Röck *et al.*, unpublished data) based on target predictions, which were derived from TargetScan (<http://www.targetscan.org>). We then integrated gene expression measurements and fitted a linear model with the gene expression data as response and the expression data of its predicted targeting miRNAs as predictor variables. We then performed a multiple linear regression analysis for each gene with elastic net penalty in order to select for miRNAs that have an influence on the gene expression data. For this purpose, we used the *glmnet* package for the R (<http://cran.r-project.org/web/packages/glmnet/index.html>) and introduced a negativity constraint to select only for negative miRNA effects. The penalty parameter was determined by 10-fold cross-validation. We finally obtained two networks by applying this procedure to the mRNA and the protein expression data, respectively.

ACKNOWLEDGEMENTS

This work was supported by the Deutsche Forschungsgemeinschaft (SFB 728 and GK 1033 to EF, FB and JK), and by the German Ministry of Research and Education (BMBF) within the GerontoSys consortium on stromal aging.

AUTHOR CONTRIBUTIONS

DWL: study design, preparation of cells/proteomes, collection and assembly of data, proteome analysis, interpretation of data and results, writing of the manuscript; AMF: data interpretation, miRNA analysis; FK: acquisition and preparation of cells; SS: miRNA-gene/protein regulatory networks; FK: correlation analysis of mRNA/protein data; JT: acquisition and preparation of cells; HB: interpretation of results; HM: financial support; FB: study design; FT: interpretation of results; GR: study design, interpretation of results and manuscript writing; KS: study design, interpretation of results and manuscript writing.

CONFLICT OF INTEREST

None declared.

REFERENCES

- Boraldi F, Bini L, Liberatori S, Armini A, Pallini V, Tiozzo R, Pasquali-Ronchetti I, Quaglino D (2003). Proteome analysis of dermal fibroblasts cultured *in vitro* from human healthy subjects of different ages. *Proteomics*. **3**, 917-929
- Boukamp P (2005). Skin aging: a role for telomerase and telomere dynamics? *Current molecular medicine*. **5**, 171-177
- Burton DG (2009). Cellular senescence, ageing and disease. *Age*. **31**, 1-9
- Calabrese V, Cornelius C, Mancuso C, Lentile R, Stella AM, Butterfield DA (2010). Redox homeostasis and cellular stress response in aging and neurodegeneration. *Methods in molecular biology*. **610**, 285-308
- Campbell KA, Minashima T, Zhang Y, Hadley S, Lee YJ, Giovino J, Quirno M, Kirsch T (2013). Annexin A6 interacts with p65 and stimulates NF-kappaB activity and catabolic events in articular chondrocytes. *Arthritis and rheumatism*. **65**, 3120-3129
- Cookson MR (2012). Aging--RNA in development and disease. *Wiley interdisciplinary reviews. RNA*. **3**, 133-143
- Coppe JP, Desprez PY, Krtolica A, Campisi J (2010). The senescence-associated secretory phenotype: the dark side of tumor suppression. *Annu Rev Pathol*. **5**, 99-118
- Fukazawa A, Alonso C, Kurachi K, Gupta S, Lesser CF, McCormick BA, Reinecker HC (2008). GEF-H1 mediated control of NOD1 dependent NF-kappaB activation by Shigella effectors. *PLoS pathogens*. **4**, e1000228
- Gale M, Jr., Blakely CM, Hopkins DA, Melville MW, Wambach M, Romano PR, Katze MG (1998). Regulation of interferon-induced protein kinase PKR: modulation of P58IPK inhibitory function by a novel protein, P52rIPK. *Molecular and cellular biology*. **18**, 859-871
- Goldstein S, Moerman EJ, Jones RA, Baxter RC (1991). Insulin-like growth factor binding protein 3 accumulates to high levels in culture medium of senescent and quiescent human fibroblasts. *Proceedings of the National Academy of Sciences of the United States of America*. **88**, 9680-9684
- Greussing R, Hackl M, Charoentong P, Pauck A, Monteforte R, Cavinato M, Hofer E, Scheideler M, Neuhaus M, Micutkova L, Mueck C, Trajanoski Z, Grillari J, Jansen-Durr P (2013). Identification of microRNA-mRNA functional interactions in UVB-induced senescence of human diploid fibroblasts. *BMC genomics*. **14**, 224

- Gry M, Rimini R, Stromberg S, Asplund A, Ponten F, Uhlen M, Nilsson P (2009). Correlations between RNA and protein expression profiles in 23 human cell lines. *BMC genomics*. **10**, 365
- Johnson SC, Rabinovitch PS, Kaeberlein M (2013). mTOR is a key modulator of ageing and age-related disease. *Nature*. **493**, 338-345
- Kalfalah F, Sobek S, Bornholz B, Gotz-Rosch C, Tigges J, Fritsche E, Krutmann J, Korner K, Deenen R, Ohse S, Boerries M, Busch H, Boege F (2014). Inadequate mito-biogenesis in primary dermal fibroblasts from old humans is associated with impairment of PGC1A-independent stimulation. *Experimental gerontology*
- Kim YM, Byun HO, Jee BA, Cho H, Seo YH, Kim YS, Park MH, Chung HY, Woo HG, Yoon G (2013). Implications of time-series gene expression profiles of replicative senescence. *Aging cell*. **12**, 622-634
- Lai MC, Chang WC, Shieh SY, Tarn WY (2010). DDX3 regulates cell growth through translational control of cyclin E1. *Molecular and cellular biology*. **30**, 5444-5453
- Laroia G, Cuesta R, Brewer G, Schneider RJ (1999). Control of mRNA decay by heat shock-ubiquitin-proteasome pathway. *Science*. **284**, 499-502
- Lautenschlaeger J, Prell T, Grosskreutz J (2012). Endoplasmic reticulum stress and the ER mitochondrial calcium cycle in amyotrophic lateral sclerosis. *Amyotrophic lateral sclerosis : official publication of the World Federation of Neurology Research Group on Motor Neuron Diseases*. **13**, 166-177
- Lee KW, Ma L, Yan X, Liu B, Zhang XK, Cohen P (2005). Rapid apoptosis induction by IGFBP-3 involves an insulin-like growth factor-independent nucleomitochondrial translocation of RXRalpha/Nur77. *J Biol Chem*. **280**, 16942-16948
- Leyvraz C, Charles RP, Rubera I, Guitard M, Rotman S, Breiden B, Sandhoff K, Hummler E (2005). The epidermal barrier function is dependent on the serine protease CAP1/Prss8. *The Journal of cell biology*. **170**, 487-496
- Li L, Monckton EA, Godbout R (2008). A role for DEAD box 1 at DNA double-strand breaks. *Molecular and cellular biology*. **28**, 6413-6425
- Lopez-Otin C, Blasco MA, Partridge L, Serrano M, Kroemer G (2013). The hallmarks of aging. *Cell*. **153**, 1194-1217
- Luders J, Demand J, Hohfeld J (2000). The ubiquitin-related BAG-1 provides a link between the molecular chaperones Hsc70/Hsp70 and the proteasome. *J Biol Chem*. **275**, 4613-4617

- Mancini M, Saintigny G, Mahe C, Annicchiarico-Petruzzelli M, Melino G, Candi E (2012). MicroRNA-152 and -181a participate in human dermal fibroblasts senescence acting on cell adhesion and remodeling of the extra-cellular matrix. *Aging*. **4**, 843-853
- Marcotte R, Lacelle C, Wang E (2004). Senescent fibroblasts resist apoptosis by downregulating caspase-3. *Mechanisms of ageing and development*. **125**, 777-783
- Midgley AC, Bowen T, Phillips AO, Steadman R (2014). MicroRNA-7 inhibition rescues age-associated loss of epidermal growth factor receptor and hyaluronan-dependent differentiation in fibroblasts. *Aging cell*. **13**, 235-244
- Mondello C, Petropoulou C, Monti D, Gonos ES, Franceschi C, Nuzzo F (1999). Telomere length in fibroblasts and blood cells from healthy centenarians. *Experimental cell research*. **248**, 234-242
- Moriyama K, Yahara I (2002). Human CAP1 is a key factor in the recycling of cofilin and actin for rapid actin turnover. *J Cell Sci*. **115**, 1591-1601
- Nguyen LH, Erzberger JP, Root J, Wilson DM, 3rd (2000). The human homolog of Escherichia coli Orn degrades small single-stranded RNA and DNA oligomers. *J Biol Chem*. **275**, 25900-25906
- Paavilainen VO, Hellman M, Helfer E, Bovellan M, Annala A, Carlier MF, Permi P, Lappalainen P (2007). Structural basis and evolutionary origin of actin filament capping by twinfilin. *Proceedings of the National Academy of Sciences of the United States of America*. **104**, 3113-3118
- Park SH, Choi HJ, Yang H, Do KH, Kim J, Lee DW, Moon Y (2010). Endoplasmic reticulum stress-activated C/EBP homologous protein enhances nuclear factor-kappaB signals via repression of peroxisome proliferator-activated receptor gamma. *J Biol Chem*. **285**, 35330-35339
- Paschen W, Doutheil J (1999). Disturbances of the functioning of endoplasmic reticulum: a key mechanism underlying neuronal cell injury? *Journal of cerebral blood flow and metabolism : official journal of the International Society of Cerebral Blood Flow and Metabolism*. **19**, 1-18
- Peterson LN, Eva KW, Rusticus SA, Lovato CY (2012). The readiness for clerkship survey: can self-assessment data be used to evaluate program effectiveness? *Academic medicine : journal of the Association of American Medical Colleges*. **87**, 1355-1360
- Ribeil JA, Zermati Y, Vandekerckhove J, Cathelin S, Kersual J, Dussiot M, Coulon S, Moura IC, Zeuner A, Kirkegaard-Sorensen T, Varet B, Solary E, Garrido C, Hermine O

- (2007). Hsp70 regulates erythropoiesis by preventing caspase-3-mediated cleavage of GATA-1. *Nature*. **445**, 102-105
- Schulze C, Wetzel F, Kueper T, Malsen A, Muhr G, Jaspers S, Blatt T, Wittern KP, Wenck H, Kas JA (2010). Stiffening of human skin fibroblasts with age. *Biophys J*. **99**, 2434-2442
- Simpson RM, Meran S, Thomas D, Stephens P, Bowen T, Steadman R, Phillips A (2009). Age-related changes in pericellular hyaluronan organization leads to impaired dermal fibroblast to myofibroblast differentiation. *The American journal of pathology*. **175**, 1915-1928
- Steinman RM, Mellman IS, Muller WA, Cohn ZA (1983). Endocytosis and the recycling of plasma membrane. *The Journal of cell biology*. **96**, 1-27
- Tigges J, Krutmann J, Fritsche E, Haendeler J, Schaal H, Fischer JW, Kalfalah F, Reinke H, Reifenberger G, Stuhler K, Ventura N, Gundermann S, Boukamp P, Boege F (2014). The hallmarks of fibroblast ageing. *Mechanisms of ageing and development*
- Tilstra JS, Clauson CL, Niedernhofer LJ, Robbins PD (2011). NF-kappaB in Aging and Disease. *Aging and disease*. **2**, 449-465
- Torres M, Encina G, Soto C, Hetz C (2011). Abnormal calcium homeostasis and protein folding stress at the ER: A common factor in familial and infectious prion disorders. *Communicative & integrative biology*. **4**, 258-261
- van Huizen R, Martindale JL, Gorospe M, Holbrook NJ (2003). P58IPK, a novel endoplasmic reticulum stress-inducible protein and potential negative regulator of eIF2alpha signaling. *J Biol Chem*. **278**, 15558-15564
- Yamauchi M, Imajoh-Ohmi S, Shibuya M (2007). Novel antiangiogenic pathway of thrombospondin-1 mediated by suppression of the cell cycle. *Cancer science*. **98**, 1491-1497
- Yokota S, Yanagi H, Yura T, Kubota H (2001). Cytosolic chaperonin-containing t-complex polypeptide 1 changes the content of a particular subunit species concomitant with substrate binding and folding activities during the cell cycle. *European journal of biochemistry / FEBS*. **268**, 4664-4673
- Zhang H, Ghai P, Wu H, Wang C, Field J, Zhou GL (2013). Mammalian adenylyl cyclase-associated protein 1 (CAP1) regulates cofilin function, the actin cytoskeleton, and cell adhesion. *J Biol Chem*. **288**, 20966-20977

Zhang W, Lane RD, Mellgren RL (1996). The major calpain isozymes are long-lived proteins. Design of an antisense strategy for calpain depletion in cultured cells. *J Biol Chem.* **271**, 18825-18830

TABLES

Table 1 Significantly altered proteins with age. Quantitative label-free proteome analysis of *in situ* aged fibroblasts' proteome revealed 43 proteins that are differentially altered during *in situ* ageing (ANOVA: $p \leq 0.05$; Pearson correlation: $p \leq 0.05$). For ANOVA analysis donors were grouped according to calendar age into groups 20-30, 40-50 and 60-70 years, with five individual donors in each group.

Accession	Gene	Description	p-value	Fold change	Regulation
P08133	ANXA6	Annexin A6	0.001	1.5	up
P47897	QARS	Glutaminyl-tRNA synthetase	0.002	1.3	up
P11717	IGF2R	Cation-independent mannose-6-phosphate receptor	0.003	2.8	up
Q6IBS0	TWF2	Twinfilin-2	0.005	1.4	down
P46782	RPS5	40S ribosomal protein S5	0.007	2.2	down
O43143	DHX15	Putative pre-mRNA-splicing factor ATP-dependent RNA helicase DHX15	0.008	1.4	up
Q99460	PSMD1	26S proteasome non-ATPase regulatory subunit 1	0.012	1.4	down
P62273	RPS29	40S ribosomal protein S29	0.012	1.3	up
Q9UMS6	SYNPO2	Synaptopodin-2	0.012	1.8	up
P40227	CCT6A	T-complex protein 1 subunit zeta	0.012	1.7	down
P08758	ANXA5	Annexin A5	0.012	1.4	up
Q9Y310	C22orf28	tRNA-splicing ligase RtcB homolog	0.013	2.8	down
Q13242	SRSF9	Serine/arginine-rich splicing factor 9	0.013	1.2	up
P60660	MYL6	Myosin light polypeptide 6	0.017	1.2	up
Q15435	PPP1R7	Protein phosphatase 1 regulatory subunit 7	0.022	1.6	down
Q9Y224	C14orf166	UPF0568 protein C14orf166	0.022	1.9	down
O00487	PSMD14	26S proteasome non-ATPase regulatory subunit 14	0.022	1.4	down
P34897	SHMT2	Serine hydroxymethyltransferase, mitochondrial	0.022	1.7	down
P08107	HSPA1A	Heat shock 70 kDa protein 1A/1B	0.022	1.7	up
Q92499	DDX1	ATP-dependent RNA helicase DDX1	0.023	1.3	down
P62158	CALM1	Calmodulin	0.024	2.7	up
O94973	AP2A2	AP-2 complex subunit alpha-2	0.027	1.6	down
Q92974	ARHGEF2	Rho guanine nucleotide exchange factor 2	0.028	2.6	down
P09525	ANXA4	Annexin A4	0.030	1.3	up
P27105	STOM	Erythrocyte band 7 integral membrane protein	0.031	2.0	up
O00571	DDX3X	ATP-dependent RNA helicase DDX3X	0.034	1.3	down
P04632	CAPNS1	Calpain small subunit 1	0.034	1.6	down
P15559	NQO1	NAD(P)H dehydrogenase [quinone] 1	0.035	3.2	up
Q96FQ6	S100A16	Protein S100-A16	0.036	1.4	down
P09497	CLTB	Clathrin light chain B	0.037	1.5	up
P80723	BASP1	Brain acid soluble protein 1	0.037	1.6	up
Q13217	DNAJC3	DnaJ homolog subfamily C member 3	0.037	2.6	down
O95782	AP2A1	AP-2 complex subunit alpha-1	0.039	1.4	down

P62753	RPS6	40S ribosomal protein S6	0.039	1.3	up
P41250	GARS	Glycyl-tRNA synthetase	0.039	1.2	down
Q9NZN4	EHD2	EH domain-containing protein 2	0.039	1.4	up
Q9Y3B8	REXO2	Oligoribonuclease, mitochondrial	0.040	2.5	down
P07996	THBS1	Thrombospondin-1	0.044	1.5	up
P30419	NMT1	Glycylpeptide N-tetradecanoyltransferase 1	0.045	1.4	down
Q01518	CAP1	Adenylyl cyclase-associated protein 1	0.048	1.1	down
P54652	HSPA2	Heat shock-related 70 kDa protein 2	0.048	1.5	up
Q96QV6	HIST1H2AA	Histone H2A type 1-A	0.049	3.8	down
P17987	TCP1	T-complex protein 1 subunit alpha	0.050	1.2	down

Table 2 Highest ranked miRNAs whose expression profiles correlate most with age (Röck *et al.*, unpublished data). Positive p-values indicate correlation and negative p-values anti-correlation with age. Matched mRNAs were obtained from the published data set of Kalfalah *et al.* (2014). For matching of the miRNAs with proteins the identified proteins of label-free proteome analysis were used. Matched proteins which were also identified as altered during ageing were indicated in bold.

miRNA	p-value	correlation	Matched mRNA	Matched Protein (alteration on protein level)
miR-100	0.458 (up)	0.086	EIF2C2, MTOR, NOX4	
miR-107	0.578 (up)	0.024	ANK1, C5ORF13, CCNYL1, FERMT2, KLF4, NFIB, PDE3B, SEMA6A, UQCC, ZC3H7B, ZNF711	ABCF1, ADD1, AK2, ANKFY1, CAPZA2, CARM1, CTNND1, DNAJC3 (down) , FERMT2, IPO9, KPNA3, PAFAH1B2, SMCHD1, SUN2
miR-125b	-0.503 (down)	0.056	ANKH, BCL2L2, CDS2, CLDN12, CORO2A, ENPP1, GOPC, LOC645978, LRRC10B, NOS1AP, PIK3CD, PSMD7, PTAR1, RBAK, RET, RPS6KA1, SOCS4, TMBIM6, TMEM168, TRPS1, USP46, ZC3H7B	ARCN1, DPP9, ESYT1, FAM129B, MEMO1, OGFR, PIP4K2B, SRSF6, STAT3, TGOLN2
miR-130b	0.503 (up)	0.056	BAG5, BCAT1, BPTF, CSF1, EREG, FERMT2, FIBIN, FLJ36031, GPATCH8, HSPA8, INO80, IRF1, KIAA0319L, LMTK2, LRRTM2, MAP3K9, MED15, MLEC, NCKIPSD, NFIB, PDE5A, RAB5B, SKP1, SMOC2, SNAP25, SPG20, TNRC6B, TSPYL2, WNK1, ZBTB4, ZNF711	CEP170, HOOK3, MAP1B, TRIM3
miR-181a	-0.58 (down)	0.023	ANK1, ARL5A, ATP2B3, BPTF, C15ORF29, CCP110, CDH13, CDS2, CPEB4, CTTNBP2NL, DEK, FAM122B, FAM13B, FAM160A2, INO80, LIMS1, LRRC8D, LRRFIP1, MCL1, METAP1, MOSPD1, NDRG2, NPTXR, NR1D2, NUDT21, PI4K2B, PIK3C2A, PRKCD, RAD21, RALGAPA2, RBAK, SACM1L, SCN9A, SHOC2, SLC10A7, SLC16A6, SLC19A2, SOCS4, STRN, TBPL1, TMEM151B, TMEM71, TRPM7, UBE2B, WSB1, ZNF83	ANXA11, ARF6, CALM1 (up) , CLIP1, FKBP1A, G3BP2, HYOU1, MARCKS, PDCD6IP, PI4K2A, PRRC2C, SYNC, TMEM165, YWHAB, YWHAZ

miR-20b	0.441 (up)	0.100	BCL6B, EREG, FBXO31, FIBIN, GUCY1A3, HSPA8, INO80, MAP3K9, MAST3, MCF2L, PANX2, PEX5L, PLA2G6, RAB5B, SERTAD2, SMOC2, SPG20, TMBIM6, TNFRSF21, TNS1, TPRG1L, WEE1, ZC3H7B	ACTR1A, AP2B1, ARHGAP1, FAM129A, HOOK3, KPNA2, MARS, MCM3, PTBP1, SYNCRIP, TRIM3
miR-23a	0.499 (up)	0.058	BTAF1, EGLN2, GABRB3, GABRB3, MAP3K9, MBTD1, PRKCSH, PTAR1, RAB35, RBPMS2, SIX4, TCF20, TNFAIP3	CUL3, DDAH1, EPN1, GNPDA1, LAMP1, MRC2, NEDD4, PICALM, PIGS, PXDN, SET, TMED5, TXNRD1
miR-494	-0.564 (down)	0.029	APC, ARHGEF12, ATP7A, ATRX, C11ORF61, C20ORF103, C5ORF24, CNTN3, ENPP1, FAM169A, GK3P, GLIS3, GPATCH8, GRIK2, INHBB, KDM5C, KIAA0776, KIAA1549, KIAA2022, LANCL2, LOC344593, LRP1B, MBNL3, NANOS1, PNOC, PSD3, PTPRE, RAB40B, RTF1, SCN2B, SLC26A3, SLC38A2, SSX2IP, TAC1, TACC2, TCF20, TRAF3, TRPS1, ZBTB39, ZBTB43	SEPT9, DPYSL3, FAM120A, H3F3A, MAP4, MTDH, PIP4K2B, PITPNB, PTPN11, PURB, SYNCRIP, THRAP3
miR-29c	0.488 (up)	0.065		ARF5, COL6A3, CSPG4, DDX3X (down) , HNRNPF, ITGB1, LOX, PRKRA, PRRC2C, PTX3, SYNCRIP
miR-28-3p	0.454 (up)	0.089		ARF6, PRPF19
miR-409-3p	-0.461 (down)	0.083		BUB3, CALM1 (up) , CDV3, COL5A2, EWSR1, HNRNPK, LARP1, MYLK, SH3BGRL3, SLC2A12, TMED7, UBE2N, YWHAE
miR-409-5p	-0.522 (down)	0.046		DLST, FAM129A

FIGURES

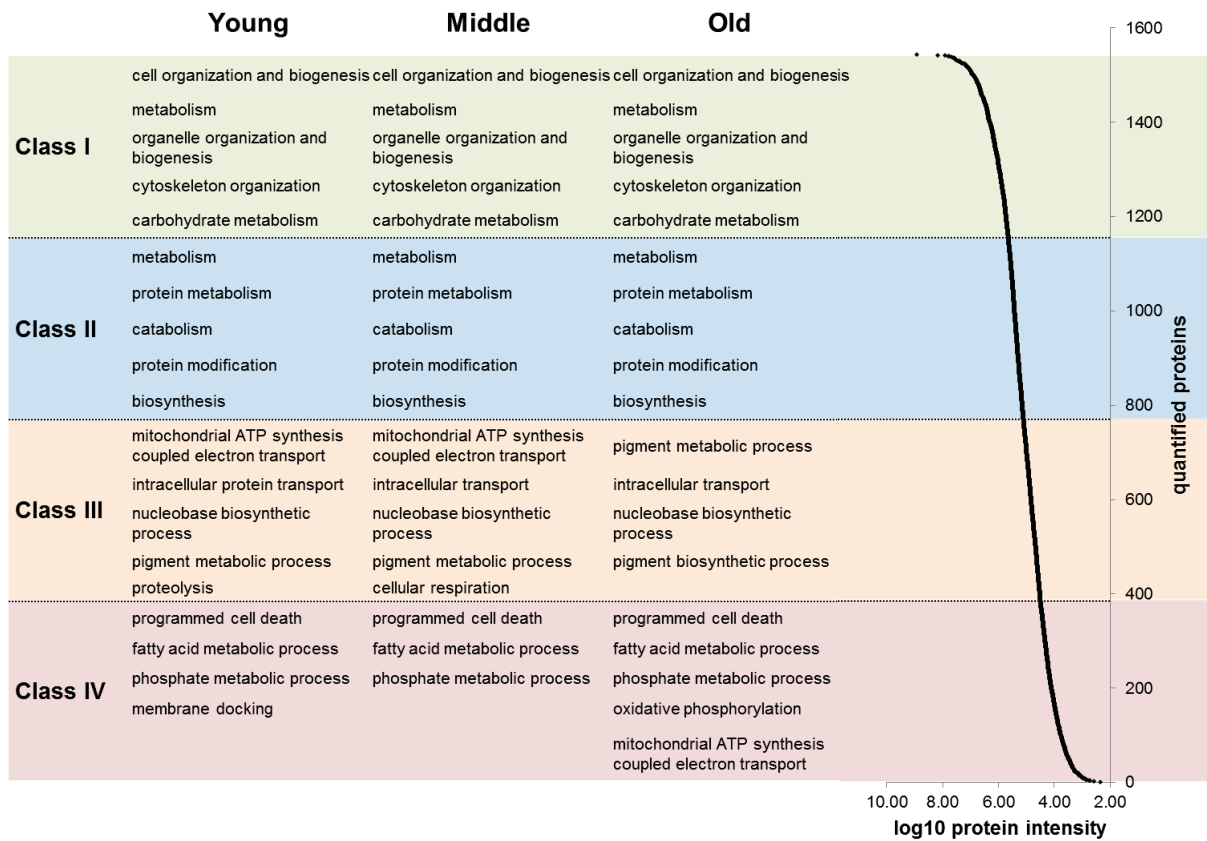


Figure 1 Abundance ranges of quantified proteins. For each age group (young, middle and old) the quantified proteins were ranked into four classes based on their abundance (log10 of protein intensities). Abundances of quantified proteins spanned approximately five orders of magnitude (right). For each abundance class and age group an enrichment analysis of biological processes was applied. The five most significant biological processes are indicated in the figure.

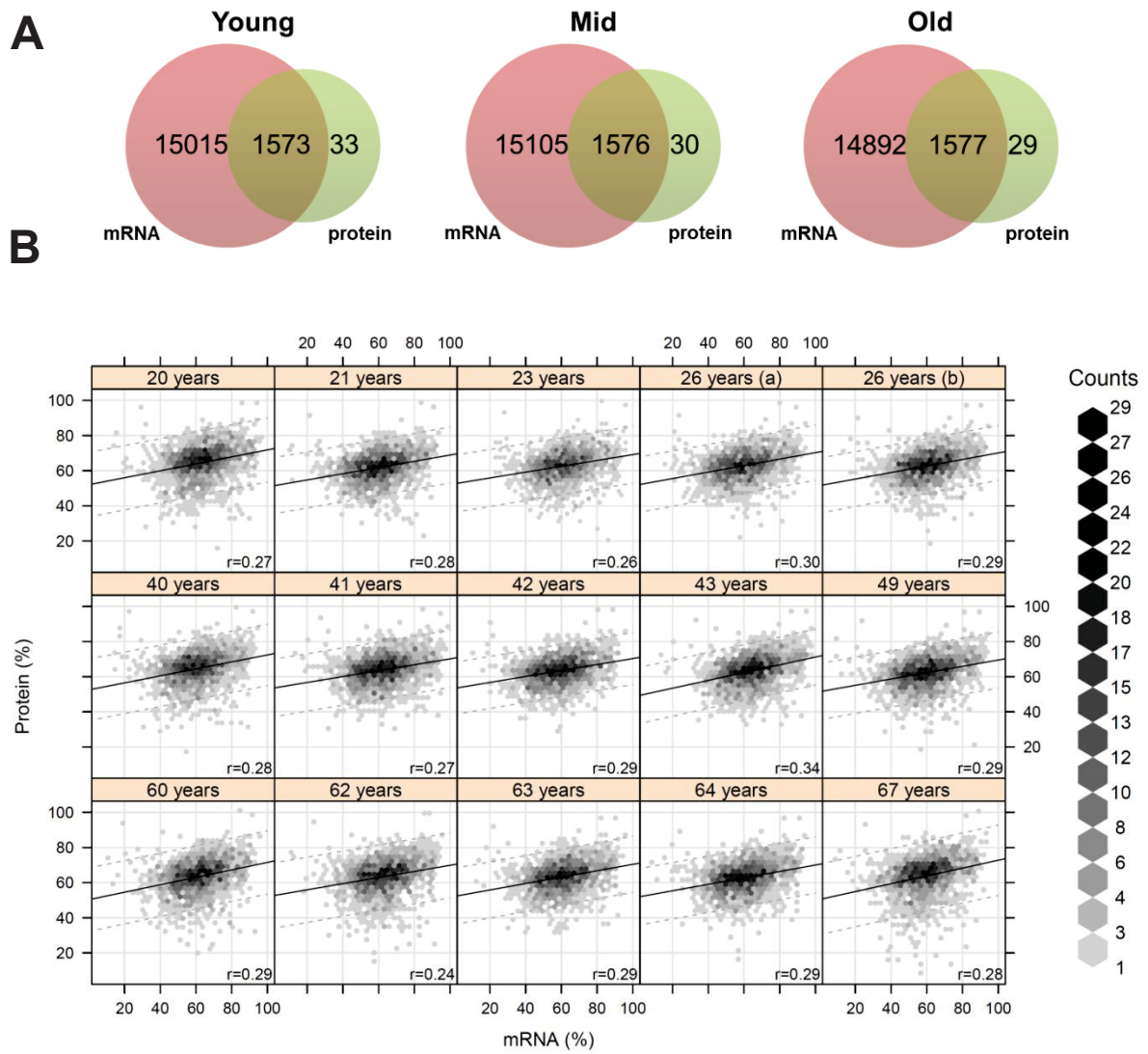


Figure 2 Coverage and correlation of mRNA and protein data. **A:** For each age group the quantified transcripts and proteins were compared. Almost all quantified proteins were also present on mRNA level. **B:** Correlation analysis of mRNA and protein abundances for each individual. The mRNA/protein pairs were drawn as hexagons whereby accumulations of pairs are indicated in different colors. Correlation analysis revealed a correlation of about 28 % on average between proteins and mRNAs.

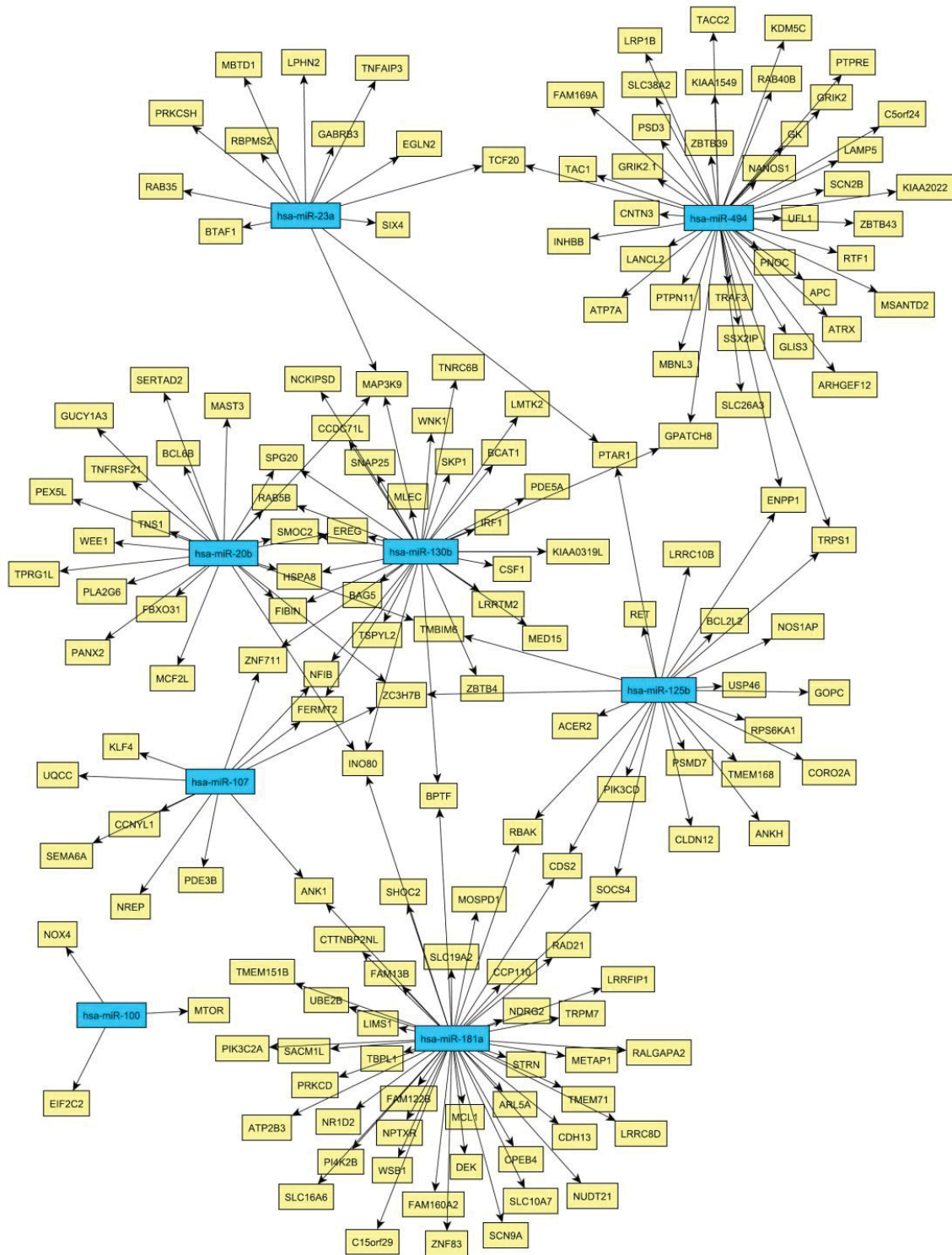


Figure 3 Network of miRNA-mRNA relationships obtained by the combination of target predictions and a penalised regression analysis integrating miRNA and mRNA expression measurements. Only miRNAs were considered which are associated with age. The miRNA nodes are colored blue and the identified target genes yellow.

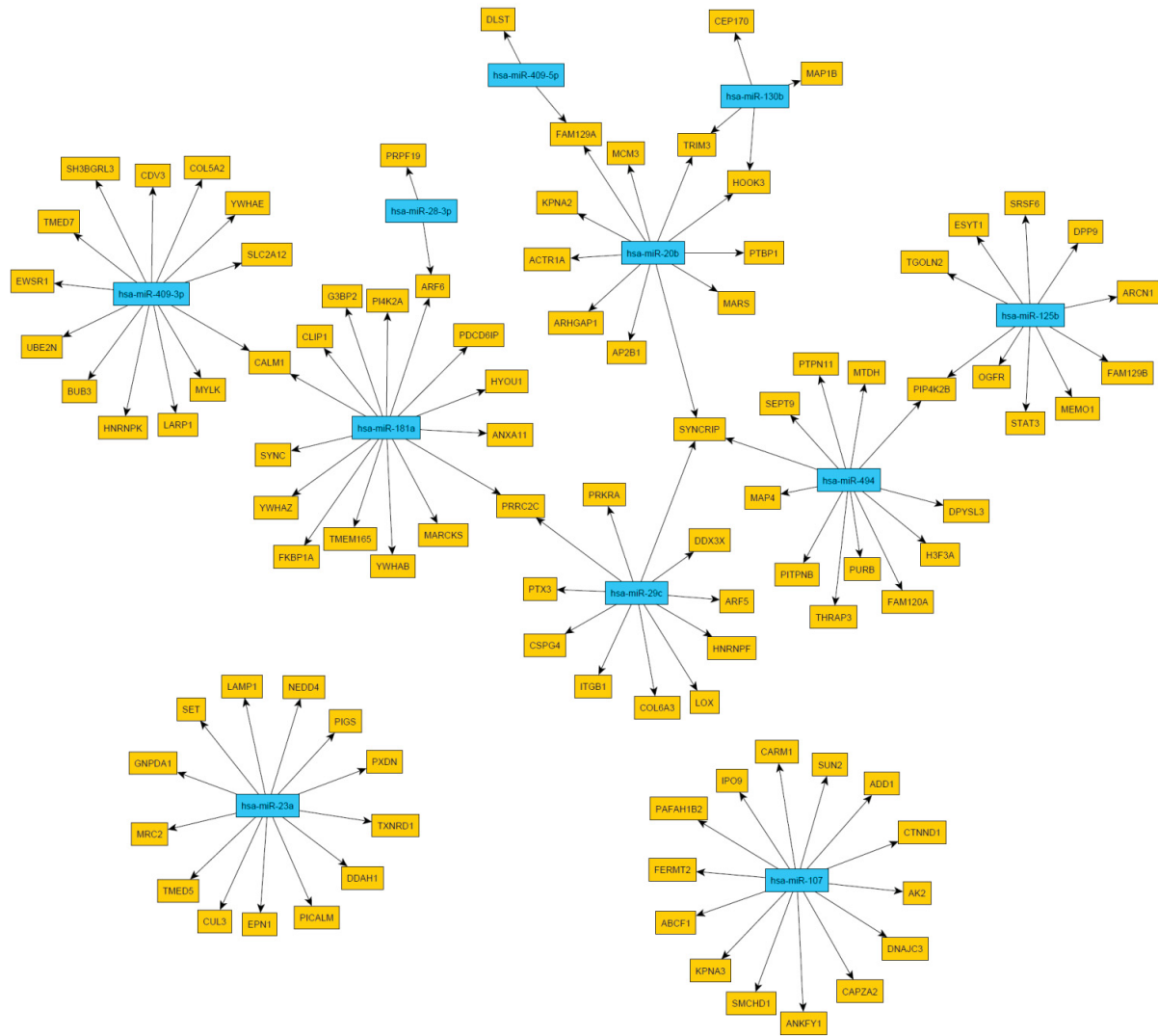


Figure 4 Network of miRNA-protein relationships obtained by the combination of target predictions and a penalised regression analysis integrating miRNA and protein expression measurements. Only miRNAs were considered which are associated with age. The miRNA nodes are colored blue and the identified target genes yellow.

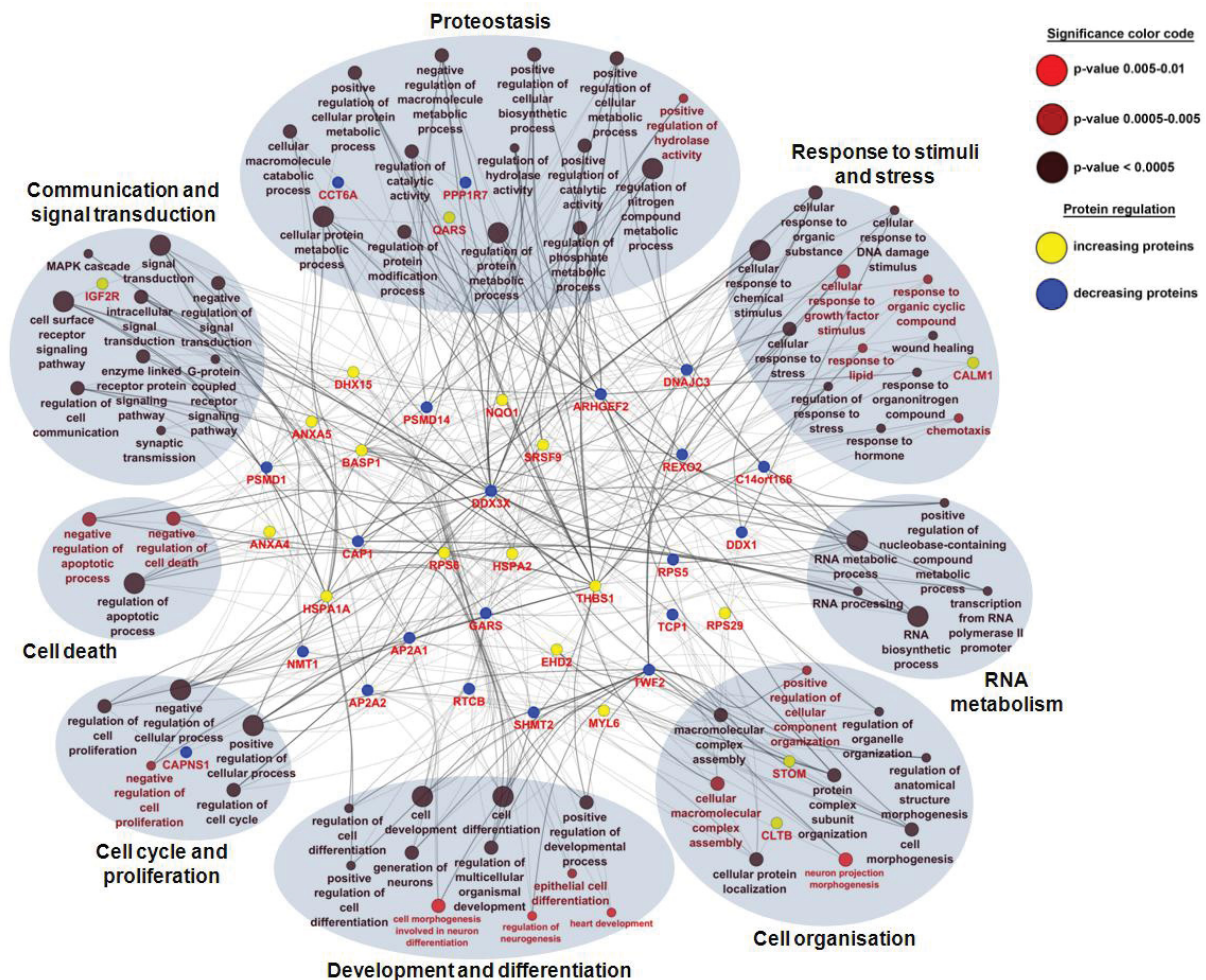


Figure 5 Network and enrichment analysis of age-associated altered proteins using Gene Ontology categories for biological processes. For the 43 age-associated altered proteins, a total of 71 unique biological processes were identified as highly enriched ($p \leq 0.01$). Proteins were color coded according to their regulation profile: increasing (yellow) and decreasing (blue). Terms describing a similar biological process were grouped according to GO slim categories. A total of eight main categories of GO terms were identified: proteostasis (8 proteins), response to stimuli and stress (9 proteins), development and differentiation (7 proteins), cell organisation (15 proteins), cell communication and signal transduction (13 proteins), RNA metabolism (17 proteins), cell cycle and proliferation (25 proteins) and cell death (13 proteins).

SUPPORTING INFORMATION

Data S1 Experimental procedure.

Fig. S1 Principle component analysis (PCA) of quantified proteins.

Fig. S2 Distributions of confidence intervals of quantifiable proteins.

Fig. S3 Cluster analysis of expression of mitochondria-related proteins.

Fig. S4 Correlation analysis of mRNA and protein abundances for quantified mRNA/protein pairs.

Fig. S5 Distributions of confidence intervals of quantifiable mRNAs.

Fig. S6 Overview of *m/z* ranges for LC-MS/MS analysis using gas-phase fractionation.

Tab. S1 Significantly altered proteins with age.

Tab. S2 Confidence intervals of quantifiable proteins.

Tab. S3 Enrichment analysis of biological processes of proteins with constant expression during aging.

Tab. S4 Enrichment analysis of abundance classes of young donor' proteins.

Tab. S5 Enrichment analysis of abundance classes of middle donor' proteins.

Tab. S6 Enrichment analysis of abundance classes of old donor' proteins.

Tab. S7 Enrichment analysis of age-associated decreasing (14) and increasing (9) mitochondrial proteins obtained from cluster analysis ($p \leq 0.1$).

Tab. S8 Significantly altered genes with age published by Kalfalah *et al.* (2014).

Tab. S9 Confidence intervals of quantifiable mRNAs.

Tab. S10 Genes contained in the miRNA/mRNA network.

Tab. S11 Biological processes significantly altered with age published by Kalfalah *et al.* (2014).

Tab. S12 Enriched biological processes of proteins found with an age-associated alteration.

Tab. S13 Significantly enriched biological processes of the genes identified in the miRNA/mRNA network.

SUPPORTING INFORMATION (EXPERIMENTAL PROCEDURES)

Sample preparation for MS-analysis

Human dermal fibroblasts were cultivated under standardised conditions until passage three as described above. Cells were harvested, homogenised and lysed in urea-buffer (2 M thiourea, 7 M urea, 30 mM Tris-HCL, pH 8.0). Subsequently, total protein amount was determined using BCA protein assay (Thermo Scientific Pierce, Rockford, USA) and 10 µg of each sample were proteolytic digested with trypsin (Promega, Mannheim, Germany). Here, the proteins were incubated with 10 mM dithiothreitol at 56 °C for 45 min in Amicon Ultra filters (3 kDa cut-off; Millipore, Billerica, USA). Subsequently, 0.55 M iodoacetamide was added to the mixture and incubated for 30 min at room temperature and light protected. The mixture was centrifuged for 30 min at 14,000 x g and 4 °C. Next, 50 mM ammonium hydrogen carbonate was added and again centrifuged for 60 min at 14,000 x g and 4 °C. Proteins were recovered and 1:50 trypsin was added. Digestion was performed at 37 °C for 12 h. Afterwards, 0.1 % trifluoroacetic acid (TFA) was added to stop the digestion.

Mass spectrometric analysis

Mass spectrometric analyses of proteomes were carried out using highly reproducible and stable LC-MS/MS system and a label-free approach for quantification. Peptides of each sample were analysed with a nano-HPLC/ESI-MS system composed of an RSLCnano HPLC and a LTQ Orbitrap Velos (Thermo Fisher Scientific, Bremen, Germany) mass spectrometer equipped with a nano-electrospray ion source. Each sample was loaded onto a trap C₁₈ trapping column (2 cm × 100 µm × 5 µm, 100 Å, Thermo Fisher Scientific) and desalted with 0.1 % TFA for 10 minutes. Peptides were eluted from the trap, separated with an analytical column (Acclaim PepMap RSLC C₁₈; 25 cm × 75 µm × 2 µm, 100 Å, Thermo Fisher Scientific) for 120 minutes with a flow rate of 300 nL/min, and sprayed into the MS. The Orbitrap parameters were as follows: spray voltage, 1.4 kV; ion transfer tube temperature, 275 °C; collision gas, helium; collision gas pressure, 1.3 mTorr; normalised collision energy for MS/MS, 35 %. MS-spectra were acquired in the Orbitrap with a mass range of 300-1500 m/z and a resolution of 60,000. The Orbitrap was operated in a TOP4 data-dependent mode to automatically switch between MS and MS/MS acquisition. MS/MS-spectra were acquired applying gas-phase fractionation. Therefore, five m/z areas were used for precursor selection: 300-450 m/z, 450-550 m/z, 550-650 m/z, 650-800 m/z and 800-1500 m/z (for more

information see Fig. S6). Polysiloxane (445.120030 Th) was used as lock mass. For MS/MS, ions were isolated with an isolation width of 2 m/z and fragmented using collision-induced dissociation. MS/MS-spectra were acquired in the linear ion trap in centroid mode. Target ions selected for MS/MS were dynamically excluded for 45 sec. The ion selection thresholds were 500 counts for MS/MS. An activation Q of 0.25 and activation time of 10 ms was applied in MS/MS acquisitions.

Protein identification and quantification

For protein identification, the Proteome Discoverer (version 1.3, Thermo Fisher Scientific) and MASCOT search engine (version 2.4.1, Matrix Science, London, UK) were used. MS/MS-spectra were searched against the UniProtKB database (date 04/03/2013). Search parameters were as follows: enzyme, trypsin; missed cleavage sites, 2; taxonomy, homo sapiens; precursor mass tolerance, 10 ppm; fragment mass tolerance, 0.4 Da; oxidation of methionine as dynamic modification; carbamidomethylation of cysteine as fixed modification. The false discovery rate was set to 1 % ($p \leq 0.01$). Label-free quantification of proteins was carried out using Progenesis LC-MS (Nonlinear Dynamics, Newcastle upon Tyne, UK). A minimum of 2 unique peptides were required for quantification. Only proteins identified in 14 of 15 samples were regarded for quantification. Statistical analysis for the proteomes was performed using two approaches: multiple t-tests (ANOVA) and Pearson correlation. For ANOVA analysis a significance threshold of 5 % ($p \leq 0.05$) was applied. Pearson correlation was performed without any grouping with a significance threshold of 5 % ($p \leq 0.05$). Stability of protein and mRNA abundance was determined as described elsewhere (Peterson *et al.*, 2012). Therefore, protein/mRNA intensities were logarithmised (\log_{10}) and for each protein/mRNA the absolute mean difference between the age-groups ('mean young' – 'mean middle'; 'mean young' – 'mean old'; 'mean middle' – 'mean old') was calculated. Afterwards, the 'two one-sided test' for equivalence (TOST) was applied to test for similarity of the groups (e.g. $H_1: |\text{'mean young' - 'mean middle'}| < \text{equivalence range } (\epsilon)$). As equivalence range, the three-fold standard deviation ($\epsilon = 0.3$) was used. Proteins/mRNAs whose p-value was significant ($p \leq 0.05$) in all of the three pairwise comparisons were marked as unchanged.

Functional annotation, network and enrichment analysis of proteins

Gene set analysis of unchanged proteins was carried out using Consensus Path DB (<http://cpdb.molgen.mpg.de/>). The entire identified proteome was used as background list. Enrichment was applied on Gene Ontology, Reactome, Wikipathways and Pathway Interaction Database biological processes. We discarded gene sets that were redundant, had ≤ 5 members or a p-value above 0.01. Enrichment analyses of abundance classes and mitochondria related proteins were carried out using DAVID (<http://david.abcc.ncifcrf.gov/>) and the Gene Ontology Biological Process categorisation. We discarded processes that had a p-value above 0.05. Network and enrichment analysis was carried out using Cytoscape environment (<http://www.cytoscape.org/>) and ClueGo plug-in (<http://www.ici.upmc.fr/cluego/>). Parameters for network analyses were applied as follows: Ontology source, Gene Ontology biological processes or cellular components (date 12/10/2013); statistical test, enrichment/depletion (two-sided hypergeometric test); p-value correction, Benjamini-Hochberg; p-value restriction, $p \leq 0.01$; network specificity, ‘medium’; GO term restriction ‘min level = 4’, ‘max level = 8’, min percentage = 4.0; use GO term fusion; use GO term grouping; GO term connection restriction, kappa score ≥ 0.5 . The entire identified proteome was used as reference set.

mRNA/protein correlation analysis

Correlation analysis between measured mRNA-expression levels and protein abundance was performed using R (<http://www.r-project.org>). The mRNA intensities were log₂-scaled, the lowest 25 % based on the median intensities as well as probes with no corresponding EntrezID were discarded. In the case of Entrez GeneIDs corresponding to multiple AgilentIDs the mean intensities were used for further analysis, whereas the maximum value was set to 100 %. For each identified protein the sum intensities were divided by the underlying number of quantified peptides. The data was log₂-scaled and the maximum value was set to 100 %.

miRNA network and enrichment analysis

The age-associated miRNAs reported by Röck *et al.* (unpublished data) were used to build up a miRNA-gene regulatory network as follows: We built up an initial network for these miRNAs based on target predictions, which were derived from TargetScan

(<http://www.targetscan.org>). We then integrated gene expression measurements in order to find relationships between miRNAs and genes, which can be deduced by the data. We fitted a linear model with the gene expression data as response and the expression data of its predicted targeting miRNAs as predictor variables. We then performed a multiple linear regression analysis for each gene with elastic net penalty in order to select for miRNAs that have an influence on the gene expression data. For this purpose, we used the *glmnet* package for the R (<http://cran.r-project.org/web/packages/glmnet/index.html>) and introduced a negativity constraint to select only for negative miRNA effects. The penalty parameter was determined by 10-fold cross-validation. We finally obtained two networks by applying this procedure to the mRNA and the protein expression data, respectively.

SUPPORTING INFORMATION (FIGURES)

Supporting figures can also be found on the enclosed compact disk.

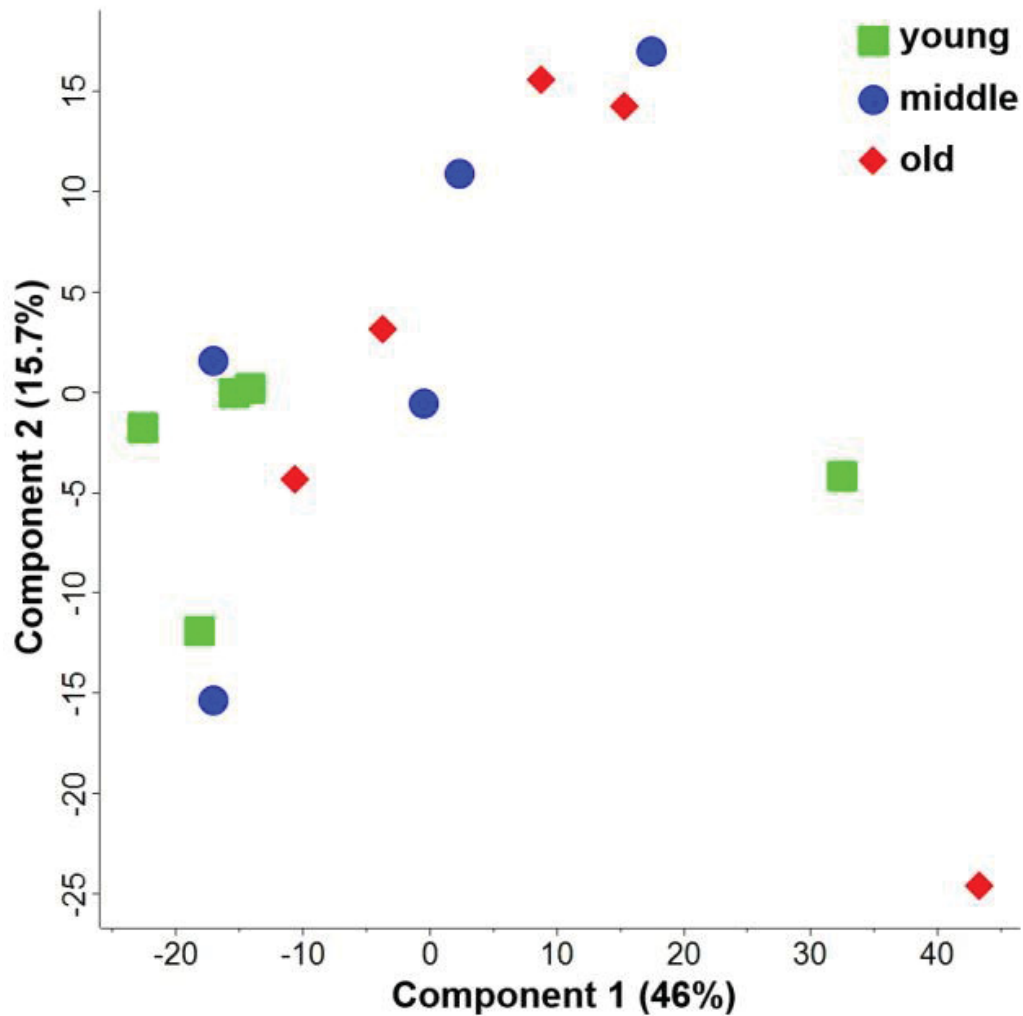


Figure S1 Principle component analysis (PCA) of quantified proteins. The individual age groups are indicated with different colors and signs: young, green squares; middle-aged, blue circles; old, red diamonds. Principal component revealed a heterogeneous protein expression pattern in fibroblasts of the three age groups.

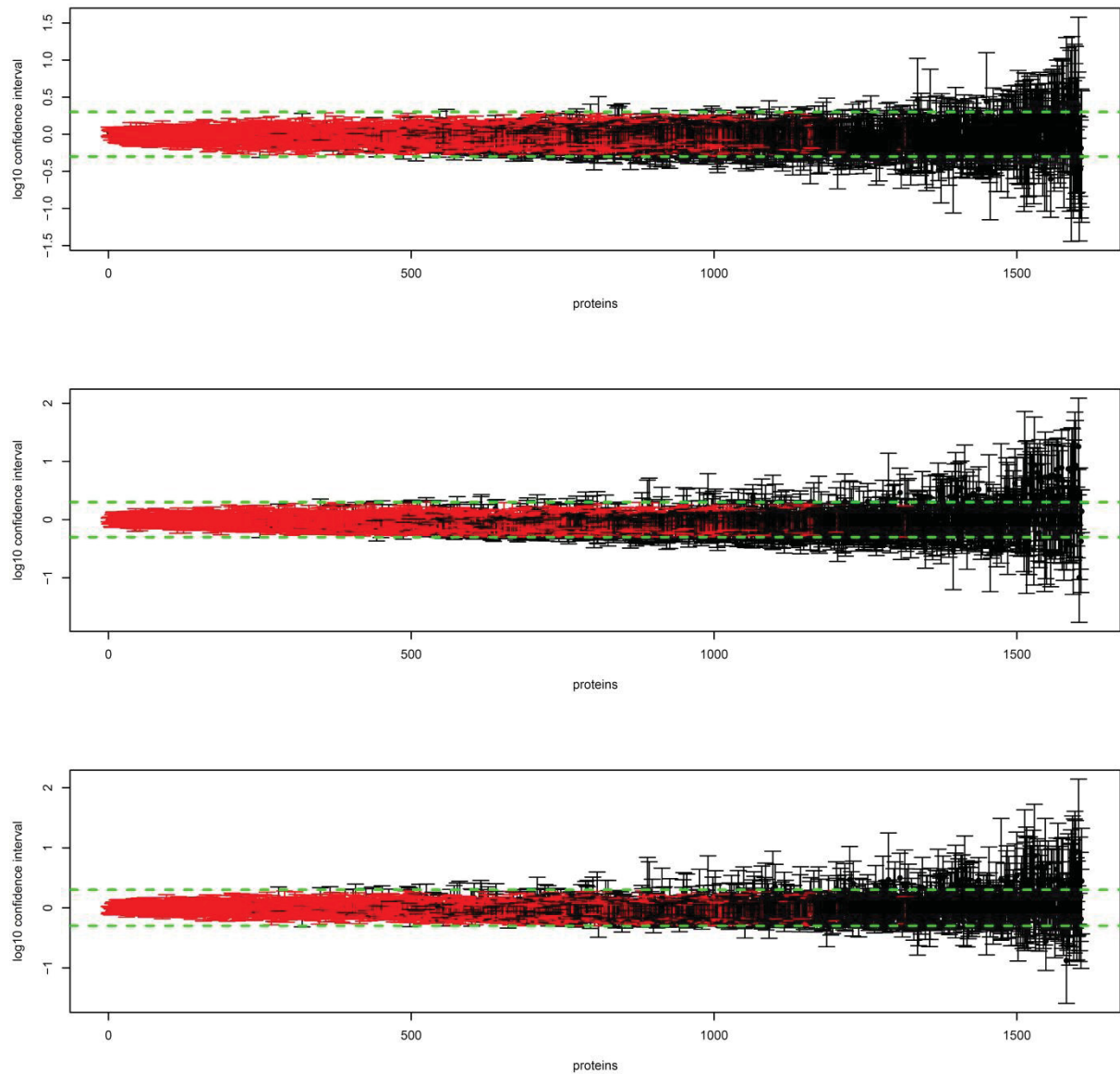


Figure S2 Distributions of confidence intervals of quantifiable proteins. Green line indicates upper and lower limits calculated from the technical variance (three times standard deviation). Significantly unchanged proteins during aging are indicated in red. Remarkably, over 47 % (755 proteins) of quantified proteins exhibited a stable abundance in cultivated fibroblasts across the different donor age groups.

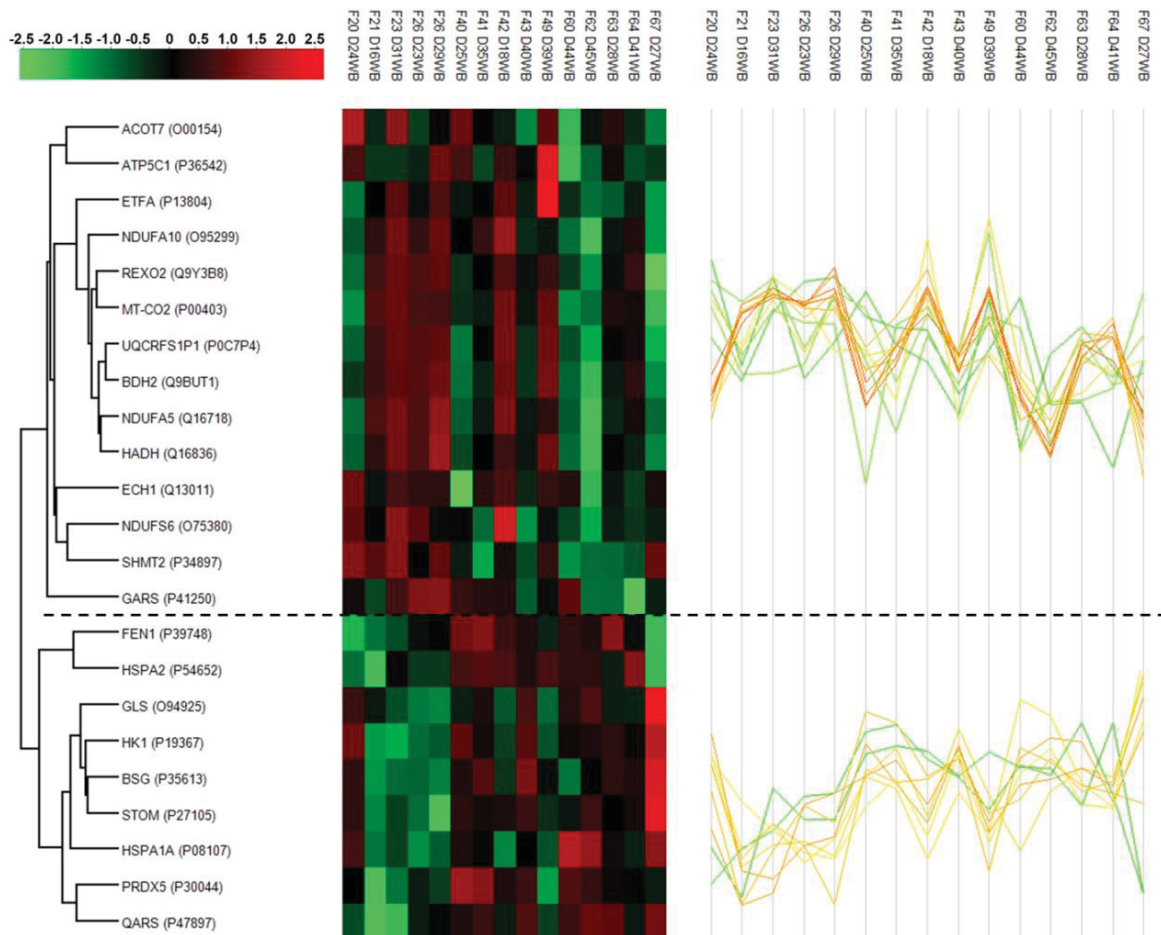


Figure S3 Cluster analysis of expression of mitochondria-related proteins. Cluster analysis of proteins related to mitochondria revealed 14 proteins showing decreasing and 9 proteins showing increasing expression levels with increasing age ($p \leq 0.1$).

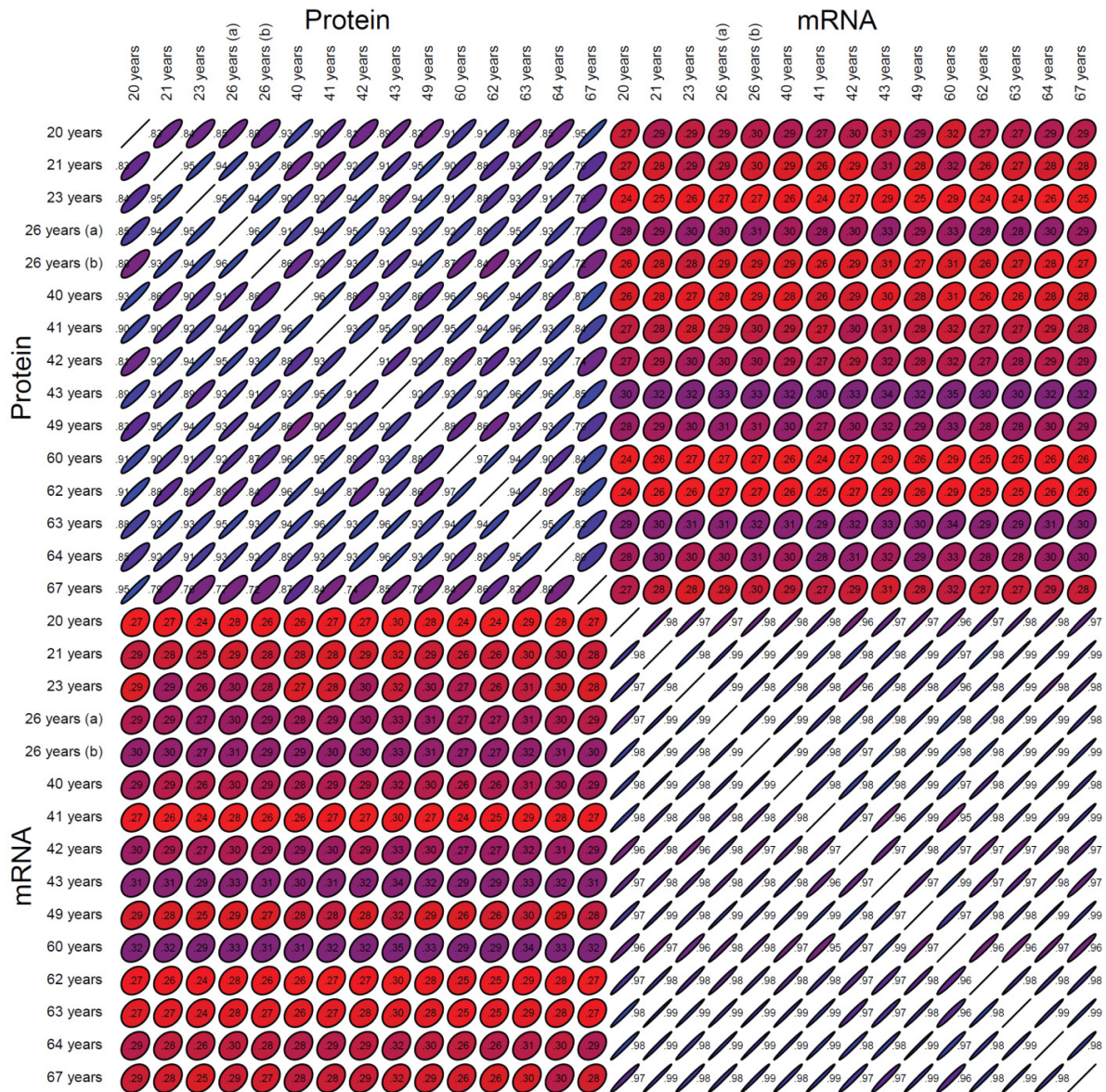


Figure S4 Correlation analysis of mRNA and protein abundances for quantified mRNA/protein pairs. Correlation coefficients are indicated by the ellipse shape. In each column the color code is sorted from highest (blue) to lowest (red) value. Neither inside age group in mRNA or protein data nor in same-sample comparison was an increased correlation observed.

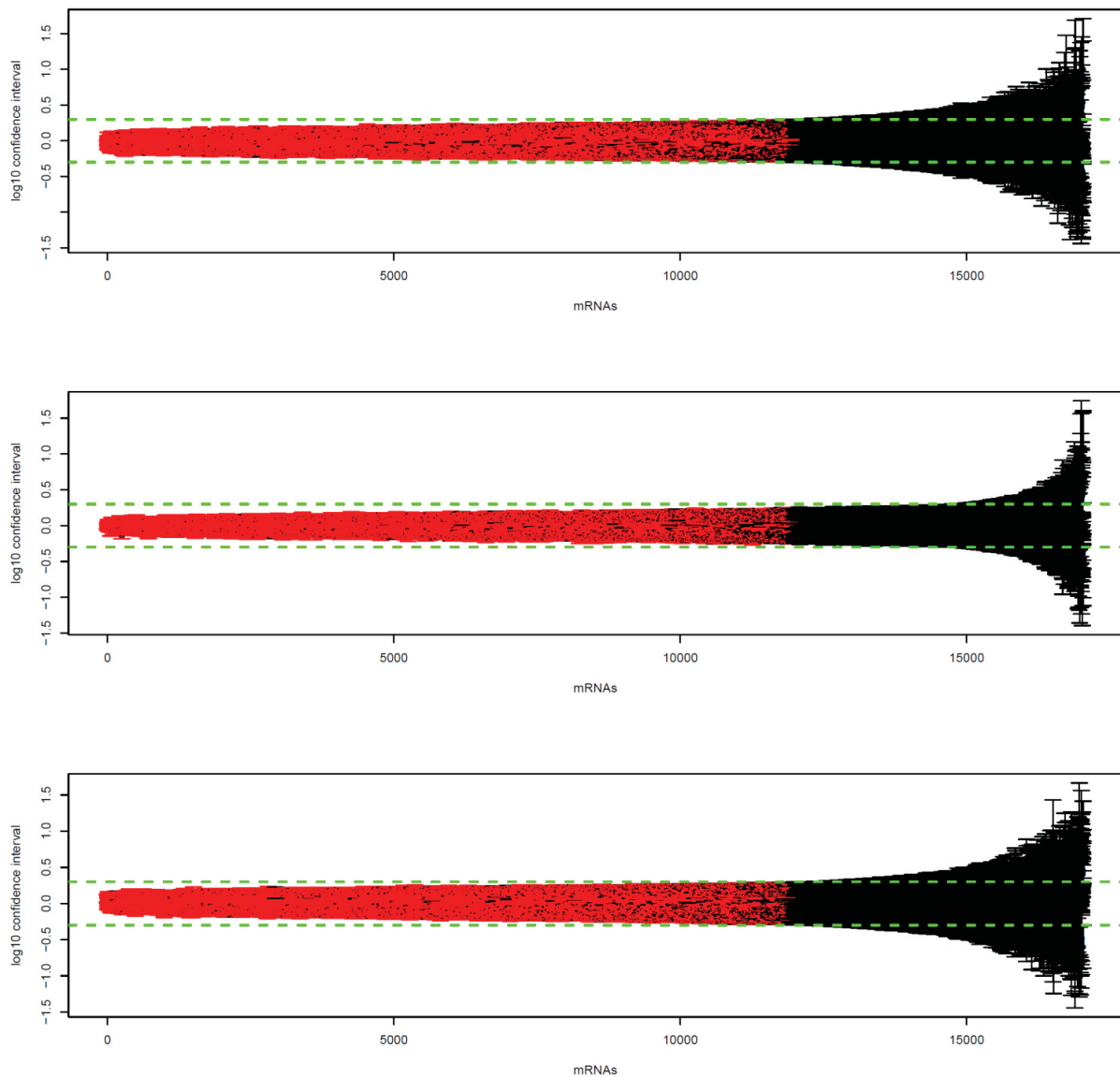


Figure S5 Distributions of confidence intervals of quantifiable mRNAs. Green line indicates upper and lower limits calculated from the technical variance (three times standard deviation). Significantly unchanged mRNAs across the different age groups are indicated in red. Remarkably, over 63 % (10665 mRNAs) of quantified mRNAs exhibited a stable abundance in fibroblasts across the distinct age groups.

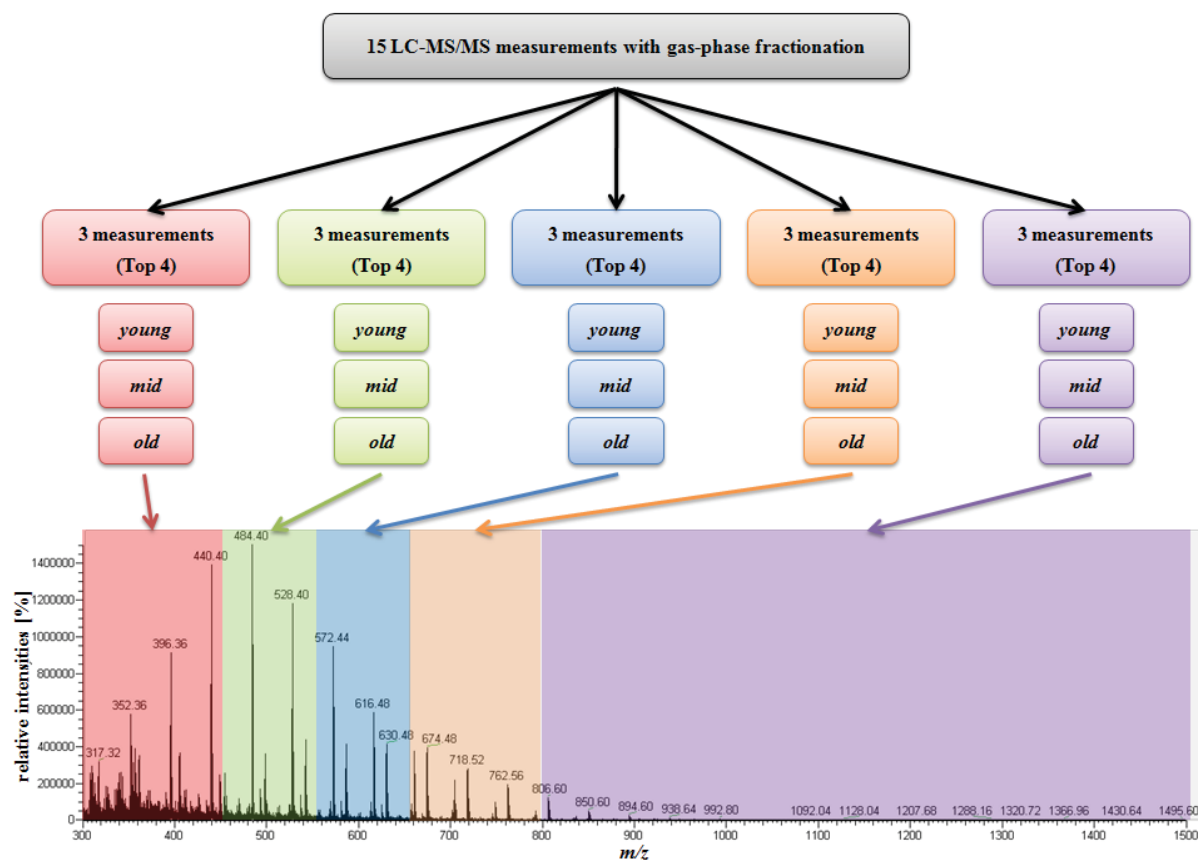


Figure S6 Overview of m/z ranges for LC-MS/MS analysis using gas-phase fractionation. The m/z segments for precursor selection are color coded as follows: (red: 300-450 m/z , green: 450-550 m/z , blue: 550-650 m/z , orange: 650-800 m/z , purple: 800-1500 m/z). Each segment was used for three measurements of each age group.

SUPPORTING INFORMATION (TABLES)

Supporting tables can be found on the enclosed compact disk.

Table S1 Significantly altered proteins with age. Quantitative label-free proteome analysis of *in situ* aged fibroblasts' proteome revealed 43 proteins that are differentially altered during *in situ* ageing (ANOVA: $p \leq 0.05$; Pearson correlation: $p \leq 0.05$). For ANOVA analysis donors were grouped according to calendar age into groups 20-30, 40-50 and 60-70 years, with five individual donors in each group.

Table S2 Confidence intervals of quantifiable proteins. Indicated are the quantifiable proteins according to their Uniprot accession. Stability of protein abundance was determined as described elsewhere (Peterson *et al.*, 2012). Therefore, protein intensities were logarithmised (\log_{10}) and for each protein the absolute mean difference between the age-groups ('mean young' – 'mean middle'; 'mean young' – 'mean old'; 'mean middle' – 'mean old') was calculated. Afterwards, the 'two one-sided test' for equivalence (TOST) was applied to test for similarity of the groups (e.g. H1: $|\text{'mean young' – 'mean middle'}| < \text{equivalence range } (\epsilon)$). As equivalence range, the three-fold standard deviation ($\epsilon = 0.3$) was used. Proteins whose p-value was significant ($p \leq 0.05$) in all of the three pairwise comparisons were marked as unchanged (yes).

Table S3 Enrichment analysis of biological processes of proteins with constant expression during aging. The entire identified proteome was used as background list. Enrichment was applied on Gene Ontology, Reactome, Wikipathways and Pathway Interaction Database (PID) biological processes. We discarded gene sets that were redundant, had < 5 members or a p-value above 0.01.

Table S4 Enrichment analysis of abundance classes of young donor' proteins. Enrichment analysis was carried out using DAVID and Gene Ontology biological processes. We discarded processes that had a p-value above 0.05.

Table S5 Enrichment analysis of abundance classes of middle donor' proteins. Enrichment analysis was carried out using DAVID and Gene Ontology biological processes. We discarded processes that had a p-value above 0.05.

Table S6 Enrichment analysis of abundance classes of old donor' proteins. Enrichment analysis was carried out using DAVID and Gene Ontology biological processes. We discarded processes that had a p-value above 0.05.

Table S7 Enrichment analysis of age-associated decreasing (14) and increasing (9) mitochondrial proteins obtained from cluster analysis ($p \leq 0.1$). Enrichment analysis was carried out using DAVID and Gene Ontology biological processes. We discarded processes that had a p-value above 0.05. A total of 19 biological processes were significantly decreased and 16 biological processes were significantly increased with age.

Table S8 Significantly altered genes with age published by Kalfalah *et al.* (2014). Statistical analysis of transcriptome data revealed 137 significantly altered genes with age.

Table S9 Confidence intervals of quantifiable mRNAs. Indicated are the quantifiable mRNAs according to their Entrez Gene ID. Stability of mRNA abundance was determined as described elsewhere (Peterson *et al.*, 2012). Therefore, mRNA intensities were logarithmised (\log_{10}) and for each mRNA the absolute mean difference between the age-groups ('mean young' – 'mean middle'; 'mean young' – 'mean old'; 'mean middle' – 'mean old') was calculated. Afterwards, the 'two one-sided test' for equivalence (TOST) was applied to test for similarity of the groups (e.g. H1: $|\text{'mean young' – 'mean middle'|} < \text{equivalence range } (\epsilon)$). As equivalence range, the three-fold standard deviation ($\epsilon = 0.3$) was used. mRNAs whose p-value was significant ($p \leq 0.05$) in all of the three pairwise comparisons were marked as unchanged (yes).

Table S10 Genes contained in the miRNA/mRNA network. Network analysis revealed 164 mRNAs as targets of significantly altered miRNAs (Röck *et al.*, unpublished data).

Table S11 Biological processes significantly altered with age published by Kalfalah *et al.* (2014). Statistical analysis of transcriptome data revealed 117 enriched biological processes altered with age.

Table S12 Enriched biological processes of proteins found with an age-associated alteration. To uncover biological processes linked to age-associated proteins in the proteome of *in situ* aged fibroblasts, we performed a detailed network and enrichment analysis using Gene Ontology biological processes. For the 43 age-associated altered proteins, we assigned 71 unique biological processes as highly enriched ($p \leq 0.01$). Correction for multiple testing was applied using Benjamini-Hochberg method.

Table S13 Significantly enriched biological processes of the genes identified in the miRNA/mRNA network. Enrichment analysis revealed biological processes such as 'signal transduction', 'cell death', 'RNA and protein metabolism', 'cell communication', 'response to stimuli', 'development' and 'RNA and protein biosynthesis' as highly enriched.

3.5 Publikation IV

Characterization of skin aging associated secreted proteins (SAASP) produced by dermal fibroblast isolated from intrinsically aged human skin

Daniel M. Waldera-Lupa^{1,2}, Faiza Kalfalah³, Petra Boukamp⁴, Kai Safferling⁵, Gereon Poschmann^{1,2}, Christine Götz-Rösch⁶, Francoise Bernerd⁷, Laura Haag³, Hanzen Birgit³, Ulrike Huebenthal⁵, Ellen Fritsche⁶, Niels Grabe⁵, Fritz Boege³, Julia Tigges^{6*}, Jean Krutmann^{1,6*}, Kai Stühler^{1,2*}

* Authors contributed equally

¹Institute of Molecular Medicine, University of Duesseldorf, Duesseldorf, Germany

²Molecular Proteomics Laboratory, Heinrich-Heine-University, Düsseldorf, Germany

³Institute of Clinical Chemistry and Laboratory Diagnostics, Heinrich-Heine-University, Med. Faculty, Düsseldorf, Germany

⁴German Cancer Research Centre, Heidelberg, Germany

⁵Hamamatsu Tissue Imaging and Analysis Center, BIOQUANT, Ruprecht-Karls-University, Heidelberg, Germany

⁶IUF – Leibniz Research Institute for Environmental Medicine, Düsseldorf, Germany

⁷L'Oréal Recherche, Clichy, Paris, France

ABSTRACT

Most molecular hallmarks of cellular senescence have been identified in studies in which cells were aged *in vitro* either by driving them into replicative or stress-induced senescence. In contrast, less is known about the characteristic features of cells which have aged *in vivo*. Here we provide a systematic molecular analysis of human dermal fibroblasts (NHDFs) which were isolated from intrinsically aged human skin of young *versus* middle aged *versus* old donors. We have found that intrinsically aged fibroblasts encompass ‘DNA segments with chromatin alterations reinforcing senescence (DNA-SCARS)’, which are, however, neither accompanied by induced DNA double strand breaks, nor decreased cell viability, nor telomere shortening, but the development of a secretory phenotype. Using a combined approach of (i) quantitative proteomic analysis of the entire secretome applying high-resolution mass spectrometry and (ii) a commercially available cytokine multiplex assay we identified 998 proteins secreted by intrinsically aged NHDFs. Seventy of these proteins exhibited an age-dependent secretion pattern. Bioinformatical comparison of these skin aging-associated secreted proteins (SAASP) with the classically described senescence-associated secretory phenotype (SASP) revealed that matrix degrading as well as pro-inflammatory processes are common aspects of both, also indicating their functional relevance for skin aging. Twenty-seven proteins involved in metabolism and adherens junction interactions, however, were unique for NHDFs isolated from intrinsically aged skin. In conclusion, fibroblasts isolated from intrinsically aged skin exhibit some, but not all molecular hallmarks of cellular senescence. Most importantly, they secrete a unique pattern of proteins which is distinct from the classically described SASP and might contribute to skin aging.

ABBREVIATIONS

ADAMTSL1: A Disintegrin And Metalloproteinase with Thrombospondin Motifs-like protein 1, BP: binding protein, CD248: endosialin, CDH: cadherin, COL: Collagen, CXCL: C-X-C motif chemokine, DNA-SCARS: DNA segments with chromatin alterations reinforcing senescence, ECM: extracellular matrix, ENO2: enolase 2, ERBB2: human epidermal growth factor receptor 2 (HER2), EREG: epiregulin, ESI: electrospray ionization, F2: Prothrombin, FBN: Fibrillin, GBA: glucosylceramidase, GGCT: γ -glutamylcyclo-transferase, GRB2: growth factor receptor-bound protein, GSN: Gelsolin, H: Histon, IGF: insulin-like growth factor, IL: interleukin, IL1RN: IL-1 receptor antagonist protein, IFNG: interferon γ , ITGBP: integrin beta-like protein, kbp: kilo base pairs, LC: liquid chromatography, LGALS1: Galectin, LMAN2: Lectin, mannose-binding protein 2, MEF: mouse embryonic fibroblast, MFAP: microfibrillar-associated protein, MIF: migration inhibitory factor, MMP: matrix metalloproteinase, MS: mass spectrometry, MUC: Mucin, MXRA: matrix-remodeling-associated protein, NEU1: Sialidase-1, NHDF: normal human dermal fibroblasts, NRG1: heregulin, NT5E: 5'nucleotidase (CD73), PLAT: tissue-type plasminogen activator (tPA), PLAUR: urokinase plasminogen activator surface receptor (uPAR), PI: propidium iodide, PIKK: phosphatidylinositol 3'kinase-related kinases, PML: promyelocytic leukemia protein, PN: passage number, PRELP: prolargin, PRNP: major prion protein, PSAP: prosaposin, SAASP: skin aging-associated secreted proteins, SASP: senescence associated secretory phenotype, SERPINE1: plasminogen activator inhibitor 1 (PAI-1), SERPINB2: plasminogen activator inhibitor 2 (PAI-2), SILAC: stable isotope labeling by amino acids in cell culture, SMS: senescence-messaging secretome, STC1: stanniocalcin-1, SUMF1: sulfatase-modifying factor 1, TFPI: tissue factor pathway inhibitor, THBS: Thrombospondin, TPST: protein-tyrosine sulfotransferase, TNF: tumor necrosis factor, TRFL: telomere restriction fragment length, VEGF: *Vascular Endothelial Growth Factor*, *VIT1: F-box only protein 11*

INTRODUCTION

Skin aging is characterized by structural and functional alterations of the dermis (Gilchrest BA and Krutmann J, 2006). The dermal stroma consists mainly of fibroblasts and their surrounding matrix (Boukamp, 2005, Parrinello *et al.*, 2005) and is a mostly post-mitotic tissue which allows for dysfunctional cells to accumulate over time. Therefore the homeostasis of the dermis depends strongly on cellular adaptation and damage clearance. The dermal fibroblast is a long-lived cell system, where one expects aging-associated alterations to accumulate and cellular functions to adapt / maladapt, accordingly.

A well described adaptive / maladaptive response of fibroblasts subjected to aging is a genetic program termed cellular senescence that limits cell proliferation (d'Adda di Fagagna *et al.*, 2003, Campisi and d'Adda di, 2007). *In vitro* in cultured skin fibroblasts, cellular senescence has been found to be induced by replicative telomere shortening (= replicative senescence, d'Adda di Fagagna *et al.*, 2003) or stress (= stress-induced senescence, Campisi and d'Adda di, 2007). The resulting senescent phenotypes have been intensively studied and found to encompass irreversible cell cycle arrest (d'Adda di Fagagna *et al.*, 2003, Herbig *et al.*, 2004, Hayflick and Moorhead, 1961), flat and enlarged cell morphology (Elzi *et al.*, 2012), enhanced heterochromatinisation (Narita *et al.*, 2003, Kreiling *et al.*, 2011) and the acquisition of a senescence-associated secretory phenotype (SASP, Coppe *et al.*, 2008) also termed senescence-messaging secretome (SMS, Kuilman and Peeper, 2009), which at least to some extent requires the formation of 'DNA segments with chromatin alterations reinforcing senescence' (DNA-SCARS, Rodier *et al.*, 2011). For the SASP aberrant secretion of over 80 factors including many cytokines, growth factors and matrix metalloproteinases (MMPs) has been reported (Coppe *et al.*, 2010a, Coppe *et al.*, 2011, Coppe *et al.*, 2008, Young and Narita, 2009). The relevance of these findings for fibroblasts present in aged human skin, i.e. for *in situ* aged fibroblasts is not known, because most studies characterizing SASP, but also other molecular hallmarks defining cellular senescence, have employed cultured cells which were either driven into replicative senescence by long-term passaging (Passi *et al.*, 1997, Lehmann *et al.*, 2008, Bhaumik *et al.*, 2009, Freund *et al.*, 2011), or into stress-induced senescence by overexpressing oncogenes (Coppe *et al.*, 2011, Orjalo *et al.*, 2009, Wajapeyee *et al.*, 2008) or by causing nuclear DNA damage e.g. by ionizing radiation (Coppe *et al.*, 2011, Coppe *et al.*, 2008, Freund *et al.*, 2011, Lehmann *et al.*, 2008, Rodier *et al.*, 2011, Laberge *et al.*, 2012, Pitiyage *et al.*, 2012). Expression of a SASP by *in situ* aged skin fibroblasts, however, might

be of clinical relevance for skin aging because some of the key proteins defined to constitute a classical SASP include Matrixmetalloproteinase-1 (MMP-1), Vascular Endothelial Growth Factor (VEGF), Interleukin (IL)-6 and IL-8 (Coppe *et al.*, 2010a), i.e. secreted proteins which are thought to be critically involved in the pathogenesis of skin aging (Gilchrest BA and Krutmann J, 2006). It is thus tempting to speculate that by virtue of producing a SASP senescent dermal fibroblasts might drive aging at the organ level.

In the present study we have therefore systematically analyzed primary human dermal fibroblasts (NHDFs) which were isolated from intrinsically aged skin of adult donors from three different age groups. Given the potential functional relevance for skin aging we were particularly interested in the capacity of these cells to secrete proteins. We therefore decided to use methods which allowed us to analyze the secretome of these cells in the most comprehensive manner. Specifically, we employed a combination of an unbiased quantitative proteomic approach of the entire secretome applying high-resolution mass spectrometry with a candidate-driven approach using a commercially available multiplex cytokine assay with state-of-the-art bioinformatics tools including a detailed enrichment and network analysis. In order to be able to do so, we used skin fibroblasts which had been isolated from intrinsically aged skin and then kept in culture for less than six passages prior to analysis. We are aware that this strategy poses the risk of introducing *in vitro* artefacts, but strongly believe that this potential disadvantage is weighed out by the comprehensibility of our analytical approach. In support of this assumption and as discussed in detail in the following paragraph, fibroblasts analyzed under these conditions indeed displayed hallmarks of cellular senescence (reviewed in Tigges *et al.*, 2014) and secrete proteins known to be of functional relevance for skin aging.

RESULTS AND DISCUSSION

In this study we asked whether hallmarks of cellular aging which previously were described to be present in *in vitro* aged fibroblast were also present in fibroblasts which had aged *in situ*, i.e. in human skin. For this purpose we analyzed primary human skin fibroblasts which had been isolated from skin samples obtained from donors from three different age groups (five donors per group, 20 -29 *versus* 40-49 *versus* ≥ 60 years of age, Table S8). In order to detect alterations truly associated with donor age and to minimize confounding aspects we ensured that (i) all cells were studied at low passage numbers (≤ 6) during the phase of exponential growth, (ii) the study was restricted to dermal fibroblasts from female donors to avoid hormonal and other sex-specific influences (Makrantonaki *et al.*, 2012, reviewed in Makrantonaki *et al.*, 2010) and (iii) all cells studied were isolated from the same intrinsically aged skin area (i.e. the bottom side of the female breast), thereby minimizing variances due to body location or different exposure to the external milieu (Irwin *et al.*, 1994).

We were interested in telomere shortening, which, although controversial (Boukamp, 2005, Krunic *et al.*, 2009), has been described as a major driving force of fibroblast senescence *in vitro* (Herbig *et al.*, 2004, Figueroa *et al.*, 2000). We measured telomere restriction fragment length (TRFL) and observed that all cells, when studied at the same low passage number (PN < 5), had a similar TRFL-value of around 3.6 kilo base pairs (kbp, Fig. 1A). Thus *in situ* aged NHDFs are not subjected to a significant extent of replicative telomere shortening. We also excluded that our data is compromised by decreased viability due to replicative senescence, as the analysis of markers for apoptosis (annexin V) and necrosis/late apoptosis (propidium iodide (PI)) did not increase in a donor-age dependent manner in our cells (Fig. 1B). Although others have reported on longer telomeres in their fibroblast cultures of aged donors in general (7-11 kbp, von Zglinicki *et al.*, 1995, Krunic *et al.*, 2009), there is evidence from the literature that even the same cell type from different aged donors exhibits varying rates of telomere shortening (Figueroa *et al.*, 2000, Harley *et al.*, 1990), which might explain this discrepancy. Also and in line with our findings, Kunic and co-workers provided evidence that adult dermal fibroblasts had a low rate of telomere loss and concluded that overall telomere erosion is not a driving force for skin aging (Krunic *et al.*, 2009). Similarly, it has been reported that the replicative lifespan of fibroblasts isolated from various human tissues does not correlate with chronological age, morbidity or mortality of the donors (Cristofalo *et al.*, 1998, Maier *et al.*, 2007).

Rodier *et al.* were first to identify DNA-SCARS as 53BP1/promyelocytic leukemia protein (PML) co-stained persistent foci within the nucleus of different senescent human cell types and mouse tissues (Rodier *et al.*, 2011). We therefore next asked whether intrinsically aged NHDFs have a higher inclination to form DNA-SCARS. We found that large nuclear foci double positive for 53BP1 and PML were more frequent in cells from aged donors (representative images in Fig. 1C). The percentage of cells containing one or more of such foci was significantly increased in an age-dependent manner (Fig. 1D, left). Furthermore, quantitative scores of DNA-SCARS did not significantly correlate with basal γ Histon 2AX (H2AX) levels (Fig. 1D, right), which is the phosphatidyl inositol 3'kinase-related kinases (PIKK)-phosphorylated form of the histone variant H2AX and an established marker for DNA double strand breaks (Celeste *et al.*, 2003, Lobrich *et al.*, 2010, Rogakou *et al.*, 1999). Together with the fact that DNA-SCARS form independently of p53, pRB and several other checkpoint proteins (Rodier *et al.*, 2011) this suggests that their formation is indeed indicative of cellular senescence, regardless of its type.

As DNA-SCARS are also thought to be involved in the development of a SASP (Rodier *et al.*, 2011) we next assessed whether intrinsically aged NHDFs display a classical SASP (reviewed in Coppe *et al.*, 2010a). We addressed this hypothesis (i) by an unbiased quantitative proteomic approach of the entire secretome applying high-resolution mass spectrometry combined with (ii) a candidate-driven approach using a commercially available multiplex cytokine assay. It should be noted that the secretome analysis presented here were carried out on cells in logarithmic growth in aerobic (20 % O₂), two-dimensional culture, which is a stress condition for NHDFs compared to their physiological, quiescent and mostly anaerobic state in the dermal stroma. In particular O₂ partial pressure is known to modulate the secretory phenotype in mouse fibroblasts (Coppe *et al.*, 2010b), as does cell cycle arrest provoked by serum starvation, which we applied on our cells (see material and methods section for details). The latter has been described to induce similar inflammatory changes as oncogene-induced SASP (Rovillain *et al.*, 2011). Nevertheless, we believe that our chosen study approach is suitable to characterize the secretory phenotype of *in situ* aged NHDFs and to test the hypothesis whether or not it differs from the classically described SASP of stress-induced senescence. Our study design differs from most previously performed studies on the secretory phenotype of cells, where alterations in protein secretion were deduced from mRNA data (Mu and Higgins, 1995, Edwards *et al.*, 1996) or where only a small group of proteins like e.g.

interleukins (Coppe *et al.*, 2008, Kuilman *et al.*, 2008) or MMPs (West *et al.*, 1989, Parrinello *et al.*, 2005) was analyzed.

The liquid chromatography(LC)-electrospray ionization(ESI)-mass spectrometry(MS)/MS (LC-ESI-MS/MS) analysis of the secretomes of intrinsically aged NHDF lines led to the identification of 1331 unique proteins. Using bioinformatics (see supplementary material and methods) we confirmed the likelihood of these proteins to be secreted by accepting all proteins confirmed by SignalP (Petersen *et al.*, 2011) known to have a N-terminal signal sequence for secretion (531 proteins), being predicted by SecretomeP (Bendtsen *et al.*, 2004) due to appropriate sequence characteristics relevant for non-classical secretion (336 proteins) and documented extracellular localization (44 proteins, Fig. S1). As known secreted factors such as Fibroblast Growth Factor (FGF)1, FGF2 and IL1 are also secreted through various non-classical pathways (Nickel and Seedorf, 2008), we added 336 proteins predicted to be non-classically secreted to our candidate list as well, whereof four proteins (IL1B, Migration Inhibitory Factor (MIF), Plasminogen Activator Inhibitor (SERPINB/PAI)2 and FGF2) are known SASP factors. Furthermore it is well known that transmembrane proteins can be shedded by proteinases and therefore are likely to be found in the secretome (Schlondorff and Blobel, 1999, Mullberg *et al.*, 2000). Consequently we identified six shedded membrane proteins (CD14, Cadherin-2 (CDH2), Galectin (LGALS)1, Lectin, mannose binding protein (LMAN)2, Mucin (MUC)16 and Tissue Factor Pathway Inhibitor (TFPI), Tab. S9) in the analyzed secretomes. Therefore we also included 66 membrane or membrane-associated proteins as candidate secretory proteins. Although we could not exclude exosomal associated proteins to be abundant in the analyzed secretomes, we did not consider this group for further analysis.

Thus via the unbiased proteomic approach we identified a total of 977 unique proteins likely to be secreted by classical or non-classical pathways whereas 354 proteins were possible contaminants. Although we identified three cytokines by our LC-ESI-MS/MS approach we could not exclude that some cytokines were missed due to their small size, limited production of tryptic peptides and/or low protein concentration. Therefore we analyzed cytokines by a targeted approach as they are relevant factors involved in the para- and autocrine effects of SASP (Hoare and Narita, 2013). This confirmed 21 additional cytokines (Fig. 3, Fig. S2 + Tab. S1).

Altogether we identified 998 proteins in the secretome of intrinsically aged NHDFs. Others, who used similar proteomic approaches analyzing replicative senescent fibroblasts, identified 407 secreted proteins using LC-MS/MS (Micutkova *et al.*, 2011). Via a stable isotope labeling by amino acids in cell culture (SILAC) approach on oncogene-induced senescent fibroblasts 1602 proteins in total of which 429 proteins were determined to be secreted were identified in another study (Acosta *et al.*, 2013). Thus our approach revealed the highest number of secreted proteins for *in situ* aged NHDFs, which allowed us to characterize the skin aging associated pattern of secreted proteins in greater detail.

Accordingly, we next analyzed whether NHDFs change their secretory phenotype during *in situ* aging. Therefore, we first performed detailed functional annotation analysis based on the 998 identified secreted proteins and identified 14 different biological processes, e.g. ‘apoptosis’, ‘cell cycle’, ‘cell-cell communication’, ‘ECM organization’, ‘hemostasis’, ‘metabolism of proteins’ and ‘signal transduction’ with at least five assigned proteins per term and age to be enriched in the secretomes (Fig. 2A). Among these enriched biological processes ‘ECM organization’ was the most abundant one. Also, the biological processes of ‘immune system’ and ‘hemostasis’ detected here reflect the role of fibroblasts in wound healing and inflammation (Midwood *et al.*, 2004). Surprisingly comparison of the different age groups revealed no significant alterations during *in situ* aging of the cells (Fig. 2B). Remarkably, about 30 % of all quantified proteins were stably abundant during aging (Fig. S3). Categorization of these proteins using the Consensus Path DB (Kamburov *et al.*, 2009) revealed ‘carbohydrate metabolism’, ‘catabolism’, ‘developmental process’, ‘hormone metabolism’ and ‘extracellular structure organization’ as the most prominent biological processes (Tab. S2) within this group. Thus the *in situ* aging process of NHDFs is accompanied by only slight rather than dramatic changes of the secretome and it seems that the cells thus maintain their canonical function in preserving the overall integrity of the skin during aging.

Therefore in a next step we examined the age-associated alterations on single protein level. Statistical analysis of the proteins identified by unbiased LS-ESI-MS/MS-analysis revealed that 63 secreted proteins altered their abundance during aging (Tab.1). Additionally seven proteins identified using the multiplex cytokine assay were significantly increased with age: IL-1B, IL-1RN, IL-4, IL-15, Interferon (IFN)G, CXCL-10 and Tumor Necrosis Factor (TNF) alpha (Fig. 3 A-G). IL-6 and Granulocyte Colony Stimulation Factor (G-CSF, Fig. 3 H+I)

were also age-dependently up-regulated in the supernatants of our cells by trend but did not quite reach statistical significance with p-values of 0.0566 and 0.0593, respectively.

For subsequent analysis proteins were grouped according to their regulation profile as immediate, late and long-term regulated proteins (Fig. 2C+D). 39 proteins (24 up and 15 down) were assigned to the immediate group with significant changes in abundance between the young and middle group, 7 proteins (2 up and 5 down) showed a late regulation with significant abundance changes between the middle and old group and 24 proteins (9 up and 15 down) were long-term regulated with a continuous increase or decrease of protein abundance during aging. Roughly, proteins with an age-associated decrease in abundance were associated with extracellular matrix (ECM) remodeling (A Disintegrin And Metalloproteinase with Thrombospondin motifs-like protein (ADAMTSL)1, F-box only protein 11 (VIT1), Fibrillin (FBN)2, Collagen (COL)1A1, Sulfatase-modifying Factor (SUMF)1, Prothrombin (F2), Microfibrillar-associated Protein (MFAP)5, Gelsolin (GSN)) and cell adhesion (Integrin beta-like protein (ITGBL1), ISLR, CDH2), whereas proteins with an age-associated increase in abundance were associated with cell cycle arrest (Major Prion Protein (PRNP), Interferon- γ (IFNG), Thrombospondin (THBS)1, SERPINE1), inflammatory responses (Protein-tyrosine sulfotransferase (TPST)1, IL15, IL-1 receptor antagonist protein (IL1RN), IL1 β , Tumor necrosis factor (TNF), IL4, C-X-C motif chemokine (CXCL)10, IL8, CD14) and ECM breakdown (MMP1, MMP10, MMP3, MMP14, Matrix-remodeling-associated protein (MXRA)5).

One ECM protein we identified was ADAMTSL1 which is a secreted metalloproteinase (Hirohata *et al.*, 2002) and has been described as a direct MMP10 substrate (Schlage *et al.*, 2014). This assumption is in line with our present observation that MMP10 is increased and ADAMTSL1 is decreased with intrinsic aging of skin.

Stanniocalcin-1 (STC1) is a glycoprotein hormone originally identified as a regulator of calcium and phosphate homeostasis in bony fish. In STC1^{-/-} mouse embryonic fibroblasts (MEFs) which are resistant to growth inhibition and cell death induced by H₂O₂ or by 20 % O₂, it was demonstrated that STC1 expression down-regulated pro-survival ERK1/2 signaling and reduces survival under conditions of oxidative stress (Nguyen *et al.*, 2009). In our study we found this protein to be significantly up-regulated with increasing donor age which suggests that *in situ* aged NHDFs are more sensitive to oxidative stress.

Furthermore, we here obtained evidence that protein shedding plays a role in *in situ* aging of NHDFs, as four of the six known membrane proteins that undergo shedding were significantly altered in their secretome (CD14, CDH2, LMAN2 and TFPI). CD14 is a possible key regulator of VEGF production (Umazume *et al.*, 2013) which is a known SASP-factor (Coppe *et al.*, 2010a, Coppe *et al.*, 2010a) and thought to be critically involved in skin aging (Yano *et al.*, 2004) and which we here found to be up-regulated in the secretomes of *in situ* aged NHDFs. CDH2 on the other hand is significantly down-regulated. The decline of CDH2 in kidneys of aged rats is associated with a loss of cell polarity (Jung *et al.*, 2004) and in fibroblasts cell polarity is an important factor for cell migration and therefore wound healing (Ridley *et al.*, 2003). In this context we also identified endosialin (CD248) as being decreased in *in situ* aged NHDFs. This ECM protein is involved in cell adhesion and migration (Tomkowicz *et al.*, 2007) whereas down-regulation results in a decline in migratory capacity. Taken together this may lead to an impaired wound healing response as it is present in elderly people (Gosain and DiPietro, 2004, Bentov and Reed, 2014).

LMAN2 is also down-regulated in our *in situ* aged NHDFs. It is shedded by macrophages thereby regulating phagocytosis (Shirakabe *et al.*, 2011) but has never been described to be secreted by fibroblasts or in the context of skin aging before. The same holds true for TFPI which was also down-regulated in *in situ* aged NHDFs. It is known to be shedded to maintain hemostatic balance in the vascular system (Schuepbach *et al.*, 2011) and to be up-regulated in the blood of menopausal women (Regnault *et al.*, 2011), but to our knowledge has not yet been described in the context of skin aging.

Taken together the combination of both approaches led to the identification of 70 secreted proteins which define the secretory phenotype of NHDFs isolated from intrinsically aged human skin (Tab. 1, for detailed information see Tab. S3) and subsequently will be referred to throughout this study as Skin Aging Associated Secreted Proteins (SAASP).

In order to reveal biological processes linked to age-dependently altered proteins in the secretome of *in situ* aged NHDFs we next performed a detailed enrichment and network analysis of the 70 SAASP (Tab. 1) using Reactome database (Matthews *et al.*, 2009, Fig.4). In total 45 proteins (64.3 %) were successfully assigned to 45 unique biological processes (Tab. S4) representing the alteration of the secretory phenotype of *in situ* aged NHDFs. The four biological processes with the lowest p-values were associated with ECM remodeling: ‘extracellular matrix organization’ ($p = 4.1 \times 10^{-8}$), ‘elastic fiber formation’ ($p = 3.1 \times 10^{-6}$),

‘activation of matrix metalloproteinases’ ($p = 2.6 \times 10^{-5}$) and ‘collagen degradation’ ($p = 5.8 \times 10^{-5}$). Furthermore, we identified ‘glycosphingolipid metabolism’ ($p = 6.4 \times 10^{-5}$), ‘regulation of insulin-like growth factor (IGF) transport and uptake by insulin-like growth factor binding proteins’(IGFBPs, $p = 1.6 \times 10^{-4}$), ‘molecules associated with elastic fibers’ ($p = 4.8 \times 10^{-4}$) and ‘sphingolipid metabolism’ ($p = 6.7 \times 10^{-4}$) as significantly enriched biological processes.

We next compared the SAASP identified in this study with the previously reported classical SASP. Among the 998 secreted proteins found in the secretome of *in situ* aged fibroblasts we identified 43 of the known 80 SASP factors (summarized in Coppe *et al.*, 2010a, Tabl. S5). Altogether, nine classical SASP proteins were significantly age-dependently altered in the secretomes of our cells, whereof eight were up- (IL-8: 8.1-fold, IL-1b: 4.0-fold, MMP-1: 3.9-fold, MMP-10: 3.2-fold, MMP-3: 3.0-fold, IFNG: 2.6-fold, IL-15: 2.0-fold, MMP-14: 1.4-fold) and one was down-regulated (IGFBP6, 2.8-fold).

As the applied analytical platforms for the discovery of SASP factors differ between the studies (Coppe *et al.*, 2010a) we cannot exclude system inherent biases leading to incomplete representation of candidate proteins. Therefore we decided to consider biological processes of the candidate-proteins expecting a higher coverage between SASP- and SAASP-factors and performed a detailed enrichment and network analysis of the involved biological processes (Fig.5).

A total of 141 proteins (94.0 %) were successfully mapped to 239 biological processes using Reactome database (Matthews *et al.*, 2009, Fig. 4). Thirty-three (93 proteins) of the 239 biological processes were identified as shared between SASP and SAASP regulated protein networks (Fig. 5A+B, pink, Tab. S7). The comparison of significant biological processes revealed that ‘chemokine receptors bind chemokines/signaling by interleukins’ ($p = 4.2 \times 10^{-14}$), ‘regulation of IGF activity by IGF binding proteins (IGFBPs)’ ($p = 7.9 \times 10^{-8}$) and ‘activation of MMPs/degradation of the ECM’ ($p = 1.5 \times 10^{-7}/p = 4.4 \times 10^{-5}$) are shared biological processes between SASP- and SAASP-proteins.

In the blood of primates several cytokines were found to be significantly altered with age (Didier *et al.*, 2012). This is in agreement with our findings that seven cytokines (INFG, IL1B, IL1RN, IL4, IL15, CXCL10 and TNF) were positively correlated with intrinsic aging of dermal fibroblasts.

Hundred twenty-six (73 proteins) of the 239 biological processes though were unique to SASP-proteins as described by Coppe and coworkers (Coppe *et al.*, 2010a, Fig. 5A+B, red circles, Tab. S6). The comparison of significant biological processes revealed that ‘integrin cell surface interactions’ ($p = 1.9 \times 10^{-9}$), ‘dissolution of fibrin clot’ ($p = 1.5 \times 10^{-4}$) and ‘GRB2 events in ERBB2 (human epidermal growth factor receptor 2, HER2) signaling’ ($p = 2.8 \times 10^{-4}$) are biological processes unique to SASP-proteins.

The proteins linked to ‘dissolution of fibrin clot’ (PLAT: tissue-type plasminogen activator, tPA, PLAUR: urokinase plasminogen activator surface receptor, uPAR, SERPINE1, SERPINB2: plasminogen activator inhibitor 2, PAI-2) have been described as up-regulated in classical SASP (Coppe *et al.*, 2010a) and were identified in a model of replicative senescence by population doublings *in vitro* (Comi *et al.*, 1995, West *et al.*, 1996, Martens *et al.*, 2003). They are actors of the fibrinolytic system and involved in the blood clotting cascade. PLAT is an activator of plasmin which plays also an important role in tissue remodeling and degradation and cell migration (Westergaard *et al.*, 2003) and is able to regulate other proteases, such as MMPs and elastases, which results in the cleavage of collagens, elastin and proteoglycans (Murphy *et al.*, 1999). Some of these proteins, PAI-1 and PLAUR, are also associated with tumorigenesis (Giacoaia *et al.*, 2014, Nowicki *et al.*, 2011), which is a known function of some SASP-factors (Coppe *et al.*, 2010a).

The biological process ‘GRB2 events in ERBB2 signaling’ defined by EGF, EGFR, epiregulin (EREG) and heregulin (NRG1) is also overexpressed in SASP-proteins only. The receptor tyrosine kinase EGFR is decreased in replicative senescent fibroblasts which results in a reduced EGF responsiveness (Shiraha *et al.*, 2000) and NRG1, a ligand of the ErbB receptors HER3 and HER4 is both a candidate oncogene and a candidate tumor suppressor gene (Chua *et al.*, 2009).

Eighty-one (33 proteins) of the 239 biological processes though were unique to SAASP (Fig. 5A+B, blue circles, Tab. S6). The comparison of significant biological processes revealed that ‘metabolism’ ($p = 6.0 \times 10^{-4}$, subdivided into ‘glycosphingolipid/sphingolipid metabolism’ ($p = 2.1 \times 10^{-3}$ and $p = 1.9 \times 10^{-2}$), ‘purine catabolism’ ($p = 1.4 \times 10^{-1}$), ‘glutathione synthesis and recycling’ ($p = 1.3 \times 10^{-1}$) and ‘metabolism of carbohydrates’ ($p = 5.8 \times 10^{-1}$)) and ‘adherens junctions interactions’ ($p = 6.4 \times 10^{-2}$) are unique proteins for SAASP.

Up to our knowledge the process of ‘sphingolipid/glycosphingolipid metabolism’ has not been described as directly associated with cellular senescence or dermal aging before. Sphingolipids are bioactive lipids normally secreted by differentiated keratinocytes that are intimately involved in skin biology, inflammation and immunity and therefore play a crucial role in terms of structural integrity as well as functionality which includes epidermal barrier function (reviewed in Kendall and Nicolaou, 2013). The proteins we identified belonging to this biological process were glucosylceramidase (GBA, up-regulated), Sialidase-1 (NEU1, up-regulated), Prosaposin (PSAP, down-regulated) and SUMF1 (down-regulated). An at least partial loss of function of all of these proteins is associated with lysosomal storage disorders, which can be accompanied by more or less severe ichthyosis (Breecher and Dworken, 1986). NEU1 is also required for the normal assembly of elastic fibers and the ECM (Starcher *et al.*, 2008) but has not been described with regard to (skin) aging before.

Only recently sphingolipids have also been profiled in dermal fibroblasts (Scherer *et al.*, 2010) and further studies are required to define their biological functions in fibroblasts in general and with for intrinsic skin aging in particular.

The biological process of ‘purine catabolism’ is reflected by the protein 5’-nucleotidase (NT5E/CD73). It is an ectonucleotidase that hydrolyzes extracellular AMP into membrane permeable adenosine (Street *et al.*, 2013) and is expressed in fibroblasts where it participates in immune and inflammatory reactions (Nemoto *et al.*, 2004). As CD73 is also a marker for mesenchymal stem cells but regularly found in fibroblasts it has been suggested, that dermal fibroblasts are a heterogeneous population containing progenitors with various levels of differentiation potentials (Chen *et al.*, 2007, Brohem *et al.*, 2013). Since NT5E is down-regulated in SAASP this might indicate a loss of dermal progenitor cells during *in situ* aging.

The process of ‘glutathione synthesis and recycling’ is also reflected by a single protein, in this case γ -glutamylcyclo-transferase (GGCT). GGCT plays a key role in the γ -glutamyl cycle, a pathway for the synthesis and degradation of glutathione and drug/xenobiotic detoxification (Courtay *et al.*, 1992) and is down-regulated in our *in situ* aged NHDFs which indicates a loss of detoxification capability in intrinsically aged skin.

The biological process contributing to the comprehensive term ‘metabolism’ is ‘metabolism of carbohydrates’, represented by enolase 2 (ENO2) and prolargin (PRELP). Enolase, unfortunately the authors do not state which isoform, has been described as present and

unaltered during aging in the epidermis of both men and women (Yamasawa *et al.*, 1972) and is down-regulated with increasing donor age in our cells. PRELP on the other hand is being up-regulated. PRELP is a small leucine rich proteoglycan and in canine skin an important constituent to production, organization and remodeling of collagen and elastin through complex biological systems (Yang *et al.*, 2012). It was also suggested to be involved in the pathogenesis of the premature aging syndrome Hutchinson-Gilford progeria (Lewis, 2003).

A novel biological process we identified while analyzing the secretomes of *in situ* aged NHDFs are alterations in ‘adherens junctions interactions’, represented by the proteins CDH2 and CDH11. As discussed earlier CDH2 is down-regulated in our cells and might be important for wound healing. The same holds true for CDH11 (Schneider *et al.*, 2012).

In summary, in the present study we clearly show that some, but not all hallmarks of *in vitro* fibroblast aging may also be detected in human fibroblasts which have been isolated from intrinsically aged skin. This is consistent with previous reports that cells expressing markers of cellular senescence are present at increased frequencies in aged skin of primates and humans (Ressler *et al.*, 2006, Dimri *et al.*, 1995). Most importantly, we found that intrinsically aged skin fibroblasts express a secretome, for which we here coined the term SAASP, which differs from the classical SASP, and which is most likely of functional relevance for intrinsic skin aging. Accordingly, with our unbiased approach we corroborated the assumption that pro-inflammatory and matrix degrading processes are critically involved in intrinsic aging of the skin thus validating our experimental approach. In addition, we identified new candidate proteins of relevant aging processes and obtained detailed information about biological processes which point beyond ECM remodeling such as immune and inflammatory reactions, wound healing, protein shedding, as well as sphingolipid and glycosphingolipid metabolism. Further studies are required to validate these findings by *in situ* analysis in intrinsically aged human skin. Also, in addition to intrinsic mechanisms skin aging is strongly driven by environmental factors including solar radiation. In follow-up studies the molecular characteristics of fibroblasts isolated from extrinsically skin will therefore have to be determined.

MATERIAL AND METHODS

Cell isolation and culture

We obtained cells from healthy female breast skin of 15 adult donors who had undergone breast reduction surgery (bottom side) in the Clinic of Plactical Surgery of the Kaiserswerther Diakonie Dusseldorf, Germany. The procedure is conform to the principles of the Declaration of Helsinki and was approved by the Ethical Committee of the Medical Faculty of the University of Düsseldorf (TOX_EF_Do1/2008). Informed consent was obtained from all donors. The samples were derived from three distinct groups of 5 donors each, based on their age: ‘young’ (20-29 years), ‘middle’ (40-49 years) and ‘old’ (< 60 years), respectively (for details see Table S8).

Fibroblasts were isolated and cultivated as described elsewhere (Kalfalah F *et al.*, 2014). Cells were not expanded beyond passage number (PN) 6 to exclude replicative senescence.

Telomere restriction fragment length (TFRL-) analysis

Genomic DNA was restricted and subjected to Southern blotting (Baird *et al.*, 2006, Figueroa *et al.*, 2000). TFRL-values were derived from digital chemi-luminescence images of telomere-probed blots as described in (Krunic *et al.*, 2009) using the formula described in (Harley *et al.*, 1990).

Western blotting and immunocytochemical staining

H2AX phosphorylation was assessed using a monoclonal mouse antibody specific for histone H2AX phosphorylated at Ser139 and a polyclonal rabbit antibody against total histone H2AX (Millipore, Schwalbach, Germany) to control for loading, as previously described (Kalfalah *et al.*, 2011).

Immunocytochemical staining and imaging followed own published procedures (Kalfalah *et al.*, 2011). Promyelocytic leukemia nuclear (PML-) bodies and nuclear foci positive for P53 binding protein 1 (53BP1) were detected using antibodies from Santa Cruz Biotechnology (Heidelberg, Germany), and distinct nuclear structures that sustain damage-induced senescence growth arrest and inflammatory cytokine secretion (DNA-SCARS) were scored in cells double stained for PML and 53BP1 as described in (Rodier *et al.*, 2011). For each donor, three individual cell cultures (biological replicates) were stained, and from each staining 50

cell images were documented and separately scored by two investigators, who were blinded regarding donor identity (technical replicates).

Flow cytometry

Annexin V and propidium iodide staining followed the prescribed protocol of a commercial apoptosis detection kit (Sigma Aldrich, Martinsried, Germany).

Statistics

If not stated otherwise, each variable stated for a given donor and parameter represents mean results from the analysis of three independent primary cell cultures serving as biological replicates. Errors (SEM) refer to the biological replicates and were calculated from the mean of the technical replicates of the assays. Whenever errors are omitted for the sake of clarity they were less than 20 % of the values or smaller than the symbols of the data plots. Arbitrary units (AU) derived from relative quantifications (e.g. the densitometry of immunoblots or qPCR) were normalized to the result obtained with the cells of the youngest donor or to the mean of all values obtained in the same analytical run. GraphPad PRISM 4.0a (GraphPad Software Inc., USA) was used for linear regression (Pearson), normal data distribution analysis (Shapiro-Wilk) and group comparisons (Wilcoxon's signed rank test or Welch's unpaired T-test). Differences considered statistically significant are marked by * ($p < 0.05$), ** ($p < 0.01$), or *** ($p < 0.001$).

Cytokine multiplex assay

Cytokine, chemokine and growth factor concentrations in NHDF supernatants were quantified using the Bio-Plex Pro™ cytokine, chemokine and growth factor assay (Bio-Rad Laboratories GmbH, Munich, Germany) according to manufacturer's instructions.

Secretome preparation

HNDFs were washed three times with DMEM and incubated in serum-free medium for 48 hours before the conditioned media (secretomes) were collected and cooled down on ice. Floating cells and cellular debris were removed by sterile filtration (pore size: 0.2 µm). Protease inhibitors (Inhibitor Cocktail Complete™, Roche, Mannheim, Germany) were added and the secretomes were concentrated using Vivaspin™ 15R ultrafiltration spin columns (Sartorius, Göttingen, Germany, 3 kDa cut-off) according to the manufacturer's instructions.

Concentrated secretomes were desalted by the use of Micro Bio-Spin™ P-6 chromatography columns (BioRad, Munich, Germany, 6 kDa cut-off) and TCA precipitation as described elsewhere (Link and LaBaer, 2011). Precipitated secretomes were dried in a SpeedVac™ and resuspended in urea-buffer (2 M thiourea, 7 M urea, 30 mM Tris-HCL, pH 8.0). Subsequently, total protein amount was determined using BCA protein assay (Thermo Scientific Pierce, Rockford, IL, USA) and 10 µg of each sample were loaded onto a SDS-PAGE gel (Life Technologies, Darmstadt, Germany). After complete entry into the gel, the electrophoresis was stopped and the gel was stained with silver as described elsewhere (Nesterenko *et al.*, 1994). The silver-stained protein gel bands, one for each sample, were then cut out and each gel slice was transferred into an Eppendorf tube. Bands were destained, washed and proteins were digested with trypsin (sequencing grade modified trypsin, Promega, Mannheim, Germany).

For details on mass spectrometry, protein identification and quantification as well as functional annotation, network and enrichment analysis please see supplementary material.

CONFLICT OF INTEREST

The authors state no conflict of interest.

ACKNOWLEDGMENTS

This work was supported by the Deutsche Forschungsgemeinschaft [SFB 728 and GK 1033 to EF, FB and JK and Kr871/5-1 to JK] and the German Ministry of Research and Education [Network Gerontosys, Stromal Aging to FB, JK, KS and PB] as well as L'Oréal Recherche [JT and JK].

REFERENCE LIST

- 1 Acosta JC, Banito A, Wuestefeld T, Georgilis A, Janich P, Morton JP, Athineos D, Kang TW, Lasitschka F, Andrulis M, Pascual G, Morris KJ, Khan S, Jin H, Dharmalingam G, Snijders AP, Carroll T, Capper D, Pritchard C, Inman GJ, Longerich T, Sansom OJ, Benitah SA, Zender L, Gil J: A complex secretory program orchestrated by the inflammasome controls paracrine senescence. *Nat Cell Biol* 15:978-990 (2013).
- 2 Baird DM, Britt-Compton B, Rowson J, Amso NN, Gregory L, Kipling D: Telomere instability in the male germline. *Hum Mol Genet* 15:45-51 (2006).
- 3 Bendtsen JD, Jensen LJ, Blom N, von HG, Brunak S: Feature-based prediction of non-classical and leaderless protein secretion. *Protein Eng Des Sel* 17:349-356 (2004).
- 4 Bentov I, Reed MJ: Anesthesia, microcirculation, and wound repair in aging. *Anesthesiology* 120:760-772 (2014).
- 5 Bhaumik D, Scott GK, Schokrpur S, Patil CK, Orjalo AV, Rodier F, Lithgow GJ, Campisi J: MicroRNAs miR-146a/b negatively modulate the senescence-associated inflammatory mediators IL-6 and IL-8. *Aging (Albany NY)* 1:402-411 (2009).
- 6 Boukamp P: Skin aging: a role for telomerase and telomere dynamics? *Curr Mol Med* 5:171-177 (2005).
- 7 Breecher MM, Dworken AM: The Merck Manual. *Med Herit* 2:229-231 (1986).
- 8 Brohem CA, de Carvalho CM, Radoski CL, Santi FC, Baptista MC, Swinka BB, de AU, de Araujo LR, Graf RM, Feferman IH, Lorencini M: Comparison between fibroblasts and mesenchymal stem cells derived from dermal and adipose tissue. *Int J Cosmet Sci* 35:448-457 (2013).
- 9 Campisi J, d'Adda di FF: Cellular senescence: when bad things happen to good cells. *Nat Rev Mol Cell Biol* 8:729-740 (2007).
- 10 Celeste A, Fernandez-Capetillo O, Kruhlak MJ, Pilch DR, Staudt DW, Lee A, Bonner RF, Bonner WM, Nussenzweig A: Histone H2AX phosphorylation is dispensable for the initial recognition of DNA breaks. *Nat Cell Biol* 5:675-679 (2003).

- 11 Chen FG, Zhang WJ, Bi D, Liu W, Wei X, Chen FF, Zhu L, Cui L, Cao Y: Clonal analysis of nestin(-) vimentin(+) multipotent fibroblasts isolated from human dermis. *J Cell Sci* 120:2875-2883 (2007).
- 12 Chua YL, Ito Y, Pole JC, Newman S, Chin SF, Stein RC, Ellis IO, Caldas C, O'Hare MJ, Murrell A, Edwards PA: The NRG1 gene is frequently silenced by methylation in breast cancers and is a strong candidate for the 8p tumour suppressor gene. *Oncogene* 28:4041-4052 (2009).
- 13 Comi P, Chiaramonte R, Maier JA: Senescence-dependent regulation of type 1 plasminogen activator inhibitor in human vascular endothelial cells. *Exp Cell Res* 219:304-308 (1995).
- 14 Coppe JP, Desprez PY, Krtolica A, Campisi J: The senescence-associated secretory phenotype: the dark side of tumor suppression. *Annu Rev Pathol* 5:99-118 (2010a).
- 15 Coppe JP, Patil CK, Rodier F, Krtolica A, Beausejour CM, Parrinello S, Hodgson JG, Chin K, Desprez PY, Campisi J: A human-like senescence-associated secretory phenotype is conserved in mouse cells dependent on physiological oxygen. *PLoS One* 5:e9188 (2010b).
- 16 Coppe JP, Patil CK, Rodier F, Sun Y, Munoz DP, Goldstein J, Nelson PS, Desprez PY, Campisi J: Senescence-associated secretory phenotypes reveal cell-nonautonomous functions of oncogenic RAS and the p53 tumor suppressor. *PLoS Biol* 6:2853-2868 (2008).
- 17 Coppe JP, Rodier F, Patil CK, Freund A, Desprez PY, Campisi J: Tumor suppressor and aging biomarker p16(INK4a) induces cellular senescence without the associated inflammatory secretory phenotype. *J Biol Chem* 286:36396-36403 (2011).
- 18 Courtay C, Oster T, Michelet F, Visvikis A, Diederich M, Wellman M, Siest G: Gamma-glutamyltransferase: nucleotide sequence of the human pancreatic cDNA. Evidence for a ubiquitous gamma-glutamyltransferase polypeptide in human tissues. *Biochem Pharmacol* 43:2527-2533 (1992).

- 19 Cristofalo VJ, Allen RG, Pignolo RJ, Martin BG, Beck JC: Relationship between donor age and the replicative lifespan of human cells in culture: a reevaluation. *Proc Natl Acad Sci U S A* 95:10614-10619 (1998).
- 20 d'Adda di Fagagna F, Reaper PM, Clay-Farrace L, Fiegler H, Carr P, von ZT, Saretzki G, Carter NP, Jackson SP: A DNA damage checkpoint response in telomere-initiated senescence. *Nature* 426:194-198 (2003).
- 21 Didier ES, Sugimoto C, Bowers LC, Khan IA, Kuroda MJ: Immune correlates of aging in outdoor-housed captive rhesus macaques (*Macaca mulatta*). *Immun Ageing* 9:25 (2012).
- 22 Dimri GP, Lee X, Basile G, Acosta M, Scott G, Roskelley C, Medrano EE, Linskens M, Rubelj I, Pereira-Smith O: A biomarker that identifies senescent human cells in culture and in aging skin in vivo. *Proc Natl Acad Sci U S A* 92:9363-9367 (1995).
- 23 Edwards DR, Leco KJ, Beaudry PP, Atadja PW, Veillette C, Riabowol KT: Differential effects of transforming growth factor-beta 1 on the expression of matrix metalloproteinases and tissue inhibitors of metalloproteinases in young and old human fibroblasts. *Exp Gerontol* 31:207-223 (1996).
- 24 Elzi DJ, Song M, Hakala K, Weintraub ST, Shiio Y: Wnt antagonist SFRP1 functions as a secreted mediator of senescence. *Mol Cell Biol* 32:4388-4399 (2012).
- 25 Figueroa R, Lindenmaier H, Hergenbahn M, Nielsen KV, Boukamp P: Telomere erosion varies during *in vitro* aging of normal human fibroblasts from young and adult donors. *Cancer Res* 60:2770-2774 (2000).
- 26 Freund A, Patil CK, Campisi J: p38MAPK is a novel DNA damage response-independent regulator of the senescence-associated secretory phenotype. *EMBO J* 30:1536-1548 (2011).
- 27 Giacoia EG, Miyake M, Lawton A, Goodison S, Rosser CJ: PAI-1 Leads to G1-Phase Cell-Cycle Progression through Cyclin D3/cdk4/6 Upregulation. *Mol Cancer Res* 12:322-334 (2014).
- 28 Gilchrist BA, Krutmann J: *Skin Aging*. (Springer-Verlag Berlin Heidelberg, 2006).

- 29 Gosain A, DiPietro LA: Aging and wound healing. *World J Surg* 28:321-326 (2004).
- 30 Harley CB, Futcher AB, Greider CW: Telomeres shorten during ageing of human fibroblasts. *Nature* 345:458-460 (1990).
- 31 Hayflick L, Moorhead PS: The serial cultivation of human diploid cell strains. *Exp Cell Res* 25:585-621 (1961).
- 32 Herbig U, Jobling WA, Chen BP, Chen DJ, Sedivy JM: Telomere shortening triggers senescence of human cells through a pathway involving ATM, p53, and p21(CIP1), but not p16(INK4a). *Mol Cell* 14:501-513 (2004).
- 33 Hirohata S, Wang LW, Miyagi M, Yan L, Seldin MF, Keene DR, Crabb JW, Apte SS: Punctin, a novel ADAMTS-like molecule, ADAMTSL-1, in extracellular matrix. *J Biol Chem* 277:12182-12189 (2002).
- 34 Hoare M, Narita M: Transmitting senescence to the cell neighbourhood. *Nat Cell Biol* 15:887-889 (2013).
- 35 Irwin CR, Picardo M, Ellis I, Sloan P, Grey A, McGurk M, Schor SL: Inter- and intra-site heterogeneity in the expression of fetal-like phenotypic characteristics by gingival fibroblasts: potential significance for wound healing. *J Cell Sci* 107 (Pt 5):1333-1346 (1994).
- 36 Jung KY, Dean D, Jiang J, Gaylor S, Griffith WH, Burghardt RC, Parrish AR: Loss of N-cadherin and alpha-catenin in the proximal tubules of aging male Fischer 344 rats. *Mech Ageing Dev* 125:445-453 (2004).
- 37 Kalfalah F, Sobe S, Bornholz B, Götz-Rösch C, Tigges J, Fritsche E, Krutmann J, Köhrer K, Deenen R, Ohse S, Boerries M, Busch H, Boege F: Inadequate mitobiogenesis in primary dermal fibroblasts from old humans is associated with impairment of PGC1A-independent stimulation (2014).
- 38 Kalfalah FM, Mielke C, Christensen MO, Baechler S, Marko D, Boege F: Genotoxicity of dietary, environmental and therapeutic topoisomerase II poisons is uniformly correlated to prolongation of enzyme DNA residence. *Mol Nutr Food Res* 55 Suppl 1:S127-S142 (2011).

- 39 Kamburov A, Wierling C, Lehrach H, Herwig R: ConsensusPathDB--a database for integrating human functional interaction networks. *Nucleic Acids Res* 37:D623-D628 (2009).
- 40 Kendall AC, Nicolaou A: Bioactive lipid mediators in skin inflammation and immunity. *Prog Lipid Res* 52:141-164 (2013).
- 41 Kreiling JA, Tamamori-Adachi M, Sexton AN, Jeyapalan JC, Munoz-Najar U, Peterson AL, Manivannan J, Rogers ES, Pchelintsev NA, Adams PD, Sedivy JM: Age-associated increase in heterochromatic marks in murine and primate tissues. *Aging Cell* 10:292-304 (2011).
- 42 Krunic D, Moshir S, Greulich-Bode KM, Figueroa R, Cerezo A, Stammer H, Stark HJ, Gray SG, Nielsen KV, Hartschuh W, Boukamp P: Tissue context-activated telomerase in human epidermis correlates with little age-dependent telomere loss. *Biochim Biophys Acta* 1792:297-308 (2009).
- 43 Kuilman T, Michaloglou C, Vredeveld LC, Douma S, van DR, Desmet CJ, Aarden LA, Mooi WJ, Peeper DS: Oncogene-induced senescence relayed by an interleukin-dependent inflammatory network. *Cell* 133:1019-1031 (2008).
- 44 Kuilman T, Peeper DS: Senescence-messaging secretome: SMS-ing cellular stress. *Nat Rev Cancer* 9:81-94 (2009).
- 45 Laberge RM, Zhou L, Sarantos MR, Rodier F, Freund A, de Keizer PL, Liu S, DeMaria M, Cong YS, Kapahi P, Desprez PY, Hughes RE, Campisi J: Glucocorticoids suppress selected components of the senescence-associated secretory phenotype. *Aging Cell* 11:569-578 (2012).
- 46 Lehmann BD, Paine MS, Brooks AM, McCubrey JA, Renegar RH, Wang R, Terrian DM: Senescence-associated exosome release from human prostate cancer cells. *Cancer Res* 68:7864-7871 (2008).
- 47 Lewis M: PRELP, collagen, and a theory of Hutchinson-Gilford progeria. *Ageing Res Rev* 2:95-105 (2003).

- 48 Link AJ, LaBaer J: Trichloroacetic acid (TCA) precipitation of proteins. *Cold Spring Harb Protoc* 2011:993-994 (2011).
- 49 Lobrich M, Shibata A, Beucher A, Fisher A, Ensminger M, Goodarzi AA, Barton O, Jeggo PA: gammaH2AX foci analysis for monitoring DNA double-strand break repair: strengths, limitations and optimization. *Cell Cycle* 9:662-669 (2010).
- 50 Maier AB, le CS, de Koning-Treurniet C, Blom J, Westendorp RG, van HD: Persistence of high-replicative capacity in cultured fibroblasts from nonagenarians. *Aging Cell* 6:27-33 (2007).
- 51 Makrantonaki E, Brink TC, Zampeli V, Elewa RM, Mlody B, Hossini AM, Hermes B, Krause U, Knolle J, Abdallah M, Adjaye J, Zouboulis CC: Identification of biomarkers of human skin ageing in both genders. Wnt signalling - a label of skin ageing? *PLoS One* 7:e50393 (2012).
- 52 Makrantonaki E, Schonknecht P, Hossini AM, Kaiser E, Katsouli MM, Adjaye J, Schroder J, Zouboulis CC: Skin and brain age together: The role of hormones in the ageing process. *Exp Gerontol* 45:801-813 (2010).
- 53 Martens JW, Sieuwerts AM, Bolt-deVries J, Bosma PT, Swiggers SJ, Klijn JG, Foekens JA: Aging of stromal-derived human breast fibroblasts might contribute to breast cancer progression. *Thromb Haemost* 89:393-404 (2003).
- 54 Matthews L, Gopinath G, Gillespie M, Caudy M, Croft D, de BB, Garapati P, Hemish J, Hermjakob H, Jassal B, Kanapin A, Lewis S, Mahajan S, May B, Schmidt E, Vastrik I, Wu G, Birney E, Stein L, D'Eustachio P: Reactome knowledgebase of human biological pathways and processes. *Nucleic Acids Res* 37:D619-D622 (2009).
- 55 Micutkova L, Diener T, Li C, Rogowska-Wrzesinska A, Mueck C, Huetter E, Weinberger B, Grubeck-Loebenstein B, Roepstorff P, Zeng R, Jansen-Duerr P: Insulin-like growth factor binding protein-6 delays replicative senescence of human fibroblasts. *Mech Ageing Dev* 132:468-479 (2011).
- 56 Midwood KS, Williams LV, Schwarzbauer JE: Tissue repair and the dynamics of the extracellular matrix. *Int J Biochem Cell Biol* 36:1031-1037 (2004).

- 57 Mu XC, Higgins PJ: Differential growth state-dependent regulation of plasminogen activator inhibitor type-1 expression in senescent IMR-90 human diploid fibroblasts. *J Cell Physiol* 165:647-657 (1995).
- 58 Mullberg J, Althoff K, Jostock T, Rose-John S: The importance of shedding of membrane proteins for cytokine biology. *Eur Cytokine Netw* 11:27-38 (2000).
- 59 Murphy G, Stanton H, Cowell S, Butler G, Knauper V, Atkinson S, Gavrilovic J: Mechanisms for pro matrix metalloproteinase activation. *APMIS* 107:38-44 (1999).
- 60 Narita M, Nunez S, Heard E, Narita M, Lin AW, Hearn SA, Spector DL, Hannon GJ, Lowe SW: Rb-mediated heterochromatin formation and silencing of E2F target genes during cellular senescence. *Cell* 113:703-716 (2003).
- 61 Nemoto E, Kunii R, Tada H, Tsubahara T, Ishihata H, Shimauchi H: Expression of CD73/ecto-5'-nucleotidase on human gingival fibroblasts and contribution to the inhibition of interleukin-1alpha-induced granulocyte-macrophage colony stimulating factor production. *J Periodontal Res* 39:10-19 (2004).
- 62 Nesterenko MV, Tilley M, Upton SJ: A simple modification of Blum's silver stain method allows for 30 minute detection of proteins in polyacrylamide gels. *J Biochem Biophys Methods* 28:239-242 (1994).
- 63 Nguyen A, Chang AC, Reddel RR: Stanniocalcin-1 acts in a negative feedback loop in the prosurvival ERK1/2 signaling pathway during oxidative stress. *Oncogene* 28:1982-1992 (2009).
- 64 Nickel W, Seedorf M: Unconventional mechanisms of protein transport to the cell surface of eukaryotic cells. *Annu Rev Cell Dev Biol* 24:287-308 (2008).
- 65 Nowicki TS, Zhao H, Darzynkiewicz Z, Moscatello A, Shin E, Schantz S, Tiwari RK, Geliebter J: Downregulation of uPAR inhibits migration, invasion, proliferation, FAK/PI3K/Akt signaling and induces senescence in papillary thyroid carcinoma cells. *Cell Cycle* 10:100-107 (2011).

- 66 Orjalo AV, Bhaumik D, Gengler BK, Scott GK, Campisi J: Cell surface-bound IL-1alpha is an upstream regulator of the senescence-associated IL-6/IL-8 cytokine network. *Proc Natl Acad Sci U S A* 106:17031-17036 (2009).
- 67 Parrinello S, Coppe JP, Krtolica A, Campisi J: Stromal-epithelial interactions in aging and cancer: senescent fibroblasts alter epithelial cell differentiation. *J Cell Sci* 118:485-496 (2005).
- 68 Passi A, Albertini R, Campagnari F, De LG: Modifications of proteoglycans secreted into the growth medium by young and senescent human skin fibroblasts. *FEBS Lett* 402:286-290 (1997).
- 69 Petersen TN, Brunak S, von HG, Nielsen H: SignalP 4.0: discriminating signal peptides from transmembrane regions. *Nat Methods* 8:785-786 (2011).
- 70 Pitiyage GN, Lim KP, Gemenitzidis E, Teh MT, Waseem A, Prime SS, Tilakaratne WM, Fortune F, Parkinson EK: Increased secretion of tissue inhibitors of metalloproteinases 1 and 2 (TIMPs -1 and -2) in fibroblasts are early indicators of oral sub-mucous fibrosis and ageing. *J Oral Pathol Med* 41:454-462 (2012).
- 71 Regnault V, Perret-Guillaume C, Kearney-Schwartz A, Max JP, Labat C, Louis H, Wahl D, Pannier B, Lecompte T, Weryha G, Challande P, Safar ME, Benetos A, Lacolley P: Tissue factor pathway inhibitor: a new link among arterial stiffness, pulse pressure, and coagulation in postmenopausal women. *Arterioscler Thromb Vasc Biol* 31:1226-1232 (2011).
- 72 Ressler S, Bartkova J, Niederegger H, Bartek J, Scharffetter-Kochanek K, Jansen-Durr P, Wlaschek M: p16INK4A is a robust in vivo biomarker of cellular aging in human skin. *Aging Cell* 5:379-389 (2006).
- 73 Ridley AJ, Schwartz MA, Burridge K, Firtel RA, Ginsberg MH, Borisy G, Parsons JT, Horwitz AR: Cell migration: integrating signals from front to back. *Science* 302:1704-1709 (2003).
- 74 Rodier F, Munoz DP, Teachenor R, Chu V, Le O, Bhaumik D, Coppe JP, Campeau E, Beausejour CM, Kim SH, Davalos AR, Campisi J: DNA-SCARS: distinct nuclear

- structures that sustain damage-induced senescence growth arrest and inflammatory cytokine secretion. *J Cell Sci* 124:68-81 (2011).
- 75 Rogakou EP, Boon C, Redon C, Bonner WM: Megabase chromatin domains involved in DNA double-strand breaks in vivo. *J Cell Biol* 146:905-916 (1999).
- 76 Rovillain E, Mansfield L, Caetano C, Alvarez-Fernandez M, Caballero OL, Medema RH, Hummerich H, Jat PS: Activation of nuclear factor-kappa B signalling promotes cellular senescence. *Oncogene* 30:2356-2366 (2011).
- 77 Scherer M, Leuthauser-Jaschinski K, Ecker J, Schmitz G, Liebisch G: A rapid and quantitative LC-MS/MS method to profile sphingolipids. *J Lipid Res* 51:2001-2011 (2010).
- 78 Schlage P, Egli FE, Nanni P, Wang LW, Kizhakkedathu JN, Apte SS, auf dem KU: Time-resolved analysis of the matrix metalloproteinase 10 substrate degradome. *Mol Cell Proteomics* 13:580-593 (2014).
- 79 Schlondorff J, Blobel CP: Metalloprotease-disintegrins: modular proteins capable of promoting cell-cell interactions and triggering signals by protein-ectodomain shedding. *J Cell Sci* 112 (Pt 21):3603-3617 (1999).
- 80 Schneider DJ, Wu M, Le TT, Cho SH, Brenner MB, Blackburn MR, Agarwal SK: Cadherin-11 contributes to pulmonary fibrosis: potential role in TGF-beta production and epithelial to mesenchymal transition. *FASEB J* 26:503-512 (2012).
- 81 Schuepbach RA, Velez K, Riewald M: Activated protein C up-regulates procoagulant tissue factor activity on endothelial cells by shedding the TFPI Kunitz 1 domain. *Blood* 117:6338-6346 (2011).
- 82 Shiraha H, Gupta K, Drabik K, Wells A: Aging fibroblasts present reduced epidermal growth factor (EGF) responsiveness due to preferential loss of EGF receptors. *J Biol Chem* 275:19343-19351 (2000).
- 83 Shirakabe K, Hattori S, Seiki M, Koyasu S, Okada Y: VIP36 protein is a target of ectodomain shedding and regulates phagocytosis in macrophage Raw 264.7 cells. *J Biol Chem* 286:43154-43163 (2011).

- 84 Starcher B, d'Azzo A, Keller PW, Rao GK, Nadarajah D, Hinek A: Neuraminidase-1 is required for the normal assembly of elastic fibers. *Am J Physiol Lung Cell Mol Physiol* 295:L637-L647 (2008).
- 85 Street SE, Kramer NJ, Walsh PL, Taylor-Blake B, Yadav MC, King IF, Vihko P, Wightman RM, Millan JL, Zylka MJ: Tissue-nonspecific alkaline phosphatase acts redundantly with PAP and NT5E to generate adenosine in the dorsal spinal cord. *J Neurosci* 33:11314-11322 (2013).
- 86 Tigges J, Krutmann J, Fritsche E, Haendeler J, Schaal H, Fischer JW, Kalfalah F, Reinke H, Reifenberger G, Stühler K, Ventura N, Gundermann S, Boukamp P, Boege F: The Hallmarks of Fibroblast Ageing 2014).
- 87 Tigges J, Weighardt H, Wolff S, Gotz C, Forster I, Kohne Z, Huebenthal U, Merk HF, Abel J, Haarmann-Stemmann T, Krutmann J, Fritsche E: Aryl Hydrocarbon Receptor Repressor (AhRR) Function Revisited: Repression of CYP1 Activity in Human Skin Fibroblasts Is Not Related to AhRR Expression. *J Invest Dermatol* (2012).
- 88 Tomkowicz B, Rybinski K, Foley B, Ebel W, Kline B, Routhier E, Sass P, Nicolaides NC, Grasso L, Zhou Y: Interaction of endosialin/TEM1 with extracellular matrix proteins mediates cell adhesion and migration. *Proc Natl Acad Sci U S A* 104:17965-17970 (2007).
- 89 Umazume K, Usui Y, Wakabayashi Y, Okunuki Y, Kezuka T, Goto H: Effects of soluble CD14 and cytokine levels on diabetic macular edema and visual acuity. *Retina* 33:1020-1025 (2013).
- 90 von Zglinicki T, Saretzki G, Docke W, Lotze C: Mild hyperoxia shortens telomeres and inhibits proliferation of fibroblasts: a model for senescence? *Exp Cell Res* 220:186-193 (1995).
- 91 Wajapeyee N, Serra RW, Zhu X, Mahalingam M, Green MR: Oncogenic BRAF induces senescence and apoptosis through pathways mediated by the secreted protein IGFBP7. *Cell* 132:363-374 (2008).

- 92 West MD, Pereira-Smith OM, Smith JR: Replicative senescence of human skin fibroblasts correlates with a loss of regulation and overexpression of collagenase activity. *Exp Cell Res* 184:138-147 (1989).
- 93 West MD, Shay JW, Wright WE, Linskens MH: Altered expression of plasminogen activator and plasminogen activator inhibitor during cellular senescence. *Exp Gerontol* 31:175-193 (1996).
- 94 Westergaard UB, Andersen MH, Heegaard CW, Fedosov SN, Petersen TE: Tetraneectin binds hepatocyte growth factor and tissue-type plasminogen activator. *Eur J Biochem* 270:1850-1854 (2003).
- 95 Yamasawa S, Cerimele D, Serri F: The activity of metabolic enzymes of human epidermis in relation to age. *Br J Dermatol* 86:134-140 (1972).
- 96 Yang CH, Culshaw GJ, Liu MM, Lu CC, French AT, Clements DN, Corcoran BM: Canine tissue-specific expression of multiple small leucine rich proteoglycans. *Vet J* 193:374-380 (2012).
- 97 Yano K, Kajiya K, Ishiwata M, Hong YK, Miyakawa T, Detmar M: Ultraviolet B-induced skin angiogenesis is associated with a switch in the balance of vascular endothelial growth factor and thrombospondin-1 expression. *J Invest Dermatol* 122:201-208 (2004).
- 98 Young AR, Narita M: SASP reflects senescence. *EMBO Rep* 10:228-230 (2009).

TABLES

Table 1: Skin Aging Associated Secreted Proteins (SAASP) proteins of human dermal fibroblasts isolated from intrinsically aged skin. Cytokine assay (in grey) and quantitative label-free proteome analysis (in black) of *in situ* aged fibroblasts' secretome revealed 70 extracellular proteins that are differentially altered during *in situ* aging (ANOVA: $p \leq 0.05$, fold change ≥ 1.3 , Pearson correlation: $p \leq 0.05$, fold change ≥ 1.3). For ANOVA analysis donors were grouped according to calendar age into groups 20-30, 40-50 and 60-70 years, with five individual donors in each group.

UniprotID	Gene name	Protein description	p-value	Fold change	Regulation	Profile
Q8N6G6	ADAMTSL1	ADAMTS-like protein 1	4,80E-02	3,6	↓	long-term
Q15904	ATP6AP1	V-type proton ATPase subunit S1	2,50E-02	1,6	↓	late
P08571	CD14	Monocyte differentiation antigen CD14	3,00E-03	3,1	↑	immediate
Q9HCU0	CD248	Endosialin	3,10E-02	1,5	↓	immediate
P55287	CDH11	Cadherin-11	4,60E-02	1,8	↑	immediate
P19022	CDH2	Cadherin-2	1,00E-02	5,4	↓	immediate
Q15782	CHI3L2	Chitinase-3-like protein 2	4,80E-02	5,6	↑	long-term
P02452	COL1A1	Collagen alpha-1(I) chain	2,00E-02	2,1	↓	immediate
P16870	CPE PE	Carboxypeptidase E	3,00E-02	1,7	↓	immediate
P02778	CXCL10	C-X-C motif chemokine 10	1,00E-02	5,1	↑	long-term
P09104	ENO2	Gamma-enolase	4,90E-02	1,5	↓	long-term
P00734	F2	Prothrombin	4,40E-02	1,6	↓	long-term
P98095	FBLN2	Fibulin-2	1,00E-02	3,1	↑	immediate
Q9UBX5	FBLN5	Fibulin-5	3,70E-02	2	↑	immediate
P35556	FBN2	Fibrillin-2	3,00E-02	2,9	↓	immediate
Q9Y680	FKBP7	Peptidyl-prolyl cis-trans isomerase FKBP7	4,80E-02	2,4	↑	immediate
O95302	FKBP9	Peptidyl-prolyl cis-trans isomerase FKBP9	3,20E-02	1,5	↑	immediate
Q14315	FLNC	Filamin-C	4,00E-02	1,8	↓	immediate
P19883	FST	Follistatin	3,30E-02	1,6	↓	long-term
Q12841	FSTL1	Follistatin-related protein 1	5,00E-03	2	↓	immediate
P04062	GBA	Glucosylceramidase	8,00E-03	1,8	↑	immediate
O75223	GGCT	Gamma-glutamylcyclotransferase	4,10E-02	2,9	↓	long-term
Q68CQ7	GLT8D1	Glycosyltransferase 8 domain-containing protein 1	6,00E-03	2	↓	immediate
P06396	GSN	Gelsolin	2,10E-02	1,5	↓	immediate
P48723	HSPA13	Heat shock 70 kDa	3,70E-02	1,9	↓	immediate

		protein 13				
P01579	IFNG	Interferon gamma	2,00E-02	2,6	↑	long-term
P24592	IGFBP6	Insulin-like growth factor-binding protein 6	3,00E-02	4,9	↓	long-term
P40933	IL15	Interleukin-15	3,30E-02	2	↑	long-term
P01584	IL1B	Interleukin-1 beta	5,00E-03	4	↑	long-term
P18510	IL1RN	Interleukin-1 receptor antagonist protein	4,20E-02	2,2	↑	long-term
P05112	IL4	Interleukin-4	2,40E-02	2,9	↑	long-term
P10145	IL8	Interleukin-8	4,90E-02	8,1	↑	immediate
O14498	ISLR	Immunoglobulin superfamily containing leucine-rich repeat protein	1,00E-03	1,3	↓	late
O95965	ITGBL1	Integrin beta-like protein 1	1,00E-03	2,7	↓	immediate
P17931	LGALS3	Galectin-3	4,80E-02	1,7	↑	immediate
Q12907	LMAN2	Vesicular integral-membrane protein VIP36	3,80E-02	1,5	↓	immediate
Q08397	LOXL1	Lysyl oxidase homolog 1	3,50E-02	1,4	↓	long-term
Q9NR34	MAN1C1	Mannosyl-oligosaccharide 1,2-alpha-mannosidase IC	1,80E-02	1,4	↑	late
Q13361	MFAP5	Microfibrillar-associated protein 5	4,30E-02	4,7	↓	long-term
P03956	MMP1	Interstitial collagenase	3,20E-02	3,9	↑	immediate
P09238	MMP10	Stromelysin-2	4,30E-02	3,2	↑	immediate
P50281	MMP14	Matrix metalloproteinase-14	1,00E-02	1,4	↑	immediate
P08254	MMP3	Stromelysin-1	4,10E-02	3	↑	immediate
Q9NR99	MXRA5	Matrix-remodeling-associated protein 5	8,00E-03	2	↑	immediate
P19105	MYL12A	Myosin regulatory light chain 12A	4,90E-02	2,7	↓	long-term
Q99519	NEU1	Sialidase-1	3,70E-02	2,3	↑	long-term
Q14112	NID2	Nidogen-2	5,00E-03	2,3	↑	immediate
P21589	NT5E	5'-nucleotidase	1,80E-02	2,5	↓	long-term
Q9Y2I2	NTNG1	Netrin-G1	2,30E-02	1,9	↓	immediate
P80303	NUCB2	Nucleobindin-2	3,40E-02	1,5	↓	long-term
Q86UD1	OAF	Out at first protein homolog	4,60E-02	2,4	↓	long-term
Q99784	OLFM1	Noelin	3,20E-02	2,1	↑	immediate
Q9H488	POFUT1	GDP-fucose protein O-fucosyltransferase 1	1,30E-02	2,1	↑	immediate
P51888	PRELP	Prolargin	1,00E-03	1,5	↑	immediate
P04156	PRNP	Major prion protein	2,70E-02	2	↓	late
O95084	PRSS23	Serine protease 23	3,00E-03	3,3	↑	immediate
P07602	PSAP	Proactivator polypeptide	9,00E-03	1,5	↓	immediate

P13489	RNH1	Ribonuclease inhibitor	1,20E-02	1,8	↑	immediate
P07093	SERPINE2	Glia-derived nexin	2,00E-03	2,1	↑	immediate
P78324	SIRPA	Tyrosine-protein phosphatase non-receptor type substrate 1	2,30E-02	1,6	↑	immediate
P08195	SLC3A2	4F2 cell-surface antigen heavy chain	4,40E-02	1,6	↓	long-term
P52823	STC1	Stanniocalcin-1	4,80E-02	2,7	↑	immediate
Q8NBK3	SUMF1	Sulfatase-modifying factor 1	2,70E-02	1,5	↓	long-term
P10646	TFPI	Tissue factor pathway inhibitor	2,20E-02	1,8	↓	long-term
P07996	THBS1	Thrombospondin-1	1,30E-02	1,8	↑	immediate
P01375	TNF	Tumor necrosis factor	1,20E-02	3,1	↑	long-term
O60507	TPST1	Protein-tyrosine sulfotransferase 1	1,10E-02	1,6	↑	late
Q9GZX9	TWSG1	Twisted gastrulation protein homolog 1	1,70E-02	2,3	↓	late
Q8NBS9	TXNDC5	Thioredoxin domain-containing protein 5	1,30E-02	1,4	↓	late
Q6UXI7	VIT	Vitrin	3,80E-02	1,9	↓	immediate

FIGURES

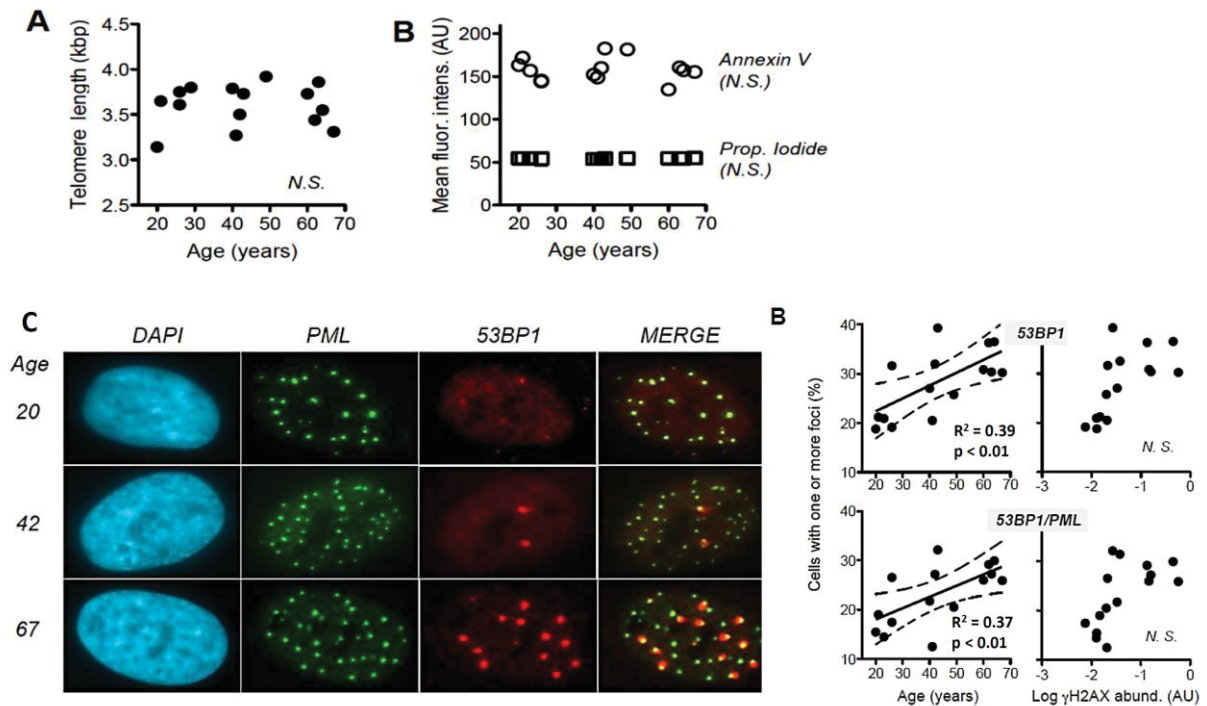


Figure 1 A: Telomere length was determined by Southern blotting. TFRL-values are plotted over the corresponding calendar age of the donor. **B:** Levels of apoptosis (annexin V) and necrosis (PI) were determined by FACS analysis. Medians of fluorescence intensities are plotted over calendar age of the donors. Mean values, $n = 3$, SEM was smaller than the size of the plotted symbols. **C:** DNA-SCARS: Representative immunofluorescent images of NHDFs dermal fibroblasts from a young, middle aged and old donor stained for PML and 53BP1. **D:** Percentage of cells having one or more foci positive for 53BP1 (top) or positive for 53BP1 and PML (bottom) plotted over donor age (left) or corresponding values of baseline H2AX-phosphorylation determined by immunoblotting. Results of linear regression are stated as R^2 : Pearson's coefficient for goodness of fit, p : probability for slope = 0, dotted lines: 95 % confidence limits of linear regression. *N.S.*: linear regression revealed no significant age-related change.

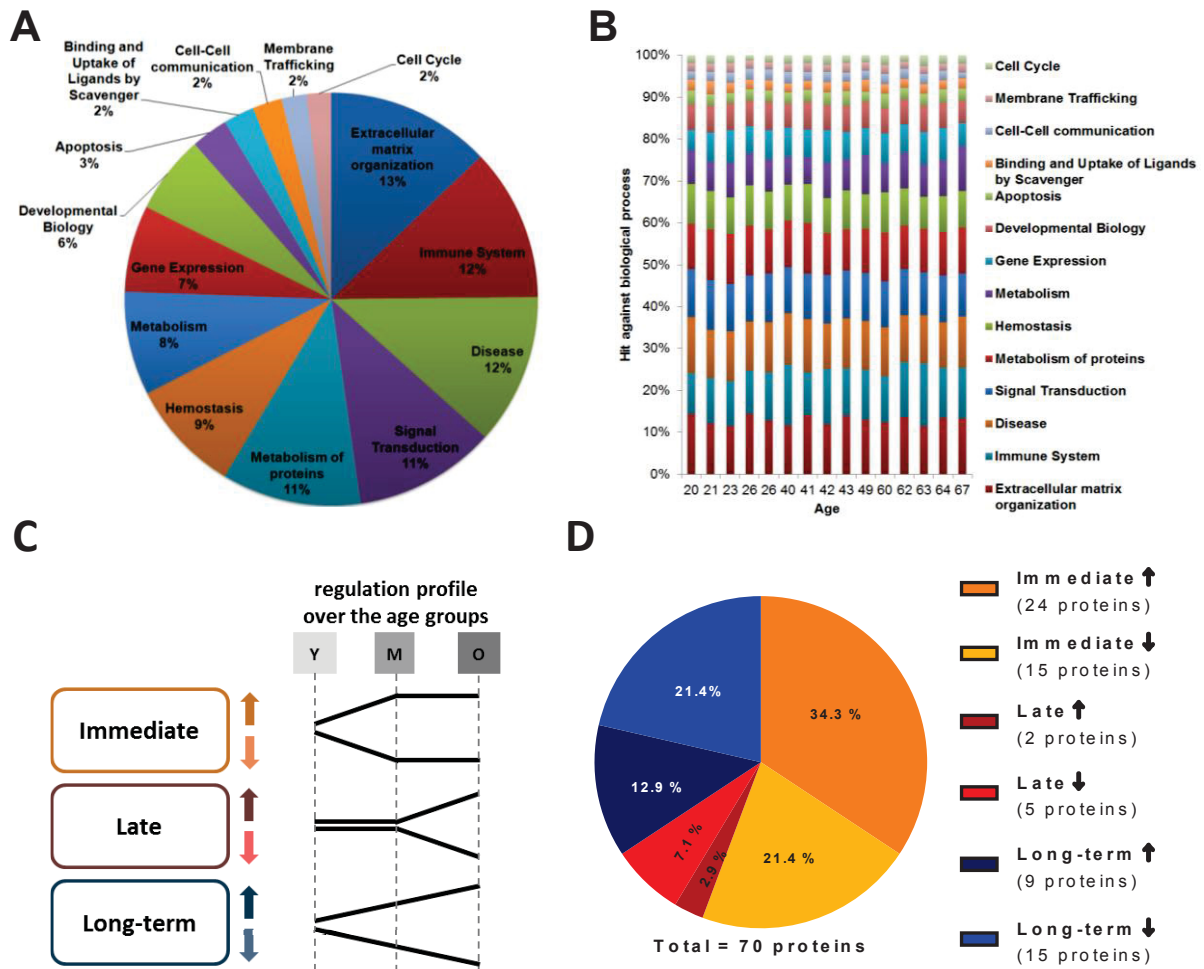


Figure 2: Functional annotation of secreted proteins using Reactome database (Matthews *et al.*, 2009). The secretome of each donor was categorized into 14 different biological processes. **A:** Functional annotation of overall identified fibroblasts' secretome. **B:** Annotation of secreted proteins for each individual. Proportion of each biological process is plotted over the corresponding calendar age of the donor. **C:** Regulation profiles of age-associated significantly altered proteins. Proteins were categorized into three groups: immediate (significant between young and middle), late (significant between middle and old) and long-term (significant correlation). All groups are subdivided into up and down altered profiles. **D:** Pie chart of age-associated alteration profiles.

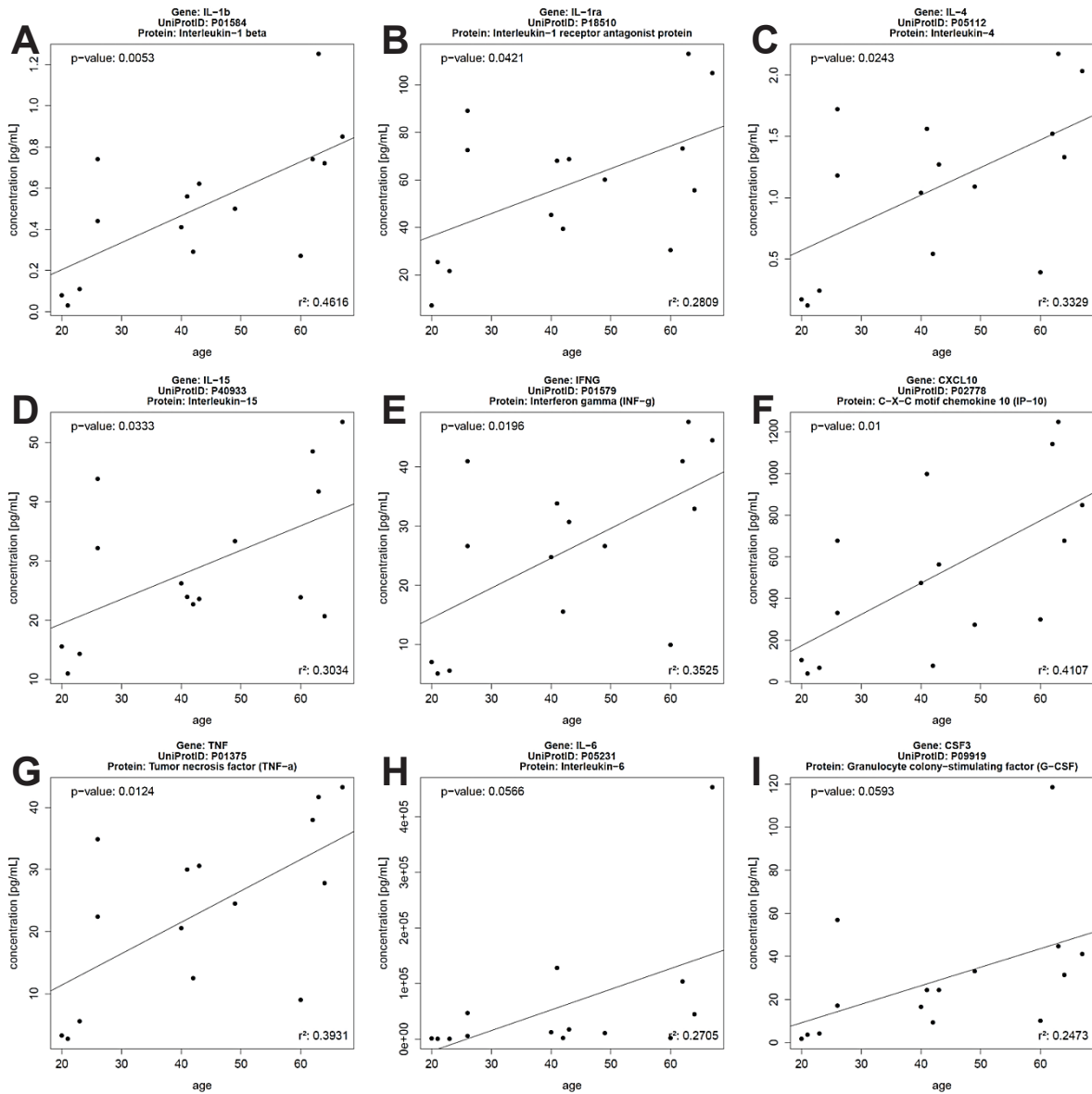


Figure 3: Results from the cytokine multiplex analysis. Concentrations of cytokines (pg/mL) are plotted over calendar age of the donors. UniProt ID and protein name are shown as identifiers. Statistical analysis of proteins analyzed in cytokine assay was applied using Pearson correlation. R^2 : Pearson's coefficient for goodness of fit. **A-G:** Age-associated significantly altered cytokines ($p < 0.05$). **H-I:** Correlation of known SASP factors (IL-6 and G-CSF) measured in cytokine assay. Regression of both cytokines revealed no significant age-related change.

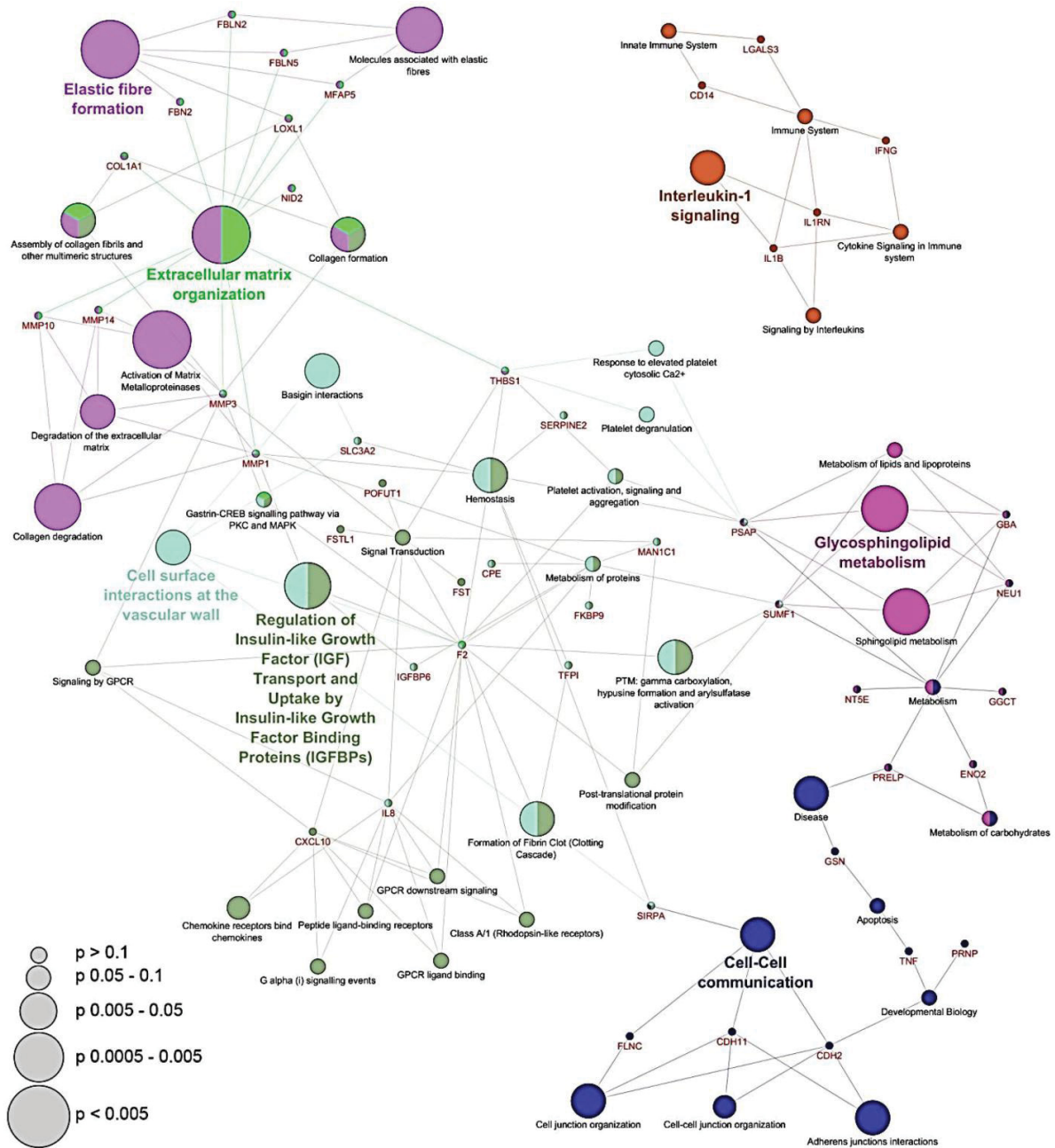


Figure 4: Detailed network and enrichment analysis of skin aging associated secreted proteins (SAASP) using biological ontology terms of Reactome database. A total of 70 proteins were used for generating the network of biological processes. About 45 proteins (64.3 %) were successfully mapped to 45 unique biological processes. Terms were labeled according to functional grouping using Kappa Score (Bindea *et al.*, 2009). Representative terms for each group are highlighted in bold. Significance level of biological processes is illustrated by the size of the dots. Interactions of proteins in biological processes are indicated by connective lines.

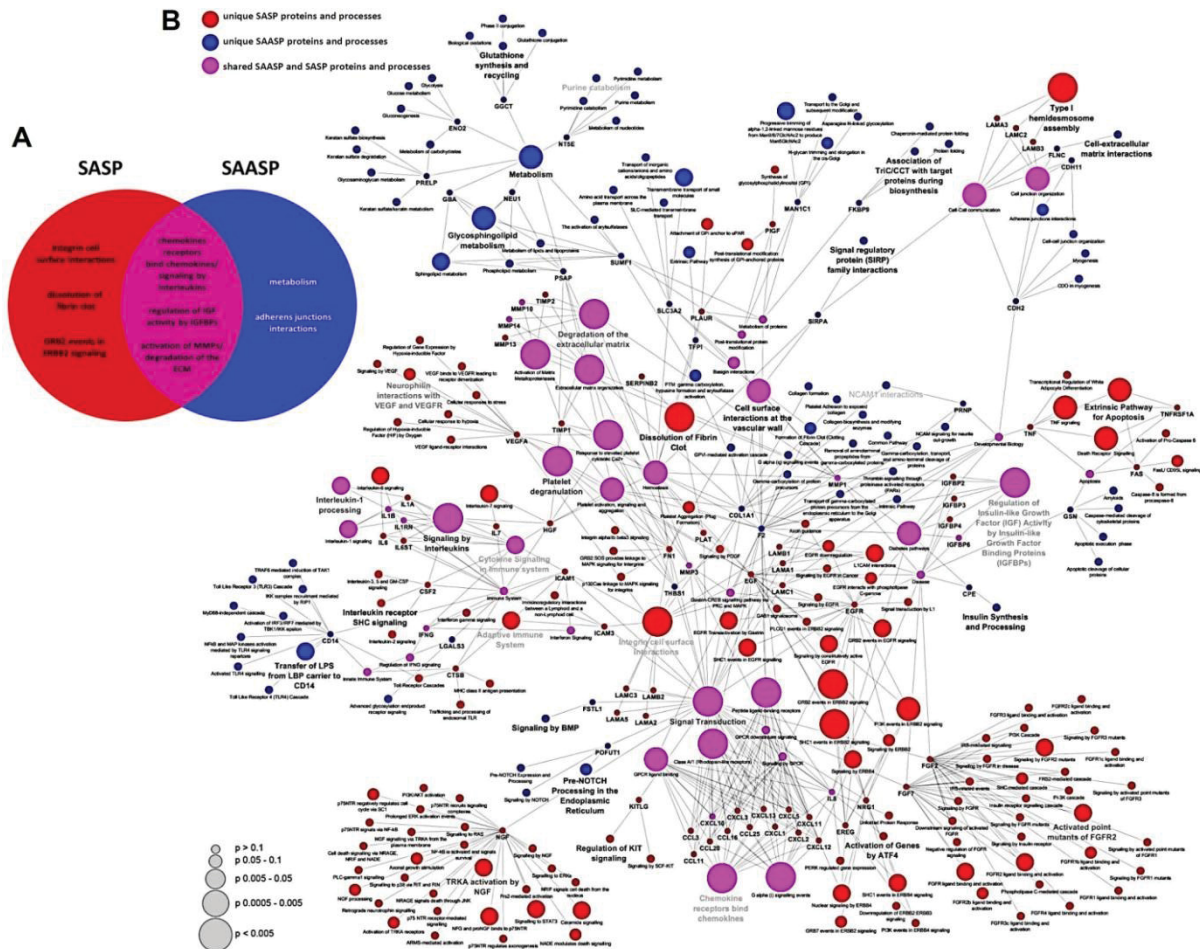


Figure 5: Detailed network and enrichment analysis of SAASP and SASP proteins using biological ontology terms of Reactome database. **A:** Summary of figure 5B showing the most important biological processes for SAASP, SASP and the overlap. **B:** A total of 151 proteins were used for generating the network of biological processes. About 109 proteins were successfully mapped to 148 biological processes. Terms were labeled as follows: red circles are unique to SASP (96 processes, 64.9 %) proteins, pink dots are shared between SASP and SAASP proteins (42 processes, 28.4 %) and blue circles are unique to SAASP proteins (10 processes, 6.8 %). Significance level of biological processes is illustrated by the size of the dots. Interactions of proteins in biological processes are indicated by connective lines.

SUPPLEMENTARY MATERIAL (MATERIAL AND METHODS)

Mass spectrometry

Mass spectrometric analyses of secretomes were carried out using the highly reproducible and stable LC-MS/MS system and a label-free approach for quantitation as described elsewhere (Sitek *et al.*, 2012). Extracted peptides of each sample were analyzed with a nano-HPLC/ESI-MS system composed of an RSLCnanoTM U3000 HPLC (Thermo Fisher Scientific, Bremen, Germany) and a LTQ Orbitrap EliteTM (Thermo Fisher Scientific, Bremen, Germany) mass spectrometer equipped with a nano-electrospray ion source (nano-ESI). Each sample (15 μ L) was loaded onto a trap C₁₈ trapping column (Acclaim PepMap C₁₈, 2 cm \times 100 μ m \times 5 μ m, 100 Å , Thermo Fisher Scientific) and desalted with 0.1 % trifluoroacetic acid (TFA) for 10 minutes. Peptides were eluted from the trap, separated with an analytical column (Acclaim PepMap RSLC C₁₈, 25 cm \times 75 μ m \times 2 μ m, 100 Å , Thermo Fisher Scientific) for 120 minutes with a flow rate of 300 nL/min, and sprayed into the MS. The mobile phase for chromatography consisted of 0.1 % formic acid in water (solvent A) and 84 % acetonitrile (ACN), 0.1% formic acid in water (solvent B). The gradient was designed as follows: starting with 4 % B, ramped to 10 % B in 5 min, 20 % B in 62 min, 30 % B in 35 min, 40 % B in 15 min and 95 % B in 2 min. The Orbitrap Elite parameters were as follows: spray voltage, 1.4 kV, ion transfer tube temperature, 275 °C, collision gas, helium, collision gas pressure, 1.3 mTorr, normalized collision energy for MS/MS, 35 %. The Orbitrap Elite was operated in a TOP20 data-dependent mode to automatically switch between MS and MS/MS acquisition. MS-spectra were acquired in the Orbitrap with a mass range of 350-1700 m/z and a resolution of 60.000. Polysiloxane (445.120030 Th) was used as lock mass. For MS/MS, ions were isolated with an isolation width of 2 m/z and fragmented using collision-induced dissociation (CID). MS/MS-spectra were acquired in the linear ion trap in centroid mode. Target ions selected for MS/MS were dynamically excluded for 45 sec. The ion selection thresholds were 500 counts for MS/MS. An activation Q of 0.25 and activation time of 10 ms was applied in MS/MS acquisitions.

Protein identification and quantification

For peptide and protein identification Proteome DiscovererTM (version 1.3, Thermo Fisher Scientific) and MASCOTTM search engine (version 2.4.1, Matrix Science, London, UK) were

used. MS/MS-spectra were searched against the UniProtKB/Swiss-Prot database (human sequences, 20255, date 04/03/2013). Search parameters were as follows: enzyme, trypsin, maximum missed cleavage sites, 2, taxonomy, homo sapiens, precursor mass tolerance, 10 ppm, fragment mass tolerance, 0.4 Da, oxidation of methionine as dynamic modification, carbamidomethylation of cysteine as fixed modification. The false discovery rate (FDR) was set to 5 % ($p \leq 0.05$). In the case of identified peptides that are shared between two proteins, these were combined and reported as one protein group.

The identified proteins of the fibroblasts' secretome were categorized by SignalP (Petersen *et al.*, 2011), SecretomeP (Bendtsen *et al.*, 2004), Exocarta (Mathivanan *et al.*, 2012) and UniProt databases (The UniProt Consortium, 2014) to confirm their extracellular occurrence and to identified potential contaminants. Proteins with missing signal peptide (SignalP), secretion prediction (SecretomeP: NN-score < 0.5) and known intracellular localization (UniProt: cytoplasm, mitochondria, nucleus, organelle lumen) were classified as potential contaminants. Although we could not exclude exosomal associated proteins to be abundant in the secretome we did not to include them in the following analysis.

Label-free quantification proteins, which were confirmed as secreted, was carried out using ProgenesisTM LC-MS (Nonlinear Dynamics, Newcastle upon Tyne, UK, Sitek *et al.*, 2012). A minimum of 2 unique peptides were required for quantification. Furthermore, only proteins identified in all secretomes were regarded for quantification. The significant threshold for the minimum fold change was determined calculating the technical variance of the LC-MS/MS measurements. Mean technical variance was calculated with a CV about 25 % and the minimum fold change was set to ≥ 1.3 . Statistical analysis for the secretomes was performed using two approaches: multiple t-tests (ANOVA) and Pearson correlation. For ANOVA analysis the samples were grouped into three ageing groups (young, middle, old) and statistical test was performed with a significance threshold of 5 % ($p \leq 0.05$). Pearson correlation was performed without any grouping using an R-script with a significance threshold of 5 % ($p \leq 0.05$).

Stability of protein abundance was determined as described elsewhere (Peterson *et al.*, 2012). Therefore, protein intensities were logarithmised (\log_{10}) and for each protein the absolute mean difference between the age-groups ('mean young' – 'mean middle', 'mean young' – 'mean old', 'mean middle' – 'mean old') was calculated. Afterwards, the 'two one-sided test' for equivalence (TOST) was applied to test for similarity of the groups (e.g. H_1 : |'mean

young' – 'mean middle'| < equivalence range (ϵ) (Robinson *et al.*, 2005). As equivalence range, the three-fold standard deviation ($\epsilon = 0.3$) was used. Proteins whose p-value was significant ($p \leq 0.05$) in all of the three pairwise comparisons were marked as unchanged.

Functional annotation, network and enrichment analysis

For global functional annotation of secreted proteins we used the Reactome database (Matthews *et al.*, 2009, Fig.4). We considered only biological processes which had at least five assigned proteins per term. Gene set analysis of unchanged proteins was carried out using Consensus Path DB (Kamburov *et al.*, 2009). The entire identified secretome was used as background list. Enrichment was applied on Gene Ontology biological processes. We discarded gene sets that were redundant, had ≤ 5 members or a p-value above 0.01. Network and enrichment analysis was carried out using ClueGO (v.2.0.7, Bindea *et al.*, 2009), CluePedia (v1.0.8, Bindea *et al.*, 2013) and Cytoscape environment (v3.0.2, Shannon *et al.*, 2003). Therefore, proteins/genes were loaded into ClueGo with UniProt accessions as identifiers. Parameters for network analyses were applied as follows: Ontology source, Reactome database (date 12/10/2013), statistical test, enrichment/depletion (two-sided hypergeometric test), p-value correction, Benjamini-Hochberg, network specificity, 'medium', GO term restriction, 'all', use GO term fusion, GO term connection restriction, kappa score ≥ 0.3 , use GO term grouping. For network analysis of SAASP proteins the entire identified secretome was used as reference set. For network analysis of SASP proteins the reference set of Reactome database was used. Proteins and biological processes of SAASP/SASP network were marked manually. Therefore, unique SASP proteins/processes were marked in red, unique SAASP proteins/processes in blue and shared proteins/processes in pink.

REFERENCE LIST

- 1 Bendtsen JD, Jensen LJ, Blom N, von HG, Brunak S: Feature-based prediction of non-classical and leaderless protein secretion. *Protein Eng Des Sel* 17:349-356 (2004).
- 2 Bindea G, Galon J, Mlecnik B: CluePedia Cytoscape plugin: pathway insights using integrated experimental and in silico data. *Bioinformatics* 29:661-663 (2013).
- 3 Bindea G, Mlecnik B, Hackl H, Charoentong P, Tosolini M, Kirilovsky A, Fridman WH, Pages F, Trajanoski Z, Galon J: ClueGO: a Cytoscape plug-in to decipher functionally grouped gene ontology and pathway annotation networks. *Bioinformatics* 25:1091-1093 (2009).
- 4 Kamburov A, Wierling C, Lehrach H, Herwig R: ConsensusPathDB--a database for integrating human functional interaction networks. *Nucleic Acids Res* 37:D623-D628 (2009).
- 5 Mathivanan S, Fahner CJ, Reid GE, Simpson RJ: ExoCarta 2012: database of exosomal proteins, RNA and lipids. *Nucleic Acids Res* 40:D1241-D1244 (2012).
- 6 Matthews L, Gopinath G, Gillespie M, Caudy M, Croft D, de BB, Garapati P, Hemish J, Hermjakob H, Jassal B, Kanapin A, Lewis S, Mahajan S, May B, Schmidt E, Vastrik I, Wu G, Birney E, Stein L, D'Eustachio P: Reactome knowledgebase of human biological pathways and processes. *Nucleic Acids Res* 37:D619-D622 (2009).
- 7 Petersen TN, Brunak S, von HG, Nielsen H: SignalP 4.0: discriminating signal peptides from transmembrane regions. *Nat Methods* 8:785-786 (2011).
- 8 Peterson LN, Eva KW, Rusticus SA, Lovato CY: The readiness for clerkship survey: can self-assessment data be used to evaluate program effectiveness? *Acad Med* 87:1355-1360 (2012).
- 9 Robinson AP, Duursma RA, Marshall JD: A regression-based equivalence test for model validation: shifting the burden of proof. *Tree Physiol* 25:903-913 (2005).
- 10 Shannon P, Markiel A, Ozier O, Baliga NS, Wang JT, Ramage D, Amin N, Schwikowski B, Ideker T: Cytoscape: a software environment for integrated models of biomolecular interaction networks. *Genome Res* 13:2498-2504 (2003).

- 11 Sitek B, Waldera-Lupa DM, Poschmann G, Meyer HE, Stuhler K: Application of label-free proteomics for differential analysis of lung carcinoma cell line A549. *Methods Mol Biol* 893:241-248 (2012).
- 12 The UniProt Consortium: Activities at the Universal Protein Resource (UniProt). *Nucleic Acids Res* 42:D191-D198 (2014).

SUPPLEMENTARY MATERIAL (FIGURES)

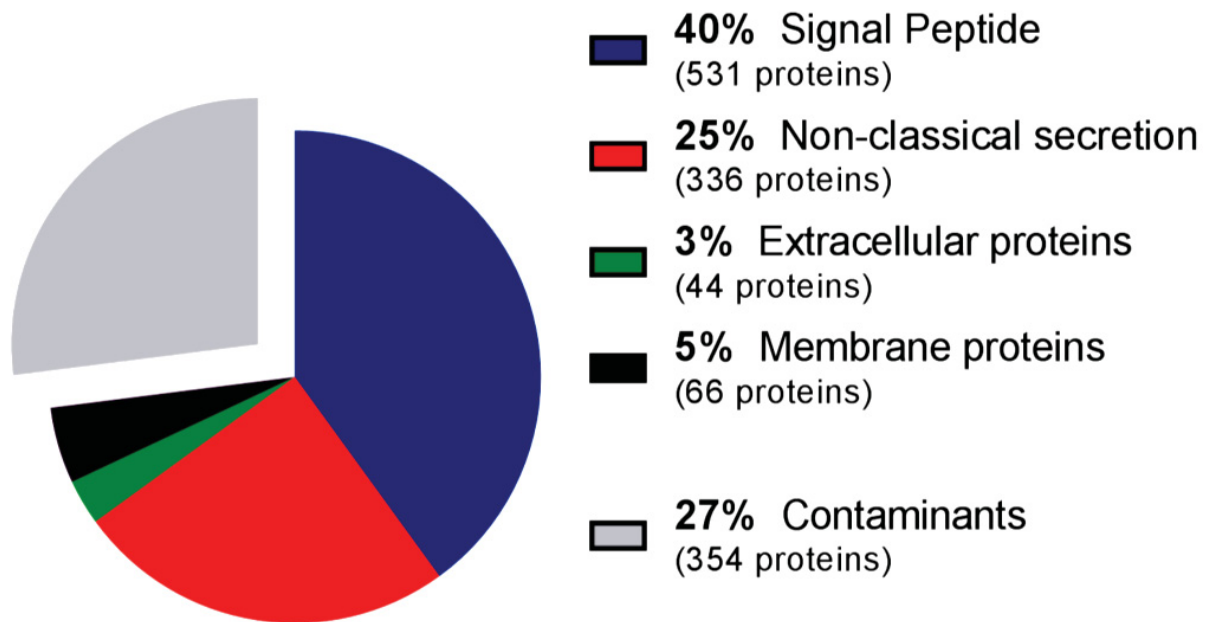


Figure S1 Categorisation of the fibroblast secretome by SignalP, SecretomeP, ExoCarta and UniProt database. A total of 1331 secretome proteins ($p < 0.05$) were identified by 15 LC-MS/MS runs. Secretome proteins were grouped into five categories: proteins with signal peptide (SignalP: 531 proteins, 40 %), classically secreted proteins (SecretomeP: 336 proteins, 25 %), extracellular (UniProt: 44 proteins, 3 %) localised proteins, membrane (UniProt: 66 proteins, 5 %) localised proteins, proteins identified in exosomes (ExoCarta: 122 proteins, 9 %) and contaminants (UniProt: 232 proteins, 18 %).

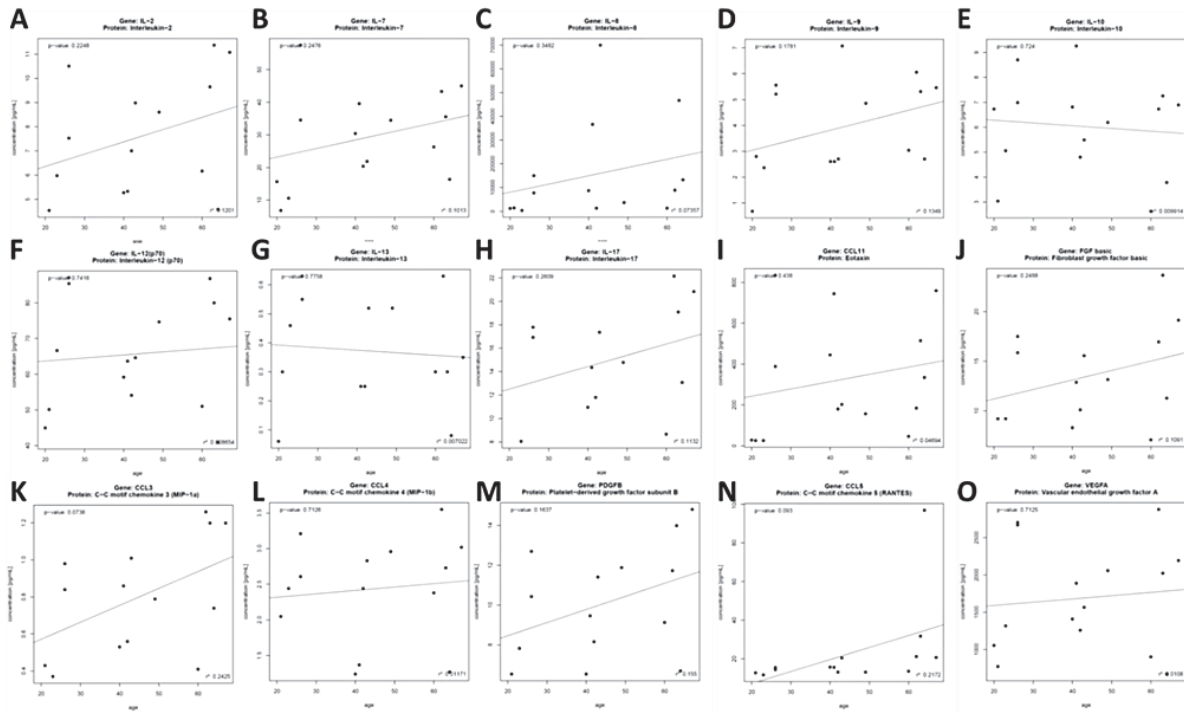


Figure S2 Results from the cytokine multiplex analysis. Concentrations of cytokines (pg/mL) are plotted over calendar age of the donors. UniProt ID and protein name are shown as identifiers. Statistical analysis of proteins analysed in cytokine assay was applied using Pearson correlation. R²: Pearson's coefficient for goodness of fit. Shown are the regressions of cytokines which revealed no significant age-related change.

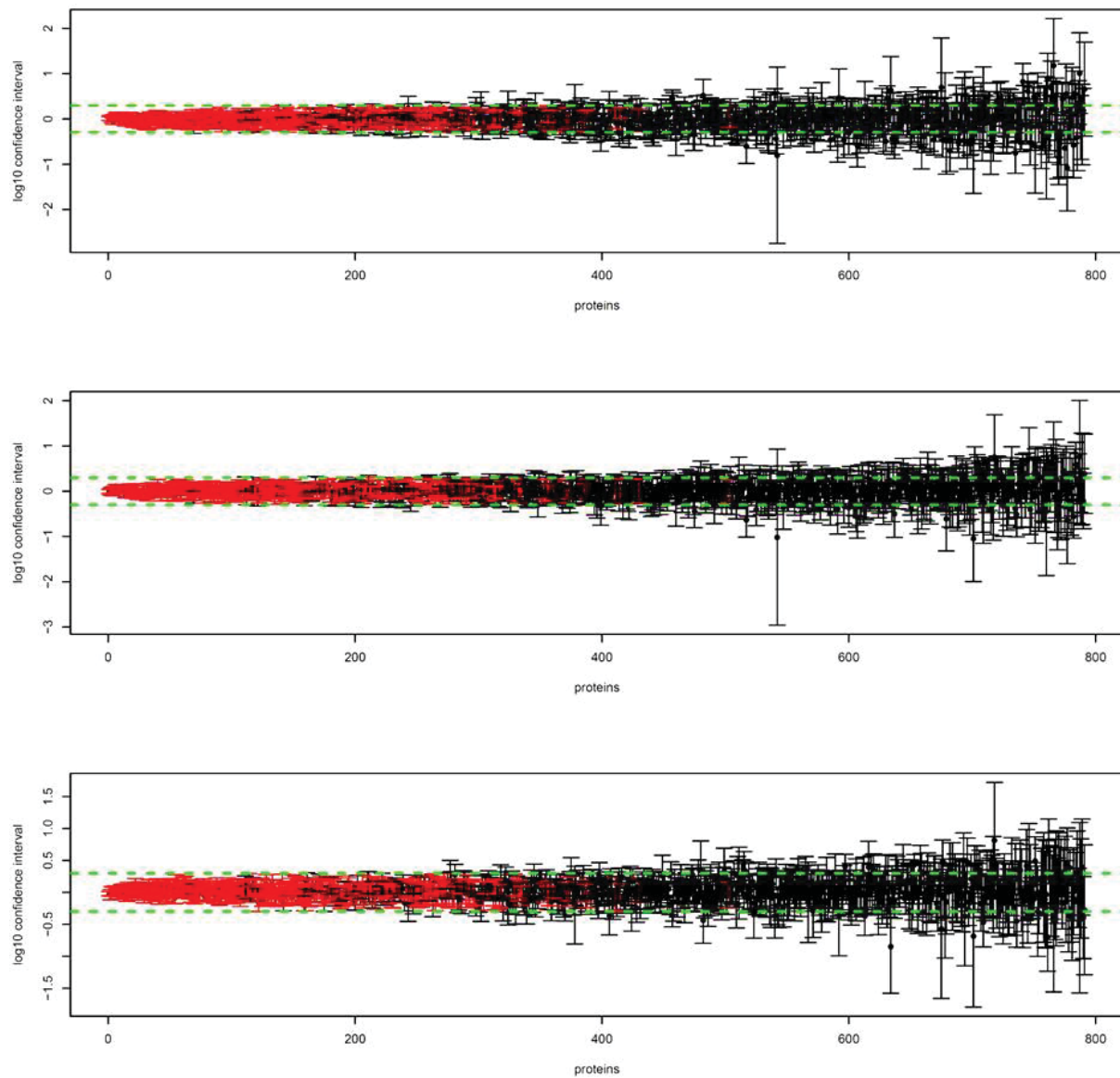


Figure S3: Confidence intervals (CI) of secreted proteins for each age-group. Logarithmised (\log_{10}) CIs are plotted over the corresponding protein. Red CIs are corresponding to significantly ($p < 0.05$) unchanged proteins. Black CIs belong to proteins which have one or more p-values above significance threshold ($p > 0.05$). Green lines indicate the equivalence range (three-fold standard deviation, $\varepsilon = 0.3$).

SUPPLEMENTARY MATERIAL (TABLES)

Supplementary tables can be found on the enclosed compact disk.

Table S1: Proteins measured in cytokine assay. Concentrations are presented in pg/mL. Values marked with * are approximated from standard curve. Values which cannot be approximated are marked with OOR (out of range) proteins which significantly alter with age are written in blue.

Table S2: Biological processes identified by gene enrichment analysis of unchanged secretome proteins using Gene Ontology database.

Table S3: Skin Aging Associated Secreted Proteins (SAASP) of *in situ* aged dermal fibroblasts. Cytokine assay (in grey) and quantitative label-free proteome analysis (in black) of *in situ* aged fibroblasts' secretome revealed 70 extracellular proteins that are differentially altered during *in situ* ageing (ANOVA: $p \leq 0.05$, fold change ≥ 1.3 , Pearson correlation: $p \leq 0.05$, fold change ≥ 1.3). For ANOVA analysis donors were grouped according to calendar age into groups 20-30, 40-50 and 60-70 years, with five individual donors in each group.

Table S4: Biological processes identified by network and enrichment analysis of SAASP proteins using biological ontology terms of Reactome database.

Table S5 Comparison of SASP proteins known from the literature identified in this study. Alterations were taken from Coppe *et al.* 2010a. Alterations (study) were classified as follows: up or down regulated proteins found with ANOVA or Pearson correlation ($p \leq 0.05$), unchanged proteins ($p \leq 0.05$ in all three CIs) and identified proteins ($p > 0.05$ in one or more CIs). (CI: confidence interval, \uparrow = up-regulated, \downarrow = down-regulated, X = no significance). Proteins identified by cytokine assay are marked in grey. Non-classically secreted proteins should obtain an NN-score exceeding the normal threshold of 0.5, but not at the same time be predicted to contain a signal peptide.

Table S6: Biological processes identified by network analysis of skin aging associated secreted proteins (SAASP) and senescence-associated secretory phenotype (SASP) proteins using biological ontology terms of Reactome database.

Table S7: Biological processes identified in both skin aging associated secreted proteins (SAASP) and senescence-associated secretory phenotype (SASP). Biological processes were determined using biological ontology terms of Reactome database. Proteins known from the literature are presented as SASP proteins and newly identified proteins as SAASP proteins.

Table S8: Demographic data from the participants included in the study.

Table S9: Shedded membrane-associated proteins identified in the secretome of *in situ* aged fibroblasts.

4 Abschlussdiskussion

Das Ziel der vorliegenden Dissertation ist es einen Beitrag zur Aufklärung des stromalen Alterungsprozesses zu leisten und die zugrundeliegenden Mechanismen des Alterns zu ergänzen. Bisher wurden dafür überwiegend induzierte Alterungsmodelle verwendet, die nur bedingt repräsentativ für das *in vivo* Altern sind. In dieser Arbeit wurde ein *ex vivo* Hautalterungsmodell unter Verwendung *in situ* gealterter primärer adulter humaner dermaler Fibroblasten mittels massenspektrometrie-basierter Proteomanalyse auf Ebene der intrazellulären und der sezernierten Proteine charakterisiert. Dafür wurde zunächst ein geeignetes Massenspektrometer evaluiert und ein Arbeitsablauf für die labelfreie Proteomanalyse humaner Proben etabliert.

4.1 Die massenspektrometrie-basierte Proteomanalyse

4.1.1 Evaluierung eines Massenspektrometers für die Identifizierung von Proteinen

Bei der Aufklärung biologischer Funktionszusammenhänge hat die technische Entwicklung der Massenspektrometer in den letzten Jahren eine wichtige Rolle gespielt (Bantscheff *et al.*, 2012). Hierbei wurden stetig die Sensitivität, die Massengenauigkeit und die Geschwindigkeit der Geräte verbessert (Olsen *et al.*, 2009, Michalski *et al.*, 2012). Eine detaillierte Charakterisierung des Proteoms wird maßgeblich vom verwendeten Massenspektrometer determiniert. Daher stellte sich zu Beginn der Arbeit aufgrund der Verfügbarkeit unterschiedlicher Massenspektrometer die Frage, welches für das geplante Experiment in Hinsicht auf Sensitivität und Genauigkeit am geeignetsten ist. So konnte bereits in einer vorangegangenen massenspektrometrie-basierten Proteomanalyse dermaler Fibroblasten gezeigt werden, dass die Anzahl identifizierter Proteine vom eingesetzten Massenspektrometer abhängig ist (Waldera-Lupa *et al.*, unveröffentlichte Daten).

Um ein geeignetes Massenspektrometer für die Analyse *in situ* gealterter Fibroblasten zu bestimmen wurde zunächst eine umfangreiche Untersuchung der Peptidfragmentierung zur Identifizierung von Proteinen mit verschiedenen Massenspektrometern durchgeführt (Publikation I: *The fate of b-ions in the two worlds of collision-induced dissociation*, Waldera-Lupa *et al.*, 2013). In Publikation I wurde gezeigt, dass b-Ionen bei den häufig verwendeten Massenspektrometern (QToF, LIT und QIT) signifikant unterrepräsentiert sind. Bei Massenspektrometern, welche die resonanz-angeregte CID (rCID) verwenden (LIT und QIT),

wurden ca. 15-20 % weniger b-Ionen als y-Ionen detektiert. Beim Beam-CID (bCID)-Massenspektrometer (QToF) wurden sogar nur etwa 20 % der möglichen b-Ionen detektiert. Letzteres steht im Einklang mit den Befunden von Lau *et al.* (2009). Durch den Vergleich verschiedener Massenspektrometer wurde zum ersten Mal gezeigt, dass die Unterrepräsentation von b-Ionen nicht wie bisher angenommen ein spezifisches Merkmal der bCID ist (Lau *et al.*, 2009), sondern auch in rCID-MS vorkommt.

Als potentielle Ursache für die Unterrepräsentation der b-Ionen wurde die in der Literatur beschriebene Zyklisierungsreaktion ausgemacht (zusammenfasst in Harrison, 2009). So konnte bei der Analyse synthetischer Peptide gezeigt werden, dass sich während der Fragmentierung von Peptiden in der Gasphase zyklische b-Ionen bilden (Yalcin *et al.*, 1995), die nach einer spontanen Ringöffnung eine veränderte Aminosäuresequenz aufweisen (Paizs und Suhai, 2005, Bleiholder *et al.*, 2008) und nicht mehr für die Identifizierung von Peptiden und Proteinen herangezogen werden können (Harrison *et al.*, 2006). Die veränderte Aminosäuresequenz resultiert somit in der Unterrepräsentation der b-Ionen in den identifizierten Spektren. Wie bereits in der Literatur beschrieben, wurden durch die Blockierung der Ringschlussreaktion mittels N-terminaler Acetylierung mehr b-Ionen detektiert (Jia *et al.*, 2007). Zudem wurde in dieser Arbeit erstmals gezeigt, dass die Ringschlussreaktion signifikant für die Unterrepräsentation von b-Ionen bei bCID-MS und rCID-MS verantwortlich ist. So konnte hier gezeigt werden, dass der Anteil der Ringschlussreaktion an der Unterrepräsentation 16 % beträgt und für alle Massenspektrometer nahezu identisch ist. Des Weiteren hat sich herausgestellt, dass die Ringschlussreaktion der hauptsächliche Grund für die Unterrepräsentation von b-Ionen bei rCID-MS ist, wohingegen b-Ionen beim bCID-MS auch nach der Acetylierung signifikant unterrepräsentiert sind. Hier spielen vermutlich weitere Degradationswege, wie beispielsweise die Degradation von b- zu a-Ionen ($b_x \rightarrow a_x$) oder die sekundäre Fragmentierung der generierten Fragmentionen aufgrund überschüssiger kinetischer Energie, eine tragende Rolle (Paizs *et al.*, 2005, Harrison, 2009). Da in dieser Arbeit keine signifikante Zunahme an a-Ionen detektiert wurde ist die Degradation von b- zu a-Ionen ein womöglich untergeordneter Prozess und eine sekundäre Fragmentierung der Fragmentionen wahrscheinlich. Ferner konnte hier gezeigt werden, dass beim bCID-MS, anders als bei rCID-MS, mehr kurz-kettige und nur wenig lang-kettige b-Ionen detektiert werden. Ein Grund hierfür könnte die bei Paizs *et al.* (2012) beschriebene Degradation von lang-kettigen b-Ionen zu kürzeren b-Ionen ($b_x \rightarrow b_{x-1}$) sein. Da b- und y-Ionen gleichwertig für die Identifizierung von Proteinen sind hat der Verlust einer der beiden

Ionenserien einen großen Einfluss auf die Identifizierungsrate. So können bei der Berücksichtigung nur einer Ionenserie etwa 75 % der Proteine einer komplexen Probe identifiziert werden, wobei vorwiegend niedrig abundante Proteine nicht mehr identifiziert werden können (Waldera-Lupa *et al.*, unveröffentlichte Daten). Aufgrund der signifikant höheren Detektionsrate von b-Ionen und auch y-Ionen bei rCID-MS und der daraus resultierenden gesteigerten Identifizierungsrate von Proteinen wurde ein Orbitrap-Massenspektrometer, ein hochauflösendes rCID-MS, für die Proteomanalyse *in situ* gealterter humaner dermaler Fibroblasten ausgewählt.

4.1.2 Etablierung eines Arbeitsablaufs zur Charakterisierung humaner Proben

Die quantitative Information der Proteinabundanz spielt eine wichtige Rolle in der Aufklärung von Signalwegen und biologischen Prozessen (Steen und Pandey, 2002). Mithilfe der massenspektrometrie-basierten Proteomanalyse ist neben der Identifizierung auch die Quantifizierung von Proteinen realisierbar. Hierfür stehen verschiedene Ansätze zur Verfügung (zusammengefasst in Bantscheff *et al.*, 2007). Diese beruhen zum einen auf der Markierung der Proteine oder Peptide mithilfe von isotoopenmarkierten Aminosäuren in der Zellkultur oder mittels Reportergruppen, die an reaktive Seitengruppen der Aminosäuren oder den N-Terminus addiert werden. Zum anderen kann die Quantifizierung auch ohne Markierung der Proteine und Peptide, also labelfrei, durchgeführt werden. Der labelfreie Ansatz hat in den letzten Jahren zunehmend an Bedeutung gewonnen (Bantscheff *et al.*, 2012). Dieser eignet sich sowohl für die Analyse von Zellkulturproben, als auch klinischer Proben (Neilson *et al.*, 2011) und ist im Gegensatz zu den markierungsbasierten Ansätzen ohne aufwendige Kultivierung der Zellen oder Markierung der Proteine durchführbar. Die labelfreie quantitative Proteomanalyse komplexer Proben setzt eine hohe Reproduzierbarkeit der Probenpräparation sowie der LC-MS/MS-Analyse voraus, weshalb der durchzuführende Arbeitsablauf zuvor evaluiert werden muss.

Für die Quantifizierung von Proteinen *in situ* gealterter Fibroblasten wurde ein labelfreier Ansatz eingesetzt. Dafür wurde zunächst ein Arbeitsablauf unter Verwendung eines nano-HPLC-ESI-Orbitrap-MS-Systems optimiert (Publikation II: *Application of label-free proteomics for differential analysis of lung carcinoma cell line A549*, Sitek *et al.*, 2012). Die Optimierung beinhaltete sowohl die Probenpräparation, die LC-MS/MS-Analyse als auch die Datenauswertung. In der Analyse von 2 x 7 Einzelproben wurden 732 Proteine quantifiziert, wovon 202 Proteine sich signifikant in ihrer Abundanz zwischen unbehandelten und TGF- β 1-

behandelten Lungenkarzinomzellen (A549) unterschieden. Die mittlere technische Varianz der LC-MS-Analyse betrug ca. 25 % und der dynamische Abundanzbereich etwa vier Größenordnungen. Im Vergleich zu vorangegangenen Proteomstudien TGF- β 1-behandelter Lungenkarzinomzellen mittels LC-MS/MS-Analyse (325 identifizierte Proteine, Keshamouni *et al.*, 2006) oder mittels gelbasierten Ansatzes (581 detektierte Proteine, Milosevic *et al.*, 2009) konnten mithilfe des etablierten labelfreien Arbeitsablaufs etwa ein Viertel bis zwei Mal so viele Proteine identifiziert werden. Durch die Verwendung der labelfreien Quantifizierung konnten zudem etwa vier Mal mehr differentielle Kandidatenproteine identifiziert werden als durch die Verwendung von iTRAQ (51 Proteine, Keshamouni *et al.*, 2006) oder der 2D-PAGE (41 Proteine, Milosevic *et al.*, 2009), wobei ein Teil der Kandidatenproteine konvergiert. Der in Publikation II beschriebene labelfreie Arbeitsablauf unter Verwendung eines Orbitrap-Massenspektrometers ermöglichte die Identifizierung und Quantifizierung hunderter Proteine aus komplexen humanen Proben.

4.1.3 Proteomanalyse humaner dermaler Fibroblasten

Für die Analyse des Proteoms und des Sekretoms humaner dermaler Fibroblasten wurde der etablierte labelfreie Arbeitsablauf adaptiert, wobei neuere Generationen des Orbitrap-Massenspektrometers (Velos und Elite) eingesetzt wurden. Diese zeichnen sich vor allem durch eine höhere Sensitivität, Massengenauigkeit sowie Geschwindigkeit aus (Olsen *et al.*, 2009, Michalski *et al.*, 2012).

Bei der Untersuchung des Proteoms dermaler Fibroblasten wurden 2409 Proteine identifiziert, wovon 1607 Proteine in mindestens 14 von 15 Proben quantifiziert werden konnten (Publikation III: *Proteome-wide analysis of primary cultures of in situ aged human fibroblasts reveals a moderate age-associated cellular phenotype*, Waldera-Lupa *et al.*, 2014a). Im Vergleich zu anderen Studien von Fibroblasten mittels labelfreien Ansatzes (1766 Proteine, Edhager *et al.*, 2014), oder unter der Verwendung von SILAC (1901 Proteine, Prins *et al.*, 2014) und iTRAQ (1609 Proteine, Zheng *et al.*, 2014) konnten in etwa gleich viele Proteine im Fibroblastenproteom quantifiziert werden. Des Weiteren wurde in dieser Arbeit mithilfe der Massenspektrometrie ein Abundanzbereich von etwa fünf Größenordnungen abgedeckt, was einem Großteil des geschätzten Abundanzbereichs einer humanen Zelle von sieben Größenordnungen abdeckt (Beck *et al.*, 2011). Der Nachweis gering abundanter Proteine wird durch Strukturproteine, wie beispielweise Vimentin, Aktin, Filamin, Lamin und Tubulin, die in Fibroblasten eine hohe Abundanz aufweisen, erschwert. Folglich kommen niedrig

abundante Proteine, wie z.B. Kinasen und Transkriptionsfaktoren (Beck *et al.*, 2011), nur im geringen Maße in einer definierten Menge des Zellysats vor und liegen somit unterhalb der Nachweisgrenze der massenspektrometrischen Analyse. Eine größere Abdeckung des Abundanzbereichs könnte beispielsweise durch eine subzelluläre Fraktionierung, bei der zelluläre Bestandteile, wie Zellkerne und Mitochondrien, aufgetrennt, angereichert und anschließend separat mittels LC-MS analysiert werden (Cox und Emili, 2006), oder durch die Verwendung einer orthogonalen 2D-Chromatographie (*multidimensional protein identification technology*, MudPIT) (Washburn *et al.*, 2001) erzielt werden.

Bei der Untersuchung des Sekretoms wurden 977 sezernierte Proteine identifiziert (Publikation IV, *Characterization of skin aging associated secreted proteins (SAASP) produced by dermal fibroblast isolated from intrinsically aged human skin*, Waldera-Lupa *et al.*, 2014b). Im Vergleich zu vorangegangenen Studien des Sekretoms replikativ seneszenten Fibroblasten (407 Proteine, Micutkova *et al.*, 2011) und onkogen-induzierter Fibroblasten (429 Proteine, Acosta *et al.*, 2013) konnten somit etwa doppelt so viele sezernierte Proteine identifiziert werden. Die Schwierigkeit in der Charakterisierung des Sekretoms besteht darin, potentielle Kontaminationen durch intrazelluläre Proteine abgestorbener Zellen zu identifizieren und somit falsch positive Sekretomproteine zu ermitteln. Hierfür wurden bioinformatische Ansätze eingesetzt, die N-terminale Signalsequenzen für die klassische Sekretion eruieren (SignalP, Petersen *et al.*, 2011) und die nicht-klassische Sekretion durch spezifische Sequenzcharakteristika vorhersagt (SecretomeP, Bendtsen *et al.*, 2004). Zudem wurden Evidenzen aus Datenbanken, wie Exocarta (Mathivanan *et al.*, 2012) und UniProt (The UniProt Consortium, 2014), für die Evaluation sezernierter Proteine verwendet. Dieser Ansatz erhöht die Wahrscheinlichkeit, dass die identifizierten Proteine keine Kontaminanten sind und von Fibroblasten sezerniert werden, obgleich falsch positive nicht gänzlich ausgeschlossen werden können.

4.2 Charakterisierung *in situ* gealterter humaner dermaler Fibroblasten

4.2.1 Intrazelluläre altersassoziierte Veränderungen

Ziel der Analyse des Proteoms ist es die altersassoziierten intrazellulären Veränderungen *in situ* gealterter humaner dermaler Fibroblasten zu charakterisieren. Da die Fibroblasten dafür aus dem Gewebe extrahiert und anschließend in einem 2D-Zellkultursystem kultiviert wurden, wurden zunächst klassische Merkmale der induzierten Alterung, wie Telomerverkürzungen und DNA-Doppelstrangbrüche (Tigges *et al.*, 2014), untersucht. In Publikation IV wurde gezeigt, dass während der Alterung keine signifikante Verkürzung der Telomere, wie bei der induzierten Alterung beschrieben (Hayflick, 1980, Harley *et al.*, 1990, Harley *et al.*, 1992), zu beobachten ist. Dies steht im Einklang mit den Befunden aus der Literatur (Boukamp, 2005, Kronic *et al.*, 2009) und ist eine Bestätigung dafür, dass die analysierten Fibroblasten während der Kultivierung nicht replikativ seneszent wurden. Des Weiteren weisen die Fibroblasten keine signifikante Erhöhung an DNA-Doppelstrangbrüchen auf, wie es für replikativ und stress-induzierte Fibroblasten beschrieben wurde (Sedelnikova *et al.*, 2004, Fumagalli *et al.*, 2012). Auf Basis dieser Resultate kann davon ausgegangen werden, dass die analysierten Fibroblasten keinen seneszenz-assoziierten Phänotyp ausgebildet haben.

Als nächstes wurden weitere altersassoziierte Merkmale dermaler Fibroblasten, wie die Zellviabilität und die Ausbildung von DNA-SCARS, untersucht. Mit zunehmendem Alter konnte keine Abnahme der Zellviabilität beobachtet werden, wie es in der Literatur bisher postuliert wurde (Mandavilli, 2002). Hingegen gibt es Hinweise auf Ebene der intrazellulären Proteine, dass womöglich die Fähigkeit der Zelle in die Apoptose zu gehen mit zunehmendem Alter vermindert ist. Darüber Hinaus wurde in Publikation IV erstmals die altersabhängige Zunahme von DNA-SCARS während der *in situ* Alterung nachgewiesen. Diese wurde bisher ausschließlich in induzierten Altersmodellen im Zusammenhang mit der zellulären Seneszenz beschrieben (Rodier *et al.*, 2011). Die Bildung von DNA-SCARS ist unabhängig von *cellular tumor antigen p53* (p53), *retinoblastoma-associated protein* (pRB) oder anderen Zellzykluskontrollproteinen, gleichwohl kann diese zu einem permanenten Zellzyklusarrest führen (Rodier *et al.*, 2011). Ein Grund für die Bildung von DNA-SCARS kann der Verlust der Proteostase mit zunehmendem Alter sein (Rodier *et al.*, 2011). Der Verlust der Proteostase durch die Abnahme der proteasomalen Funktion wurde bereits in stress-induzierten Fibroblasten beschrieben (Bulteau *et al.*, 2007). In Publikation III wurde gezeigt,

dass es während des *in situ* Alterns zu einer Abnahme zweier proteasomaler Untereinheiten (PSMD1 und PSMD14) kommt, was dafür spricht, dass die proteasomale Funktion beeinträchtigt sowie die Proteostase gestört sein kann.

Auf Ebene des Proteoms konnten 43 altersabhängig veränderte Proteine identifiziert werden, die in die Differenzierung, die Proliferation, die Proteostase, den RNA-Metabolismus, die interzelluläre Kommunikation, die intrazelluläre Organisation, das Zytoskelett, die Stressantwort und den Zelltod involviert sind. Darüber Hinaus korrelierte die Abundanz von Proteinen des mitochondrialen Energiemetabolismus, insbesondere Proteine der Elektronentransportkette und der oxidativen Phosphorylierung, negativ mit dem Alter. Dies stimmt mit den Befunden aus der vorangegangenen Genexpressionsanalyse überein (Kalfalah *et al.*, 2014). In Kombination mit den Hinweisen für eine altersabhängig verminderte Proliferation auf Ebene des Proteoms unterstützt dies die Hypothese, dass die Dysfunktion der Mitochondrien mit zunehmendem Alter, und die daraus resultierende inadäquate Kommunikation zwischen Mitochondrien und Zellkern zu einer Abnahme der Proliferation führt (Kalfalah *et al.*, 2014). Die Abnahme der Proliferation könnte der Hauptgrund für die Reduktion der Gesamtanzahl an Fibroblasten in der Dermis mit zunehmendem Alter sein und negative Auswirkungen auf die Gewebemöostase und die Instandhaltung der ECM haben (Gunin *et al.*, 2011). Die meisten der biologischen Prozesse und ein Großteil der altersassoziierten Proteine sind noch nicht im Zusammenhang mit der *in situ* Alterung von Fibroblasten beschrieben worden und ergänzen die bereits bekannten Alterungsprozesse dermaler Fibroblasten (Tigges *et al.*, 2014).

Ferner wurden unter Berücksichtigung von mRNA-Daten Evidenzen gefunden, dass die identifizierten altersassoziierten Proteine nicht auf Ebene der Genexpression reguliert werden. Darüber Hinaus wurden durch den Abgleich der Proteomdaten mit den miRNA-Daten Hinweise gefunden, dass drei altersassoziierte Proteine potentiell durch miRNAs reguliert werden, die bisher noch nicht als gero-miRs (Boulias und Horvitz, 2012, Ugalde *et al.*, 2011) beschrieben wurden. Die Befunde auf Ebene des Proteoms deuten darauf hin, dass *in situ* gealterte dermale Fibroblasten einen moderaten altersassoziierten zellulären Phänotyp ausbilden, wobei 47 % des Proteoms und 63 % des Transkriptoms nachweislich keine Abundanzveränderung aufweisen. Dies deutet darauf hin, dass die Fibroblasten, wie erwartet, ihre kanonische Funktion im Alter aufrechterhalten. Obgleich können die altersabhängigen Veränderungen der Fibroblasten, wie die Abnahme der Proliferation, der Differenzierung und der Motilität, einen großen Einfluss auf das umliegende Stroma haben (Gunin *et al.*, 2011,

Midgley *et al.*, 2014). Es wurde postuliert, dass eine Reduktion dieser Prozesse ein Grund für die verminderte Wundheilung mit zunehmendem Alter sein kann (Gosain und DiPietro, 2004). Bei der Wundheilung migrieren Fibroblasten zunächst in das Wundgebiet, proliferieren und produzieren Zytokine sowie Wachstumsfaktoren. Dadurch werden Keratinozyten zur Migration und Proliferation stimuliert damit die Wunde geschlossen werden kann (Mirastschijski *et al.*, 2004). Im Weiteren differenzieren Fibroblasten zu Myofibroblasten, welche Kollagen-Fasern produzieren und essentiell für die Wundkontraktion sind (Grinnell, 1994, Eichler und Carlson, 2006). Die Evidenzen der Reduktion der Proliferation, der Differenzierung und der Motilität auf Proteomebene lässt den Schluss zu, dass Fibroblasten ein möglicher Ausgangspunkt für die Abnahme der Wundheilungskapazität mit zunehmendem Alter sind und dadurch einen Beitrag zur Hautalterung leisten.

4.2.2 Altersassoziierte Veränderungen des Sekretoms

Ziel der Analyse des Sekretoms ist es den altersassoziierten sekretorischen Phänotyp *in situ* gealterter humaner dermaler Fibroblasten zu charakterisieren. In vorangegangenen Studien wurden dafür überwiegend induzierte Alterungsmodelle von Fibroblasten analysiert (zusammengefasst in Coppe *et al.*, 2010). Hierbei kommt es jedoch zur Ausbildung eines seneszenz-assoziierten sekretorischen Phänotyps, dem sogenannten SASP (Coppe *et al.*, 2008). Dieser zeichnet sich durch die erhöhte Sekretion pro-inflammatorischer Proteine, ECM-Degradationsproteinen und Wachstumsfaktoren aus (Coppe *et al.*, 2010, Kuilman *et al.*, 2010). Es wird postulieren, dass der SASP eine negative Wirkung auf benachbarte Zellen und das Gewebe hat, und Karzinogenese stimulieren sowie die Gewebekomöostase stören kann (Coppe *et al.*, 2010). Allerdings ist bisher ungeklärt, ob sich der SASP während der *in vivo* Alterung ausbildet. Eine detaillierte Untersuchung des Sekretoms *in situ* gealterter Fibroblasten wurde bisher nicht durchgeführt.

In Publikation IV wurde erstmals der sekretorische Phänotyp *in situ* gealterter humaner dermaler Fibroblasten detailliert auf Ebene der Proteine charakterisiert. Hierbei wurden 70 altersabhängig veränderte Proteine identifiziert, die in der Organisation und dem Umbau bzw. Abbau der ECM, der Formation von elastischen Fasern, der Inflammation und der interzellulären Kommunikation eine Rolle spielen. Der Vergleich des in dieser Arbeit charakterisierten mit dem in der Literatur beschriebenen SASP zeigte, dass die Sekretion pro-inflammatorischer Zytokine und MMPs ein gemeinsamer Aspekt der induzierten Seneszenz

und des *in situ* Alters sind, obgleich viele der beschriebenen Proteine, wie z.B. Metalloproteinase-Inhibitoren oder insulinähnliche Wachstumsfaktoren, im *in situ* Alterungsmodell nicht verifiziert wurden (Coppe *et al.*, 2010, Kuilman *et al.*, 2010, Rodier und Campisi, 2011). Insgesamt wurden 27 Proteine identifiziert, die bisher nicht durch den SASP beschrieben wurden, wobei die extrazelluläre Funktion einiger Proteine noch unbekannt ist.

Die sekretierten Proteine *in situ* gealterter dermaler Fibroblasten können zu einer gestörten Gewebemöostase mit zunehmendem Alter führen und somit signifikant zur Hautalterung bzw. Gewebeergerung beitragen. So zeichnen sich die *in situ* gealterten Fibroblasten durch eine verminderte Sekretion von Kollagen und einer gesteigerten Sekretion von MMPs (MMP1, MMP3, MMP10 und MMP14) aus. Dies steht womöglich mit Beobachtungen in Verbindung, die zeigen, dass die ECM zunehmend durch die Degradation von Kollagenen und Elastin abgebaut wird (Naylor *et al.*, 2011), wodurch die Haut an Regenerationskapazität verliert (Krutmann *et al.*, 2008) und die Gewebemöostase gestört wird (Domyati *et al.*, 2002). Der Abbau der ECM durch eine geminderte Kollagensekretion und eine erhöhte Degradation durch Fibroblasten kann somit ein Grund für den zunehmenden Verlust der Elastizität der Haut und die Bildung von Falten im Alter sein (Escoffier *et al.*, 1989), wobei die Ausprägung der erkennbaren Altersmerkmale durch exogene Faktoren und den Lebensstil stark beeinflusst werden kann (Warren *et al.*, 1991). Des Weiteren zeichnen sich die *in situ* gealterten Fibroblasten durch eine erhöhte Sekretion pro-inflammatorischer Zytokine, wie Interleukin-1 (IL1), Interleukin-4 (IL4), Interleukin-8 (IL8), Interleukin-15 (IL15), Gamma-Interferon (INFG) und Tumornekrosefaktoren (TNF), aus. Dies könnte zu einem Anstieg von Entzündungsreaktionen in der Haut bzw. dem betroffenen Organ führen (Coppe *et al.*, 2010) und ist ein Hinweis für das Entzündungsaltern (Salminen *et al.*, 2012), welches die Proliferation epidermaler Stammzellen inhibieren (Doles *et al.*, 2012) und altersassoziierte Krankheiten induzieren kann (Barzilai *et al.*, 2012, Deeks, 2011). Somit könnten Fibroblasten durch die erhöhte Sekretion pro-inflammatorischer Zytokine und MMPs in die Verdünnung der Epidermis mit zunehmendem Alter involviert sein, was zu einer Abnahme der Barrierefunktion und der Wundheilung führt (zusammengefasst in Tigges *et al.*, 2014). Des Weiteren könnten Fibroblasten, die in jedem Bindegewebe des Körpers präsent sind, durch erhöhte inflammatorische Reaktionen einen schädlichen Einfluss auf lebenswichtige Organe haben (Cevenini *et al.*, 2010) und so ein Teilaspekt des systemischen Alterns darstellen (Jayanthi *et al.*, 2010). Ein weiterer Aspekt des altersassoziierten sekretorischen Phänotyps

dermaler Fibroblasten ist die immunsuppressive und tumorfördernde Wirkung, die durch Zytokine und MMPs vermittelt wird (Frey, 2006, Hoare und Narita, 2013). So sind Fibroblasten in die Initiation und Promotion maligner Melanome (Krtolica *et al.*, 2001, Hill *et al.*, 2005, Collado *et al.*, 2005), die Initiation und Progression von Ovarialkarzinomen (Yang *et al.*, 2006), die Promotion von Prostatakarzinomen (Yang *et al.*, 2005) und die Progression von Mammakarzinomen involviert (Wiseman und Werb, 2002). Die potentiell tumorfördernde Wirkung sezernierter Proteine *in situ* gealterter dermaler Fibroblasten könnte somit ein Teilaspekt der Karzinogenese und ein Grund für das erhöhte Krebsrisiko mit zunehmendem Alter (Berger *et al.*, 2006) sein. Zudem könnte die immunsuppressive Wirkung ein Grund für die Abnahme der Leistungsfähigkeit des Immunsystems und die Zunahme von Autoimmunreaktionen mit zunehmendem Alter sein (Walford, 1974). Die altersassoziierten Veränderungen dermaler Fibroblasten können einen negativen Effekt auf die Wundheilung, die Regenerationsfähigkeit, die Gewebekomöostase und die Elastizität der Haut haben. Darüber hinaus können die sezernierten Proteine inflammatorisch und immunmodulatorisch wirken und so das Immunsystem schwächen und die Karzinogenese fördern. Infolgedessen könnten Fibroblasten maßgeblich zum systemischen Altern des Organismus beitragen.

4.3 Schlussfolgerung

Die in dieser Arbeit etablierte labelfreie massenspektrometrie-basierte Proteomanalyse eignet sich für die Untersuchung primärer humaner Fibroblasten. Sie liefert im Vergleich zu anderen Quantifizierungsmethoden, wie SILAC oder iTRAQ, eine vergleichbare Anzahl quantifizierbarer Proteine über einen Abundanzbereich von etwa fünf Größenordnungen. Die kombinierte Untersuchung des Proteoms und Sekretoms *in situ* gealterter humaner dermaler Fibroblasten gab Hinweise darauf, dass viele verschiedene Prozesse in die Alterung von Fibroblasten involviert sind (Abb. 7). Diese bestätigen die bekannten Charakteristika des Alterns (Lopez-Otin *et al.*, 2013) und ergänzen die altersassoziierten Merkmale von Fibroblasten (Tigges *et al.*, 2014).

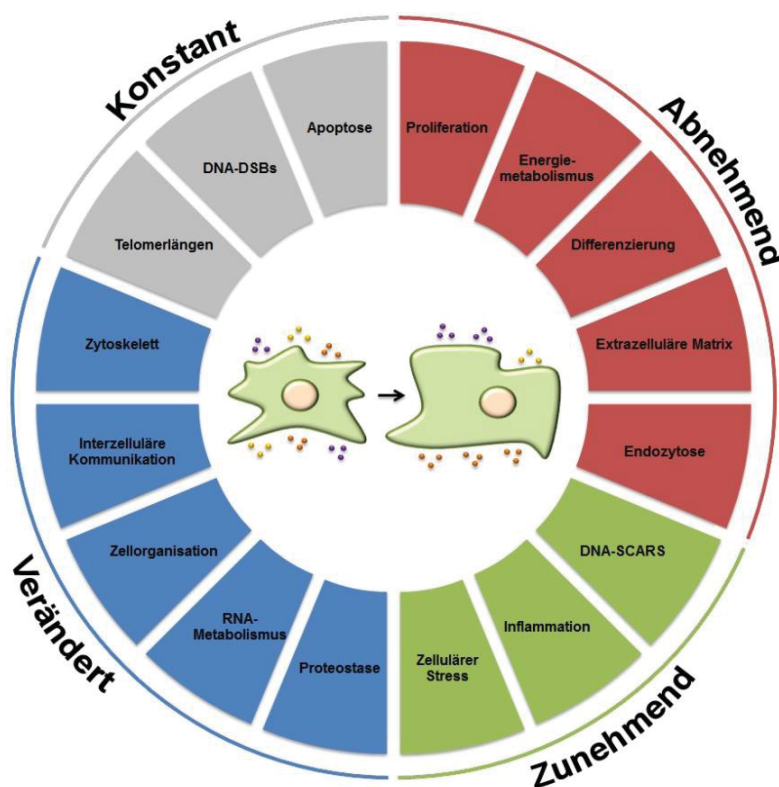


Abbildung 7: Intra- und extrazelluläre Veränderungen *in situ* gealterter humaner dermaler Fibroblasten. Zu den altersabhängig abnehmenden Funktionen gehören die Proliferation, der Energiemetabolismus, die Differenzierung, die Instandhaltung der ECM und die Endozytose. Zu den zunehmenden Charakteristika zählen die Bildung von DNA-SCARS, die Inflammation und zellulärer Stress. Zu den Funktionen, die mit zunehmendem Alter beeinträchtigt sind, gehören die Proteostase, der RNA-Metabolismus, die Zellorganisation, die interzelluläre Kommunikation und die Organisation des Zytoskeletts. Nachweislich unverändert sind die Längen der Telomere, das Vorkommen von DNA-Doppelstrangbrüchen (DNA-DSBs) und die Anzahl apoptotischer Zellen.

Der Vergleich des in dieser Arbeit charakterisierten Phänotyps *in situ* gealterter Fibroblasten mit dem in der Literatur beschriebenen SASP hat gezeigt, dass die Sekretion proinflammatorischer Zytokine und Matrix-Metalloproteinasen ein gemeinsamer Aspekt der induzierten Seneszenz und des *in situ* Alters sind, obgleich viele der im SASP beschriebenen Proteine, wie beispielweise Metalloproteinase-Inhibitoren oder Wachstumsfaktoren, im *ex vivo* Alterungsmodell nicht verifiziert werden konnten. Zudem konnten 27 sezernierte Proteine mit einer altersabhängigen Veränderung identifiziert werden, die bisher nicht durch den SASP beschrieben wurden. Hieraus lässt sich der Schluss ziehen, dass sich das in dieser Arbeit eingesetzt *ex vivo* Alterungsmodell unter Verwendung *in situ* gealterter humaner dermaler Fibroblasten von den induzierten Alterungsmodellen (Tigges *et al.*, 2014) unterscheidet. Des Weiteren konnte gezeigt werden, dass die intra- und extrazellulären Veränderungen mit zunehmendem Alter einen kleinen Teil der Proteine und miRNAs betrifft und ein großer Teil des Proteoms und Sekretoms aber auch des Transkriptoms signifikant unverändert bleibt. Dies lässt darauf schließen, dass die Fibroblasten ihre kanonische Funktion im Alter aufrechterhalten. Diese Arbeit hat einen Beitrag zum Verständnis der Mechanismen des Alterungsprozesses, der Hautalterung und der Rolle der Fibroblasten bei der stromalen und der systemischen Alterung geleistet.

4.4 Ausblick

Die Ergebnisse der vorliegenden Arbeit erlauben es Rückschlüsse auf die intra- und extrazellulären Veränderungen der Fibroblasten während des Alterns zu ziehen und geben einen Hinweis auf die Bedeutung der Fibroblasten für die Gewebemöostase und deren Beteiligung an der stromalen sowie systemischen Alterung. Obgleich ein *ex vivo* Alterungsmodell mit den Vorzügen der direkten Analyse *in situ* gealterter primärer Fibroblasten gewählt wurde, bedarf es zur Übertragung der erzielten Ergebnisse auf die *in vivo* Situation weiterführende Untersuchungen. Hierfür kommen, in Ergänzungen zum gewählten 2D-Zellkultursystem, 3D-Zellkultursysteme, beispielweise als Kokulturmodell mit Keratinozyten in Frage (Sun *et al.*, 2007). Ferner ließen sich die altersassoziierten Kandidatenproteine mithilfe der im GerontoSys-Konsortium gesammelten Gewebebiopsate, als auch in Tiermodellen validieren. Des Weiteren hat sich gezeigt, dass für viele der sezernierten Kandidatenproteine die extrazelluläre Funktion noch nicht beschrieben ist. Aus diesem Grund kommt der Aufklärung der unbekanntenen Wirkmechanismen der sezernierten Proteine eine bedeutende Rolle zu. Ziel ist es unter anderem, die Kandidatenproteine in die bereits beschriebenen Prozesse des sekretorischen Phänotyps, wie beispielweise seneszenzfördernd, tumorfördernd und immunmodulatorisch, mithilfe beispielweise von *knock down* Experimenten oder Überexpression der Kandidatengene, einzuordnen. Ein weiterer interessanter Aspekt betrifft die Charakterisierung der Proteine, die über nicht-klassische Sekretionswege sezerniert werden. Bisher sind etwa 20 Proteine experimentell bestätigt, die über nicht-klassische Wege sezerniert werden (Nickel und Seedorf, 2008). Im Rahmen dieser Arbeit wurden 336 Proteine vorhergesagt, die aufgrund des Fehlens einer Signalsequenz für die klassische Sekretion sehr wahrscheinlich über nicht-klassische Sekretionswege, wie z.B. Plasmamembrantransporter, intrazellulär gebildete Vesikel oder Membran-Flip-Flop (Nickel, 2003), sezerniert werden. Die Validierung dieser Proteine und auch die funktionelle Aufklärung der für den altersassoziierten sekretorischen Phänotyp erstmals identifizierten Proteine, werden zu einem besseren Verständnis der Rolle des Stromas im systemischen Alterungsprozess beitragen und dabei helfen ein molekulares Bild für diesen zu entwerfen.

5 Literaturverzeichnis

- Acosta JC, Banito A, Wuestefeld T, Georgilis A, Janich P, Morton JP, Athineos D, Kang TW, Lasitschka F, Andrulis M, Pascual G, Morris KJ, Khan S, Jin H, Dharmalingam G, Snijders AP, Carroll T, Capper D, Pritchard C, Inman GJ, Longerich T, Sansom OJ, Benitah SA, Zender L, Gil J (2013). A complex secretory program orchestrated by the inflammasome controls paracrine senescence. *Nature cell biology*. **15**, 978-990.
- Aebersold R, Mann M (2003). Mass spectrometry-based proteomics. *Nature*. **422**, 198-207.
- Alers S, Loffler AS, Wesselborg S, Stork B (2012). Role of AMPK-mTOR-Ulk1/2 in the regulation of autophagy: cross talk, shortcuts, and feedbacks. *Molecular and cellular biology*. **32**, 2-11.
- Amor-Gueret M (2006). Bloom syndrome, genomic instability and cancer: the SOS-like hypothesis. *Cancer letters*. **236**, 1-12.
- Anderson NG, Anderson NL (1996). Twenty years of two-dimensional electrophoresis: past, present and future. *Electrophoresis*. **17**, 443-453.
- Arike L, Valgepea K, Peil L, Nahku R, Adamberg K, Vilu R (2012). Comparison and applications of label-free absolute proteome quantification methods on *Escherichia coli*. *Journal of proteomics*. **75**, 5437-5448.
- Armanios M, Alder JK, Parry EM, Karim B, Strong MA, Greider CW (2009). Short telomeres are sufficient to cause the degenerative defects associated with aging. *American journal of human genetics*. **85**, 823-832.
- Baird DM, Britt-Compton B, Rowson J, Amso NN, Gregory L, Kipling D (2006). Telomere instability in the male germline. *Hum Mol Genet*. **15**, 45-51.
- Balch WE, Morimoto RI, Dillin A, Kelly JW (2008). Adapting proteostasis for disease intervention. *Science*. **319**, 916-919.
- Bantscheff M, Lemeer S, Savitski MM, Kuster B (2012). Quantitative mass spectrometry in proteomics: critical review update from 2007 to the present. *Analytical and bioanalytical chemistry*. **404**, 939-965.
- Bantscheff M, Schirle M, Sweetman G, Rick J, Kuster B (2007). Quantitative mass spectrometry in proteomics: a critical review. *Analytical and bioanalytical chemistry*. **389**, 1017-1031.
- Barrilleaux B, Phinney DG, Prockop DJ, O'Connor KC (2006). Review: *ex vivo* engineering of living tissues with adult stem cells. *Tissue engineering*. **12**, 3007-3019.

- Barsnes H, Eidhammer I, Martens L (2011). A global analysis of peptide fragmentation variability. *Proteomics*. **11**, 1181-1188.
- Barzilai N, Huffman DM, Muzumdar RH, Bartke A (2012). The critical role of metabolic pathways in aging. *Diabetes*. **61**, 1315-1322.
- Beck M, Schmidt A, Malmstroem J, Claassen M, Ori A, Szymborska A, Herzog F, Rinner O, Ellenberg J, Aebersold R (2011). The quantitative proteome of a human cell line. *Molecular systems biology*. **7**, 549.
- Beck S, Rakyant VK (2008). The methylome: approaches for global DNA methylation profiling. *Trends in genetics : TIG*. **24**, 231-237.
- Bendtsen JD, Jensen LJ, Blom N, Von Heijne G, Brunak S (2004). Feature-based prediction of non-classical and leaderless protein secretion. *Protein engineering, design & selection : PEDS*. **17**, 349-356.
- Bentov I, Reed MJ (2014). Anesthesia, microcirculation, and wound repair in aging. *Anesthesiology*. **120**, 760-772.
- Berger NA, Savvides P, Koroukian SM, Kahana EF, Deimling GT, Rose JH, Bowman KF, Miller RH (2006). Cancer in the elderly. *Transactions of the American Clinical and Climatological Association*. **117**, 147-155; discussion 155-146.
- Bernardes de Jesus B, Vera E, Schneeberger K, Tejera AM, Ayuso E, Bosch F, Blasco MA (2012). Telomerase gene therapy in adult and old mice delays aging and increases longevity without increasing cancer. *EMBO molecular medicine*. **4**, 691-704.
- Bhaumik D, Scott GK, Schokrpur S, Patil CK, Orjalo AV, Rodier F, Lithgow GJ, Campisi J (2009). MicroRNAs miR-146a/b negatively modulate the senescence-associated inflammatory mediators IL-6 and IL-8. *Aging*. **1**, 402-411.
- Bindea G, Galon J, Mlecnik B (2013). CluePedia Cytoscape plugin: pathway insights using integrated experimental and in silico data. *Bioinformatics*. **29**, 661-663.
- Bindea G, Mlecnik B, Hackl H, Charoentong P, Tosolini M, Kirilovsky A, Fridman WH, Pages F, Trajanoski Z, Galon J (2009). ClueGO: a Cytoscape plug-in to decipher functionally grouped gene ontology and pathway annotation networks. *Bioinformatics*. **25**, 1091-1093.
- Blackburn EH (2000). Telomere states and cell fates. *Nature*. **408**, 53-56.
- Blagosklonny MV (2008). Aging: ROS or TOR. *Cell cycle*. **7**, 3344-3354.
- Blasco MA (2007a). The epigenetic regulation of mammalian telomeres. *Nature reviews. Genetics*. **8**, 299-309.

- Blasco MA (2007b). Telomere length, stem cells and aging. *Nature chemical biology*. **3**, 640-649.
- Bleiholder C, Osburn S, Williams TD, Suhai S, Van Stipdonk M, Harrison AG, Paizs B (2008). Sequence-scrambling fragmentation pathways of protonated peptides. *Journal of the American Chemical Society*. **130**, 17774-17789.
- Boraldi F, Annovi G, Tiozzo R, Sommer P, Quaglino D (2010). Comparison of *ex vivo* and *in vitro* human fibroblast ageing models. *Mechanisms of ageing and development*. **131**, 625-635.
- Boraldi F, Bini L, Liberatori S, Armini A, Pallini V, Tiozzo R, Pasquali-Ronchetti I, Quaglino D (2003). Proteome analysis of dermal fibroblasts cultured *in vitro* from human healthy subjects of different ages. *Proteomics*. **3**, 917-929.
- Boukamp P (2005). Skin aging: a role for telomerase and telomere dynamics? *Current molecular medicine*. **5**, 171-177.
- Boulias K, Horvitz HR (2012). The *C. elegans* microRNA mir-71 acts in neurons to promote germline-mediated longevity through regulation of DAF-16/FOXO. *Cell metabolism*. **15**, 439-450.
- Bowen RL, Atwood CS (2004). Living and dying for sex. A theory of aging based on the modulation of cell cycle signaling by reproductive hormones. *Gerontology*. **50**, 265-290.
- Breecher MM, Dworken AM (1986). The Merck Manual. *Medical heritage*. **2**, 229-231.
- Brett D, Pospisil H, Valcarcel J, Reich J, Bork P (2002). Alternative splicing and genome complexity. *Nature genetics*. **30**, 29-30.
- Brohem CA, de Carvalho CM, Radoski CL, Santi FC, Baptista MC, Swinka BB, de AUC, de Araujo LR, Graf RM, Feferman IH, Lorencini M (2013). Comparison between fibroblasts and mesenchymal stem cells derived from dermal and adipose tissue. *International journal of cosmetic science*. **35**, 448-457.
- Bulteau AL, Moreau M, Nizard C, Friguet B (2007). Proteasome and photoaging: the effects of UV irradiation. *Annals of the New York Academy of Sciences*. **1100**, 280-290.
- Burtner CR, Kennedy BK (2010). Progeria syndromes and ageing: what is the connection? *Nature reviews. Molecular cell biology*. **11**, 567-578.
- Burton DG (2009). Cellular senescence, ageing and disease. *Age*. **31**, 1-9.

- Calabrese V, Cornelius C, Mancuso C, Lentile R, Stella AM, Butterfield DA (2010). Redox homeostasis and cellular stress response in aging and neurodegeneration. *Methods in molecular biology*. **610**, 285-308.
- Calderwood SK, Murshid A, Prince T (2009). The shock of aging: molecular chaperones and the heat shock response in longevity and aging--a mini-review. *Gerontology*. **55**, 550-558.
- Campbell KA, Minashima T, Zhang Y, Hadley S, Lee YJ, Giovinazzo J, Quirno M, Kirsch T (2013). Annexin A6 interacts with p65 and stimulates NF-kappaB activity and catabolic events in articular chondrocytes. *Arthritis and rheumatism*. **65**, 3120-3129.
- Campisi J, d'Adda di Fagagna F (2007). Cellular senescence: when bad things happen to good cells. *Nature reviews. Molecular cell biology*. **8**, 729-740.
- Catalgol B, Ziaja I, Breusing N, Jung T, Hohn A, Alpertunga B, Schroeder P, Chondrogianni N, Gonos ES, Petropoulos I, Friguet B, Klotz LO, Krutmann J, Grune T (2009). The proteasome is an integral part of solar ultraviolet a radiation-induced gene expression. *J Biol Chem*. **284**, 30076-30086.
- Catherman AD, Skinner OS, Kelleher NL (2014). Top Down proteomics: Facts and perspectives. *Biochemical and biophysical research communications*. **445**, 683-693.
- Celeste A, Fernandez-Capetillo O, Kruhlak MJ, Pilch DR, Staudt DW, Lee A, Bonner RF, Bonner WM, Nussenzweig A (2003). Histone H2AX phosphorylation is dispensable for the initial recognition of DNA breaks. *Nature cell biology*. **5**, 675-679.
- Cevenini E, Caruso C, Candore G, Capri M, Nuzzo D, Duro G, Rizzo C, Colonna-Romano G, Lio D, Di Carlo D, Palmas MG, Scurti M, Pini E, Franceschi C, Vasto S (2010). Age-related inflammation: the contribution of different organs, tissues and systems. How to face it for therapeutic approaches. *Current pharmaceutical design*. **16**, 609-618.
- Chelius D, Bondarenko PV (2002). Quantitative profiling of proteins in complex mixtures using liquid chromatography and mass spectrometry. *Journal of proteome research*. **1**, 317-323.
- Chen FG, Zhang WJ, Bi D, Liu W, Wei X, Chen FF, Zhu L, Cui L, Cao Y (2007). Clonal analysis of nestin(-) vimentin(+) multipotent fibroblasts isolated from human dermis. *J Cell Sci*. **120**, 2875-2883.
- Chu DH, Haake AR, Holbrook K, Loomis CA: The Structure and Development of Skin: Fitzpatrick's dermatology in general medicine, pp 58-88 (McGraw-Hill Professional, New York 2003)

- Chua YL, Ito Y, Pole JC, Newman S, Chin SF, Stein RC, Ellis IO, Caldas C, O'Hare MJ, Murrell A, Edwards PA (2009). The NRG1 gene is frequently silenced by methylation in breast cancers and is a strong candidate for the 8p tumour suppressor gene. *Oncogene*. **28**, 4041-4052.
- Collado M, Blasco MA, Serrano M (2007). Cellular senescence in cancer and aging. *Cell*. **130**, 223-233.
- Collado M, Gil J, Efeyan A, Guerra C, Schuhmacher AJ, Barradas M, Benguria A, Zaballos A, Flores JM, Barbacid M, Beach D, Serrano M (2005). Tumour biology: senescence in premalignant tumours. *Nature*. **436**, 642.
- Comi P, Chiamonte R, Maier JA (1995). Senescence-dependent regulation of type 1 plasminogen activator inhibitor in human vascular endothelial cells. *Experimental cell research*. **219**, 304-308.
- Conboy IM, Conboy MJ, Wagers AJ, Girma ER, Weissman IL, Rando TA (2005). Rejuvenation of aged progenitor cells by exposure to a young systemic environment. *Nature*. **433**, 760-764.
- Conboy IM, Rando TA (2012). Heterochronic parabiosis for the study of the effects of aging on stem cells and their niches. *Cell cycle*. **11**, 2260-2267.
- Cookson MR (2012). Aging--RNA in development and disease. *Wiley interdisciplinary reviews. RNA*. **3**, 133-143.
- Coppe JP, Desprez PY, Krtolica A, Campisi J (2010a). The senescence-associated secretory phenotype: the dark side of tumor suppression. *Annu Rev Pathol*. **5**, 99-118.
- Coppe JP, Patil CK, Rodier F, Krtolica A, Beausejour CM, Parrinello S, Hodgson JG, Chin K, Desprez PY, Campisi J (2010b). A human-like senescence-associated secretory phenotype is conserved in mouse cells dependent on physiological oxygen. *PloS one*. **5**, e9188.
- Coppe JP, Patil CK, Rodier F, Sun Y, Munoz DP, Goldstein J, Nelson PS, Desprez PY, Campisi J (2008). Senescence-associated secretory phenotypes reveal cell-nonautonomous functions of oncogenic RAS and the p53 tumor suppressor. *PLoS biology*. **6**, 2853-2868.
- Coppe JP, Rodier F, Patil CK, Freund A, Desprez PY, Campisi J (2011). Tumor suppressor and aging biomarker p16(INK4a) induces cellular senescence without the associated inflammatory secretory phenotype. *J Biol Chem*. **286**, 36396-36403.

- Courtay C, Oster T, Michelet F, Visvikis A, Diederich M, Wellman M, Siest G (1992). Gamma-glutamyltransferase: nucleotide sequence of the human pancreatic cDNA. Evidence for a ubiquitous gamma-glutamyltransferase polypeptide in human tissues. *Biochemical pharmacology*. **43**, 2527-2533.
- Cox B, Emili A (2006). Tissue subcellular fractionation and protein extraction for use in mass-spectrometry-based proteomics. *Nat Protoc*. **1**, 1872-1878.
- Cox J, Mann M (2011). Quantitative, high-resolution proteomics for data-driven systems biology. *Annual review of biochemistry*. **80**, 273-299.
- Cox TR, Erler JT (2011). Remodeling and homeostasis of the extracellular matrix: implications for fibrotic diseases and cancer. *Disease models & mechanisms*. **4**, 165-178.
- Craven NM, Watson RE, Jones CJ, Shuttleworth CA, Kielty CM, Griffiths CE (1997). Clinical features of photodamaged human skin are associated with a reduction in collagen VII. *Br J Dermatol*. **137**, 344-350.
- Crea F, Hurt EM, Mathews LA, Cabarcas SM, Sun L, Marquez VE, Danesi R, Farrar WL (2011). Pharmacologic disruption of Polycomb Repressive Complex 2 inhibits tumorigenicity and tumor progression in prostate cancer. *Molecular cancer*. **10**, 40.
- Cristofalo VJ, Allen RG, Pignolo RJ, Martin BG, Beck JC (1998). Relationship between donor age and the replicative lifespan of human cells in culture: a reevaluation. *Proceedings of the National Academy of Sciences of the United States of America*. **95**, 10614-10619.
- Cuervo AM, Bergamini E, Brunk UT, Droge W, Ffrench M, Terman A (2005). Autophagy and aging: the importance of maintaining "clean" cells. *Autophagy*. **1**, 131-140.
- d'Adda di Fagagna F, Reaper PM, Clay-Farrace L, Fiegler H, Carr P, Von Zglinicki T, Saretzki G, Carter NP, Jackson SP (2003). A DNA damage checkpoint response in telomere-initiated senescence. *Nature*. **426**, 194-198.
- De Cecco M, Criscione SW, Peckham EJ, Hillenmeyer S, Hamm EA, Manivannan J, Peterson AL, Kreiling JA, Neretti N, Sedivy JM (2013). Genomes of replicatively senescent cells undergo global epigenetic changes leading to gene silencing and activation of transposable elements. *Aging cell*. **12**, 247-256.
- de Magalhaes JP (2004). From cells to ageing: a review of models and mechanisms of cellular senescence and their impact on human ageing. *Experimental cell research*. **300**, 1-10.

- de Magalhaes JP, Curado J, Church GM (2009). Meta-analysis of age-related gene expression profiles identifies common signatures of aging. *Bioinformatics*. **25**, 875-881.
- Deeks SG (2011). HIV infection, inflammation, immunosenescence, and aging. *Annual review of medicine*. **62**, 141-155.
- Desiderio DM, Kai M (1983). Preparation of stable isotope-incorporated peptide internal standards for field desorption mass spectrometry quantification of peptides in biologic tissue. *Biomedical mass spectrometry*. **10**, 471-479.
- Didier ES, Sugimoto C, Bowers LC, Khan IA, Kuroda MJ (2012). Immune correlates of aging in outdoor-housed captive rhesus macaques (*Macaca mulatta*). *Immunity & ageing : I & A*. **9**, 25.
- Dimri GP, Lee X, Basile G, Acosta M, Scott G, Roskelley C, Medrano EE, Linskens M, Rubelj I, Pereira-Smith O *et al.* (1995). A biomarker that identifies senescent human cells in culture and in aging skin in vivo. *Proceedings of the National Academy of Sciences of the United States of America*. **92**, 9363-9367.
- Doles J, Storer M, Cozzuto L, Roma G, Keyes WM (2012). Age-associated inflammation inhibits epidermal stem cell function. *Genes & development*. **26**, 2144-2153.
- Edelberg JM, Ballard VL (2008). Stem cell review series: regulating highly potent stem cells in aging: environmental influences on plasticity. *Aging cell*. **7**, 599-604.
- Edgar D, Shabalina I, Camara Y, Wredenberg A, Calvaruso MA, Nijtmans L, Nedergaard J, Cannon B, Larsson NG, Trifunovic A (2009). Random point mutations with major effects on protein-coding genes are the driving force behind premature aging in mtDNA mutator mice. *Cell metabolism*. **10**, 131-138.
- Edhager AV, Stenbroen V, Nielsen NS, Bross P, Olsen RK, Gregersen N, Palmfeldt J (2014). Proteomic investigation of cultivated fibroblasts from patients with mitochondrial short-chain acyl-CoA dehydrogenase deficiency. *Molecular genetics and metabolism*. **111**, 360-368.
- Edman P, Begg G (1967). A protein sequenator. *European journal of biochemistry / FEBS*. **1**, 80-91.
- Edwards DR, Leco KJ, Beaudry PP, Atadja PW, Veillette C, Riabowol KT (1996). Differential effects of transforming growth factor-beta 1 on the expression of matrix metalloproteinases and tissue inhibitors of metalloproteinases in young and old human fibroblasts. *Experimental gerontology*. **31**, 207-223.

- Eichler MJ, Carlson MA (2006). Modeling dermal granulation tissue with the linear fibroblast-populated collagen matrix: a comparison with the round matrix model. *Journal of dermatological science*. **41**, 97-108.
- El-Domyati M, Attia S, Saleh F, Brown D, Birk DE, Gasparro F, Ahmad H, Uitto J (2002). Intrinsic aging vs. photoaging: a comparative histopathological, immunohistochemical, and ultrastructural study of skin. *Experimental dermatology*. **11**, 398-405.
- Ellis RJ, van der Vies SM (1991). Molecular chaperones. *Annual review of biochemistry*. **60**, 321-347.
- Elzi DJ, Song M, Hakala K, Weintraub ST, Shiio Y (2012). Wnt antagonist SFRP1 functions as a secreted mediator of senescence. *Molecular and cellular biology*. **32**, 4388-4399.
- Eng J, McCormack A, Yates J (1994) An approach to correlate tandem mass spectral data of peptides with amino acid sequences in a protein database. *J. Am. Soc. Mass Spectrom.* **5**, 976-989
- Escoffier C, de Rigal J, Rochefort A, Vasselet R, Leveque JL, Agache PG (1989). Age-related mechanical properties of human skin: an in vivo study. *J Invest Dermatol.* **93**, 353-357.
- Fenn JB, Mann M, Meng CK, Wong SF, Whitehouse CM (1989). Electrospray ionization for mass spectrometry of large biomolecules. *Science*. **246**, 64-71.
- Figuroa R, Lindenmaier H, Hergenhahn M, Nielsen KV, Boukamp P (2000). Telomere erosion varies during *in vitro* aging of normal human fibroblasts from young and adult donors. *Cancer research*. **60**, 2770-2774.
- Finley LW, Haigis MC (2009). The coordination of nuclear and mitochondrial communication during aging and calorie restriction. *Ageing research reviews*. **8**, 173-188.
- Fontana L, Partridge L, Longo VD (2010). Extending healthy life span--from yeast to humans. *Science*. **328**, 321-326.
- Freund A, Patil CK, Campisi J (2011). p38MAPK is a novel DNA damage response-independent regulator of the senescence-associated secretory phenotype. *The EMBO journal*. **30**, 1536-1548.
- Frey AB (2006). Myeloid suppressor cells regulate the adaptive immune response to cancer. *The Journal of clinical investigation*. **116**, 2587-2590.

- Fritsch: Dermatologie and Venerologie für das Studium. (Springer Medizin Verlag, Heidelberg 2009)
- Fukazawa A, Alonso C, Kurachi K, Gupta S, Lesser CF, McCormick BA, Reinecker HC (2008). GEF-H1 mediated control of NOD1 dependent NF-kappaB activation by Shigella effectors. *PLoS pathogens*. **4**, e1000228.
- Fumagalli M, Rossiello F, Clerici M, Barozzi S, Cittaro D, Kaplunov JM, Bucci G, Dobrev M, Matti V, Beausejour CM, Herbig U, Longhese MP, d'Adda di Fagagna F (2012). Telomeric DNA damage is irreparable and causes persistent DNA-damage-response activation. *Nature cell biology*. **14**, 355-365.
- Gale M, Jr., Blakely CM, Hopkins DA, Melville MW, Wambach M, Romano PR, Katze MG (1998). Regulation of interferon-induced protein kinase PKR: modulation of P58IPK inhibitory function by a novel protein, P52rIPK. *Molecular and cellular biology*. **18**, 859-871.
- Garinis GA, van der Horst GT, Vijg J, Hoeijmakers JH (2008). DNA damage and ageing: new-age ideas for an age-old problem. *Nature cell biology*. **10**, 1241-1247.
- Geiger T, Cox J, Ostasiewicz P, Wisniewski JR, Mann M (2010). Super-SILAC mix for quantitative proteomics of human tumor tissue. *Nature methods*. **7**, 383-385.
- Gerber SA, Rush J, Stemman O, Kirschner MW, Gygi SP (2003). Absolute quantification of proteins and phosphoproteins from cell lysates by tandem MS. *Proceedings of the National Academy of Sciences of the United States of America*. **100**, 6940-6945.
- Giacoaia EG, Miyake M, Lawton A, Goodison S, Rosser CJ (2014). PAI-1 Leads to G1-Phase Cell-Cycle Progression through Cyclin D3/cdk4/6 Upregulation. *Molecular cancer research: MCR*. **12**, 322-334.
- Giangreco A, Qin M, Pinter JE, Watt FM (2008). Epidermal stem cells are retained in vivo throughout skin aging. *Aging cell*. **7**, 250-259.
- Gilchrist BA (1989). Skin aging and photoaging: an overview. *Journal of the American Academy of Dermatology*. **21**, 610-613.
- Gilchrist BA, Krutmann J: Photoaging of skin, Gilchrist BA, Krutmann J (eds): Skin Aging, pp 33-44 (Springer, New York 2006)
- Gimble JM, Katz AJ, Bunnell BA (2007). Adipose-derived stem cells for regenerative medicine. *Circulation research*. **100**, 1249-1260.

- Goldstein S, Moerman EJ, Jones RA, Baxter RC (1991). Insulin-like growth factor binding protein 3 accumulates to high levels in culture medium of senescent and quiescent human fibroblasts. *Proceedings of the National Academy of Sciences of the United States of America*. **88**, 9680-9684.
- Gompertz, B. On the nature of the function expressive of the law of human mortality, and on a new mode of determining the value of life contingencies (1825). *Philosophical Transactions of the Royal Society of London* **115**, 513-585.
- Gosain A, DiPietro LA (2004). Aging and wound healing. *World journal of surgery*. **28**, 321-326.
- Graves PR, Haystead TA (2002). Molecular biologist's guide to proteomics. *Microbiology and molecular biology reviews : MMBR*. **66**, 39-63; table of contents.
- Greco M, Villani G, Mazzucchelli F, Bresolin N, Papa S, Attardi G (2003). Marked aging-related decline in efficiency of oxidative phosphorylation in human skin fibroblasts. *Faseb J*. **17**, 1706-1708.
- Green DR (1998). Apoptotic pathways: the roads to ruin. *Cell*. **94**, 695-698.
- Green DR, Galluzzi L, Kroemer G (2011). Mitochondria and the autophagy-inflammation-cell death axis in organismal aging. *Science*. **333**, 1109-1112.
- Gregg SQ, Gutierrez V, Robinson AR, Woodell T, Nakao A, Ross MA, Michalopoulos GK, Rigatti L, Rothermel CE, Kamileri I, Garinis GA, Stolz DB, Niedernhofer LJ (2012). A mouse model of accelerated liver aging caused by a defect in DNA repair. *Hepatology*. **55**, 609-621.
- Greider CW (1996). Telomere length regulation. *Annual review of biochemistry*. **65**, 337-365.
- Greider CW, Blackburn EH (1985). Identification of a specific telomere terminal transferase activity in Tetrahymena extracts. *Cell*. **43**, 405-413.
- Greussing R, Hackl M, Charoentong P, Pauck A, Monteforte R, Cavinato M, Hofer E, Scheideler M, Neuhaus M, Micutkova L, Mueck C, Trajanoski Z, Grillari J, Jansen-Durr P (2013). Identification of microRNA-mRNA functional interactions in UVB-induced senescence of human diploid fibroblasts. *BMC genomics*. **14**, 224.
- Grinnell F (1994). Fibroblasts, myofibroblasts, and wound contraction. *The Journal of cell biology*. **124**, 401-404.

- Grossmann J, Roschitzki B, Panse C, Fortes C, Barkow-Oesterreicher S, Rutishauser D, Schlapbach R (2010). Implementation and evaluation of relative and absolute quantification in shotgun proteomics with label-free methods. *Journal of proteomics*. **73**, 1740-1746.
- Gry M, Rimini R, Stromberg S, Asplund A, Ponten F, Uhlen M, Nilsson P (2009). Correlations between RNA and protein expression profiles in 23 human cell lines. *BMC genomics*. **10**, 365.
- Gunin AG, Kornilova NK, Petrov VV, Vasil'eva OV (2011). [Age-related changes in the number and proliferation of fibroblasts in the human skin]. *Advances in gerontology = Uspekhi gerontologii / Rossiiskaia akademiia nauk, Gerontologicheskoe obshchestvo*. **24**, 43-47.
- Gygi SP, Rist B, Gerber SA, Turecek F, Gelb MH, Aebersold R (1999). Quantitative analysis of complex protein mixtures using isotope-coded affinity tags. *Nature biotechnology*. **17**, 994-999.
- Hajnoczky G, Csordas G, Das S, Garcia-Perez C, Saotome M, Sinha Roy S, Yi M (2006). Mitochondrial calcium signalling and cell death: approaches for assessing the role of mitochondrial Ca²⁺ uptake in apoptosis. *Cell calcium*. **40**, 553-560.
- Hardy K, Mansfield L, Mackay A, Benvenuti S, Ismail S, Arora P, O'Hare MJ, Jat PS (2005). Transcriptional networks and cellular senescence in human mammary fibroblasts. *Molecular biology of the cell*. **16**, 943-953.
- Harley CB, Futcher AB, Greider CW (1990). Telomeres shorten during ageing of human fibroblasts. *Nature*. **345**, 458-460.
- Harley CB, Vaziri H, Counter CM, Allsopp RC (1992). The telomere hypothesis of cellular aging. *Experimental gerontology*. **27**, 375-382.
- Harman D (1972). The biologic clock: the mitochondria? *Journal of the American Geriatrics Society*. **20**, 145-147.
- Harries LW, Hernandez D, Henley W, Wood AR, Holly AC, Bradley-Smith RM, Yaghootkar H, Dutta A, Murray A, Frayling TM, Guralnik JM, Bandinelli S, Singleton A, Ferrucci L, Melzer D (2011). Human aging is characterized by focused changes in gene expression and deregulation of alternative splicing. *Aging cell*. **10**, 868-878.
- Harrison AG (2009a). Cyclization of peptide b9 ions. *Journal of the American Society for Mass Spectrometry*. **20**, 2248-2253.

- Harrison AG (2009b). TO b OR NOT TO b: THE ONGOING SAGA OF PEPTIDE b IONS. *Mass spectrometry reviews*. **28**, 640-654.
- Harrison AG, Young AB, Bleiholder C, Suhai S, Paizs B (2006). Scrambling of sequence information in collision-induced dissociation of peptides. *Journal of the American Chemical Society*. **128**, 10364-10365.
- Hayflick L (1980). Recent advances in the cell biology of aging. *Mechanisms of ageing and development*. **14**, 59-79.
- Hayflick L, Moorhead PS (1961). The serial cultivation of human diploid cell strains. *Experimental cell research*. **25**, 585-621.
- Herbig U, Ferreira M, Condel L, Carey D, Sedivy JM (2006). Cellular senescence in aging primates. *Science*. **311**, 1257.
- Herbig U, Jobling WA, Chen BP, Chen DJ, Sedivy JM (2004). Telomere shortening triggers senescence of human cells through a pathway involving ATM, p53, and p21(CIP1), but not p16(INK4a). *Molecular cell*. **14**, 501-513.
- Hill R, Song Y, Cardiff RD, Van Dyke T (2005). Selective evolution of stromal mesenchyme with p53 loss in response to epithelial tumorigenesis. *Cell*. **123**, 1001-1011.
- Hiona A, Sanz A, Kujoth GC, Pamplona R, Seo AY, Hofer T, Someya S, Miyakawa T, Nakayama C, Samhan-Arias AK, Servais S, Barger JL, Portero-Otin M, Tanokura M, Prolla TA, Leeuwenburgh C (2010). Mitochondrial DNA mutations induce mitochondrial dysfunction, apoptosis and sarcopenia in skeletal muscle of mitochondrial DNA mutator mice. *PloS one*. **5**, e11468.
- Hirohata S, Wang LW, Miyagi M, Yan L, Seldin MF, Keene DR, Crabb JW, Apte SS (2002). Punctin, a novel ADAMTS-like molecule, ADAMTSL-1, in extracellular matrix. *J Biol Chem*. **277**, 12182-12189.
- Hoare M, Narita M (2013). Transmitting senescence to the cell neighbourhood. *Nature cell biology*. **15**, 887-889.
- Hoeijmakers JH (2009). DNA damage, aging, and cancer. *The New England journal of medicine*. **361**, 1475-1485.
- Horvath S (2013). DNA methylation age of human tissues and cell types. *Genome biology*. **14**, R115.
- Houtkooper RH, Williams RW, Auwerx J (2010). Metabolic networks of longevity. *Cell*. **142**, 9-14.

- Hughes KA, Reynolds RM (2005). Evolutionary and mechanistic theories of aging. *Annual review of entomology*. **50**, 421-445.
- Hwang ES, Yoon G, Kang HT (2009). A comparative analysis of the cell biology of senescence and aging. *Cell Mol Life Sci*. **66**, 2503-2524.
- Irwin CR, Picardo M, Ellis I, Sloan P, Grey A, McGurk M, Schor SL (1994). Inter- and intra-site heterogeneity in the expression of fetal-like phenotypic characteristics by gingival fibroblasts: potential significance for wound healing. *J Cell Sci*. **107 (Pt 5)**, 1333-1346.
- Ishihama Y, Oda Y, Tabata T, Sato T, Nagasu T, Rappsilber J, Mann M (2005). Exponentially modified protein abundance index (emPAI) for estimation of absolute protein amount in proteomics by the number of sequenced peptides per protein. *Molecular & cellular proteomics : MCP*. **4**, 1265-1272.
- Jacobs KB, Yeager M, Zhou W, Wacholder S, Wang Z, Rodriguez-Santiago B, Hutchinson A, Deng X, Liu C, Horner MJ, Cullen M, Epstein CG, Burdett L, Dean MC, Chatterjee N, Sampson J, Chung CC, Kovaks J, Gapstur SM, Stevens VL, Teras LT, Gaudet MM, Albanes D, Weinstein SJ, Virtamo J, Taylor PR, Freedman ND, Abnet CC, Goldstein AM, Hu N, Yu K, Yuan JM, Liao L, Ding T, Qiao YL, Gao YT, Koh WP, Xiang YB, Tang ZZ, Fan JH, Aldrich MC, Amos C, Blot WJ, Bock CH, Gillanders EM, Harris CC, Haiman CA, Henderson BE, Kolonel LN, Le Marchand L, McNeill LH, Rybicki BA, Schwartz AG, Signorello LB, Spitz MR, Wiencke JK, Wrensch M, Wu X, Zanetti KA, Ziegler RG, Figueroa JD, Garcia-Closas M, Malats N, Marenne G, Prokunina-Olsson L, Baris D, Schwenn M, Johnson A, Landi MT, Goldin L, Consonni D, Bertazzi PA, Rotunno M, Rajaraman P, Andersson U, Beane Freeman LE, Berg CD, Buring JE, Butler MA, Carreon T, Feychting M, Ahlbom A, Gaziano JM, Giles GG, Hallmans G, Hankinson SE, Hartge P, Henriksson R, Inskip PD, Johansen C, Landgren A, McKean-Cowdin R, Michaud DS, Melin BS, Peters U, Ruder AM, Sesso HD, Severi G, Shu XO, Visvanathan K, White E, Wolk A, Zeleniuch-Jacquotte A, Zheng W, Silverman DT, Kogevinas M, Gonzalez JR, Villa O, Li D, Duell EJ, Risch HA, Olson SH, Kooperberg C, Wolpin BM, Jiao L, Hassan M, Wheeler W, Arslan AA, Bueno-de-Mesquita HB, Fuchs CS, Gallinger S, Gross MD, Holly EA, Klein AP, LaCroix A, Mandelson MT, Petersen G, Boutron-Ruault MC, Bracci PM, Canzian F, Chang K, Cotterchio M, Giovannucci EL, Goggins M, Hoffman Bolton JA, Jenab M, Khaw KT, Krogh V, Kurtz RC, McWilliams RR,

- Mendelsohn JB, Rabe KG, Riboli E, Tjonneland A, Tobias GS, Trichopoulos D, Elena JW, Yu H, Amundadottir L, Stolzenberg-Solomon RZ, Kraft P, Schumacher F, Stram D, Savage SA, Mirabello L, Andrulis IL, Wunder JS, Patino Garcia A, Sierrasesumaga L, Barkauskas DA, Gorlick RG, Purdue M, Chow WH, Moore LE, Schwartz KL, Davis FG, Hsing AW, Berndt SI, Black A, Wentzensen N, Brinton LA, Lissowska J, Peplonska B, McGlynn KA, Cook MB, Graubard BI, Kratz CP, Greene MH, Erickson RL, Hunter DJ, Thomas G, Hoover RN, Real FX, Fraumeni JF, Jr., Caporaso NE, Tucker M, Rothman N, Perez-Jurado LA, Chanock SJ (2012). Detectable clonal mosaicism and its relationship to aging and cancer. *Nature genetics*. **44**, 651-658.
- Jaskelioff M, Muller FL, Paik JH, Thomas E, Jiang S, Adams AC, Sahin E, Kost-Alimova M, Protopopov A, Cadinanos J, Horner JW, Maratos-Flier E, Depinho RA (2011). Telomerase reactivation reverses tissue degeneration in aged telomerase-deficient mice. *Nature*. **469**, 102-106.
- Jayanthi P, Joshua E, Ranganathan K (2010). Ageing and its implications. *Journal of oral and maxillofacial pathology : JOMFP*. **14**, 48-51.
- Jia C, Qi W, He Z (2007). Cyclization reaction of peptide fragment ions during multistage collisionally activated decomposition: an inducement to lose internal amino-acid residues. *Journal of the American Society for Mass Spectrometry*. **18**, 663-678.
- Johnson SC, Rabinovitch PS, Kaeberlein M (2013). mTOR is a key modulator of ageing and age-related disease. *Nature*. **493**, 338-345.
- Jung EG: Dermatologie 4 ed. (Hippokrates Verlag, Stuttgart 1998)
- Jung KY, Dean D, Jiang J, Gaylor S, Griffith WH, Burghardt RC, Parrish AR (2004). Loss of N-cadherin and alpha-catenin in the proximal tubules of aging male Fischer 344 rats. *Mechanisms of ageing and development*. **125**, 445-453.
- Jungblut PR, Zimny-Arndt U, Zeindl-Eberhart E, Stulik J, Koupilova K, Pleissner KP, Otto A, Muller EC, Sokolowska-Kohler W, Grabher G, Stoffler G (1999). Proteomics in human disease: cancer, heart and infectious diseases. *Electrophoresis*. **20**, 2100-2110.
- Kadoya K, Sasaki T, Kostka G, Timpl R, Matsuzaki K, Kumagai N, Sakai LY, Nishiyama T, Amano S (2005). Fibulin-5 deposition in human skin: decrease with ageing and ultraviolet B exposure and increase in solar elastosis. *Br J Dermatol*. **153**, 607-612.

- Kalfalah F, Sobek S, Bornholz B, Gotz-Rosch C, Tigges J, Fritsche E, Krutmann J, Kohrer K, Deenen R, Ohse S, Boerries M, Busch H, Boege F (2014). Inadequate mito-biogenesis in primary dermal fibroblasts from old humans is associated with impairment of PGC1A-independent stimulation. *Experimental gerontology*. **56**, 59-68.
- Kalfalah FM, Mielke C, Christensen MO, Baechler S, Marko D, Boege F (2011). Genotoxicity of dietary, environmental and therapeutic topoisomerase II poisons is uniformly correlated to prolongation of enzyme DNA residence. *Molecular nutrition & food research*. **55 Suppl 1**, S127-142.
- Kamburov A, Wierling C, Lehrach H, Herwig R (2009). ConsensusPathDB--a database for integrating human functional interaction networks. *Nucleic acids research*. **37**, D623-628.
- Karas M, Hillenkamp F (1988). Laser desorption ionization of proteins with molecular masses exceeding 10,000 daltons. *Analytical chemistry*. **60**, 2299-2301.
- Karve TM, Cheema AK (2011). Small changes huge impact: the role of protein posttranslational modifications in cellular homeostasis and disease. *Journal of amino acids*. **2011**, 207691.
- Kendall AC, Nicolaou A (2013). Bioactive lipid mediators in skin inflammation and immunity. *Progress in lipid research*. **52**, 141-164.
- Keshamouni VG, Michailidis G, Grasso CS, Anthwal S, Strahler JR, Walker A, Arenberg DA, Reddy RC, Akulapalli S, Thannickal VJ, Standiford TJ, Andrews PC, Omenn GS (2006). Differential protein expression profiling by iTRAQ-2DLC-MS/MS of lung cancer cells undergoing epithelial-mesenchymal transition reveals a migratory/invasive phenotype. *Journal of proteome research*. **5**, 1143-1154.
- Kim YM, Byun HO, Jee BA, Cho H, Seo YH, Kim YS, Park MH, Chung HY, Woo HG, Yoon G (2013). Implications of time-series gene expression profiles of replicative senescence. *Aging cell*. **12**, 622-634.
- Klose J, Kobalz U (1995). Two-dimensional electrophoresis of proteins: an updated protocol and implications for a functional analysis of the genome. *Electrophoresis*. **16**, 1034-1059.
- Koch CM, Suschek CV, Lin Q, Bork S, Goergens M, Jousen S, Pallua N, Ho AD, Zenke M, Wagner W (2011). Specific age-associated DNA methylation changes in human dermal fibroblasts. *PloS one*. **6**, e16679.

- Koga H, Kaushik S, Cuervo AM (2011). Protein homeostasis and aging: The importance of exquisite quality control. *Ageing research reviews*. **10**, 205-215.
- Konermann L, Pan J, Liu YH (2011). Hydrogen exchange mass spectrometry for studying protein structure and dynamics. *Chemical Society reviews*. **40**, 1224-1234.
- Koziel R, Greussing R, Maier AB, Declercq L, Jansen-Durr P (2011). Functional interplay between mitochondrial and proteasome activity in skin aging. *J Invest Dermatol*. **131**, 594-603.
- Kreiling JA, Tamamori-Adachi M, Sexton AN, Jeyapalan JC, Munoz-Najar U, Peterson AL, Manivannan J, Rogers ES, Pchelintsev NA, Adams PD, Sedivy JM (2011). Age-associated increase in heterochromatic marks in murine and primate tissues. *Aging cell*. **10**, 292-304.
- Krtolica A, Parrinello S, Lockett S, Desprez PY, Campisi J (2001). Senescent fibroblasts promote epithelial cell growth and tumorigenesis: a link between cancer and aging. *Proceedings of the National Academy of Sciences of the United States of America*. **98**, 12072-12077.
- Kruegel U, Robison B, Dange T, Kahlert G, Delaney JR, Kotireddy S, Tsuchiya M, Tsuchiyama S, Murakami CJ, Schleit J, Sutphin G, Carr D, Tar K, Dittmar G, Kaeberlein M, Kennedy BK, Schmidt M (2011). Elevated proteasome capacity extends replicative lifespan in *Saccharomyces cerevisiae*. *PLoS genetics*. **7**, e1002253.
- Krunic D, Moshir S, Greulich-Bode KM, Figueroa R, Cerezo A, Stammer H, Stark HJ, Gray SG, Nielsen KV, Hartschuh W, Boukamp P (2009). Tissue context-activated telomerase in human epidermis correlates with little age-dependent telomere loss. *Biochimica et biophysica acta*. **1792**, 297-308.
- Krutmann J (2003). [Premature skin aging by ultraviolet radiation and other environmental hazards. The molecular basis]. *Der Hautarzt; Zeitschrift für Dermatologie, Venerologie, und verwandte Gebiete*. **54**, 809-817.
- Krutmann J, Diepgen TL, Billmann-Krutmann C. Hautalterung: Grundlagen - Prävention - Therapie. Springer Berlin Heidelberg, 2008
- Kuilman T, Michaloglou C, Mooi WJ, Peeper DS (2010). The essence of senescence. *Genes & development*. **24**, 2463-2479.
- Kuilman T, Michaloglou C, Vredeveld LC, Douma S, van Doorn R, Desmet CJ, Aarden LA, Mooi WJ, Peeper DS (2008). Oncogene-induced senescence relayed by an interleukin-dependent inflammatory network. *Cell*. **133**, 1019-1031.

- Kuilman T, Peeper DS (2009). Senescence-messaging secretome: SMS-ing cellular stress. *Nature reviews. Cancer.* **9**, 81-94.
- Laberge RM, Zhou L, Sarantos MR, Rodier F, Freund A, de Keizer PL, Liu S, Demaria M, Cong YS, Kapahi P, Desprez PY, Hughes RE, Campisi J (2012). Glucocorticoids suppress selected components of the senescence-associated secretory phenotype. *Aging cell.* **11**, 569-578.
- Lai MC, Chang WC, Shieh SY, Tarn WY (2010). DDX3 regulates cell growth through translational control of cyclin E1. *Molecular and cellular biology.* **30**, 5444-5453.
- Laroya G, Cuesta R, Brewer G, Schneider RJ (1999). Control of mRNA decay by heat shock-ubiquitin-proteasome pathway. *Science.* **284**, 499-502.
- Lau KW, Hart SR, Lynch JA, Wong SCC, Hubbard SJ, Gaskell SJ (2009). Observations on the detection of b- and y-type ions in the collisionally activated decomposition spectra of protonated peptides. *Rapid Commun Mass Sp.* **23**, 1508-1514.
- Lautenschlaeger J, Prell T, Grosskreutz J (2012). Endoplasmic reticulum stress and the ER mitochondrial calcium cycle in amyotrophic lateral sclerosis. *Amyotrophic lateral sclerosis : official publication of the World Federation of Neurology Research Group on Motor Neuron Diseases.* **13**, 166-177.
- Lavasani M, Robinson AR, Lu A, Song M, Feduska JM, Ahani B, Tilstra JS, Feldman CH, Robbins PD, Niedernhofer LJ, Huard J (2012). Muscle-derived stem/progenitor cell dysfunction limits healthspan and lifespan in a murine progeria model. *Nature communications.* **3**, 608.
- Lee BH, Lee MJ, Park S, Oh DC, Elsasser S, Chen PC, Gartner C, Dimova N, Hanna J, Gygi SP, Wilson SM, King RW, Finley D (2010). Enhancement of proteasome activity by a small-molecule inhibitor of USP14. *Nature.* **467**, 179-184.
- Lee HC, Yin PH, Chi CW, Wei YH (2002). Increase in mitochondrial mass in human fibroblasts under oxidative stress and during replicative cell senescence. *Journal of biomedical science.* **9**, 517-526.
- Lee KW, Ma L, Yan X, Liu B, Zhang XK, Cohen P (2005). Rapid apoptosis induction by IGFBP-3 involves an insulin-like growth factor-independent nucleomitochondrial translocation of RXRalpha/Nur77. *J Biol Chem.* **280**, 16942-16948.
- Lehmann BD, Paine MS, Brooks AM, McCubrey JA, Renegar RH, Wang R, Terrian DM (2008). Senescence-associated exosome release from human prostate cancer cells. *Cancer research.* **68**, 7864-7871.

- Lener T, Moll PR, Rinnerthaler M, Bauer J, Aberger F, Richter K (2006). Expression profiling of aging in the human skin. *Experimental gerontology*. **41**, 387-397.
- Lewis M (2003). PRELP, collagen, and a theory of Hutchinson-Gilford progeria. *Ageing research reviews*. **2**, 95-105.
- Leyvraz C, Charles RP, Rubera I, Guitard M, Rotman S, Breiden B, Sandhoff K, Hummler E (2005). The epidermal barrier function is dependent on the serine protease CAP1/Prss8. *The Journal of cell biology*. **170**, 487-496.
- Li L, Monckton EA, Godbout R (2008). A role for DEAD box 1 at DNA double-strand breaks. *Molecular and cellular biology*. **28**, 6413-6425.
- Link AJ, LaBaer J (2011). Trichloroacetic acid (TCA) precipitation of proteins. *Cold Spring Harbor protocols*. **2011**, 993-994.
- Liu N, Landreh M, Cao K, Abe M, Hendriks GJ, Kennerdell JR, Zhu Y, Wang LS, Bonini NM (2012). The microRNA miR-34 modulates ageing and neurodegeneration in *Drosophila*. *Nature*. **482**, 519-523.
- Lobrich M, Shibata A, Beucher A, Fisher A, Ensminger M, Goodarzi AA, Barton O, Jeggo PA (2010). gammaH2AX foci analysis for monitoring DNA double-strand break repair: strengths, limitations and optimization. *Cell cycle*. **9**, 662-669.
- Lopez-Otin C, Blasco MA, Partridge L, Serrano M, Kroemer G (2013). The hallmarks of aging. *Cell*. **153**, 1194-1217.
- Lottspeich F, In Lottspeich, F. und Zorbas, H. (Hrsg.) Bioanalytik. Spektrum Akademischer Verlag, Heidelberg, 2006.
- Lottspeich F (2009). Introduction to proteomics. *Methods in molecular biology*. **564**, 3-10.
- Lu P, Vogel C, Wang R, Yao X, Marcotte EM (2007). Absolute protein expression profiling estimates the relative contributions of transcriptional and translational regulation. *Nature biotechnology*. **25**, 117-124.
- Luders J, Demand J, Hohfeld J (2000). The ubiquitin-related BAG-1 provides a link between the molecular chaperones Hsc70/Hsp70 and the proteasome. *J Biol Chem*. **275**, 4613-4617.
- Luo M (2012). Current chemical biology approaches to interrogate protein methyltransferases. *ACS chemical biology*. **7**, 443-463.
- MacBeath G, Schreiber SL (2000). Printing proteins as microarrays for high-throughput function determination. *Science*. **289**, 1760-1763.

- Maegawa S, Hinkal G, Kim HS, Shen L, Zhang L, Zhang J, Zhang N, Liang S, Donehower LA, Issa JP (2010). Widespread and tissue specific age-related DNA methylation changes in mice. *Genome research*. **20**, 332-340.
- Maier AB, le Cessie S, de Koning-Treurniet C, Blom J, Westendorp RG, van Heemst D (2007). Persistence of high-replicative capacity in cultured fibroblasts from nonagenarians. *Aging cell*. **6**, 27-33.
- Makarov A (2000). Electrostatic axially harmonic orbital trapping: a high-performance technique of mass analysis. *Analytical chemistry*. **72**, 1156-1162.
- Makarov A, Denisov E, Lange O, Horning S (2006). Dynamic range of mass accuracy in LTQ Orbitrap hybrid mass spectrometer. *Journal of the American Society for Mass Spectrometry*. **17**, 977-982.
- Makrantonaki E, Brink TC, Zampeli V, Elewa RM, Mlody B, Hossini AM, Hermes B, Krause U, Knolle J, Abdallah M, Adjaye J, Zouboulis CC (2012). Identification of biomarkers of human skin ageing in both genders. Wnt signalling - a label of skin ageing? *PloS one*. **7**, e50393.
- Makrantonaki E, Schonknecht P, Hossini AM, Kaiser E, Katsouli MM, Adjaye J, Schroder J, Zouboulis CC (2010). Skin and brain age together: The role of hormones in the ageing process. *Experimental gerontology*. **45**, 801-813.
- Mancini M, Saintigny G, Mahe C, Annicchiarico-Petruzzelli M, Melino G, Candi E (2012). MicroRNA-152 and -181a participate in human dermal fibroblasts senescence acting on cell adhesion and remodeling of the extra-cellular matrix. *Aging*. **4**, 843-853.
- Mandavilli BS, Santos JH, Van Houten B (2002). Mitochondrial DNA repair and aging. *Mutation research*. **509**, 127-151.
- Mann M, Hojrup P, Roepstorff P (1993). Use of mass spectrometric molecular weight information to identify proteins in sequence databases. *Biological mass spectrometry*. **22**, 338-345.
- Mann M, Kelleher NL (2008). Precision proteomics: the case for high resolution and high mass accuracy. *Proceedings of the National Academy of Sciences of the United States of America*. **105**, 18132-18138.
- Marcotte R, Lacelle C, Wang E (2004). Senescent fibroblasts resist apoptosis by downregulating caspase-3. *Mechanisms of ageing and development*. **125**, 777-783.
- Marcus K, Joppich C, May C, Pfeiffer K, Sitek B, Meyer H, Stuehler K (2009). High-resolution 2DE. *Methods in molecular biology*. **519**, 221-240.

- Martens JW, Sieuwerts AM, Bolt-deVries J, Bosma PT, Swiggers SJ, Klijn JG, Foekens JA (2003). Aging of stromal-derived human breast fibroblasts might contribute to breast cancer progression. *Thrombosis and haemostasis*. **89**, 393-404.
- Martens UM, Chavez EA, Poon SS, Schmoor C, Lansdorp PM (2000). Accumulation of short telomeres in human fibroblasts prior to replicative senescence. *Experimental cell research*. **256**, 291-299.
- Martinez P, Blasco MA (2010). Role of shelterin in cancer and aging. *Aging cell*. **9**, 653-666.
- Mathivanan S, Fahner CJ, Reid GE, Simpson RJ (2012). ExoCarta 2012: database of exosomal proteins, RNA and lipids. *Nucleic acids research*. **40**, D1241-1244.
- Matthews L, Gopinath G, Gillespie M, Caudy M, Croft D, de Bono B, Garapati P, Hemish J, Hermjakob H, Jassal B, Kanapin A, Lewis S, Mahajan S, May B, Schmidt E, Vastrik I, Wu G, Birney E, Stein L, D'Eustachio P (2009). Reactome knowledgebase of human biological pathways and processes. *Nucleic acids research*. **37**, D619-622.
- Mattison JA, Roth GS, Beasley TM, Tilmont EM, Handy AM, Herbert RL, Longo DL, Allison DB, Young JE, Bryant M, Barnard D, Ward WF, Qi W, Ingram DK, de Cabo R (2012). Impact of caloric restriction on health and survival in rhesus monkeys from the NIA study. *Nature*. **489**, 318-321.
- McGrath JA, Eady RAJ, Pope FM. (2004). "Anatomy and Organization of Human Skin". In Burns T, Breathnach S, Cox N, Griffiths C. Rook's Textbook of Dermatology (7th ed.). Blackwell Publishing. p. 4190.
- Michalski A, Damoc E, Lange O, Denisov E, Nolting D, Muller M, Viner R, Schwartz J, Remes P, Belford M, Dunyach JJ, Cox J, Horning S, Mann M, Makarov A (2012). Ultra high resolution linear ion trap Orbitrap mass spectrometer (Orbitrap Elite) facilitates top down LC MS/MS and versatile peptide fragmentation modes. *Molecular & cellular proteomics : MCP*. **11**, O111 013698.
- Micutkova L, Diener T, Li C, Rogowska-Wrzesinska A, Mueck C, Huetter E, Weinberger B, Grubeck-Loebenstein B, Roepstorff P, Zeng R, Jansen-Duerr P (2011). Insulin-like growth factor binding protein-6 delays replicative senescence of human fibroblasts. *Mechanisms of ageing and development*. **132**, 468-479.
- Midgley AC, Bowen T, Phillips AO, Steadman R (2014). MicroRNA-7 inhibition rescues age-associated loss of epidermal growth factor receptor and hyaluronan-dependent differentiation in fibroblasts. *Aging cell*. **13**, 235-244.

- Midwood KS, Valenick LV, Hsia HC, Schwarzbauer JE (2004a). Coregulation of fibronectin signaling and matrix contraction by tenascin-C and syndecan-4. *Molecular biology of the cell*. **15**, 5670-5677.
- Midwood KS, Williams LV, Schwarzbauer JE (2004b). Tissue repair and the dynamics of the extracellular matrix. *The international journal of biochemistry & cell biology*. **36**, 1031-1037.
- Milosevic J, Bulau P, Mortz E, Eickelberg O (2009). Subcellular fractionation of TGF-beta1-stimulated lung epithelial cells: a novel proteomic approach for identifying signaling intermediates. *Proteomics*. **9**, 1230-1240.
- Min JN, Whaley RA, Sharpless NE, Lockyer P, Portbury AL, Patterson C (2008). CHIP deficiency decreases longevity, with accelerated aging phenotypes accompanied by altered protein quality control. *Molecular and cellular biology*. **28**, 4018-4025.
- Minden JS, Dowd SR, Meyer HE, Stuhler K (2009). Difference gel electrophoresis. *Electrophoresis*. **30 Suppl 1**, S156-161.
- Mirastschijski U, Haaksma CJ, Tomasek JJ, Agren MS (2004). Matrix metalloproteinase inhibitor GM 6001 attenuates keratinocyte migration, contraction and myofibroblast formation in skin wounds. *Experimental cell research*. **299**, 465-475.
- Mondello C, Petropoulou C, Monti D, Gonos ES, Franceschi C, Nuzzo F (1999). Telomere length in fibroblasts and blood cells from healthy centenarians. *Experimental cell research*. **248**, 234-242.
- Moriyama K, Yahara I (2002). Human CAP1 is a key factor in the recycling of cofilin and actin for rapid actin turnover. *J Cell Sci*. **115**, 1591-1601.
- Moskalev AA, Shaposhnikov MV, Plyusnina EN, Zhavoronkov A, Budovsky A, Yanai H, Fraifeld VE (2013). The role of DNA damage and repair in aging through the prism of Koch-like criteria. *Ageing research reviews*. **12**, 661-684.
- Mu XC, Higgins PJ (1995). Differential growth state-dependent regulation of plasminogen activator inhibitor type-1 expression in senescent IMR-90 human diploid fibroblasts. *Journal of cellular physiology*. **165**, 647-657.
- Mullberg J, Althoff K, Jostock T, Rose-John S (2000). The importance of shedding of membrane proteins for cytokine biology. *European cytokine network*. **11**, 27-38.
- Murphy G, Stanton H, Cowell S, Butler G, Knauper V, Atkinson S, Gavrilovic J (1999). Mechanisms for pro matrix metalloproteinase activation. *APMIS : acta pathologica, microbiologica, et immunologica Scandinavica*. **107**, 38-44.

- Nagaraj N, Kulak NA, Cox J, Neuhauser N, Mayr K, Hoerning O, Vorm O, Mann M (2012). System-wide perturbation analysis with nearly complete coverage of the yeast proteome by single-shot ultra HPLC runs on a bench top Orbitrap. *Molecular & cellular proteomics : MCP*. **11**, M111 013722.
- Narita M, Nunez S, Heard E, Lin AW, Hearn SA, Spector DL, Hannon GJ, Lowe SW (2003). Rb-mediated heterochromatin formation and silencing of E2F target genes during cellular senescence. *Cell*. **113**, 703-716.
- Naylor EC, Watson RE, Sherratt MJ (2011). Molecular aspects of skin ageing. *Maturitas*. **69**, 249-256.
- Neilson KA, Ali NA, Muralidharan S, Mirzaei M, Mariani M, Assadourian G, Lee A, van Sluyter SC, Haynes PA (2011). Less label, more free: approaches in label-free quantitative mass spectrometry. *Proteomics*. **11**, 535-553.
- Nemoto E, Kunii R, Tada H, Tsubahara T, Ishihata H, Shimauchi H (2004). Expression of CD73/ecto-5'-nucleotidase on human gingival fibroblasts and contribution to the inhibition of interleukin-1alpha-induced granulocyte-macrophage colony stimulating factor production. *Journal of periodontal research*. **39**, 10-19.
- Nesterenko MV, Tilley M, Upton SJ (1994). A simple modification of Blum's silver stain method allows for 30 minute detection of proteins in polyacrylamide gels. *Journal of biochemical and biophysical methods*. **28**, 239-242.
- Nguyen A, Chang AC, Reddel RR (2009). Stanniocalcin-1 acts in a negative feedback loop in the prosurvival ERK1/2 signaling pathway during oxidative stress. *Oncogene*. **28**, 1982-1992.
- Nguyen LH, Erzberger JP, Root J, Wilson DM, 3rd (2000). The human homolog of Escherichia coli Orn degrades small single-stranded RNA and DNA oligomers. *J Biol Chem*. **275**, 25900-25906.
- Nickel W (2003). The mystery of nonclassical protein secretion. A current view on cargo proteins and potential export routes. *European journal of biochemistry / FEBS*. **270**, 2109-2119.
- Nickel W, Seedorf M (2008). Unconventional mechanisms of protein transport to the cell surface of eukaryotic cells. *Annual review of cell and developmental biology*. **24**, 287-308.

- Nishio K, Inoue A (2005). Senescence-associated alterations of cytoskeleton: extraordinary production of vimentin that anchors cytoplasmic p53 in senescent human fibroblasts. *Histochemistry and cell biology*. **123**, 263-273.
- Nowicki TS, Zhao H, Darzynkiewicz Z, Moscatello A, Shin E, Schantz S, Tiwari RK, Geliebter J (2011). Downregulation of uPAR inhibits migration, invasion, proliferation, FAK/PI3K/Akt signaling and induces senescence in papillary thyroid carcinoma cells. *Cell cycle*. **10**, 100-107.
- Old WM, Meyer-Arendt K, Aveline-Wolf L, Pierce KG, Mendoza A, Sevinsky JR, Resing KA, Ahn NG (2005). Comparison of label-free methods for quantifying human proteins by shotgun proteomics. *Molecular & cellular proteomics : MCP*. **4**, 1487-1502.
- O'Farrell PH (1975). High resolution two-dimensional electrophoresis of proteins. *J Biol Chem*. **250**, 4007-4021.
- Olovnikov AM (1996). Telomeres, telomerase, and aging: origin of the theory. *Experimental gerontology*. **31**, 443-448.
- Olsen JV, Schwartz JC, Griep-Raming J, Nielsen ML, Damoc E, Denisov E, Lange O, Remes P, Taylor D, Splendore M, Wouters ER, Senko M, Makarov A, Mann M, Horning S (2009). A dual pressure linear ion trap Orbitrap instrument with very high sequencing speed. *Molecular & cellular proteomics : MCP*. **8**, 2759-2769.
- Ong SE, Blagoev B, Kratchmarova I, Kristensen DB, Steen H, Pandey A, Mann M (2002). Stable isotope labeling by amino acids in cell culture, SILAC, as a simple and accurate approach to expression proteomics. *Molecular & cellular proteomics : MCP*. **1**, 376-386.
- Ono Y, Torii K, Fritsche E, Shintani Y, Nishida E, Nakamura M, Shirakata Y, Haarmann-Stemmann T, Abel J, Krutmann J, Morita A (2013). Role of the aryl hydrocarbon receptor in tobacco smoke extract-induced matrix metalloproteinase-1 expression. *Experimental dermatology*. **22**, 349-353.
- Orjalo AV, Bhaumik D, Gengler BK, Scott GK, Campisi J (2009). Cell surface-bound IL-1alpha is an upstream regulator of the senescence-associated IL-6/IL-8 cytokine network. *Proceedings of the National Academy of Sciences of the United States of America*. **106**, 17031-17036.

- Paavilainen VO, Hellman M, Helfer E, Bovellan M, Annala A, Carlier MF, Permi P, Lappalainen P (2007). Structural basis and evolutionary origin of actin filament capping by twinfilin. *Proceedings of the National Academy of Sciences of the United States of America*. **104**, 3113-3118.
- Paizs B, Bythell BJ, Maitre P (2012). Rearrangement Pathways of the a(4) Ion of Protonated YGGFL Characterized by IR Spectroscopy and Modeling. *Journal of the American Society for Mass Spectrometry*. **23**, 664-675.
- Paizs B, Suhai S (2005). Fragmentation pathways of protonated peptides. *Mass spectrometry reviews*. **24**, 508-548.
- Park SH, Choi HJ, Yang H, Do KH, Kim J, Lee DW, Moon Y (2010). Endoplasmic reticulum stress-activated C/EBP homologous protein enhances nuclear factor-kappaB signals via repression of peroxisome proliferator-activated receptor gamma. *J Biol Chem*. **285**, 35330-35339.
- Parrinello S, Coppe JP, Krtolica A, Campisi J (2005). Stromal-epithelial interactions in aging and cancer: senescent fibroblasts alter epithelial cell differentiation. *J Cell Sci*. **118**, 485-496.
- Paschen W, Doutheil J (1999). Disturbances of the functioning of endoplasmic reticulum: a key mechanism underlying neuronal cell injury? *Journal of cerebral blood flow and metabolism : official journal of the International Society of Cerebral Blood Flow and Metabolism*. **19**, 1-18.
- Passi A, Albertini R, Campagnari F, De Luca G (1997). Modifications of proteoglycans secreted into the growth medium by young and senescent human skin fibroblasts. *Febs Lett*. **402**, 286-290.
- Paul W (1989). Electromagnetic Traps for Charged and Neutral Particles (Nobel Lecture). *Angewandete Chemie International Edition in Englisch* **29**, 739-748.
- Paul W and Raether M (1995). Das elektrische Massenfiter. *Zeitschrift für Physik A Hadrons and Nuclei* **140**, 262-273.
- Perkins DN, Pappin DJ, Creasy DM, Cottrell JS (1999). Probability-based protein identification by searching sequence databases using mass spectrometry data. *Electrophoresis*. **20**, 3551-3567.
- Petersen TN, Brunak S, von Heijne G, Nielsen H (2011). SignalP 4.0: discriminating signal peptides from transmembrane regions. *Nature methods*. **8**, 785-786.

- Peterson LN, Eva KW, Rusticus SA, Lovato CY (2012). The readiness for clerkship survey: can self-assessment data be used to evaluate program effectiveness? *Academic medicine : journal of the Association of American Medical Colleges*. **87**, 1355-1360.
- Phillips TJ, Demircay Z, Sahu M (2001). Hormonal effects on skin aging. *Clinics in geriatric medicine*. **17**, 661-672, vi.
- Pitiyage GN, Lim KP, Gemenitzidis E, Teh MT, Waseem A, Prime SS, Tilakaratne WM, Fortune F, Parkinson EK (2012). Increased secretion of tissue inhibitors of metalloproteinases 1 and 2 (TIMPs -1 and -2) in fibroblasts are early indicators of oral sub-mucous fibrosis and ageing. *Journal of oral pathology & medicine : official publication of the International Association of Oral Pathologists and the American Academy of Oral Pathology*. **41**, 454-462.
- Powers ET, Morimoto RI, Dillin A, Kelly JW, Balch WE (2009). Biological and chemical approaches to diseases of proteostasis deficiency. *Annual review of biochemistry*. **78**, 959-991.
- Pratsch K, Wellhausen R, Seitz H (2014). Advances in the quantification of protein microarrays. *Current opinion in chemical biology*. **18**, 16-20.
- Prins JM, Fu L, Guo L, Wang Y (2014). Cd(2)(+)-induced alteration of the global proteome of human skin fibroblast cells. *Journal of proteome research*. **13**, 1677-1687.
- Raffaello A, Rizzuto R (2011). Mitochondrial longevity pathways. *Biochimica et biophysica acta*. **1813**, 260-268.
- Rando TA (2006). Stem cells, ageing and the quest for immortality. *Nature*. **441**, 1080-1086.
- Rando TA, Chang HY (2012). Aging, rejuvenation, and epigenetic reprogramming: resetting the aging clock. *Cell*. **148**, 46-57.
- Regnault V, Perret-Guillaume C, Kearney-Schwartz A, Max JP, Labat C, Louis H, Wahl D, Pannier B, Lecompte T, Weryha G, Challande P, Safar ME, Benetos A, Lacolley P (2011). Tissue factor pathway inhibitor: a new link among arterial stiffness, pulse pressure, and coagulation in postmenopausal women. *Arteriosclerosis, thrombosis, and vascular biology*. **31**, 1226-1232.
- Ressler S, Bartkova J, Niederegger H, Bartek J, Scharffetter-Kochanek K, Jansen-Durr P, Wlaschek M (2006). p16INK4A is a robust in vivo biomarker of cellular aging in human skin. *Aging cell*. **5**, 379-389.

- Ribeil JA, Zermati Y, Vandekerckhove J, Cathelin S, Kersual J, Dussiot M, Coulon S, Moura IC, Zeuner A, Kirkegaard-Sorensen T, Varet B, Solary E, Garrido C, Hermine O (2007). Hsp70 regulates erythropoiesis by preventing caspase-3-mediated cleavage of GATA-1. *Nature*. **445**, 102-105.
- Ridley AJ, Schwartz MA, Burridge K, Firtel RA, Ginsberg MH, Borisy G, Parsons JT, Horwitz AR (2003). Cell migration: integrating signals from front to back. *Science*. **302**, 1704-1709.
- Robinson AP, Duursma RA, Marshall JD (2005). A regression-based equivalence test for model validation: shifting the burden of proof. *Tree physiology*. **25**, 903-913.
- Röck K, Meusch M, Fuchs N, Tigges J, Zipper P, Fritsche E, Krutmann J, Homey B, Reifenberger J, Fischer JW (2012). Estradiol protects dermal hyaluronan/versican matrix during photoaging by release of epidermal growth factor from keratinocytes. *J Biol Chem*. **287**, 20056-20069.
- Röck K, Tigges J, Sass S, Florea AM, Fender A, Krutmann J, Boege F, Reifenberger G, Fischer JW (2014). miR-23a promotes dermal aging and cellular senescence by targeting hyaluronan synthase 2. *Journal of Invest Dermatology*. submitted.
- Rodier F, Campisi J (2011). Four faces of cellular senescence. *The Journal of cell biology*. **192**, 547-556.
- Rodier F, Munoz DP, Teachenor R, Chu V, Le O, Bhaumik D, Coppe JP, Campeau E, Beausejour CM, Kim SH, Davalos AR, Campisi J (2011). DNA-SCARS: distinct nuclear structures that sustain damage-induced senescence growth arrest and inflammatory cytokine secretion. *J Cell Sci*. **124**, 68-81.
- Roepstorff P, Fohlman J (1984). Proposal for a common nomenclature for sequence ions in mass spectra of peptides. *Biomedical mass spectrometry*. **11**, 601.
- Roepstorff P (2012). Mass spectrometry based proteomics, background, status and future needs. *Protein Cell*. **9**, 641-647.
- Rogakou EP, Boon C, Redon C, Bonner WM (1999). Megabase chromatin domains involved in DNA double-strand breaks in vivo. *The Journal of cell biology*. **146**, 905-916.
- Ross PL, Huang YN, Marchese JN, Williamson B, Parker K, Hattan S, Khainovski N, Pillai S, Dey S, Daniels S, Purkayastha S, Juhasz P, Martin S, Bartlet-Jones M, He F, Jacobson A, Pappin DJ (2004). Multiplexed protein quantitation in *Saccharomyces cerevisiae* using amine-reactive isobaric tagging reagents. *Molecular & cellular proteomics : MCP*. **3**, 1154-1169.

- Rossi DJ, Jamieson CH, Weissman IL (2008). Stems cells and the pathways to aging and cancer. *Cell*. **132**, 681-696.
- Rotilio D, Della Corte A, D'Imperio M, Coletta W, Marcone S, Silvestri C, Giordano L, Di Michele M, Donati MB (2012). Proteomics: bases for protein complexity understanding. *Thrombosis research*. **129**, 257-262.
- Rovillain E, Mansfield L, Caetano C, Alvarez-Fernandez M, Caballero OL, Medema RH, Hummerich H, Jat PS (2011). Activation of nuclear factor-kappa B signalling promotes cellular senescence. *Oncogene*. **30**, 2356-2366.
- Rubinsztein DC, Marino G, Kroemer G (2011). Autophagy and aging. *Cell*. **146**, 682-695.
- Salminen A, Kaarniranta K, Kauppinen A (2012). Inflammaging: disturbed interplay between autophagy and inflammasomes. *Aging*. **4**, 166-175.
- Sand M, Gambichler T, Sand D, Skrygan M, Altmeyer P, Bechara FG (2009). MicroRNAs and the skin: tiny players in the body's largest organ. *Journal of dermatological science*. **53**, 169-175.
- Scherer M, Leuthauser-Jaschinski K, Ecker J, Schmitz G, Liebisch G (2010). A rapid and quantitative LC-MS/MS method to profile sphingolipids. *Journal of lipid research*. **51**, 2001-2011.
- Schlage P, Egli FE, Nanni P, Wang LW, Kizhakkedathu JN, Apte SS, auf dem Keller U (2014). Time-resolved analysis of the matrix metalloproteinase 10 substrate degradome. *Molecular & cellular proteomics : MCP*. **13**, 580-593.
- Schlondorff J, Blobel CP (1999). Metalloprotease-disintegrins: modular proteins capable of promoting cell-cell interactions and triggering signals by protein-ectodomain shedding. *J Cell Sci*. **112** (Pt 21), 3603-3617.
- Schmidt A, Kellermann J, Lottspeich F (2005). A novel strategy for quantitative proteomics using isotope-coded protein labels. *Proteomics*. **5**, 4-15.
- Schneider DJ, Wu M, Le TT, Cho SH, Brenner MB, Blackburn MR, Agarwal SK (2012). Cadherin-11 contributes to pulmonary fibrosis: potential role in TGF-beta production and epithelial to mesenchymal transition. *FASEB J*. **26**, 503-512.
- Schuepbach RA, Velez K, Riewald M (2011). Activated protein C up-regulates procoagulant tissue factor activity on endothelial cells by shedding the TFPI Kunitz 1 domain. *Blood*. **117**, 6338-6346.

- Schulze C, Wetzel F, Kueper T, Malsen A, Muhr G, Jaspers S, Blatt T, Wittern KP, Wenck H, Kas JA (2010). Stiffening of human skin fibroblasts with age. *Biophys J.* **99**, 2434-2442.
- Schwanhausser B, Busse D, Li N, Dittmar G, Schuchhardt J, Wolf J, Chen W, Selbach M (2011). Global quantification of mammalian gene expression control. *Nature.* **473**, 337-342.
- Sedelnikova OA, Horikawa I, Zimonjic DB, Popescu NC, Bonner WM, Barrett JC (2004). Senescing human cells and ageing mice accumulate DNA lesions with unreparable double-strand breaks. *Nature cell biology.* **6**, 168-170.
- Seluanov A, Mittelman D, Pereira-Smith OM, Wilson JH, Gorbunova V (2004). DNA end joining becomes less efficient and more error-prone during cellular senescence. *Proceedings of the National Academy of Sciences of the United States of America.* **101**, 7624-7629.
- Senovilla L, Vitale I, Martins I, Tailler M, Paillet C, Michaud M, Galluzzi L, Adjemian S, Kepp O, Niso-Santano M, Shen S, Marino G, Criollo A, Boileve A, Job B, Ladoire S, Ghiringhelli F, Sistigu A, Yamazaki T, Rello-Varona S, Locher C, Poirier-Colame V, Talbot M, Valent A, Berardinelli F, Antoccia A, Ciccocanti F, Fimia GM, Piacentini M, Fueyo A, Messina NL, Li M, Chan CJ, Sigl V, Pourcher G, Ruckenstein C, Carmona-Gutierrez D, Lazar V, Penninger JM, Madeo F, Lopez-Otin C, Smyth MJ, Zitvogel L, Castedo M, Kroemer G (2012). An immunosurveillance mechanism controls cancer cell ploidy. *Science.* **337**, 1678-1684.
- Shannon P, Markiel A, Ozier O, Baliga NS, Wang JT, Ramage D, Amin N, Schwikowski B, Ideker T (2003). Cytoscape: a software environment for integrated models of biomolecular interaction networks. *Genome research.* **13**, 2498-2504.
- Shaw AC, Joshi S, Greenwood H, Panda A, Lord JM (2010). Aging of the innate immune system. *Current opinion in immunology.* **22**, 507-513.
- Shen Y, Wollam J, Magner D, Karalay O, Antebi A (2012). A steroid receptor-microRNA switch regulates life span in response to signals from the gonad. *Science.* **338**, 1472-1476.
- Sherwood SW, Rush D, Ellsworth JL, Schimke RT (1988). Defining Cellular Senescence in Imr-90 Cells - a Flow Cytometric Analysis. *Proceedings of the National Academy of Sciences of the United States of America.* **85**, 9086-9090.

- Shiraha H, Gupta K, Drabik K, Wells A (2000). Aging fibroblasts present reduced epidermal growth factor (EGF) responsiveness due to preferential loss of EGF receptors. *J Biol Chem.* **275**, 19343-19351.
- Shirakabe K, Hattori S, Seiki M, Koyasu S, Okada Y (2011). VIP36 protein is a target of ectodomain shedding and regulates phagocytosis in macrophage Raw 264.7 cells. *J Biol Chem.* **286**, 43154-43163.
- Shock, N. Handbook of the Biology of Aging, 721 (Van Nostrand Reinhold, 1985).
- Silva JC, Gorenstein MV, Li GZ, Vissers JP, Geromanos SJ (2006). Absolute quantification of proteins by LCMSE: a virtue of parallel MS acquisition. *Molecular & cellular proteomics : MCP.* **5**, 144-156.
- Simpson RM, Meran S, Thomas D, Stephens P, Bowen T, Steadman R, Phillips A (2009). Age-related changes in pericellular hyaluronan organization leads to impaired dermal fibroblast to myofibroblast differentiation. *The American journal of pathology.* **175**, 1915-1928.
- Sitek B, Waldera-Lupa DM, Poschmann G, Meyer HE, Stuhler K (2012). Application of label-free proteomics for differential analysis of lung carcinoma cell line A549. *Methods in molecular biology.* **893**, 241-248.
- Sprenger A, Kuttner V, Biniossek ML, Gretzmeier C, Boerries M, Mack C, Has C, Bruckner-Tuderman L, Dengjel J (2010). Comparative quantitation of proteome alterations induced by aging or immortalization in primary human fibroblasts and keratinocytes for clinical applications. *Molecular bioSystems.* **6**, 1579-1582.
- Starcher B, d'Azzo A, Keller PW, Rao GK, Nadarajah D, Hinek A (2008). Neuraminidase-1 is required for the normal assembly of elastic fibers. *American journal of physiology. Lung cellular and molecular physiology.* **295**, L637-647.
- Stastna M, Van Eyk JE (2012). Analysis of protein isoforms: can we do it better? *Proteomics.* **12**, 2937-2948.
- Steen H, Mann M (2004). The ABC's (and XYZ's) of peptide sequencing. *Nature reviews. Molecular cell biology.* **5**, 699-711.
- Steen H, Pandey A (2002). Proteomics goes quantitative: measuring protein abundance. *Trends in biotechnology.* **20**, 361-364.
- Steinman RM, Mellman IS, Muller WA, Cohn ZA (1983). Endocytosis and the recycling of plasma membrane. *The Journal of cell biology.* **96**, 1-27.

- Stern MM, Bickenbach JR (2007). Epidermal stem cells are resistant to cellular aging. *Aging cell*. **6**, 439-452.
- Street SE, Kramer NJ, Walsh PL, Taylor-Blake B, Yadav MC, King IF, Vihko P, Wightman RM, Millan JL, Zylka MJ (2013). Tissue-nonspecific alkaline phosphatase acts redundantly with PAP and NT5E to generate adenosine in the dorsal spinal cord. *The Journal of neuroscience : the official journal of the Society for Neuroscience*. **33**, 11314-11322.
- Stumpf MP, Thorne T, de Silva E, Stewart R, An HJ, Lappe M, Wiuf C (2008). Estimating the size of the human interactome. *Proceedings of the National Academy of Sciences of the United States of America*. **105**, 6959-6964.
- Sun T, Norton D, Ryan AJ, MacNeil S, Haycock JW (2007). Investigation of fibroblast and keratinocyte cell-scaffold interactions using a novel 3D cell culture system. *Journal of materials science. Materials in medicine*. **18**, 321-328.
- Suva ML, Riggi N, Janiszewska M, Radovanovic I, Provero P, Stehle JC, Baumer K, Le Bitoux MA, Marino D, Cironi L, Marquez VE, Clement V, Stamenkovic I (2009). EZH2 is essential for glioblastoma cancer stem cell maintenance. *Cancer research*. **69**, 9211-9218.
- Swindell WR, Masternak MM, Kopchick JJ, Conover CA, Bartke A, Miller RA (2009). Endocrine regulation of heat shock protein mRNA levels in long-lived dwarf mice. *Mechanisms of ageing and development*. **130**, 393-400.
- Syka JE, Coon JJ, Schroeder MJ, Shabanowitz J, Hunt DF (2004). Peptide and protein sequence analysis by electron transfer dissociation mass spectrometry. *Proceedings of the National Academy of Sciences of the United States of America*. **101**, 9528-9533.
- Tabb DL, Smith LL, Brechi LA, Wysocki VH, Lin D, Yates JR, 3rd (2003). Statistical characterization of ion trap tandem mass spectra from doubly charged tryptic peptides. *Analytical chemistry*. **75**, 1155-1163.
- Takahashi Y, Moriwaki S, Sugiyama Y, Endo Y, Yamazaki K, Mori T, Takigawa M, Inoue S (2005). Decreased gene expression responsible for post-ultraviolet DNA repair synthesis in aging: a possible mechanism of age-related reduction in DNA repair capacity. *J Invest Dermatol*. **124**, 435-442.

- Talens RP, Christensen K, Putter H, Willemsen G, Christiansen L, Kremer D, Suchiman HE, Slagboom PE, Boomsma DI, Heijmans BT (2012). Epigenetic variation during the adult lifespan: cross-sectional and longitudinal data on monozygotic twin pairs. *Aging cell*. **11**, 694-703.
- Talwar HS, Griffiths CE, Fisher GJ, Hamilton TA, Voorhees JJ (1995). Reduced type I and type III procollagens in photodamaged adult human skin. *J Invest Dermatol*. **105**, 285-290.
- Tanaka K, Waki H, Ido Y, Akita S, Yoshida T (1988). Protein and Polymer Analyses up to m/z 100000 by Laser Ionization Time-of-Flight Mass Spectrometry. *Rapid Commun Mass Spectrom*. **2**(20), 151-153.
- Thompson A, Schäfer J, Kuhn K, Kienle S, Schwarz J, Schmidt G, Neumann T, Johnstone R, Mohammed AKA, Hamon C (2003). Tandem mass tags: a novel quantification strategy for comparative analysis of complex protein mixtures by ms/ms. *Analytical chemistry*. **75** (8), 1895–1904.
- Tigges J, Krutmann J, Fritsche E, Haendeler J, Schaal H, Fischer JW, Kalfalah F, Reinke H, Reifenberger G, Stuhler K, Ventura N, Gundermann S, Boukamp P, Boege F (2014). The hallmarks of fibroblast ageing. *Mechanisms of ageing and development*.
- Tilstra JS, Clauson CL, Niedernhofer LJ, Robbins PD (2011). NF-kappaB in Aging and Disease. *Aging and disease*. **2**, 449-465.
- Toledano H, D'Alterio C, Czech B, Levine E, Jones DL (2012). The let-7-Imp axis regulates ageing of the Drosophila testis stem-cell niche. *Nature*. **485**, 605-610.
- Tomaru U, Takahashi S, Ishizu A, Miyatake Y, Gohda A, Suzuki S, Ono A, Ohara J, Baba T, Murata S, Tanaka K, Kasahara M (2012). Decreased proteasomal activity causes age-related phenotypes and promotes the development of metabolic abnormalities. *The American journal of pathology*. **180**, 963-972.
- Tomas-Loba A, Flores I, Fernandez-Marcos PJ, Cayuela ML, Maraver A, Tejera A, Borrás C, Matheu A, Klatt P, Flores JM, Vina J, Serrano M, Blasco MA (2008). Telomerase reverse transcriptase delays aging in cancer-resistant mice. *Cell*. **135**, 609-622.
- Tomkiewicz B, Rybinski K, Foley B, Ebel W, Kline B, Routhier E, Sass P, Nicolaidis NC, Grasso L, Zhou Y (2007). Interaction of endosialin/TEM1 with extracellular matrix proteins mediates cell adhesion and migration. *Proceedings of the National Academy of Sciences of the United States of America*. **104**, 17965-17970.

- Tonge R, Shaw J, Middleton B, Rowlinson R, Rayner S, Young J, Pognan F, Hawkins E, Currie I, Davison M (2001). Validation and development of fluorescence two-dimensional differential gel electrophoresis proteomics technology. *Proteomics*. **1**, 377-396.
- Torres M, Encina G, Soto C, Hetz C (2011). Abnormal calcium homeostasis and protein folding stress at the ER: A common factor in familial and infectious prion disorders. *Communicative & integrative biology*. **4**, 258-261.
- Toussaint O, Dumont P, Dierick JF, Pascal T, Fripiat C, Chainiaux F, Sluse F, Eliaers F, Remacle J (2000a). Stress-induced premature senescence. Essence of life, evolution, stress, and aging. *Annals of the New York Academy of Sciences*. **908**, 85-98.
- Toussaint O, Medrano EE, von Zglinicki T (2000b). Cellular and molecular mechanisms of stress-induced premature senescence (SIPS) of human diploid fibroblasts and melanocytes. *Experimental gerontology*. **35**, 927-945.
- Troen BR (2003). The biology of aging. *The Mount Sinai journal of medicine, New York*. **70**, 3-22.
- Ugalde AP, Espanol Y, Lopez-Otin C (2011). Micromanaging aging with miRNAs: new messages from the nuclear envelope. *Nucleus*. **2**, 549-555.
- Umazume K, Usui Y, Wakabayashi Y, Okunuki Y, Kezuka T, Goto H (2013). Effects of soluble CD14 and cytokine levels on diabetic macular edema and visual acuity. *Retina*. **33**, 1020-1025.
- UniProt C (2014). Activities at the Universal Protein Resource (UniProt). *Nucleic acids research*. **42**, D191-198.
- Valdiglesias V, Giunta S, Fenech M, Neri M, Bonassi S (2013). gammaH2AX as a marker of DNA double strand breaks and genomic instability in human population studies. *Mutation research*. **753**, 24-40.
- van Huizen R, Martindale JL, Gorospe M, Holbrook NJ (2003). P58IPK, a novel endoplasmic reticulum stress-inducible protein and potential negative regulator of eIF2alpha signaling. *J Biol Chem*. **278**, 15558-15564.
- Vermulst M, Wanagat J, Kujoth GC, Bielas JH, Rabinovitch PS, Prolla TA, Loeb LA (2008). DNA deletions and clonal mutations drive premature aging in mitochondrial mutator mice. *Nature genetics*. **40**, 392-394.

- von Zglinicki T, Saretzki G, Docke W, Lotze C (1995). Mild hyperoxia shortens telomeres and inhibits proliferation of fibroblasts: a model for senescence? *Experimental cell research*. **220**, 186-193.
- Wajapeyee N, Serra RW, Zhu X, Mahalingam M, Green MR (2008). Oncogenic BRAF induces senescence and apoptosis through pathways mediated by the secreted protein IGFBP7. *Cell*. **132**, 363-374.
- Waldera-Lupa DM, Kalfalah F, Florea AM, Sass S, Kruse F, Rieder V, Tigges J, Fritsche E, Krutmann J, Busch H, Boerries M, Meyer HE, Boege F, Theis F, Reifemberger G, Stühler K (2014). Proteome-wide analysis of primary cultures of *in situ* aged human fibroblasts reveals a moderate age-associated cellular phenotype. *Aging Cell*. submitted.
- Waldera-Lupa DM, Kalfalah F, Boukamp P, Safferling K, Poschmann G, Götz-Rösch C, Bernerd F, Haag L, Hanzen B, Huebenthal U, Fritsche E, Grabe N, Boege F, Tigges J, Krutmann J, Stühler K (2014). Characterization of skin aging associated secreted proteins (SAASP) produced by dermal fibroblast isolated from intrinsically aged human skin. *Journal of Invest Dermatology*. submitted.
- Walford RL (1974). Immunologic theory of aging: current status. *Federation proceedings*. **33**, 2020-2027.
- Wang C, Jurk D, Maddick M, Nelson G, Martin-Ruiz C, von Zglinicki T (2009). DNA damage response and cellular senescence in tissues of aging mice. *Aging cell*. **8**, 311-323.
- Wang E, Gundersen D (1984). Increased organization of cytoskeleton accompanying the aging of human fibroblasts *in vitro*. *Experimental cell research*. **154**, 191-202.
- Wang K, Klionsky DJ (2011). Mitochondria removal by autophagy. *Autophagy*. **7**, 297-300.
- Warren R, Gartstein V, Kligman AM, Montagna W, Allendorf RA, Ridder GM (1991). Age, sunlight, and facial skin: a histologic and quantitative study. *Journal of the American Academy of Dermatology*. **25**, 751-760.
- Washburn MP, Wolters D, Yates JR, 3rd (2001). Large-scale analysis of the yeast proteome by multidimensional protein identification technology. *Nature biotechnology*. **19**, 242-247.
- Watson RE, Griffiths CE, Craven NM, Shuttleworth CA, Kielty CM (1999). Fibrillin-rich microfibrils are reduced in photoaged skin. Distribution at the dermal-epidermal junction. *J Invest Dermatol*. **112**, 782-787.

- Weindruch R, Walford RL, Fligiel S, Guthrie D (1986). The retardation of aging in mice by dietary restriction: longevity, cancer, immunity and lifetime energy intake. *The Journal of nutrition*. **116**, 641-654.
- Weinert BT, Timiras PS (2003). Invited review: Theories of aging. *Journal of applied physiology*. **95**, 1706-1716.
- West MD, Pereira-Smith OM, Smith JR (1989). Replicative senescence of human skin fibroblasts correlates with a loss of regulation and overexpression of collagenase activity. *Experimental cell research*. **184**, 138-147.
- West MD, Shay JW, Wright WE, Linskens MH (1996). Altered expression of plasminogen activator and plasminogen activator inhibitor during cellular senescence. *Experimental gerontology*. **31**, 175-193.
- Westergaard UB, Andersen MH, Heegaard CW, Fedosov SN, Petersen TE (2003). Tetranection binds hepatocyte growth factor and tissue-type plasminogen activator. *European journal of biochemistry / FEBS*. **270**, 1850-1854.
- Wilkins MR, Sanchez JC, Gooley AA, Appel RD, Humphery-Smith I, Hochstrasser DF, Williams KL (1996). Progress with proteome projects: why all proteins expressed by a genome should be identified and how to do it. *Biotechnology & genetic engineering reviews*. **13**, 19-50.
- Winslow T (2008) Medical expertise Responsive and efficient Informed and engaging illustrations. <http://www.teresewinslow.com/>
- Wiseman BS, Werb Z (2002). Stromal effects on mammary gland development and breast cancer. *Science*. **296**, 1046-1049.
- Wollnik H (1993). Time-of-Flight Mass Analyzers. *Mass spectrometry reviews*. **12**, 89-114.
- Yaar M, Gilchrist BA (2001). Skin aging: postulated mechanisms and consequent changes in structure and function. *Clinics in geriatric medicine*. **17**, 617-630, v.
- Yalcin T, Khouw C, Csizmadia IG, Peterson MR, Harrison AG (1995). Why Are B ions stable species in peptide spectra? *Journal of the American Society for Mass Spectrometry*. **6**, 1165-1174.
- Yamasawa S, Cerimele D, Serri F (1972). The activity of metabolic enzymes of human epidermis in relation to age. *Br J Dermatol*. **86**, 134-140.
- Yamauchi M, Imajoh-Ohmi S, Shibuya M (2007). Novel antiangiogenic pathway of thrombospondin-1 mediated by suppression of the cell cycle. *Cancer science*. **98**, 1491-1497.

- Yang CH, Culshaw GJ, Liu MM, Lu CC, French AT, Clements DN, Corcoran BM (2012a). Canine tissue-specific expression of multiple small leucine rich proteoglycans. *Veterinary journal*. **193**, 374-380.
- Yang F, Tuxhorn JA, Ressler SJ, McAlhany SJ, Dang TD, Rowley DR (2005). Stromal expression of connective tissue growth factor promotes angiogenesis and prostate cancer tumorigenesis. *Cancer research*. **65**, 8887-8895.
- Yang G, Rosen DG, Zhang Z, Bast RC, Jr., Mills GB, Colacino JA, Mercado-Uribe I, Liu J (2006). The chemokine growth-regulated oncogene 1 (Gro-1) links RAS signaling to the senescence of stromal fibroblasts and ovarian tumorigenesis. *Proceedings of the National Academy of Sciences of the United States of America*. **103**, 16472-16477.
- Yang SB, Tien AC, Boddupalli G, Xu AW, Jan YN, Jan LY (2012b). Rapamycin ameliorates age-dependent obesity associated with increased mTOR signaling in hypothalamic POMC neurons. *Neuron*. **75**, 425-436.
- Yano K, Kajiya K, Ishiwata M, Hong YK, Miyakawa T, Detmar M (2004). Ultraviolet B-induced skin angiogenesis is associated with a switch in the balance of vascular endothelial growth factor and thrombospondin-1 expression. *J Invest Dermatol*. **122**, 201-208.
- Yen WL, Klionsky DJ (2008). How to Live Long and Prosper: Autophagy, Mitochondria, and Aging. *Physiology*. **23**, 248-262.
- Yokota S, Yanagi H, Yura T, Kubota H (2001). Cytosolic chaperonin-containing t-complex polypeptide 1 changes the content of a particular subunit species concomitant with substrate binding and folding activities during the cell cycle. *European journal of biochemistry / FEBS*. **268**, 4664-4673.
- Young AR, Narita M (2009). SASP reflects senescence. *EMBO reports*. **10**, 228-230.
- Zhang C, Cuervo AM (2008). Restoration of chaperone-mediated autophagy in aging liver improves cellular maintenance and hepatic function. *Nature medicine*. **14**, 959-965.
- Zhang G, Li J, Purkayastha S, Tang Y, Zhang H, Yin Y, Li B, Liu G, Cai D (2013a). Hypothalamic programming of systemic ageing involving IKK-beta, NF-kappaB and GnRH. *Nature*. **497**, 211-216.
- Zhang H, Ghai P, Wu H, Wang C, Field J, Zhou GL (2013b). Mammalian adenylyl cyclase-associated protein 1 (CAP1) regulates cofilin function, the actin cytoskeleton, and cell adhesion. *J Biol Chem*. **288**, 20966-20977.

- Zhang J, Bardot E, Ezhkova E (2012). Epigenetic regulation of skin: focus on the Polycomb complex. *Cell Mol Life Sci.* **69**, 2161-2172.
- Zhang W, Lane RD, Mellgren RL (1996). The major calpain isozymes are long-lived proteins. Design of an antisense strategy for calpain depletion in cultured cells. *J Biol Chem.* **271**, 18825-18830.
- Zhang Y, Ikeno Y, Qi W, Chaudhuri A, Li Y, Bokov A, Thorpe SR, Baynes JW, Epstein C, Richardson A, Van Remmen H (2009). Mice deficient in both Mn superoxide dismutase and glutathione peroxidase-1 have increased oxidative damage and a greater incidence of pathology but no reduction in longevity. *The journals of gerontology. Series A, Biological sciences and medical sciences.* **64**, 1212-1220.
- Zheng Y, Cretoiu D, Yan G, Cretoiu SM, Popescu LM, Wang X (2014). Comparative proteomic analysis of human lung telocytes with fibroblasts. *Journal of cellular and molecular medicine.* **18**, 568-589.
- Zubarev RA, Horn DM, Fridriksson EK, Kelleher NL, Kruger NA, Lewis MA, Carpenter BK, McLafferty FW (2000). Electron capture dissociation for structural characterization of multiply charged protein cations. *Analytical chemistry.* **72**, 563-573.
- Zuo X, Echan L, Hembach P, Tang HY, Speicher KD, Santoli D, Speicher DW (2001). Towards global analysis of mammalian proteomes using sample prefractionation prior to narrow pH range two-dimensional gels and using one-dimensional gels for insoluble and large proteins. *Electrophoresis.* **22**, 1603-1615.

Publikationen im Journalformat

Publikation I: *The fate of b-ions in the two worlds of collision-induced dissociation* XV

Publikation II: *Application of label-free proteomics for differential analysis of lung carcinoma cell line A549* XXI



Contents lists available at ScienceDirect

Biochimica et Biophysica Acta

journal homepage: www.elsevier.com/locate/bbapap

The fate of b-ions in the two worlds of collision-induced dissociation

Daniel M. Waldera-Lupa^{a,*}, Anja Stefanski^a, Helmut E. Meyer^b, Kai Stühler^a

^a Molecular Proteomics Laboratory, Biologisch-Medizinisches Forschungszentrum (BMFZ), Heinrich-Heine-Universität, Düsseldorf, Germany

^b Medizinisches Proteom-Center, Ruhr-Universität Bochum, Germany

ARTICLE INFO

Article history:

Received 26 June 2013

Received in revised form 14 August 2013

Accepted 16 August 2013

Available online 28 August 2013

Keywords:

b-Ion cyclization

Collision-induced dissociation

Mass spectrometry

Peptide acetylation

Peptide fragmentation

ABSTRACT

Fragment analysis of proteins and peptides by mass spectrometry using collision-induced dissociation (CID) revealed that the pairwise generated N-terminal b- and C-terminal y-ions have different stabilities resulting in underrepresentation of b-ions. Detailed analyses of large-scale spectra databases and synthetic peptides underlined these observations and additionally showed that the fragmentation pattern depends on utilized CID regime. To investigate this underrepresentation further we systematically compared resonant excitation energy and beam-type CID facilitated on different mass spectrometer platforms: (i) quadrupole time-of-flight, (ii) linear ion trap and (iii) three-dimensional ion trap. Detailed analysis of MS/MS data from a standard tryptic protein digest revealed that b-ions are significantly underrepresented on all investigated mass spectrometers. By N-terminal acetylation of tryptic peptides we show for the first time that b-ion cyclization reaction significantly contributes to b-ion underrepresentation even on ion trap instruments and accounts for at most 16% of b-ion loss.

© 2013 Elsevier B.V. All rights reserved.

1. Introduction

The application of mass spectrometry (MS) has become an indispensable tool in proteomics [1–4]. In combination with soft ionization techniques such as matrix-assisted laser-desorption/ionization (MALDI) [5] and electrospray ionization (ESI) [6] as well as different mass analyzers like e.g. time-of-flight, ion trap, orbitrap, MS provides a broad range of applications for detailed characterization of proteins and peptides. The commonly used bottom up approach of analyzing peptides after tryptic digestion has been successfully applied to quantify proteomes [1–3] as well as in-depth analysis of the phosphoproteome [7,8]. To obtain sequence information and characterize proteins' primary structure as well as posttranslational modifications fragment analysis using collision-induced dissociation (CID), electron transfer dissociation (ETD) or higher-energy collisional dissociation (HCD) is routinely applied [9–12]. In low-energy CID experiments the selected precursor ions undergo energetic collisions with an inert gas such as nitrogen or helium predominantly leading to so-called N-terminal b-ions and C-terminal y-ions [11–16]. At this point it must be distinguished between two different instrument specific CID fragmentation techniques: beam-type and resonance excitation CID. Beam-type CID is a quadrupole based technique (QToF, QQQ) where fragmentation is achieved

by transferring precursor ions with ultrasonic speed from the analytical quadrupole into the gas-filled collision cell [9,10]. Formed fragment ions can undergo unintended secondary fragmentation leading to non-sequence specific ions. In contrast, fragmentation in ion trap instruments (LIT, QIT) is achieved by resonance excitation of precursor ions. Here, the ions are excited with a precursor specific energy and collisions with the inert gas cause fragmentation [9,10]. The excitation energy is not sufficient for exciting previously formed fragment ions.

Due to the specific fragmentation pattern, sequence information can be deduced from the b- and y-ion series. In case of *de novo* sequencing nearly complete b- or y-ion series are mandatory, whereas searching of fragment spectra against a protein database via peptide fragment mass fingerprint analysis even partial b- and y-ion series can successfully identify a peptide sequence [17]. The broad application of CID experiments for peptide characterization revealed early that b- and y-ions have different stabilities leading to product ion spectra with high numbers of y-ions but often a minor number of b-ions [19, 20]. Especially, analyzing tryptic digest the different intensity of b- and y-ions is more pronounced because y-ion *per se* contains C-terminal basic amino acids (arginine and lysine) which produce more intense signals in the positive analysis mode [18–20].

It has been accepted that y-ions are protonated amino acids or protonated truncated peptides, whereas the structures of b-ions are much more complex and variable [21].

In general, b-ions have an oxazolone structure [14,21] and can form linear as well as cyclic conformers [21–29]. There is evidence that b₂ and larger b-ions form fully cyclic structures [21,22,30–35]. These cyclic structures are formed via a C-terminal oxazolone intermediate (ring formation) by nucleophilic attack of the N-terminal amine function on the carbonyl function of the oxazolone structure of the b-ion (head-

Abbreviations: Ac, acetylated; ETD, electron transfer dissociation; HCD, higher-energy collisional dissociation; HSD, honestly significant difference; LIT, linear ion trap; nAc, non-acetylated; QIT, quadrupole ion trap; QToF, quadrupole time-of-flight; QQQ, triple quadrupole; UPLC, ultra performance liquid chromatography

* Corresponding author at: Molecular Proteomics Laboratory, Biologisch Medizinisches Forschungszentrum, Heinrich-Heine-Universität, Universitätsstr. 1, 40225 Düsseldorf, Germany. Tel.: +49 211 81 12230; fax: +49 211 81 10469.

E-mail address: daniel.waldera-lupa@uni-duesseldorf.de (D.M. Waldera-Lupa).

1570-9639/\$ – see front matter © 2013 Elsevier B.V. All rights reserved.

<http://dx.doi.org/10.1016/j.bbapap.2013.08.007>

to-tail cyclization) [31]. The possible reopening of the cyclic peptide at several positions can lead to scrambling of the initial amino acid sequence and thus lead to a complex variety of oxazolones [21,25,31,34]. Further fragmentation of these scrambled b-ions leads to fragment ions (a-ions or lower b-ions) that are hard to assign to the initial peptide [30,31]. Quantifying the proportion of b-ion cyclization is still object of recent research [36].

Detailed analyses of large-scale spectra databases underlined these observations and additionally revealed that the fragmentation pattern depends on CID technique [37]. First reports on underrepresentation of b-ions were shown for QToF instruments (beam-type CID) [37,38], but also slight differences were reported for ion trap instruments (resonance excitation CID) [19,20]. But until now, data experimentally evaluating and quantifying the underrepresentation of b-ions on different MS platforms are missing. Here, we systematically analyzed a standard tryptic protein digest on two ion trap instruments, linear ion trap (LIT) and three-dimensional ion trap (QIT), and one quadrupole time-of-flight instrument (QToF) statistically evaluating b- and y-ion series in a prospective approach. By N-terminal acetylation of tryptic peptides we show for the first time that b-ion cyclization reaction significantly contributes to b-ion underrepresentation on all examined instrument platforms even on ion traps.

2. Materials and methods

2.1. Sample preparation

The proteins glucose oxidase (*Aspergillus niger*) (Serva, Heidelberg, Germany), lipase (*Burkholderia glumae*) (Serva, Heidelberg, Germany) and α -crystallin (*Bos taurus*) (Sigma-Aldrich, München, Germany) were separately digested and afterwards mixed together. For digestion 1 mg of each protein was solved in 100 μ L 40 mM ammonium bicarbonate with 10 μ L acetonitrile (Biosolve, Valkenswaard, Netherlands) and digested with trypsin 1:50 (Promega, Mannheim, Germany) at 37 °C for 16 h. Finally the digests were filtered using 3 kDa cut-off Centricons™ (Millipore, Schwalbach, Germany) at 16,000 \times g for 15 min and mixed together. For peptide acetylation 3 pmol of the digested 3-protein-mix was dried in a SpeedVac™, dissolved in 20 μ L 50 mM ammonium bicarbonate and incubated with acetic anhydride (Acros Organics, Nidderau, Germany) dissolved in ethanol (1:3) (Sigma-Aldrich, München, Germany) for 1 h [39,40]. The pH was adjusted to be acidic (pH 6) during the acetylation reaction to ensure that monoacetylation occurred at the amino terminus. For LC–MS/MS analysis 3 ng (25 fmol of each protein) of acetylated (Ac) and non-acetylated (nAc) protein-mix were applied.

2.2. LC–MS/MS data collection

LC–ESI–MS/MS measurements were carried out using different HPLC–MS systems. Bruker Maxis™ (QToF) and HCTultra II™ (QIT) mass spectrometers (Bruker Daltonics, Bremen, Germany) were coupled with nanoHPLC UltiMate 3000™ (Thermo Fisher Scientific, Bremen, Germany) and Thermo LTQ Velos™ (LIT) mass spectrometer (Thermo Fisher Scientific, Bremen, Germany) was coupled with RSLCnano™ UPLC (Thermo Fisher Scientific, Bremen, Germany). Both LC systems were operated with a pre-column (C₁₈) and analytical column (C₁₈) setup. After injection of 15 μ L of each sample peptides were trapped, desalted (0.1% aqueous trifluoroacetic acid) and then separated using a linear gradient from 4% to 40% (45 min) gradient solvent (84% acetonitrile and 0.1% formic acid in water). The flow rate was 400 nL/min. For all mass spectrometers the mass range for survey full scan MS spectra was m/z 300–1500. For fragmentation collision-induced dissociation (CID) was applied. All other mass spectrometer parameters were set to system specific standard values and were not changed during the acetylation experiment.

2.3. Database search and statistical analysis

Result files were converted into MASCOT Generic Format (.mgf) files using Data Analysis™ (Bruker Daltonics, Bremen, Germany) for HCTultra II™ and Maxis™ and Proteome Discoverer™ (Thermo Fisher Scientific, Bremen, Germany) for LTQ Velos™ data. The MS data were searched against a UniProtKB/Swiss-Prot shuffled decoy database (519,348 sequences) using MASCOT™ (v2.2.0) algorithm (Matrix Science, London, United Kingdom). The following parameters were applied: enzyme: trypsin, missed cleavages: allow up to one, variable modifications: oxidation (methionine) and acetylation (N-term/lysine for acetylated samples), peptide tolerance: 15 ppm (Maxis), 0.3 Da (HCTultra II™) and 0.4 Da (LTQ Velos™), MS/MS tolerance: 0.1 Da (Maxis™), 0.3 Da (HCTultra II™) and 0.4 Da (LTQ Velos™), peptide charge: 2+ and 3+ and monoisotopic mass. For the analysis of identified ion series the Fragmentation Analyzer tool [41] was used. Briefly, Fragmentation Analyzer can analyze the influence of the following parameters: (i) the instrument used for the identifications; (ii) the modification status of the N- and C-terminus of the identified peptides; (iii) the charge of the identified peptides; and (iv) post-translational modifications detected for the identified peptides. First, it is required to load an input file of a MS search engine (MASCOT, OMSSA, etc.) into the Fragmentation Analyzer tool. After selection of parameters, the tool finds a set of matching identifications, groups these by peptide sequence, and presents them for further analysis [41].

MASCOT input files (.dat) were loaded into the Fragmentation Analyzer and the peptides were filtered according to the following properties: all peptides had a precursor charge of 2+, unmodified C-terminals (acetylation of lysine and arginine were not considered) and acetylated or unmodified N-terminals. Only peptides confidently identified by a MASCOT score (≥ 30) search were considered.

Twenty common peptides (supplement) were selected for analysis eluting over the whole LC gradient and reproducibly detected in three LC–MS/MS runs per instrument at least. For statistical analysis the occurrence of ions in MS spectra was used. The calculation of b- and y-ions occurrence was performed using a fragment ion probability plot generated by the Fragmentation Analyzer tool [41]. For the comparison between different MS platforms b-ion occurrence was normalized by y-ion occurrence. For testing of statistical significance of ion occurrence between different MS platforms Tukey's honestly significant difference (HSD) Post-Hoc-Test ($p < 0.05$) was applied. For calculation of significance difference of $p < 0.05$ between b- and y-ions occurrences on the same instrument Student's *t*-test was used.

3. Results and discussion

Fragment analysis of proteins and peptides by mass spectrometry using collision-induced dissociation revealed that the pairwise generated N-terminal b- and C-terminal y-ions have different stabilities [21]. Detailed analyses of large-scale spectra databases and synthetic peptides underlined these observations and additionally revealed that the fragmentation pattern is instrument-specific [37,38]. It has been shown that instruments facilitating beam-type CID (triple quadrupole instruments, QToF) with excitation energies of around 100 eV exhibit an underrepresentation of b-ions [37,38,42]. For ion traps (QIT, LIT) utilizing resonant-excitation energy CID (<2 eV) it was reported that y-ions were more than twice as intense as b-ions; however systematically evaluation has not been performed [19]. A detailed analysis of the influence of amino acids' basicity on fragmentation ion peak intensities on ion trap instruments revealed that fragment ions containing the basic amino acids arginine, lysine and histidine generate more intense peaks [20]. But until now, no experimental approach has been undertaken to analyze underrepresentation of b-ions facilitating different CID types. For the experimental evaluation of the observation of underrepresentation of b-ions on different MS platforms we decided to analyze tryptic proteins digest instead of synthetic peptides to

approach the realistic situation of MS-based protein analysis. To avoid the above mentioned influence of basic amino acids on ion intensity we only consider tryptic peptides represented on all MS platforms containing arginine and lysine and normalized the b-ions occurrence by the y-ions. Because it has been shown that averaged spectra are more reliable to analyze ion series we decided to consider Fragment Analyzer tool instead of representative spectra [38,41]. Furthermore, we decided to consider the ion occurrence instead of the ion intensity because protein identification in common proteomics strategies relies not on ion intensities. Altogether 95 LC-MS/MS runs, including non-acetylated and acetylated samples, were performed using a QIT, a LIT and a QToF instrument. In total more than 15,000 spectra (≥ 2 per peptide) were evaluated. All peptides considered for statistic evaluation were consistently identified by MASCOT™. Over 75,000 b- and y-ions could be

assigned to the twenty common peptides (Table 1S) in all LC-MS/MS runs. The selected peptides elute over the whole LC gradient to prevent any potential bias in the data due to differing distributions of amino acid frequencies or compositions in the sequences of the peptides.

Analysis of ion statistics based on average values of b-ion and of y-ion occurrence of twenty selected peptides identified in at least three LC-MS/MS runs per MS. To avoid any potential bias by different ionization efficiency and fragmentation techniques of used MS platforms b-ion occurrence was normalized by the y-ion occurrence. Statistical significance of ion occurrence between MS platforms was determined by Tukey's HSD Post-Hoc-Test. Tukey's HSD test is a single-step multiple comparison procedure in conjunction with an ANOVA to find if normalized means of b-ions are significantly different between the instruments.

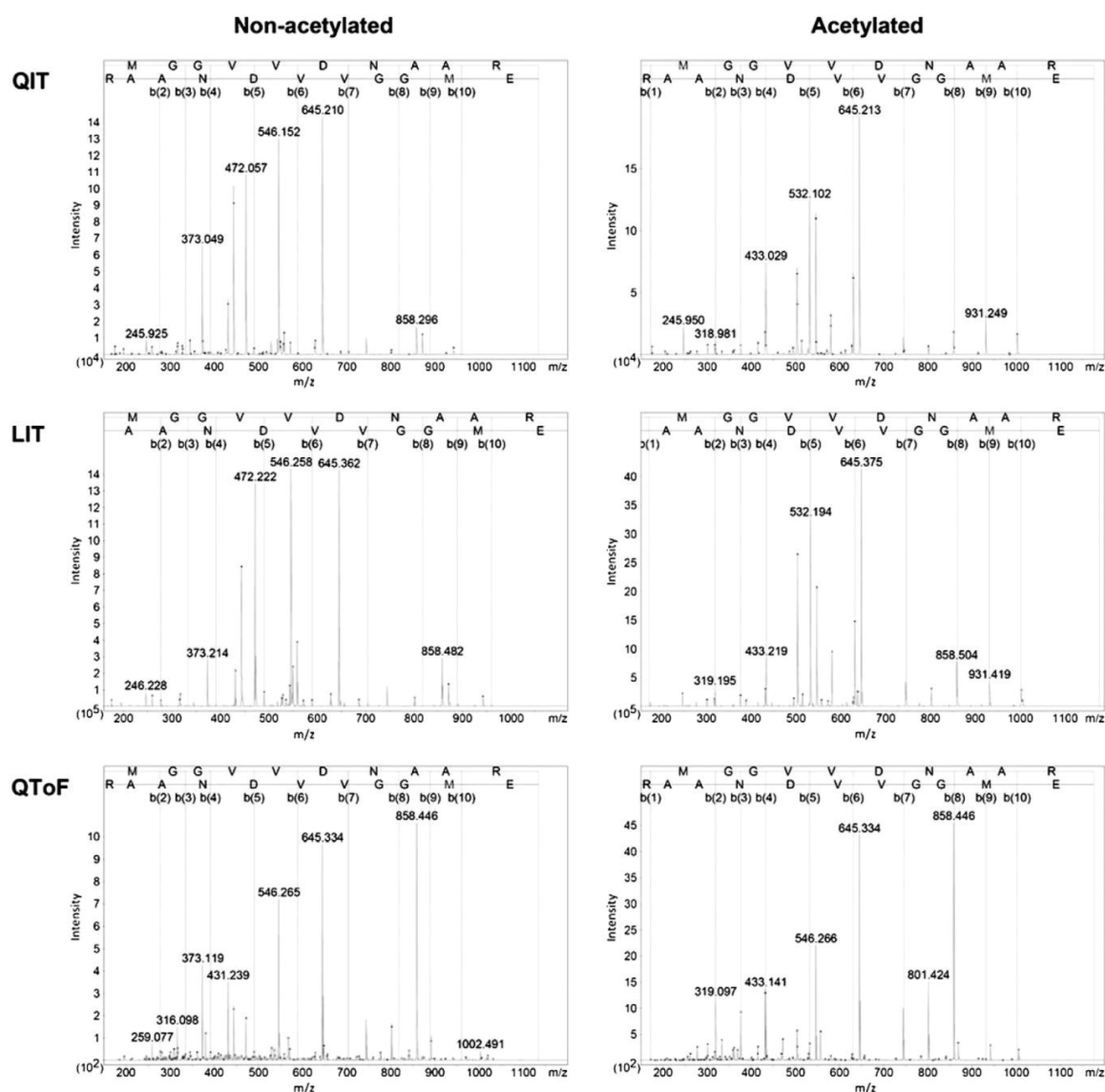


Fig. 1. Representative fragment spectra (CID) of a single peptide (sequence: EM(Ox)GGVVDNAAAR) from digested protein mix measured with different mass spectrometers (QIT, LIT and QToF) before and after acetylation. Continuous lines indicate identified b-ions, whereas the dashed lines indicate unmatched b-ions.

3.1. Determination of b-ion statistic on different mass spectrometer platforms

Fragmentation and fragment ion analysis is a favorite technique to characterize peptides primary structure by mass spectrometry. Although major processes of peptide fragmentation have already been described [15,21,25] the detailed elucidation of peptides' fragmentation reaction in the gas-phase or even prediction of fragment spectra is still far from realization. In the past experiments ranging from single synthetic peptide analysis [22–32] to the in-depth data analysis of spectra databases have been performed to elucidate the fragmentation process of peptides [37,38]. In recent years the gas-phase chemistry of b-ions became of increasing interest. The analysis of spectra databases has shown that b-ions in comparison to y-ions are underrepresented in MS/MS spectra acquired on MS instruments with beam-type CID [37,38,42]. The instability of b-ions in applied CID conditions makes them more susceptible to post-CID reactions leading to much more complex and variable structures of b-ions' gas-phase chemistry [21,25].

Our aim was to answer the question if the underrepresentation of b-ions varies significantly on different MS platforms (QIT, LIT, QToF) depending on their CID type and quantify b-ion degradation via head-to-tail-cyclization reaction as one major pathway.

In agreement with the discussed observation of Lau et al. [37] we could confirm that b-ions in comparison with y-ions are underrepresented on the QToF instrument (see Fig. 1 non-acetylated example peptide EM(Ox)GGVVDNAAR). We could also show that beside underrepresentation of b-ions on the QToF instrument b-ions are also significantly underrepresented on ion trap instruments and therewith statistically confirm the observation of Tabb et al. [19,20] (Fig. 2 QIT and LIT). Although the underrepresentation of b-ions is significant on all considered platforms, the QToF instrument with a normalized b-ion occurrence of around 25% exhibit the greatest difference between b- and y-ions. The normalized b-ion occurrence for QIT and LIT is about 71% and 82%, respectively. Furthermore, detailed inspection showed that the resonant-excitation energy CID utilizing ion trap instruments exhibit an even distribution of b-ions and y-ions over the entire m/z range without any maximum (Fig. 2 QIT and LIT), whereas the beam-type CID applying QToF instrument showed a maximum for y-ions at y_6 and for b-ions at b_3 (Fig. 2 QToF). The absence of long-chained b-ions on the QToF instrument could be a hint of secondary fragmentation of b-ions ($b_n \rightarrow a_n \rightarrow b_{n-1} \rightarrow \dots$) or other degradation pathways [25,43]. However, no significant increase of a-ions in the QToF instrument could be detected (data not shown).

3.2. Determining the influence of head-to-tail cyclization on b-ion occurrence

As a next step we were aiming at experimentally elucidating the role of b-ions' head-to-tail cyclization as one pathway of significant underrepresentation of b-ions. In contrast to stable y-ions ("protonated amino acids") b-ions tend to stabilize their structure in the gas-phase by cyclization or rearrangement reactions [21]. Beside CO loss and building of a-ions, sequence scrambling after head-to-tail cyclization and re-opening have been described as post-CID fragmentation and rearrangement processes of b-ions. Especially this unpredictable sequence scrambling infers with data analysis and hampers protein identification by common search algorithm.

The influence of initial head-to-tail cyclization on b-ion occurrence was determined by acetylation of the N-terminus of tryptic peptides.

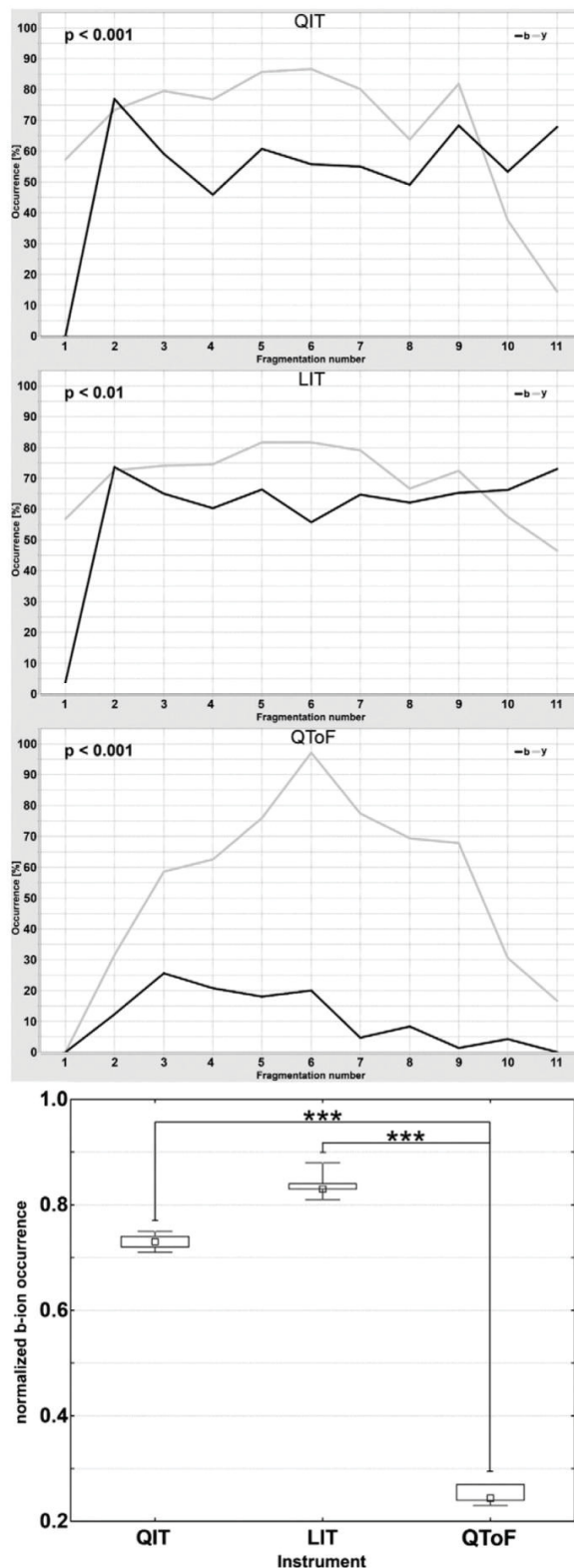


Fig. 2. Occurrence of b- and y-ions on different mass spectrometer platforms of digested protein mix. On the x-axis fragment number and on the y-axis occurrence in percent (%) is plotted. The black line represents the b-ion occurrence and the gray line the y-ion occurrence. The plotted p-value describes the difference between b- and y-ion occurrence of the same mass spectrometer calculated by Student's t-test. The box-whisker plot shows the normalized b-ion occurrence of the mass spectrometers. Significance is calculated across ion trap and QToF instruments by Tukey's HSD post-hoc test.

It has been shown that acetylation of the amino-N-atom at the N-terminus blocks the head-to-tail-cyclization reaction of b-ions [32,34,35]. Effects on b-ion stability by acetylation can be neglected because it has been shown that monoacetylation has not significant influence in the overall basicity of peptides [18]. Therefore, only monoacetylated peptides were considered for further data interpretation. As already described for single peptides N-terminal acetylation leads to an increase in b-ion occurrence [32,42] (see Fig. 1 acetylated example peptide EM(Ox)GGVVDNAAR). As depicted for the selected peptide EM(Ox)GGVVDNAAR acetylation leads to an increase in b-ion occurrence (Fig. 1). We assume that un-matched m/z values are peptide species coming from internal fragments or scrambled sequences.

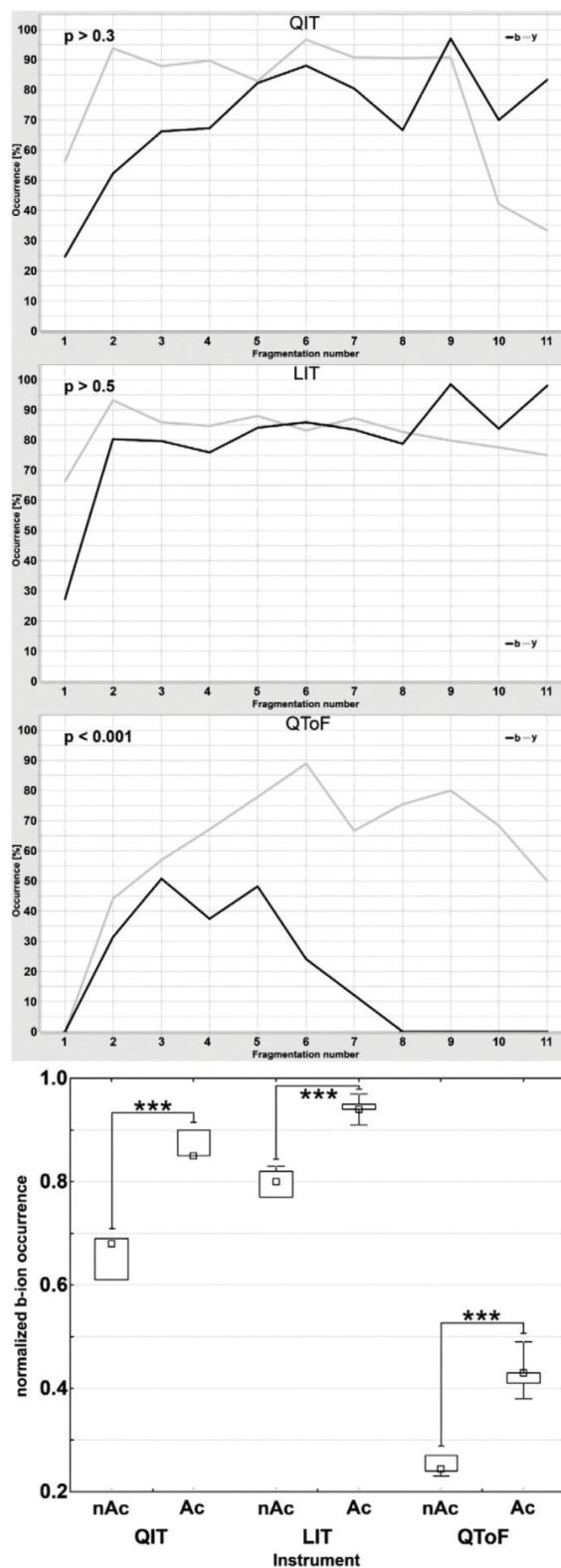
Statistical analysis revealed a significant increase of b-ions on all instruments, whereas acetylation does not influence y-ion occurrence (Fig. 3 Box-Plot). On the QToF instrument b-ion occurrence improved by 17% after blocking head-to-tail cyclization by acetylation and has its maximum at b-ion b_3 (Fig. 3 QToF). For the ion trap instruments we could observe the same effect. The b-ion occurrence on QIT and LIT increased by 16% and 15%, respectively. On ion trap instruments (performing resonant-excitation energy CID) acetylation of peptides abolishes the difference between b-ion and y-ion occurrence and therefore b-ions head-to-tail cyclization appears to be the dominant process leading to b-ion underrepresentation on ion trap instruments. For the QToF (performing beam-type CID) instrument the difference between y-ion and b-ion abundance is still statically significant (Fig. 3 QToF). A possible explanation of this observation could be the impact of collisional energies on beam-type CID fragmentation which is more likely optimal for y-ion intensities. It would be interesting to analyze the impact of different collision energies on the intensity of b- and y-ions on beam-type CID-based instruments. Our experimental approach clearly demonstrates that b-ion cyclization contributes to a maximum of 16% of the underrepresentation of b-ions independent of the utilized CID type. The comparison with recent reports relying on the prediction and assignment of scrambled ions is hindered by the unclear data situation. Goloborodko et al. reported that <1% of ions in the SwedCAD library (15,897 low energy CAD MS/MS spectra) could be matched to scrambled ion [36], whereas Dong et al. showed that in 390,000 CID spectra more than 10% of ions could be matched to scrambled ions [44]. In the work of Saminathan et al. in 35% of 43 peptides scrambling could be observed [45]. Therefore it would be interesting to combine both approaches of prediction of scrambled ions as well as experimental evaluation (N-terminal acetylation of peptides) and to adapt search engines for full interpretation of MS/MS spectra.

4. Conclusions

The underrepresentation of b-ions is a common feature of both beam-type (QToF) and resonant-excitation energy (LIT and QIT) CID type performing instruments.

The significant increase of b-ion occurrence by acetylation of peptides' N-terminus on all investigated instrument types let us conclude that the head-to-tail cyclization as an initial step for downstream degradation pathways of b-ions i.e. scrambling followed by fragmentation to a-ions and smaller species accounts for a maximum of 16% of b-ion loss. The abolition of differences between b- and y-ion occurrence revealed that the underrepresentation of b-ions not only exist on resonant-excitation energy CID performing ion trap MS but also that head-to-tail cyclization is the dominant process and responsible for this loss.

Fig. 3. Occurrence of b- and y-ions on different mass spectrometer platforms analyzing acetylated peptide mixture. On the x-axis fragment number and on the y-axis occurrence in percent (%) is plotted. The black line represents the b-ion occurrence and the gray line the y-ion occurrence. The p-value of Student's t-test was considered as a measure to analyze significance between b- and y-ions occurrences. The box-whisker plot shows the normalized b-ion occurrence of the different MS instruments with p-value calculated by Tukey's HSD post-hoc test.



As long as specific search algorithms do not reward for complete b- and y-ion series the loss of b-ions can be neglected in shotgun proteome analyses as shown by recent reports [36,45]. But, in case of detailed sequence analysis like e.g. *de novo* sequencing or phosphorylation site determination when complete sequence coverage is required, underrepresentation of b-ion becomes an issue. Therefore, the adaption of sample preparation protocols or selection of instrument facilitating resonant-excitation energy CID will help to obtain more sequence information.

Supplementary data to this article can be found online at <http://dx.doi.org/10.1016/j.bbapap.2013.08.007>.

Conflict of interest statement

The authors have declared no conflict of interest.

Acknowledgements

The authors acknowledge support for this work by GerontoSys and Protein-research Unit Ruhr within Europe (PURE). The authors thank Dr. Gereon Poschmann, Molecular Proteomics Laboratory (MPL), Düsseldorf, Germany, for the assistance in statistical analysis and Dr. Anke Schnabel, Protagen AG, Dortmund, Germany, and Sebastian Link, DKFZ-ZMBH, Heidelberg, Germany, for helpful discussion.

References

- R. Aebersold, M. Mann, Mass spectrometry-based proteomics, *Nature* 422 (2003) 198–207.
- B. Domon, R. Aebersold, Mass spectrometry and protein analysis, *Science* 312 (2006) 212–217.
- J.R. Yates III, C.I. Ruse, A. Nakorchevsky, Proteomics by mass spectrometry: approaches, advances and applications, *Annu. Rev. Biomed. Eng.* 11 (2009) 49–79.
- X. Han, A. Aslanian, J.R. Yates III, Mass spectrometry for proteomics, *Curr. Opin. Chem. Biol.* 12 (2008) 483–490.
- M. Karas, F. Hillenkamp, Laser desorption ionization of proteins with molecular masses exceeding 10,000 Da, *Anal. Chem.* 60 (1988) 2299–2301.
- J.B. Fenn, M. Mann, C.K. Meng, S.F. Wong, C.M. Whitehouse, Electrospray ionization mass spectrometry of large molecules, *Science* 246 (1989) 64–71.
- J. Muñoz, A.J. Heck, Quantitative proteome and phosphoproteome analysis of human pluripotent stem cells, *Methods Mol. Biol.* 767 (2011) 297–312.
- H. Zhou, S. Di Palma, C. Preisinger, M. Peng, A.N. Polat, A.J. Heck, S. Mohammed, Toward a comprehensive characterization of a human cancer cell phosphoproteome, *J. Proteome Res.* 12 (2013) 260–271.
- K.L. Busch, G.L. Glish, S.A. McLuckey, *Mass Spectrometry/Mass Spectrometry: Techniques and Applications of Tandem Mass Spectrometry*, VCH, New York, 1988.
- F.W. McLafferty, *Tandem Mass Spectrometry*, Wiley, New York, 1983.
- R. Johnson, S. Martin, K. Biemann, J. Stults, J. Watson, Novel fragmentation process of peptides by collision-induced decomposition in a tandem mass spectrometer: differentiation of leucine and isoleucine, *Anal. Chem.* 59 (1987) 2621–2625.
- R.A. Zubarev, N.L. Kelleher, F.W. McLafferty, Electron capture dissociation of multiply charged protein cations. A nonergodic process, *J. Am. Chem. Soc.* 120 (1998) 3265–3266.
- R.A. Zubarev, K.F. Haselmann, B. Budnik, F. Kjeldsen, F. Jensen, Towards an understanding of the mechanism of electron-capture dissociation: a historical perspective and modern ideas, *Eur. J. Mass Spectrom.* 8 (2002) 337–349.
- V.H. Wysocki, et al., *Principles of Mass Spectrometry Applied to Biomolecules*, Ed. by J. Laskin and C. Lifshitz, Wiley, New York, 2006.
- P. Roepstorff, J. Fohlman, Proposal for a common nomenclature for sequence ions in mass spectra of peptides, *Biomed. Mass Spectrom.* 11 (1984) 601.
- K. Biemann, Contributions of mass spectrometry to peptide and protein structure, *Biomed. Environ. Mass Spectrom.* 16 (1988) 99–111.
- A.L. McCormack, J. Eng, J.R. Yates III, Peptide sequence analysis on quadrupole mass spectrometers. A companion to methods in enzymology, *Acad. Press* 6 (1994) 274–283.
- A.R. Dongré, J.L. Jones, A. Somogyi, V.H. Wysocki, Influence of peptide composition, gas-phase basicity and chemical modification on fragmentation efficiency: evidence for the mobile proton model, *J. Am. Chem. Soc.* 118 (1996) 8365–8374.
- D.L. Tabb, L.L. Smith, L.A. Breci, V.H. Wysocki, D. Lin, J.R. Yates III, Statistical characterization of ion trap tandem mass spectra from doubly charged tryptic peptides, *Anal. Chem.* 75 (2003) 1155.
- D.L. Tabb, Y. Huang, V.H. Wysocki, J.R. Yates III, Influence of basic residue content on fragment ion peak intensities in low-energy collision-induced dissociation spectra of peptides, *Anal. Chem.* 76 (2004) 1243.
- A.G. Harrison, To b or not to b: the ongoing saga of peptide b ions, *Mass Spec. Rev.* 28 (2009) 640–654.
- A.G. Harrison, I.G. Csizmadia, T.H. Tang, Structure and fragmentation of b₂ ions in peptide mass spectra, *J. Am. Soc. Mass Spectrom.* 11 (2000) 427–436.
- T. Yalcin, C. Khouw, I.G. Csizmadia, M.R. Peterson, A.G. Harrison, Why are B ions stable species in peptide mass spectra? *J. Am. Soc. Mass Spectrom.* 6 (1995) 1165–1174.
- T. Yalcin, I.G. Csizmadia, M.R. Peterson, A.G. Harrison, The structures and fragmentation of B_n (n ≥ 3) ions in peptide mass spectra, *J. Am. Soc. Mass Spectrom.* 7 (1996) 233–242.
- B. Paizs, S. Suhai, Fragmentation pathways of protonated peptides, *Mass Spectrom. Rev.* 24 (2005) 508–548.
- B. Paizs, G. Lendvai, K. Vékely, S. Suhai, Formation of b₂⁺ ions from protonated peptides. An ab initio study, *Rapid Commun. Mass Spectrom.* 13 (1999) 525–533.
- M.J. Nold, C. Wesdemiotis, T. Yalcin, A.G. Harrison, Amide bond dissociation in protonated peptides. Structures of the N-terminal ionic and neutral fragments, *Int. J. Mass Spectrom. Ion Processes.* 164 (1997) 137–153.
- C.F. Rodriguez, T. Shoeib, I.K. Chu, K.W.M. Siu, A.C. Hopkinson, Comparison between protonation, lithiation and argentation of 5-oxazolones. A study of a key intermediate in gas-phase peptide sequencing, *J. Phys. Chem. A* 104 (2000) 5335–5342.
- A.G. Harrison, I.G. Csizmadia, T.H. Tang, Structures and fragmentation of b₂ ions in peptide mass spectra, *J. Am. Soc. Mass Spectrom.* 11 (2000) 427–436.
- J. Yague, A. Parada, M. Ramos, S. Ogueta, A. Marina, F. Barabona, J.A. de Castro, J. Vazquez, Peptide rearrangement during ion trap fragmentation: added complexity to MS/MS spectra, *Anal. Chem.* 75 (2003) 1524–1535.
- A.G. Harrison, A.B. Young, C. Bleiholder, S. Suhai, B. Paizs, Scrambling of sequence information in collision-induced dissociation of peptides, *J. Am. Chem. Soc.* 32 (2006) 10364–10365.
- C. Jia, W. Qi, Z. He, Cyclization reactions of peptide fragment ions during multistage collisionally activated decomposition: an inducement to lose internal amino acid residues, *J. Am. Soc. Mass Spectrom.* 18 (2007) 663–678.
- L. Mouis, J.L. Aubagnac, J. Martinez, C. Enjalbal, Low energy peptide fragmentations in an ESI-Q-ToF type mass spectrometer, *J. Proteome Res.* 6 (2007) 1378–1391.
- A.G. Harrison, Peptide sequence scrambling through cyclization of b₂ ions, *J. Am. Soc. Mass Spectrom.* 19 (2008) 1776–1780.
- A.G. Harrison, Cyclization of peptide b₃ ions, *J. Am. Soc. Mass Spectrom.* 20 (2009) 2248–2253.
- A.A. Goloborodko, M.V. Gorshkov, D.M. Good, R.A. Zubarev, Sequence scrambling in shotgun proteomics is negligible, *J. Am. Soc. Mass Spectrom.* 22 (2011) 1121–1124.
- K.W. Lau, S.R. Hart, J.A. Lynch, S.C.C. Wong, S.J. Hubbard, S.J. Gaskell, Observations on the detection of b- and y-type ions in the collisionally activated decomposition spectra of protonated peptides, *Rapid Commun. Mass Spectrom.* 23 (2009) 1508–1514.
- H. Barsnes, I. Eidhammer, L. Martens, A global analysis of peptide fragmentation variability, *Proteomics* 11 (2011) 1181–1188.
- T.Y. Samgina, S.V. Kovalev, V.A. Gorshkov, K.A. Artemenko, N.B. Poljakov, A.T. Lebedev, N-terminal tagging strategy for de novo sequencing of short peptides by ESI-MS/MS and MALDI-MS/MS, *J. Am. Soc. Mass Spectrom.* 21 (2010) 104–111.
- J.F. Riordan, B.L. Vallee, C.H. Hirs, N.T. Serge, Acetylation, *Methods in Enzymology*, 15, Academic Press, Oxford, 1972, 494–499.
- H. Barsnes, I. Eidhammer, L. Martens, Fragmentation analyzer: an open-source tool to analyze MS/MS fragmentation data, *Proteomics* 10 (2010) 1087–1090.
- R.W. Vachet, B.M. Bishop, W. Erickson, G.L. Glish, Novel peptide dissociation: gas-phase intramolecular rearrangement of internal amino acid residues, *J. Am. Chem. Soc.* 24 (1997) 5481–5488.
- B. Paizs, B.J. Bythell, P. Maître, Rearrangement pathways of the a₄ ion of protonated YGGFL characterized by IR spectroscopy and modeling, *J. Am. Soc. Mass Spectrom.* 23 (2012) 664–675.
- N. Dong, Y. Liang, L. Yi, Investigation of scrambled ions in tandem mass spectra. Part 1. Statistical characterization, *J. Am. Soc. Mass Spectrom.* 23 (2012) 1209–1220.
- I.S. Saminathan, X.S. Wang, Y. Guo, O. Kravovska, S. Voisin, A.C. Hopkinson, K.W.M. Siu, The extent and effects of peptide sequence scrambling via formation of macrocyclic b ions in model proteins, *J. Am. Soc. Mass Spectrom.* 21 (2010) 2085–2094.
- O.V. Krokhin, V. Spicer, Peptide retention standards and hydrophobicity indexes in reversed-phase high-performance liquid chromatography of peptides, *Anal. Chem.* 22 (2009) 9522–9530.

Chapter 16

Application of Label-Free Proteomics for Differential Analysis of Lung Carcinoma Cell Line A549

Barbara Sitek, Daniel M. Waldera-Lupa, Gereon Poschmann, Helmut E. Meyer, and Kai Stühler

Abstract

A label-free solution basing on a highly reproducible and stable LC-MS/MS system allows quantitative proteome analyses. Due to nonlabeling approach, the label-free method has the potential to measure samples from clinical specimen monitoring and comparing thousands of proteins. The presented label-free workflow includes in-solution digest, LC-MS analyses, data evaluation by the means of Progenesis™ software, and validation of the differential proteins. We successfully applied this workflow in a proteomics study analyzing the human lung carcinoma cell line A549 treated with transforming growth factor beta 1, a cell culture model of lung fibrosis. The differential analysis of only 1 µg protein per sample led to 202 significantly regulated proteins.

Key words: Lung fibrosis, Transforming growth factor beta 1, Peptide profiles, Label-free quantification

1. Introduction

A label-free solution for relative quantitative proteomics is based on two different strategies for protein quantification. On the one hand, the relative peptide ion intensities measured by liquid chromatography in combination with mass spectrometry to calculate expression levels of proteins can be used. The high correlation of mass spectral peak intensities of peptide ions and protein abundances has been demonstrated in numerous studies (1, 2). On the other hand, the label-free quantification can be performed by counting the number of fragment spectra identifying peptides of a

given protein (see Chapters 20 and 22). Spectral count or peptide ion intensity are measured for individual LC-MS/MS runs and differences in protein abundances are calculated by direct comparison between different runs.

In contrast to labeling-based quantification techniques such as ICAT (see Chapter 24), iTRAQ (see Chapter 8), TMT (see Chapter 9), IPTL (see Chapter 10), ICPL (see Chapter 11), or SILAC (see Chapters 13, 14, 25, and 26), the label-free approach is proceeding without any isotopic or chemical labeling. For this reason, the limitation caused by the labeling (e.g., high cost of the reagents, incomplete labeling, or higher sample concentration) can be omitted in the label-free technique. Otherwise there are some challenges which are important requirements for successful realization of label-free quantification in biological samples. Due to a high sample complexity, the reproducibility and stability of the LC-MS system as well as appropriate software solution for data analysis are essential. This is challenging, especially when a large number of biological samples is analyzed. Therefore, all steps of the label-free approach have to be optimized in order to get valid data. Usually, this approach includes the following steps: (a) sample preparation with protein extraction and digestion; (b) peptides separation by liquid chromatography; and (c) data analysis including quantification, identification, and statistical analysis. Recent improvements in the sensitivity of MS and the reproducibility of LC have shown that label-free proteomics for a proteome-wide quantification of proteins in complex biological samples is feasible. This technique has the potential to become a significant complement to current quantification methods. The high-throughput compatibility of a label-free approach allows processing of large numbers of biological samples, which is required for statistically significant quantification.

We describe the application of a label-free approach for the identification of new candidate proteins involved in the development of lung fibrosis. We used human lung carcinoma cell line A549 as a biological system. Transforming growth factor beta 1 (TGF- β 1) is a key effector cytokine in the development of lung fibrosis. The treatment of A549 cells using TGF-beta is a well-established model for lung fibrosis. For the differential proteome study, seven biological replicates of A549 cell line were treated with TGF- β 1 and as control seven cell replicates without TGF- β 1 were applied. We used nano-HPLC coupled to an LTQ-OrbitrapTM mass spectrometer for generating peptide profiles and the ProgenesisTM software for statistical analysis of the data (Fig. 1). Altogether 202 proteins have been found to be differentially expressed (fold change >1.5 or <-1.5 , $p < 0.01$).

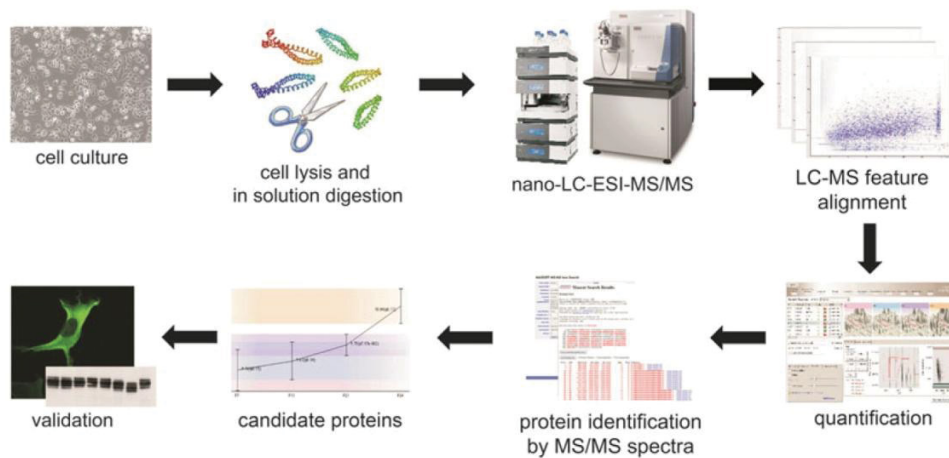


Fig. 1. Workflow of the label-free proteomic approach applying LC-MS/MS. First the proteins will be extracted and digested with trypsin. After the digest LC-MS/MS data will be generated and evaluated with Progenesis™. The differential regulated proteins will be identified by using Mascot™. For validation of candidate proteins Western blots and immunohistochemistry will be performed.

2. Materials

2.1. Sample Preparation and Digestion

1. Ultrasonic bath (VWR, Darmstadt, Germany).
2. Hand homogenizer.
3. Lysis buffer: 2 M thiourea, 7 M urea, 30 mM Tris-HCl, pH 8.0.
4. Digestion: 50 mM ammonium bicarbonate (ABC), 45 mM DTT, 100 mM iodoacetamide (IAA), 100 ng/μL trypsin, formic acid (FA).

2.2. Liquid Chromatography

1. Dionex UltiMate 3000 Nano LC System (Dionex, Idstein, Germany).
2. Trap column: Acclaim PepMap100 C18 Nano-Trap Column (C18, particle size 5 μm, pore size 300 Å, I.D. 200 μm, length 1 cm; Dionex).
3. Nano column: Acclaim PepMap100 C18 Column (C18, particle size 3 μm, pore sizes 100 Å, I.D. 75 μm, length 25 cm; Dionex).
4. Loading solvent: 0.1% (v/v) Trifluoroacetic acid (TFA) (MS grade).
5. Gradient solvent A: 0.1% (v/v) FA (MS grade).
6. Gradient solvent B: 0.1% (v/v) FA (MS grade), 84% (v/v) Acetonitrile (ACN) (HPLC-S gradient grade).

244 B. Sitek et al.

2.3. Mass Spectrometry

1. LTQ-Orbitrap XL with an online nano-ESI source (Thermo Fisher Scientific, Bremen, Germany).
2. Distal Coated SilicaTips™ (New Objective, Woburn, USA).
3. Collision gas: nitrogen.

2.4. Data Analysis

1. Mascot v. 2.2.0 (Matrix Science, London, UK) (see Chapter 28).
2. Progenesis™ v. 2.5 (Nonlinear Dynamics, Newcastle, UK).

3. Methods

3.1. General Practice

The human lung adenocarcinoma cell line A549 (ATCC CCL-185) was grown in DMEM (high glucose, GlutaMAX and Pyruvate; Invitrogen Nr. 31966047) supplemented with 10% FBS in a humidified incubator at 37°C and 5% CO₂ until cells were confluent. Subsequently, cells have been detached by trypsin and transferred to 14 cm diameter dishes (2.5 × 10⁶ cells/dish). Twenty-four hours later, the medium was removed and exchanged by serum-free medium. After 24 h of serum starvation and exchange of medium, TGF-β1 (25 ng/10 mL serum-free medium, RD-Systems 240-B, lot AV406041) was added to seven dishes and TGF-β1 reconstitution buffer to the other seven dishes. Twenty-four hours after cell stimulation cells were harvested, washed with PBS, scraped using a rubber policeman, washed with PBS again, pelleted, snap frozen, and stored at -80°C.

3.2. Sample Preparation and Enzymatic Digestion

1. Lyse the cells in lysis buffer (1.4 μL/mg sample; 4°C) and sonicate the samples six times for 10 s on ice and finally centrifuge (16,000 × g for 15 min) the lysate and store the supernatant at -80°C (see Note 1).
2. For the further analysis, it is necessary to know the concentration of the samples. To determine the concentrations a Bradford assay is performed.
3. For the proteolysis of proteins a tryptic in-solution digest is performed. Therefore, solve 5 μg protein (5 μL) in 129 μL ABC and reduce with 0.8 μL DTT (45 mM) for 15 min at 50°C. Afterwards alkylate with 0.8 μL IAA (100 mM) in the dark at room temperature for 15 min. Add trypsin (1:50, w/w) to digest the protein over night (max. 14 h) at 37°C. Stop the digestion by adding 5 μL FA to the solution.
4. Before performing the LC-MS experiments, centrifuge (16,000 × g for 30 min) the digested samples and transfer them into a clear vial (see Note 2). Afterwards add 0.1% TFA to a final concentration of 1 μg/15 μL.

3.3. Peptide Separation with Reversed Phase High-Performance Liquid Chromatography

1. For separation of digested proteins, a reversed phase high-performance liquid chromatography is performed using the UltiMate™ 3000 Nano LC System (Dionex). Therefore, a system comprising a nano-trap column (C18) and a nano-column (C18) is used. Heating the columns to a temperature of 60°C allows high flow rate (400 nL/min) at tolerable pressure (see Note 3).
2. For injection of the samples, a volume of 15 µL is used. After injection the peptides will be trapped while detergents and salts will be washed out for 5 min (see Note 4). For loading, a flow rate of 30 µL/min is used.
3. A shallow gradient is applied for separation: (a) linear gradient from 5% B to 35% B over 150 min, then (b) to 95% B in 2 min, (c) constant 95% B for 3 min and finally (d) 20 min at 5% B for equilibration (see Note 5). As flow rate of the gradient pump 400 nL/min is used.

3.4. Detection of Separated Peptides with Mass Spectrometry

1. The LTQ-Orbitrap™ mass spectrometer (Thermo Fisher Scientific) is operated in the data-dependent mode to switch automatically between MS and MS/MS acquisition.
2. Set the mass range for survey full scan MS spectra and MS/MS spectra to m/z 300–1,500.
3. For fragmentation collision-induced dissociation (CID) with nitrogen as collision gas is applied. Therefore, a top six methods based on the intensity is used (see Note 6). The minimal required signals for precursor ions are 5,000 counts and the isolation width is 2 ppm.
4. Reject charge state 1+ and prefer charge states 2+, 3+, and 4+ for precursor ion isolation.
5. Utilize dynamic exclusion with an exclusion duration of 35 s and one repeat count within 30 s. Exclusion list size of 500 precursor ions with an exclusion mass width of 5 ppm is used.
6. Finally export LC-MS analysis data as Thermo .RAW file format.

3.5. Differential Proteome Analysis

1. The differential proteome analysis is performed with Progenesis™ (Nonlinear Dynamics). Import the LC-MS analysis data files which are described previously.
2. Select the reference run that all other runs are aligned to. Therefore, select a run that has minimal noise and represents stable LC-MS conditions by consideration of the two-dimensional map (Fig. 2).
3. Alignment is the most important step in the label-free workflow. So it is necessary that the alignment will be done with high

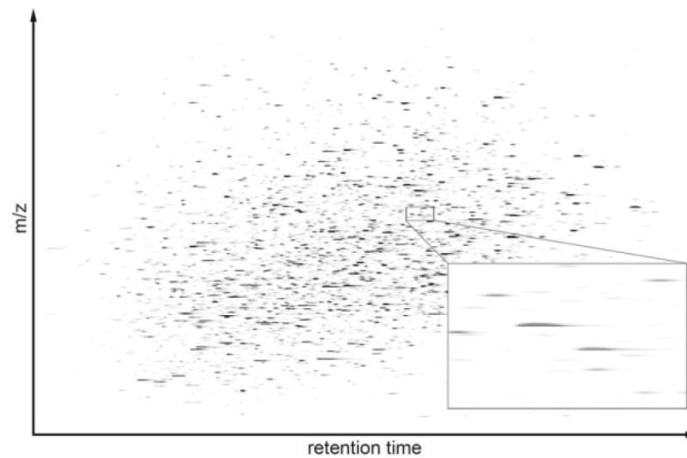


Fig. 2. Two-dimensional display of the peptide LC-MS analysis from A549. The survey view displays m/z vs. retention time of the LC-MS run. The automated alignment of Progenesis™ is based on paired feature detection at the LC-MS level and does not reduce the data to the total ion chromatogram. This is followed by regression analysis in peptides retention time and m/z to produce an alignment grid used to accurately overlay the data.

accuracy. Apply automatic alignment and afterwards check the alignment carefully. If automatic alignment does not work, manually add vectors to align the run.

4. Feature detection, normalization and quantification will be done automatically. Exclude or include features from the analysis results. Therefore, the LC washing and equilibration step is excluded. Include only charge states between 2+ and 5+ to exclude contaminations from the analysis (see Note 7).
5. Create the design of the experiment, e.g., untreated vs. treated samples. Runs which have no stable LC-MS conditions can be sorted out.
6. For differential analysis, it is necessary to have significant results. Therefore, features are filtered based on p -value ($p < 0.05$) and tagged for further analysis.
7. Perform a principal component analysis (PCA) to check the runs cluster based on the expected groups. Features also can be filtered based on their q -value to report false discovery rates and their statistical power within the experimental analysis.
8. Identify features which are differentially regulated (Fig. 3). Therefore, export these features in a .MGF file format and perform a Mascot™ (Matrix Science) (see Chapter 28) MS/MS-Ions search.

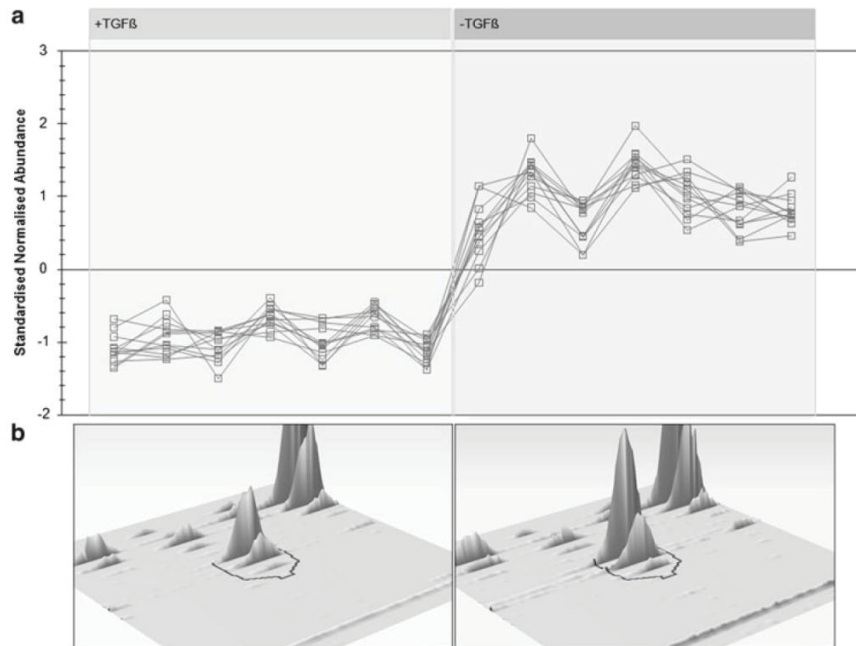


Fig. 3. Regulation of the identified peptides from one single protein. (a) Twelve differentially regulated peptides from one protein which were identified in all samples. Each *square* stands for one peptide in each replicate for the respective condition. (b) Three-dimensional display of one specific peptide in both conditions. This view shows the regulation and also the isotopic pattern of the eluting peptide.

3.6. Identification of Differentially Regulated Proteins

1. For protein identification the Mascot™ search engine is used. The following parameters are used: (a) database: ipi.human.decoy, (b) enzyme: trypsin, (c) missed cleavages: allow up to one, (d) fixed modifications: propionamide (cysteine), (e) variable modifications: oxidation (methionine), (f) peptide tolerance: 4 ppm, (g) MS/MS tolerance: 0.4 Da, (h) peptide charge: 2+ and 3+, (i) monoisotopic, and (j) data format: mascot generic.
2. Export identification data as .XML file format and import these in Progenesis™. The imported data are not filtered yet, e.g., peptides with a low mascot score are included. Filter the identified peptides based on mascot score and decoy entries.
3. Check the identified proteins manually and solve problems with protein isoforms if possible. Afterwards validate the differentially regulated proteins manually.
4. Finally create a report of the analysis results.

4. Notes

1. For tissue and body fluids the procedure can also be applied. This workflow could already be carried out successfully.
2. A tryptic digestion is never complete. To avoid clogging of the trap column it is necessary to remove undigested proteins. If the trap column is closed the LC-MS runs will not be reproducible.
3. Heating the columns is necessary to reduce the pressure of the system and to get a better separation of the peptides. But if the columns are heated the flow rate must be higher, because the HPLC need a minimum of pressure to work. The higher the flow rate, the worse the sensitivity. A compromise between separation and sensitivity is necessary.
4. The time for trapping and washing the samples depends on the length of the capillaries to the trap column and on the purity of the samples. If high salt concentrations were used it is necessary to expand the time for washing.
5. To avoid a bad reproducibility time for equilibration should be 20 min in minimum. If early eluting peptides in the LC-MS runs are not reproducible increase the time for equilibration.
6. A top six method means that the six most intense peaks of a full scan MS are selected for fragmentation (MS/MS).
7. The charge states of tryptic peptides are between 2+ and 5+. Contaminations mostly have charge state +1. If another protease as trypsin is used the charge states could be different.

Acknowledgments

The author would like to thank Dr. Katja Kuhlmann and Nadine Stoepel for the mass spectrometry measurements and Kathy Pfeiffer for excellent technical assistance.

References

1. Bondarenko PV, Chelius D, Shaler TA (2002) Identification and relative quantitation of protein mixtures by enzymatic digestion followed by capillary reversed-phase liquid chromatography-tandem mass spectrometry. *Anal Chem* 74:4741–4749
2. Chelius D, Bondarenko PV (2002) Quantitative profiling of proteins in complex mixtures using liquid chromatography and mass spectrometry. *J Proteome Res* 1:317–323

Veröffentlichungen und Präsentationen

Veröffentlichungen

Aldous, S.H., Weise, S.E., Sharkey, T.D., Waldera-Lupa, D.M., Stühler, K., Malmann, J., Groth, G., Gowik, U., Westhoff, P., Arsova, B. (2013) Evolution of the phosphoenolpyruvate carboxylase protein kinase family in C₃ and C₄ *Flaveria* species. *PlantPhys*, accepted

Waldera-Lupa, D.M., Stefanski, A., Meyer, H.E., Stühler, K. (2013) The fate of b-ions in the two worlds of collision-induced dissociation. *Biochim Biophys Acta*, **12**, 2843-2848

Sitek, B., Waldera-Lupa, D.M., Poschmann, G., Meyer, H.E., Stühler, K. (2012) Application of label-free proteomics for differential analysis of lung carcinoma cell line A549. *Methods Mol Biol*, **893**, 241-248

Eingereichte Manuskripte

Waldera-Lupa, D.M., Florea, A., Kalfalah, F., Sass, S., Kruse, F., Tigges, J., Fritsche, E., Krutmann, J., Busch, H., Meyer, H.E., Boege, F., Theis, F., Reifenberger*, G., Stühler*, K. (2014) Proteome-wide analysis of primary cultures of *in situ* aged human fibroblasts reveals a moderate age-associated cellular phenotype. *Aging Cell*, submitted

* These authors contributed equally

Waldera-Lupa, D.M., Kalfalah, F., Boukamp, P., Safferling, K., Poschmann, G., Götz-Rösch, C., Bernerd, F., Haag, L., Hanzen, B., Huebenthal, U., Fritsche, E., Grabe, N., Boege, F., Tigges*, J., Krutmann*, J., Stühler*, K. (2014) Characterization of skin aging associated secreted proteins (SAASP) produced by dermal fibroblast isolated from intrinsically aged human skin. *J Invest Dermatology*, submitted

* These authors contributed equally

Vorträge

H/D exchange & Crosslinking Mass Spectrometry, Modul "From gene to *in silico* structure" im März 2014 in Düsseldorf, Deutschland

H/D exchange & Crosslinking Mass Spectrometry, Modul “From gene to *in silico* structure” im März 2013 in Düsseldorf, Deutschland

Mass spectrometrical analysis of aged fibroblasts using a quantitative proteome approach, GerontoSys Status Meeting im Juli 2012 in Heidelberg, Deutschland

LTQ Velos ETD - Linear Ion Trap with Electron Transfer Dissociation, Tagung des Medizinischen Proteom-Center im Dezember 2011 in Rauschholzhausen, Deutschland

Progenesis – Nonlinear Dynamics, Tagung des Medizinischen Proteom-Center im Dezember 2010 in Rauschholzhausen, Deutschland

Präsentationen

Skin Ageing - Proteome-wide analysis of primary cultures of *in situ* aged human fibroblasts reveals a moderate age-associated cellular phenotype, 62th ASMS Conference on Mass Spectrometry and Allied Topics im Juni 2014 in Baltimore, Maryland, USA

Skin aging - Identification of proteins secreted by human dermal fibroblasts using a quantitative proteome approach, Annual Meeting of the German Society for Aging Research (DGfA) im Dezember 2013 in Düsseldorf, Deutschland

Skin aging - Identification of protein factors secreted by human dermal fibroblasts using a quantitative proteome approach, 61th ASMS Conference on Mass Spectrometry and Allied Topics im Juni 2013 in Minneapolis, Minnesota, USA

Y not B? The occurrence of b-ions on different mass spectrometer platforms, Proteomic Forum 2013 im März 2013 in Berlin, Deutschland

The b-ions are the cool losers, 60th ASMS Conference on Mass Spectrometry and Allied Topics im Mai 2012 in Vancouver, British Columbia, Kanada

Fragmentation on different mass spectrometer platforms, Tagung des Medizinischen Proteom-Center im Dezember 2011 in Rauschholzhausen, Deutschland

The occurrence of b-ions on different mass spectrometer platforms, 5th European Summer School "Proteomic Basics" im Juli 2011 in Brixen, Italien

Y not B? The occurrence of b-ions on different mass spectrometer platforms, 59th ASMS Conference on Mass Spectrometry and Allied Topics im Juni 2011 in Denver, Colorado, USA

Pilot study of GerontoSys project: Mass spectrometrical analysis of senescence associated protein changes in cultured human fibroblasts using a label-free proteomics approach, Proteomic Forum 2011 im April 2011 in Berlin, Deutschland

Mass spectrometrical analysis of senescence associated protein changes in cultured human fibroblasts using a label-free proteomics approach, Tagung des Medizinischen Proteom-Center im Dezember 2010 in Rauschholzhausen, Deutschland

Mass spectrometrical analysis of senescence-associated protein changes in cultured human fibroblasts using a label-free proteomics approach, 58th ASMS Conference on Mass Spectrometry and Allied Topics im Mai 2010 in Salt Lake City, Uah, USA

Proteome analysis of senescence associated protein changes in cultured human fibroblasts using a label-free mass spectrometry approach, 61. Mosbacher Kolloquium The Biology of Aging: Mechanisms and Intervention im April 2010 in Mosbach, Deutschland

Danksagung

Zuallererst danke ich meinem Doktorvater Prof. Dr. Kai Stühler ganz besonders für die Betreuung dieser Arbeit. Die zahlreichen Diskussion, Anregungen und Ideen haben mein wissenschaftliches Interesse kontinuierlich vorangetrieben und mir dabei geholfen Ergebnisse stets kritisch zu hinterfragen.

Prof. Dr. Lutz Schmitt, Inhaber des Lehrstuhls für Biochemie I, möchte ich für die Übernahme des Zweitgutachtens danken.

Für die gute Zusammenarbeit möchte ich mich herzlich bei den Mitgliedern des GerontoSys-Konsortiums bedanken. Besonderer Dank gilt hier Prof. Dr. Boege, Prof. Dr. Reifenberger, Dr. Dr. Ana-Maria Florea, Dr. Faiza Kalfalah und Dr. Julia Tigges für ausführliche biologische Diskussionen und die Bereitstellung der Proben.

Bei den Mitarbeitern des Medizinischen-Proteom-Centers bedanke ich mich für die lehrreiche Zeit und die Möglichkeit tiefgreifende Einblicke in die Proteinanalytik zu erlangen. Besonders möchte ich mich hier bei Prof. Dr. Helmut E. Meyer, Jun.-Prof. Dr. Barbara Sitek, Christian Bunse, Birgit Korte und Michael Krafzik bedanken.

Sebastian Link möchte ich für den detaillierten Einblick in die Massenspektrometrie, die Chromatographie und die Datenevaluation danken.

Bei meinen Kollegen vom Molecular Proteomics Laboratory möchte ich mich für die hervorragende Zusammenarbeit, die zahlreichen Diskussionen und die Unterstützung bedanken. Insbesondere danke ich Anja Stefanski, Dr. Gereon Poschmann, Mareike Brocksieper, Eva Hawranke und Hans Bruns (ehemals MPL).

Bedanken möchte ich mich auch bei meinen Eltern, Sylvia und Jörg Waldera, für die Unterstützung während meines Studiums und die stetige Ermutigung meine Ziele weiterhin zu verfolgen. Selbstverständlich danke ich auch meiner ganzen Familie.

Besonderer Dank gilt meinen Freunden Eugen Edengeiser (aka Otto Edengieser), Dr. Inga Ellmers und Dr. Stefanie Punsmann für die unvergessliche Zeit während des Studiums.

Außerordentlicher Dank gilt meiner Frau Nadine Lupa für die Geduld bei den zahlreichen Diskussionen und die Unterstützung während meiner Promotion. Danke!

Lebenslauf

Persönliche Daten

Name Daniel Michael Waldera-Lupa, geb. Waldera

Anschrift Gahlensche Straße 117, 44809 Bochum

Telefonnummer +49 (0) 172 16 58 977

E-Mail daniel.waldera-lupa@hhu.de

Geburtsdatum 01. November 1984, Bochum

Staatsangehörigkeit Deutsch

Familienstand Verheiratet, keine Kinder



Akademischer Werdegang

01/2012 - aktuell Molecular Proteomics Laboratory, Düsseldorf
Universitätsklinikum Düsseldorf, Düsseldorf
Wissenschaftlicher Mitarbeiter
Leitung: Prof. Dr. Kai Stühler
Mitglied der Interdisciplinary Graduate and Research Academy Düsseldorf

04/2010 - 12/2011 Medizinisches Proteom-Center, Abteilung Neuroproteomics, Bochum
Ruhr-Universität Bochum, Bochum
Wissenschaftlicher Mitarbeiter
Institutsleitung: Prof. Dr. Helmut E. Meyer
Abteilungsleitung: Prof. Dr. Kai Stühler

04/2010 - aktuell Promotionsstudium der Biochemie
Thema des Promotionsvorhabens:
Untersuchung der stromalen Alterung - Proteom- und Sekretomstudie *in situ*
gealterter humaner dermaler Fibroblasten
Erstprüfer: Prof. Dr. Kai Stühler

10/2008 - 03/2010 Studium der Biochemie
Ruhr-Universität Bochum, Bochum
Abschluss: Master of Science (Note: 1,1)
Masterarbeit am Medizinischen Proteom-Center, Bochum:
Untersuchung der altersabhängigen Veränderung des Fibroblastenproteoms
mittels differentieller Proteomanalyse (Note: 1,3)
Erstprüfer: Prof. Dr. Helmut E. Meyer

10/2005 - 09/2008 Studium der Biochemie
Ruhr-Universität Bochum, Bochum

Lebenslauf

Abschluss: Bachelor of Science (Note: 1,8)
Bachelorarbeit am Max-Planck-Institut für molekulare Physiologie, Dortmund:
Suche nach Arl6 bindenden Proteinen (Note: 1,7)
Erstprüfer: Prof. Dr. Alfred Wittinghofer

Zivildienst und Schulischer Werdegang

- 08/2004 - 08/2005** AWO Seniorenzentrum, Bochum
- 08/1995 - 07/2004** Willy-Brandt-Gesamtschule, Bochum
Abschluss: Allgemeine Hochschulreife (Note: 1,6)
- 08/1991 - 07/1995** Städtische Grundschule am Volkspark, Bochum

Ausgewählte Weiterbildungen

- 09/2012** iGRAD Workshop: Führungskompetenz
Medical Research School Düsseldorf, Düsseldorf
- 09/2012** iGRAD Workshop: Wissenschaftliches Präsentieren
Medical Research School Düsseldorf, Düsseldorf
- 06/2012** iGRAD Workshop: Introduction to Good Scientific Practice
Heinrich-Heine Universität Düsseldorf, Düsseldorf
- 05/2012** TSQ Biotech Operations Training Course
Thermo Scientific Training Institute, Bremen
- 01/2011** LTQ Orbitrap Velos Biotech Operations Training Course
Thermo Scientific Training Institute, Bremen
- 01/2011** maXis UHR-ESI-TOF Basic Operator Course
Bruker Daltonik, Bremen
- 02/2010** 5. Workshop Biochromatographie
Dionex Trainings Center, Dortmund

Stipendien

- 06/2014** DGPF-Reisestipendium zur Teilnahme an der 62st ASMS Conference on Mass Spectrometry and Allied Topics, Baltimore, Maryland, USA
- 06/2013** DGPF-Reisestipendium zur Teilnahme an der 61st ASMS Conference on Mass Spectrometry and Allied Topics, Minneapolis, Minnesota, USA
- 05/2012** DGPF-Reisestipendium zur Teilnahme an der 60st ASMS Conference on Mass Spectrometry and Allied Topics, Vancouver, Kanada
- 07/2011** DGPF-Reisestipendium zur Teilnahme an der 5th European Summer School "Proteomic Basics", Brixen, Italien

Erklärung

Hiermit erkläre ich, Daniel Michael Waldera-Lupa, dass ich die vorliegende Dissertation selbstständig verfasst und bei keiner anderen Universität bzw. Fakultät in der vorgelegten oder einer ähnlichen Form eingereicht habe. Für die Anfertigung der Dissertation habe ich keine anderen als die angegebenen Hilfsmittel verwendet. Die Stellen, die anderen Arbeiten dem Wortlaut oder dem Sinn nach entnommen sind, wurden unter Angabe der dazugehörigen Quelle kenntlich gemacht. Weiterhin erkläre ich, dass alle Abbildungen nur die originalen Daten enthalten und in keinem Fall inhaltsverändernde Bildbearbeitung vorgenommen wurde.

Düsseldorf, den

Daniel Michael Waldera-Lupa